# WMA

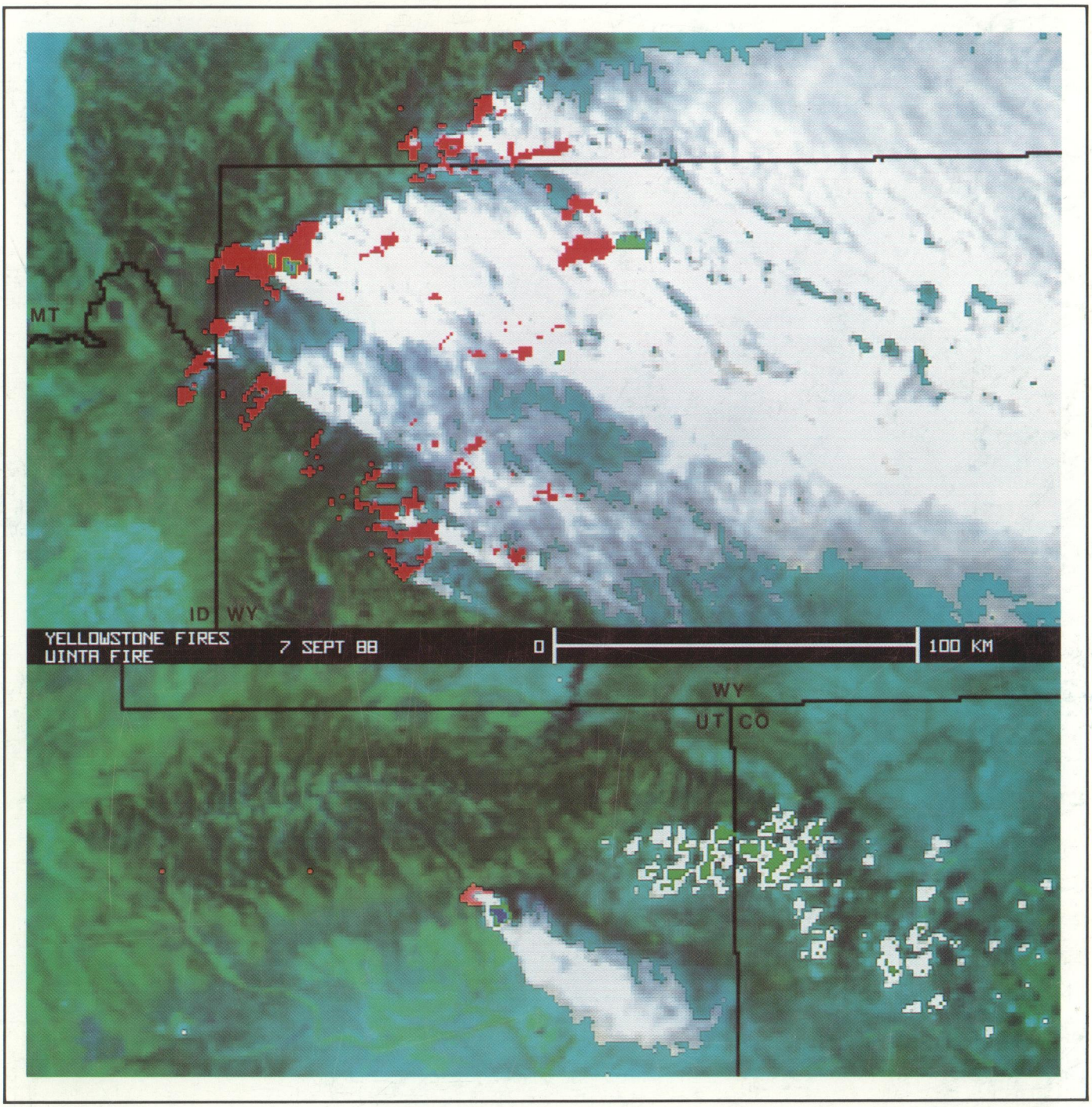


*The Journal of Weather Modification*

*Volume 21 Number 1* *April 1989*

*The various papers in Volume 21 are interesting, informative, provocative, and stimulating. They not only illuminate much of "what's going on" in cloud seeding today, but point us toward an avenue of tomorrow. The President's Message (Dennis) helps clarify a subject long in the shadows, the realism of risk. Understanding this subject has been a stumbling block in the arenas of pure science and applied cloud seeding technology.*

*The subjects in Volume 21 focus on hail suppression (Musil, Aleksic and Radinovic), the singular use of propane as a seeding material at ground level (Reynolds), thoughts on dynamic seeding (Pflaum), cloud liquid water (Super), possibilities for seeding fire induced cumulus clouds, (Holroyd), seeding effects at ground level (Ben-Zvi), and some initial field experiments and laboratory tests using pseudomonas syringae, a common occurring bacteria with strong ice nucleating properties (Ward). The subjects are exciting enough to stimulate anyone's imagination and desire to "look further".*

*As is normally the case, the subjects in this volume are a mix of both scientific investigation and the application of this scientifically based technology. It seems logical that such a mix will continue in some small way to provide forward motion to the field of weather modification.*

***Cover:***

*Satellite views of the Yellowstone and Uinta fires on the afternoon of 7 September 1988.*
*Image processing by Edmond W. Holroyd, III.*
*Fires: red and orange*
*Cloud temperatures: white and gray >0 °C;*
*0 °C > green ≥ -20 °C; -20 °C > blue.*

*See paper by Holroyd and Super for further details.*

***Published by:***

*THE WEATHER MODIFICATION ASSOCIATION*
*P. O. BOX 8116*
*FRESNO, CALIFORNIA 93747 U.S.A.*
*PHONE: 209-291-8466*

*ISBN: 0739:1781*

*ADDITIONAL COPIES OF THE JOURNAL OF WEATHER MODIFICATION ARE AVAILABLE FOR U.S. $25.00 EACH (MEMBERS) AND U.S. $40.00 (NON-MEMBERS).*

*MEMBERSHIP INFORMATION IS AVAILABLE BY CONTACTING THE ASSOCIATION AT THE ABOVE ADDRESS.*

- THE JOURNAL OF WEATHER MODIFICATION -

WEATHER MODIFICATION ASSOCIATION

VOLUME 21 NUMBER 1 APRIL 1989

TABLE OF CONTENTS: PAGE

**- NON-REVIEWED SECTION -**

# A NOTE ON THE POTENTIAL FOR SEEDING FIRE-INDUCED CONVECTIVE CLOUDS

Edmond W. Holroyd III and Arlin B. Super
Bureau of Reclamation
Denver, CO 80225

The recent outbreaks of widespread, drought-related forest and range fires in the Western United States have increased interest in reducing fire danger and damage. One possible approach that deserves serious assessment is the application of cloud seeding to convective clouds over the fire-prone areas. Such clouds may form naturally, especially over mountainous terrain, or may be produced or enhanced by the fires themselves. This note examines a September 1988 afternoon with fire-induced convective clouds as viewed with digital satellite data. It is recommended that similar studies be made of the entire 1988 fire season in the West to determine the frequency of clouds possibly suitable for seeding.

Towering cumulus or even cumulonimbus clouds may often be present during the summer months when the fire danger is greatest. In fact, thunderstorms often ignite the fires, and Project Skyfire of the 1950's was conducted to see if cloud seeding could reduce the lightning danger. Even during severe drought conditions in which there is little atmospheric water that is condensable into clouds, fires create water vapor as a product of combustion. The smoke from the fires should make the clouds extremely colloidally stable, with tiny cloud droplets. Thus, only the ice phase process should be able to make such clouds precipitate. Cloud seeding, with dry ice or AgI released from aircraft directly into the supercooled portions of fire-induced cumulus clouds, will initiate the precipitation process and might drop rain downwind of the fire, dampening the surface into which the fire is moving.

Fires which produce supercooled clouds may also create a circulation regime that could be exploited by setting AgI generators on the ground upwind of the fires. The AgI nuclei might then be drawn into the fire-induced cloud, seeding it when and if it becomes supercooled.

The idea of seeding convective clouds associated with forest fires is not new. For example, some exploratory work has been done in Alaska (Harpster and Douglas, 1971) and in Canada (Isaac et al., 1980). Perhaps a number of workers have even occasionally experimented with fire-induced cumulus. Such a cloud, labeled as Cloud 2 on 8 December 1972 in Holroyd et al. (1978), was seeded by the first author using an aircraft and dry ice pellets. It produced the second highest estimate of dry ice effectiveness of the reliable Australian experiments. This suggests that the ingested smoke did not radically alter the cloud microphysics so as to prevent seeding from starting the precipitation process.

The cover photograph of this volume shows two fire systems during the afternoon of 7 September 1988 as viewed by the NOAA-AVHRR polar orbiting satellite. The upper part is of the Yellowstone Park fires and the lower is of a fire on the south side of the Uinta Mountains of northeastern Utah. The state boundaries are shown in black. In the computer processing, fires were identified using the infrared band 3 (3.50 to 3.95 $\mu$m) with a threshold at 47 °C. They are colored in red on top of the Yellowstone smoke. A more orange tone is the fire area in the Uintas because a slightly different color processing was used to show the smoke emanating from the fire.

Of interest to weather modifiers are those parts of the clouds that were supercooled. Infrared band 4 (10.4 to 11.7 $\mu$m) was used to identify the 0 and -20 °C thresholds. Clouds between 0 and -20 °C are shown in green on top of the fires and smoke. Those clouds colder than -20 °C are shown in blue within the green ring. Five regions over the Yellowstone fires had supercooled clouds. One of them, and also the Uinta fire, had portions colder than -20 °C. A field of cumulus clouds with supercooled tops (green) was east of the Uinta fire.

Figure 1 shows cloud top temperature profiles with distance downwind of the fires. Surface temperatures adjacent to the fires and the fire locations are also indicated. The larger supercooled elements, labeled "TCU" for towering cumulus, are 5 to 7 km long, but most of the smoke is warmer than 0 °C.

The Yellowstone profile extends eastward from the large fire in the northwestern part of the park for a 29-km-wide swath through four of the supercooled cloud elements. The surface locations of the fires are marked by the broad lines at the bottom. The Uinta cloud was profiled within a similar swath in the direction of 123°. Scatter diagrams of temperatures within the swaths were prepared from which the general surface temperatures adjacent to the fires and

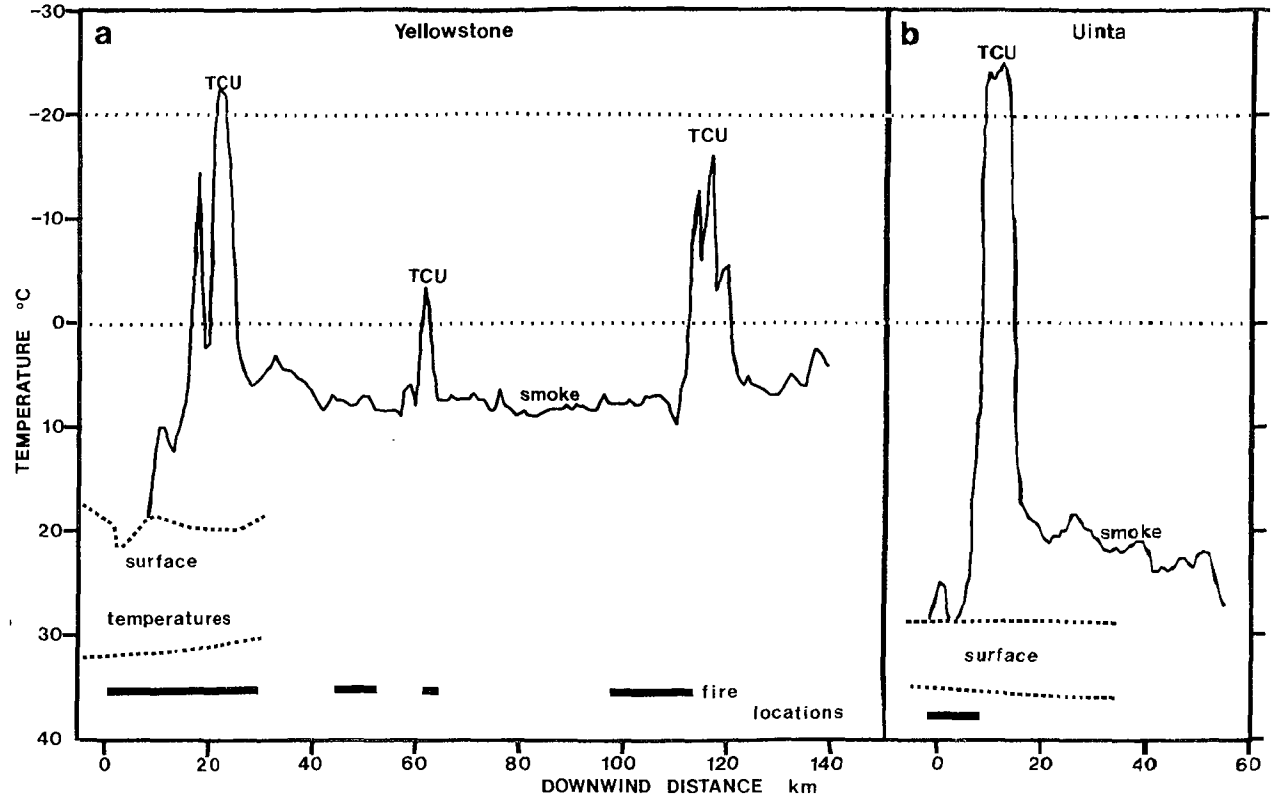


Figure 1. - Temperature profiles of the tops of clouds produced by (a) the Yellowstone fires and (b) the Uinta fire on 7 September 1988.

the coldest cloud temperatures were extracted. The larger supercooled cloud elements were 5 to 7 km long. Most of the smoke had tops at only about 7 °C for the Yellowstone fires and 21 °C for the Uinta fire, making such portions unsuitable for dry ice or AgI seeding technologies.

The ground release of AgI nuclei is perhaps the simplest strategy that can be carried out during an actual fire situation. The generators can be ignited upwind of a major fire whenever there is a possibility of the formation of supercooled fire-induced cumulus clouds. A more direct approach would be to use a high-performance aircraft to seed the developing turrets with dry ice as done in HIPLEX-1 (Smith et al., 1984). Not all large fires will produce clouds suitable for seeding, but the costs of seeding from either the ground or by aircraft are small compared to typical firefighting budgets. Minor fires are unlikely to produce fire-induced cumulus clouds that might become supercooled.

The rain from fire-induced clouds will be highly contaminated by the smoke. But those concerned with air pollution would most likely prefer to have rain wash the air rather than have the smoke travel across several states as it did from the 1988 Yellowstone fires. An ability to hinder the spread of large fires through cloud seeding could also be considered an air pollution reduction technique. The rain would reduce the smoke downwind by washing the air. The rain would reduce future smoke by hindering the future fire. Only in unusually calm air masses could the rain be expected to fall directly on the fire producing the fire-induced cumulus.

Rain from naturally occurring cumulus clouds might be initiated through cloud seeding to fall on the fire itself on some occasions. Several fires in northwestern Montana (not illustrated) had supercooled clouds near or over them on the afternoon of 7 September 1988.

This paper presents only a "snapshot" of fires during one afternoon. There were numerous other fires in the field of view of the satellite which produced only smoke and no fire-induced cumulus clouds. A study should be conducted to determine how frequently there were opportunities for seeding fire-induced clouds during the 1988 and perhaps earlier fire seasons. If the frequency was sufficient to justify it, exploratory seeding of convective clouds over fires should be carried out with

state-of-the-art instrumentation systems used to physically evaluate the results in the manner of HIPLEX-1 (Cooper and Lawson, 1984). The potential benefit-cost ratio is too high to continue to ignore cloud seeding as one of the tools that might be used to fight range and forest fires.

REFERENCES

Cooper, W.A., and R.P. Lawson, 1984. Physical interpretation of results from the HIPLEX-1 experiment. J. Climate Appl. Meteor., 23, 523-540.

Harpster, J.D., and W.J. Douglas, 1971. Weather modification - a fire control tool. J. Weather Mod., 3, 244-249.

Holroyd, Edmond W., III, Arlin B. Super, and Bernard A. Silverman, 1978. The practicability of dry ice for on-top seeding of convective clouds. J. Appl. Meteor., 17, 49-63.

Isaac, G.A., R.S. Schemenauer, J.W. Strapp, and C.L. Crozier, 1980. Weather modification experiments for forest fire control - 1978 field program results. Internal Rep., APRB 109 P 33, Atmospheric Environment Service, Downsview, Ontario, 345 pp.

Smith, Paul L., A.S. Dennis, B.A. Silverman, A.B. Super, E.W. Holroyd III, W.A. Cooper, P.W. Mielke, Jr., K.J. Berry, H.D. Orville, and J.R. Miller, Jr., 1984. HIPLEX-1: Experimental Design and Response Variables. J. Climate Appl. Meteor., 23, 497-512.

# THE NUMERICAL MODELING OF ICE-PHASE CLOUD SEEDING EFFECTS IN A WARM-BASE CLOUD: PRELIMINARY RESULTS

H. D. Orville, F. J. Kopp, R. D. Farley, and R. B. Hoffman
Institute of Atmospheric Sciences
South Dakota School of Mines and Technology
501 E. St. Joseph Street
Rapid City, South Dakota 57701-3995

Abstract. A numerical simulation of a warm-base cloud in the southeastern United States has resulted in a vigorous cloud development, much in agreement with observations by radar and aircraft on that day (20 July 1986). The case has been rerun with all of the ice processes turned off and vigorous growth still occurs. The natural ice processes enhance the cloud cell development and produce about 12% more precipitation. Simulated cloud seeding of the natural cloud case [testing both silver iodide (AgI) and solid carbon dioxide ($CO_2$)] produces about 5% less precipitation from this large convective cloud. The same sounding is used but with decreased vapor flux, to produce a smaller warm-base cloud. Simulated cloud seeding of that cloud results in 12% increases in precipitation, illustrating that the dynamics of the cloud are important for determining the seeding results.

## 1. INTRODUCTION

The use of cloud models to predict and to help understand the effects of cloud seeding has been practiced for many years now, starting with one-dimensional, steady-state cloud models in the early 60's (Simpson and Wiggert, 1969) to the two-dimensional (2D), time-dependent cloud models in more recent times (Hsie et al., 1980; Kopp et al., 1983; Orville et al., 1984; Farley, 1987; Kopp, 1988). The version of the IAS model used in the Hsie et al. paper referenced above did not include the simulation of a snow mixing ratio field, as described in Lin et al. (1983). The preliminary work reported here uses the updated version of the 2D cloud model applied to a warm-base cloud (+18°C) simulated and observed during the Cooperative Huntsville Meteorological Experiment (COHMEX) conducted in Huntsville, Alabama, USA, during the summer of 1986.

## 2. CLOUD AND MODELING SITUATION

The subject cloud formed about 1400 local time on 20 July 1986. Clouds had formed 30 to 45 min earlier and had grown to between 6 km (MSL) and 8 km producing coalescence rain in the process (Tuttle et al., 1988). At about 1400 a more vigorous growth occurred leading to a cloud topping out at about 14 km and producing copious amounts of rain and small, pea-sized hail. This precipitation led to a strong microburst.

This cloud was well-observed by multiparameter Doppler radars and simulated by the IAS 2D cloud model on the morning before the storm occurred (Tuttle et al., 1988). We have rerun this sounding two years later and on a different computer system and still obtain a realistic simulation of clouds on that day (but not exactly like the original run). We use this later sounding to produce two cloud cases -- one large and one moderate size cloud -- to study the effects of ice on the cloud growth and the effects of ice-phase cloud seeding on precipitation from warm-base clouds. Eventually we hope to run enough cases of both cold- and warm-base clouds to update our earlier cloud seeding study (Hsie et al., 1980).

## 3. CLOUD MODEL DESCRIPTION

The cloud model used in this study is two-dimensional, time-dependent (Orville and Kopp, 1977; Lin et al., 1983) with bulk water microphysics and 200 m grid intervals over a 20 km by 20 km domain. Cloud seeding simulations employ techniques described in Hsie et al. (1980), Kopp et al. (1983), and Orville et al. (1984). The model is anelastic and uses a vorticity (stream function) approach to obtain the velocity field. Chen and Orville (1980) provide additional information on the dynamic framework of the model.

The bulk water microphysical method is based on concepts suggested by Kessler (1969). Our model divides water and ice hydrometeors into five classes: cloud water, cloud ice, rain, snow and high density precipitating ice (graupel/hail). Rain, snow and graupel/hail, which are assumed to follow inverse exponential size distributions, possess appreciable terminal fall velocities. Cloud water and cloud ice have zero terminal velocities and thus travel with the air parcels. These five classes of hydrometeors interact with each other and water vapor through a variety of crude parameterizations of the physical processes of condensation/evaporation, collision/coalescence and collision/aggregation, accretion, freezing, melting and deposition/sublimation. The microphysical processes and parameterizations employed in the bulk water model are discussed in detail by Wisner et al. (1972), Orville and Kopp (1977), and Lin et al. (1983).

## 4. CLOUD MODEL RESULTS

### 4.1 N2 Case (Large Convective Storm)

#### 4.1.1 Unseeded run

The natural (unseeded) cloud develops much as was described in Tuttle et al. (1988). Early growth of the model clouds is slow and cloud tops cap out at 5 to 8 km. The 0°C level is at about 5 km so very little ice forms in these small clouds. Some small amounts of graupel/hail occur

because of the probabilistic freezing of raindrops (Bigg, 1953), formed earlier via coalescence. Cloud ice does not form until temperatures inside the model cloud drop below -20°C. Figure 1 shows the growth curves of various representative clouds appearing in the model domain. Early growth rates of cloud tops are 1 to 3.5 m $s^{-1}$ while the active main cloud top rises at nearly 7 m $s^{-1}$. Figure 2, left column, shows the general cloud outline and precipitation fields of the unseeded cloud run at various times throughout the cloud's life cycle. A series of cloud developments on the left side of the grid lead to the main cloud formation, evident at 129 min of simulated real time.

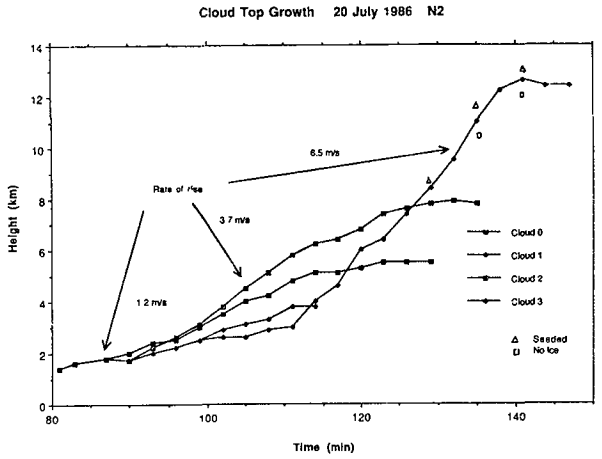


Fig. 1. Plots of various cloud top heights vs. time, which occur in the model results. The Δ and □ symbols give the cloud top height for the seeded and no-ice cases, respectively.

Coalescence growth begins in the model clouds when cloud water mixing ratios exceed 2 g $kg^{-1}$. This leads to efficient rain production with rain mixing ratios greater than 1 g $kg^{-1}$ initially showing up between 2 and 3 km height in the model.

As seen in Fig. 1, the primary cloud grows rapidly from 123 min to 140 min. The evolution of the cloud over much of this time period is also illustrated in Fig. 2. The ice processes become very active during this time and aid in the production of rain through melting processes. The rain production terms shown in Fig. 3 indicate melting of graupel increasing in magnitude to values greater than 100 kT $km^{-1}$ after 140 min.

Unfortunately for the cloud seeding efforts (as decribed below) the coalescence formation of rain dominates precipitation production in this large cloud situation, as seen in Fig. 3 in the rain accretion term (ACCR) and the autoconversion term (AUTO). As early as 110 min the ACCR term is larger than 10 kT $km^{-1}$ increasing to greater than 100 kT $km^{-1}$ at 125 min. The AUTO term represents rain initiation via coalescence and is in the range of 1 kT $km^{-1}$, by 110 min indicating an efficient rain formation process. The subsequent rain production is primarily through the accretion of cloud water by the rain.

4.1.2 No-Ice Run

As is evident in Fig. 2 the no-ice run appears to produce clouds similar in shape to the natural cloud but less dynamic. The main cloud is not quite so vigorous and does not grow as high in the atmosphere as its counterpart in either the unseeded or seeded runs. This cloud situation produces about 10% less precipitation than the natural cloud run (see Table 1).

Table 1. Precipitation production from the 20 July 1986 cloud simulations. Units are kT $km^{-1}$, numbers in parenthesis are percentage change from the unseeded case.

| Case | Rain | Hail | Total |
|---|---|---|---|
| N1 (smaller cloud) | | | |
| Unseeded | 26.7 | -- | 26.7 |
| AgI, cloud base | 30.0 (+12.4) | -- | 30.0 (+12.4) |
| $CO_2$, cloud top | 29.7 (+11.6) | -- | 29.7 (+11.6) |
| AgI, cloud top | 29.9 (+12.2) | -- | 29.9 (+12.2) |
| N2 (large cloud) | | | |
| Unseeded | 301.5 | 3.70 | 305.2 |
| No-Ice | 272.3 (-9.7) | -- | 272.3 (-10.8) |
| AgI, cloud base | 287.8 (-4.5) | 3.36 (-9.2) | 291.2 (-4.6) |
| $CO_2$, cloud top | 286.6 (-4.9) | 2.86 (-22.7) | 289.5 (-5.2) |
| AgI, cloud top | 285.3 (-5.4) | 2.92 (-21.1) | 288.2 (-5.6) |

4.1.3 Seeded Runs

Cloud-base seeding with silver iodide (AgI) and cloud-top seeding (at about -10°C) with both dry ice ($CO_2$) and AgI have been simulated, as in Orville et al. (1984) and Kopp (1988). Seeding amounts of about 200 g $km^{-1}$ were simulated at 117 min (cloud base) and 120 min (cloud top) of simulated real time. Figure 2 shows the effects of seeding in a run with AgI seeding at cloud top. More snow and graupel/hail is evident at 129 min in the seeded cloud.

For this large cloud, the icing effects were clear; production terms of rain via ice processes began earlier and radar reflectivity patterns were changed (maximum values higher in the cloud) as well as the reflectivity values increased. Also the seeded cloud grew faster than the unseeded cloud (Fig. 1). However, these changes did not result in greater precipitation fallout, in fact, less. Table 1 shows the precipitation production in the various cases.

One of the effects of cloud seeding is shown in Fig. 3. The dashed curves represent the seeded case. Note that almost immediately after seeding the GMLT (graupel melting) term deviates from the unseeded run GMLT curve. This is caused by the nearly instantaneous transformation of rain to graupel caused by the cloud ice produced by seeding, and the collection of this cloud ice by the rain (Koenig, 1966; Cotton, 1972). The graupel then falls to warmer regions of the cloud and melts to form rain.

Our preliminary analysis of these results indicate that the earlier formation of snow and graupel did not help the precipitation production in this large, vigorous cloud (vertical velocity maxima greater than 25 m $s^{-1}$). In the seeded runs too much of the snow was transported to the anvil region and never reached the ground.

4.2 Further Tests (N1 Case - Moderate Size Convective Cloud)

One further series of tests has been run at the time of this writing. A smaller, weaker cloud development was produced using this atmospheric sounding by decreasing the water vapor flux at the earth's surface. The main cloud development topped out at about 8 km (-20°C), and produced about an order of magnitude less precipitation than the previous case. The seeded runs produced about 12%

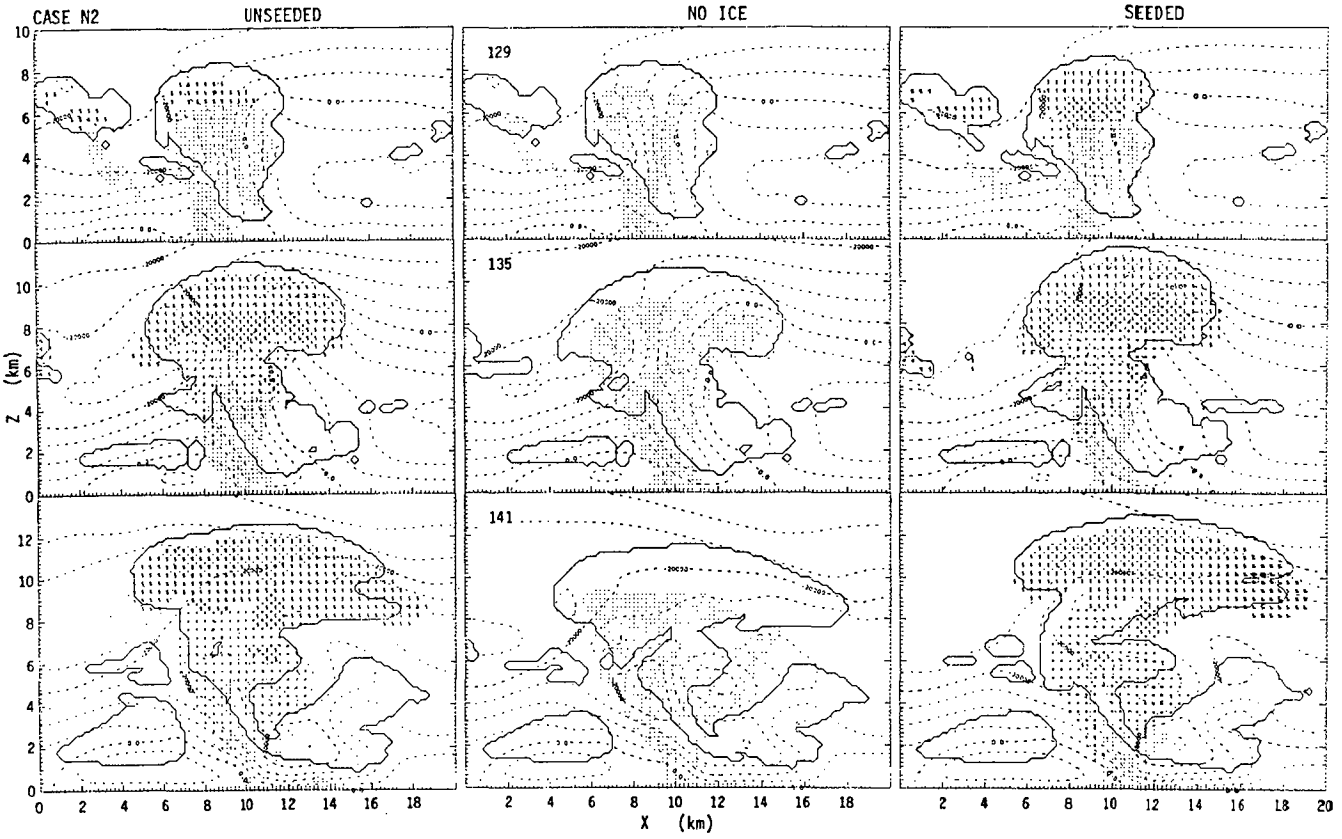


**Fig. 2.** The general cloud outline and precipitation fields for the unseeded run (left column), no-ice run (central column), and AgI cloud top (-10°C) seeded run (right column) for the large cloud case, N2. The symbols * and • represent graupel/hail and rain mixing ratios greater than 1 g kg$^{-1}$; the S represents snow mixing ratios greater than 0.5 g kg$^{-1}$. Time in simulated real time (minutes) is denoted in the upper left corner of the center panels.

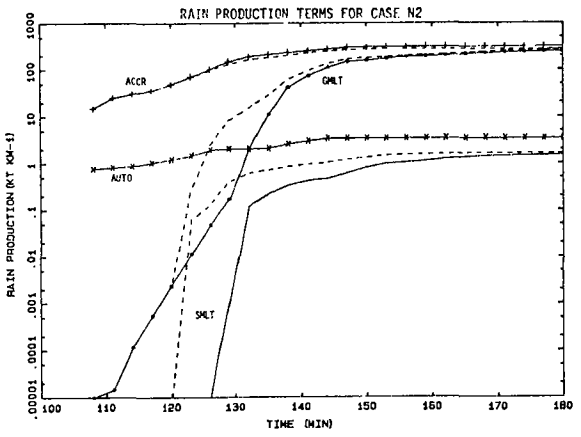


**Fig. 3.** The rain production terms in the N2 case, unseeded run. ACCR denotes accretion of cloud water by rain, AUTO is the coalescence of cloud water to form rain, GMLT is graupel melt and SMLT is snow melt to form rain. The dashed curves represent the seeded case results.

more precipitation than the unseeded run (Table 1). In this case the earlier formation of snow and graupel helped to process the cloud liquid and cloud ice into precipitation and the weaker dynamics of the cloud allowed more precipitation fallout.

Figure 4 shows the general outline of the unseeded and seeded clouds. The formation of snow and graupel/hail is evident at 186 min in the seeded case, but not until 204 min and at high altitudes in the unseeded case. Actually some graupel/hail formed via the rain freezing process, but remained much less than in the seeded case.

## 5. DISCUSSION

These modeling tests of the seeding of a large and a moderate size warm-base cloud have produced different effects on precipitation. The modeled clouds have been very efficient producers of warm rain; the ice phase seeding has decreased slightly the total precipitation in the large cloud and increased it moderately in the smaller cloud. However, note that the small percentage change in the large model cloud results in a greater absolute change in precipitation than the moderate percentage change in the smaller model cloud.

These changes due to ice-phase seeding are less dramatic than the changes we have seen in simulations of cold-base convective clouds (Kopp et al., 1983; Kopp, 1988; Orville and Kopp, 1986), where coalescence is not active. In those cases

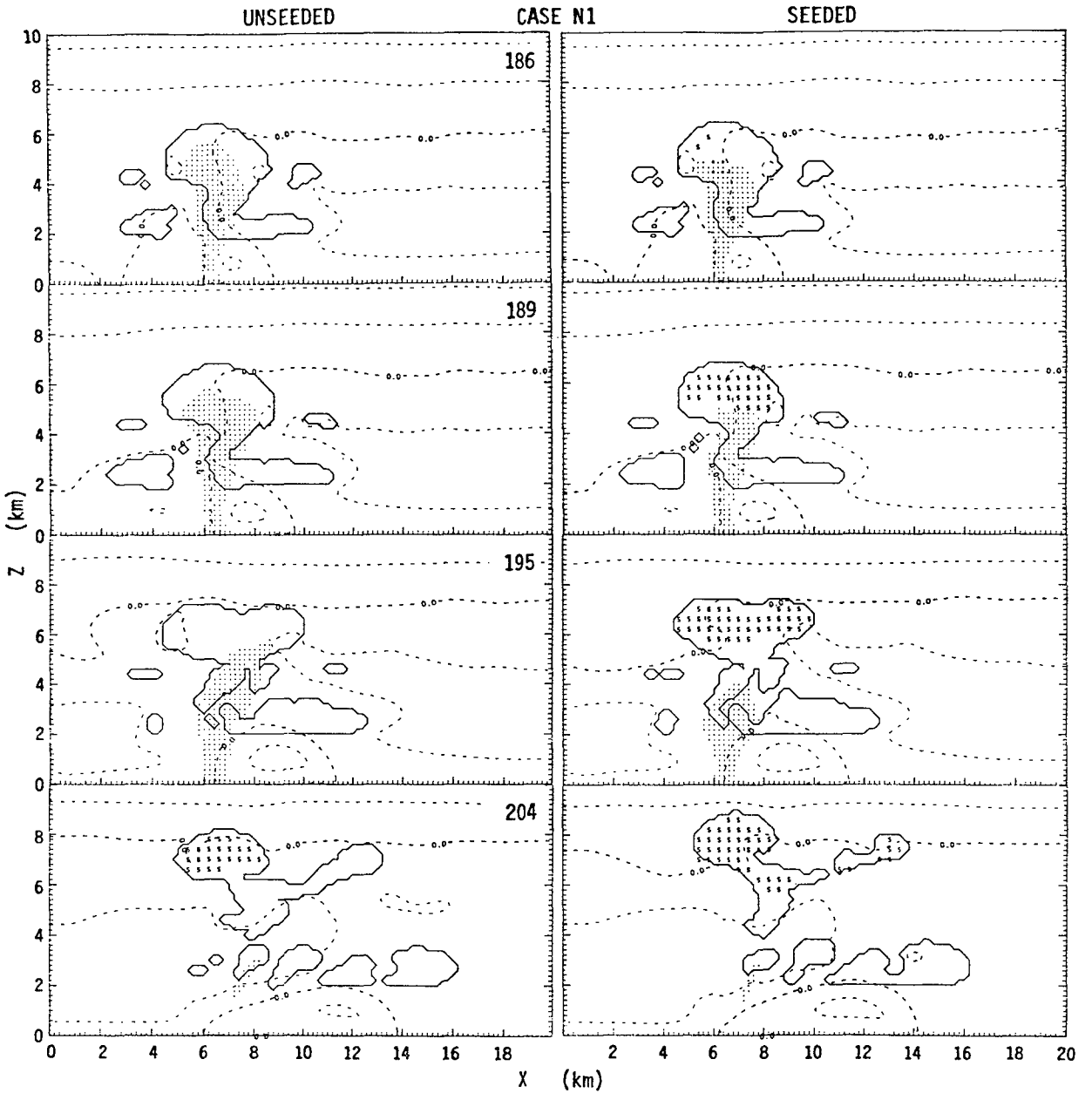


**Fig. 4.** Similar to Fig. 2, but for the smaller cloud case, N1. The unseeded run is on the left, seeded on the right.

increases ranging from 20 to 100% or more resulted, primarily by the process of creating precipitation via the cloud seeding at an early stage of the cloud's limited life history.

The results shown here regarding a large warm-base cloud do not appear consistent with the results of Hsie et al. (1980) concerning the warm-base cloud produced in the model using an atmospheric sounding from St. Louis. In that case a healthy increase in precipitation was noted.

We ascribe the differences to changes in ice microphysical simulations since that 1980 study. The inclusion of a snow mixing ratio field in the model has made the precipitation simulations more realistic. The ice-phase seeding simulations now form snow initially (via cloud ice) instead of graupel/hail immediately as in the Hsie et al. study. If the storm dynamics are great enough, the snow is carried aloft and may not result in precipitation on the ground.

The vigor of the large cloud is increased by the ice-phase seeding, but an inhibiting inversion is not present. That type of inversion situation has been hypothesized in the past to be favorable for positive cloud seeding effects, but we have not simulated such a case yet. Also, the ice-phase cloud seeding would be expected to be more effective in warm-base clouds that have a less efficient warm-rain process than that which was modeled. So far only a relatively few cases have been run. These results appear to be con-

sistent with the discussion of the seeding of isolated convective clouds presented in Dennis (1980), in which he suggests that moderate size convective clouds are the prime targets for rain enhancement via ice-phase cloud seeding.

**ACKNOWLEDGMENTS**

This research was sponsored by the National Science Foundation, Division of Atmospheric Sciences, under Grant No. ATM-8516940. The study of the unseeded cloud microphysical processes has been done partially under support from the National Aeronautics and Space Administration under NASA Grant No. NAG 8-632, which was a key supporter of the COHMEX. The calculations were performed using the facilities of the Scientific Computing Division of the National Center for Atmospheric Research, which is sponsored by the National Science Foundation.

We thank Carol Vande Bossche for typing and arranging the manuscript.

**REFERENCES**

Bigg, 1953: The supercooling of water. Proc. Phys. Soc. London, B66, 688-694.

Chen, C-H. and H. D. Orville, 1980: Effects of mesoscale convergence on cloud convection. J. Appl. Meteor., 19, 256-274.

Cotton, W. R., 1972: Numerical simulation of precipitation development in a supercooled cumuli - Part II. Mon. Wea. Rev., 100, 764-784.

Dennis, A. S., 1980: Weather Modification by Cloud Seeding. Academic Press, Inc., New York. 267 pp.

Farley, R. D., 1987: Numerical modeling of hailstorms and hailstone growth: Part III. Simulation of an Alberta hailstorm -- natural and seeded cases. J. Climate Appl. Meteor., 26, 789-812.

Hsie, E-Y., R. D. Farley and H. D. Orville, 1980: Numerical simulation of ice-phase convective cloud seeding. J. Appl. Meteor., 18, 958-977.

Kessler, E., 1969: On the distribution and continuity of water substance in atmospheric circulations. Meteor. Monogr., 10, No. 32. 84 pp.

Koenig, L. R., 1966: Numerical test of the validity of the drop-freezing/splintering hypothesis of cloud glaciation. J. Atmos. Sci., 23, 726-740.

Kopp, F. J., 1988: A simulation of Alberta cumulus. J. Appl. Meteor., 27, 626-641.

_____, H. D. Orville, R. D. Farley and J. H. Hirsch, 1983: Numerical simulation of dry ice cloud seeding experiments. J. Climate Appl. Meteor., 22, 1542-1556.

Lin, Y-L., R. D. Farley and H. D. Orville, 1983: Bulk parameterization of the snow field in a cloud model. J. Climate Appl. Meter., 22, 1065-1092.

Orville, H. D. and F. J. Kopp, 1977: Numerical simulation of the life history of a hailstorm. J. Atmos. Sci., 34, 1569-1618.

_____, and _____, 1986: Simulation of the 22 July 1979 HIPLEX case. Proc. Intn'l Cloud Modeling Workshop/Conf., WMO/TD No. 139, 15-19 July 1985, Irsee, F.R.G., 207-216.

_____, R. D. Farley and J. H. Hirsch, 1984: Some surprising results from simulated seeding of stratiform-type clouds. J. Climate Appl. Meteor., 23, 1585-1600.

Simpson, J. and V. Wiggert, 1969: Models of precipitating cumulus towers. Mon. Wea. Rev., 97, 471-489.

Tuttle, J. D., V. N. Bringi, H. D. Orville, and F. J. Kopp, 1988: Multiparameter radar study of a microburst: comparison with model results. Accepted by J. Atmos. Sci., --.

Wisner, C. E., H. D. Orville and C. Myers, 1972: A numerical model of a hail-bearing cloud. J. Atmos. Sci., 29, 1160-1181.

# Preliminary Experimental Evaluation of Snomax™ Snow Inducer, *Pseudomonas syringae*, as an Artificial Ice Nucleus for Weather Modification

Patrick J. Ward
Bio-Products Division
Eastman Kodak Company
1700 Lexington Avenue
Rochester, NY 14652

and

Paul J. DeMott
Department of Atmospheric Science
Colorado State University
Fort Collins, CO 80523

Abstract: Snomax™ Snow Inducer, *Pseudomonas syringae*, has undergone preliminary laboratory and atmospheric studies in order to assess its usefulness as an artificial ice nucleus. Initial laboratory results show that Snomax is a very efficient condensation and freezing nucleus, exhibiting activities of $10^{12}$ to $10^{13}$ nuclei per gram at temperatures colder than -4°C and showing significant activity (approximately $10^{10}$ per gram) at temperatures as warm as -2.5°C. A preliminary aerial trial has demonstrated that Snomax powder can be easily dispersed to initiate nucleation in natural supercooled clouds.

## 1. INTRODUCTION

Very much has been learned in the past 15 years regarding the ability of certain strains of naturally occurring bacteria to efficiently nucleate the formation of ice at slight supercoolings. Ice nucleation active (INA) bacteria have been implicated in frost damage to plants (Lindow et al., 1978), their role as sources of atmospheric ice nuclei has been suggested (Vali et al., 1976; Maki et al., 1978), they are being utilized to improve the efficiency of snowmaking operations at ski areas, and their utility for controlled use in cloud seeding has been suggested and investigated (Maki and Willoughby, 1978; Levin et al., 1987). While the atmospheric implications of naturally occurring concentrations of INA bacteria has been judged to be minimal (Levin and Yankofsky, 1988), the basic understanding of the nucleation properties of these bacteria is not complete and is important, particularly for potential weather modification applications. One particularly efficient organism, *Pseudomonas syringae* (Snomax Snow Inducer) is now commercially available for snowmaking and is being evaluated for its nucleation modes, activity, and rates in conditions that simulate a natural cloud environment. We present the results of the preliminary investigation here.

## 2. SNOMAX AS AN ICE NUCLEATING AEROSOL

Snomax Snow Inducer is a natural source of ice-nucleating proteins that induces the formation of ice crystals. Water molecules apparently attach to the bacterial proteins in an arrangement that mimics the structure of an ice crystal, thereby decreasing the amount of supercooling that might normally be required during the nucleation process. The efficiency of Snomax in causing nucleation by the immersion-freezing of solutions at low levels of supercooling is well defined and is the foundation for its use in snowmaking operations.

Until recently, the ability of Snomax to cause nucleation in a supercooled cloud environment was unknown. Preliminary tests of Snomax in a supercooled cloud were performed at Atmospherics Incorporated (AI) in Fresno, California. Through the use of a small freezer chest, dry powdered Snomax aerosols were qualitatively tested for nucleation ability over the temperature range of 0 to-20°C. Snomax was found to be an effective ice nucleus in supercooled clouds at temperatures between 0°C and -5°C. Formvar coated microscope slides were used to encapsulate and replicate the artificially generated ice crystals. Photos 1A through 1D are increasing magnifications of a transmission electron micrograph of an ice crystal captured after Snomax aerosol introduction into a -20°C supercooled cloud. These photos clearly show a single *Pseudomonas syringae* bacterium in the center of the crystal. It is evident that the Snomax bacterial particle was indeed the nucleation site for the formation of this ice crystal.

## 3. SNOMAX ICE NUCLEATION STUDIES

Laboratory experiments were performed in the Colorado State University (CSU) isothermal and dynamic cloud chambers (see Garvey, 1975; DeMott et al., 1983; and DeMott, 1988 for chamber descriptions). The isothermal chamber was used to quantitatively survey the fractions of bacterial particles acting to form ice crystals when dispersed into a continuously replenished, water saturated cloud at temperatures from -4 to -12°C. Computations of ice crystals formed per gram of Snomax powder dispersed permitted a standard comparison to other artifical ice nucleating aerosols that have been tested in the same chamber. Procedures outlined by DeMott et al. (1983) were used to assess the basic nucleation mode based on the kinetics of ice crystal formation. The dynamic cloud chamber was used to test the cloud condensation nucleus (CCN) activity of the bacterium by simulating adiabatic expansion-cooling of an air parcel. Continued expansion-cooling of the cloud thus formed permitted the first simulation of the continuous condensation and

Figure 1a. (3,000X) ⊢——————⊣ 20 um

Figure 1b. (4,200X) ⊢——————⊣ 15 um

Figure 1c. (15,360X) ⊢——————⊣ 5 um

Figure 1d. (30,000X) ⊢——————⊣ 2 um

Figure 1a - 1d. Increasing magnifications of a transmission electron micrograph of an ice crystal captured after Snomax aerosol introduction into a -20°C supercooled cloud.

freezing activity of a known INA bacterium. The influences of the presence of other CCN particles and of warm versus supercooled cloud base temperature on these basic nucleation processes were also examined. These studies add to the understanding of nucleation by INA bacteria and are relevant to the potential use of such materials for weather modification. Brief summaries of the isothermal and dynamic chamber results are given in this paper. A complete treatise of the laboratory experimental procedures and results is being written for future publication. We also present the results of preliminary seeding tests with Snomax in real clouds in this section.

### 3.1 Isothermal Chamber Results

Snomax aerosols were found to be highly efficient and fast-functioning ice nucleating aerosols, apparently nucleating ice by a condensation-freezing mechanism and at rates comparable to those of dry ice under similar conditions ( 90% of ice crystals formed in 3 to 5 minutes). Rates of ice crystal formation showed no significant dependence on liquid water content between 0.5 and 1.5 g/m$^3$. Figure 2 shows the average (6 tests at each temperature) active number of Snomax particles per gram dispersed as compared to dry ice and two highly efficient AgI-type ice nucleating aerosols produced by solution combustion and a pyrotechnic formulation, respectively. The Snomax aerosols were assessed under similar environmental conditions and in the same chamber as the dry ice and AgI aerosols. Snomax yield in the isothermal cloud chamber was found to decrease by less than one order of magnitude between -12°C ($5.5 \times 10^{12}$ g$^{-1}$) and -4°C ($1.3 \times 10^{12}$ g$^{-1}$). This contrasts with three to five orders of magnitude losses of effectivity for AgI-type aerosols over the same temperature range. The potential advantages of Snomax versus AgI aerosols are evident at temperatures warmer than about -5 to -7°C where AgI aerosols are very inefficient. Rapid nucleation rates compared to most AgI-type aerosols may also be advantageous. Snomax yields are within a factor of 2 of yields from dry ice seeding over the temperature range tested.

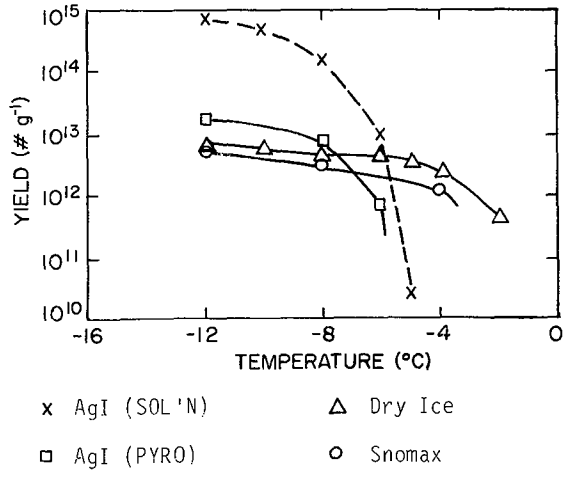


Figure 2. Comparison of the ice crystal yield versus temperature for Snomax, dry ice, and two of the more efficient AgI-type ice nucleating aerosols from solution combustion and pyrotechnic formulation.

### 3.2 Dynamic Chamber Results

Snomax yields as a function of temperature during continuous expansion cooling of clouds in the dynamic chamber were in close agreement with results from the static isothermal cloud chamber. These unique experiments also demonstrated the particularly narrow temperature ranges for the activation of large fractions of the bacteria. Initial ice formation started at temperatures as warm as -2.5°C. Figures 3a, 3b, and 3c are examples from one experiment that show the ice crystal flux (aerosol fraction nucleated s$^{-1}$), cumulative yield, and cloud droplet concentration respectively, as a function of temperature during expansion cooling. Snomax aerosols were used as CCN for cloud formation in this example. The cooling rate was approximately 1°C min$^{-1}$ after cloud formation. The observed tendency for nucleation activity to be centered in specific temperature ranges was a consistent feature in these experiments. This has been noted for other bacterial nuclei in the past (Levin and Yankofsky, 1988), but never verified for freely suspended bacterial aerosols acting first as condensation and then as freezing nuclei.

Direct injection of Snomax aerosols into cooling cloud parcels in the dynamic cloud chamber has lead to apparent enhancements of ice crystals formed compared to particles injected. This phenomenon is under investigation.

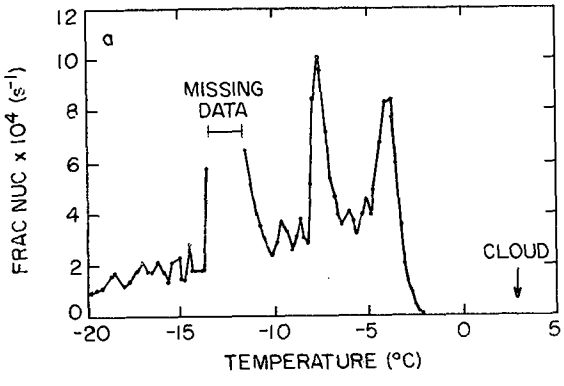


Figure 3a.

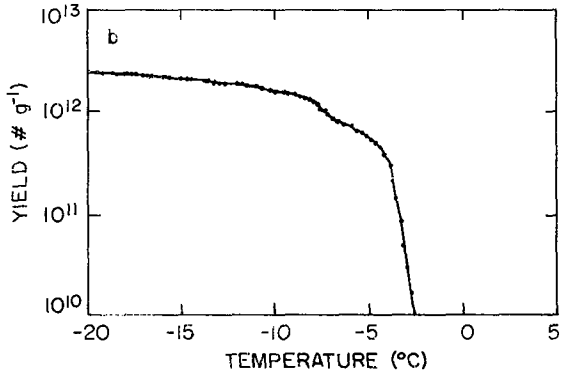


Figure 3b.

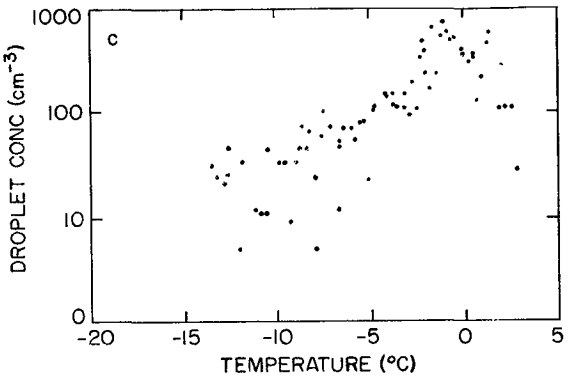


Figure 3c.

Figure 3. a) Ice crystal flux (aerosol fraction nucleated $s^{-1}$), b) cumulative yield, and c) cloud droplet concentration plotted as a function of temperature during expansion cooling. Snomax aerosols used as CCN for cloud formation in this example.

### 3.3 Preliminary Field Test Results

The results of the laboratory chamber tests were encouraging enough to warrant a preliminary aerial test. The test site chosen was in western Nevada, where occasional individual cumulus develop. The objectives of the test were to apply specific amounts of non-viable Snomax to a few small cumulus congestus and make some general observations and measurements of the subsequent cloud behavior as well as gain some experience in aerial dispersal of the product. The aerial tests were organized and directed by Atmospherics Incorporated (Fresno, CA). During a two day investigation (September 8th and 9th, 1988), it was demonstrated that Snomax dry powder can be dispersed from aircraft into the updraft region below cloud or injected directly into supercooled cloud at rates that are comparable with conventional silver iodide seeding applications. The method of generation produced a highly dispersed aerosol (the degree of dispersal is currently being quantified). In one case, visible glaciation effects were apparent as warm as the -5°C level. Liquid water data has not yet been analyzed. No ice crystal concentration data were collected. Future seeding tests will include detailed microphysical data.

## 4. POTENTIAL ADVANTAGES OF SNOMAX NUCLEI

Snomax Snow Inducer possesses some unique characteristics that may be advantageous to the weather modification community. First, Snomax is prepared in a powdered form that exhibits $10^{12}$ to $10^{13}$ ice nuclei per gram at temperatures less than -4°C and shows significant activity at temperatures as warm as -2.5°C. The activity of Snomax per gram at small supercooling is greater than that of silver iodide aerosols, which do not have a measurable response until about -5°C to -7°C. Secondly, Snomax, being a stable, aerosolizable powder can be used for seeding at cloud base at temperatures greater than 0°C. Dry ice cannot be used under these circumstances. Snomax may offer better dispersion characteristics than dry ice and should offer increased ease of material handling.

## 5. CONCLUSIONS

This preliminary investigation of the use of Snomax Snow Inducer as an artificial ice nucleus demonstrates its utility for cloud seeding. However, more seeding experiments need to be conducted in real clouds. There are several planned seeding targets: supercooled fog, wave clouds, stratus, and cumulus. Experimental procedures will be designed to investigate the advantages that Snomax should have over other seeding technologies based on the preliminary studies presented.

## 6. ACKNOWLEDGMENTS

We thank Mr. Thomas J. Henderson, President, Atmospherics Incorporated for his direction of initial cold box nucleation tests and for aircraft, personnel and technical assistance in support of the field tests. We also want to acknowledge Dr. David C. Rogers, Colorado State University, for his participation in the field tests and many helpful comments, and Mr. Edward R. Robinson, President and General Manager, Snomax Technologies, for funding support, supervision and comments. Regulatory approval for cloud seeding tests was granted by EPA, USDA, and local Nevada agencies.

## 7. REFERENCES

Demott, P.J., W.G. Finnegan and L.O. Grant, 1983: An Application of Chemical Kinetic Theory and Methodology to Characterize the Ice Nucleating Properties of Aerosols Used in Weather Modification. J. Clim. Appl. Meteor. 22, 1190-1203.

DeMott, P.J., 1988: Comparisons of the Behavior of AgI-Type Ice Nucleating Aerosols in Laboratory Simulated Clouds. J. Weather Mod., 20, 44-50.

Garvey, D.M., 1975: Testing of Cloud Seeding Materials at the Cloud Simulation and Aerosol Laboratory, 1971-1973. J. Appl. Meteor., 14, 883-890.

Levin, A. and S.A. Yankofsky, D. Pardes and N. Magal, 1987: Possible Application of Bacterial Condensation Freezing to Artificial Rainfall Enhancement. J. Clim. Appl. Meteor., 26, 1188-1197.

Levin, A. and S.A. Yankofsky, 1988: Ice Nuclei of Biological Origin. In Lecture notes in Physics: Atmospheric Aerosols and Nucleation, P. Wagner and Vali (eds.), Proc. of 12th International Conf. on Atmos. Aerosols and Nucleation, 645-647.

Lindow, S.E., D.C. Arny and C.D. Upper, 1978: Erwinia herbicola: A Bacterial Ice Nucleus Active in Increasing Frost Injury to Corn. Phytopathology, 68, 523-527.

Maki, L.R. and K.J. Willoughby, 1978: Bacteria as Biogenic Sources of Freezing Nuclei. J. Appl. Meteor., 17, 1049-1053.

Morrison, B.M., 1989: A Characterization of Dry Ice as a Glaciogenic Seeding Agent. M.S. Thesis, Dept. of Atmos. Sci., Colorado State Univ., Ft. Collins, Co. 109 pp.

Vali, G., M. Christensen, R.W. Fresh, E.L. Galyan, L.R. Maki and R.C. Schnell, 1976: Biogenic Ice Nuclei. Part II: Bacterial Sources. J. Atmos. Sci., 33, 1565-1570.

# EVALUATION OF A 2-MONTH COOPERATIVE GROUND-BASED SILVER IODIDE SEEDING PROGRAM

David W. Reynolds
Bureau of Reclamation
Sacramento CA 94236

James H. Humphries
Air Pollution Control District
San Luis Obispo CA 93401

Richard H. Stone
Desert Research Institute
Reno NV 89506

Abstract. Field investigations to determine the effectiveness of ground-based AgI seeding generators to treat Sierra Nevada winter cloud systems were conducted by the Sierra Cooperative Pilot Project (SCPP) from November 3, 1986, to January 9, 1987. Of 18 randomized events, 12 were seeded and 6 were left unseeded. A postanalysis using the data collected by a variety of in situ devices and the results of a numerical targeting model identified periods which appeared to contain the best seeding potential and estimated the effectiveness of placing the effects within the desired target area.

Criteria used in real time for declaring an experiment may have been too lenient. Nearly one-third of the seeding cases were conducted when the -5 °C level was at an elevation that would not be expected to be reached by the ground-released nucleants.

A numerical targeting model, GUIDE (Rauber et al, 1988), adapted for ground release of seeding material, computed nucleation and fallout locations from each generator on a given day. Results indicated fallout downwind of the target, primarily due to a high -5 °C level and a strong southerly wind component. During southerly winds, nucleants released from low elevation sites were often predicted to travel parallel to the barrier, displacing fallout north of the target. Meteorological conditions with low freezing levels and light westerly winds were predicted to produce the most effective targeting allowing fallout a short distance downwind of the generator, especially for those above 2000 m.

Aircraft plume tracing studies, using airborne ice nucleus counters under both visual flight rules (VFR) and instrument flight rules (IFR) conditions, detected the plumes downwind of the release sites. The observations indicated a 10- to 15-degree angle of spread and an approximate 0.3 m $s^{-1}$ rise rate for plumes over mountainous terrain. Although it was difficult to map the horizontal and vertical extent of the plumes, the GUIDE model appeared to provide reasonable estimates of plume transport and diffusion.

In addition to the above studies, a chemistry analysis of snowpack samples showed very limited silver dispersion, with less than 15 percent of the samples indicating any silver above background. This rather poor result may indicate inadequate generator coverage and/or poor generator performance.

## 1.0 INTRODUCTION

Operational cloud seeding programs have been conducted in California since the early 1950's in attempts to increase water supplies and hydroelectric power generation. Although the effectiveness of large scale cloud seeding operations still has not been firmly established, public and private programs continue their attempts to modify cloud systems for the purpose of increasing precipitation and runoff. Such expenditures are considered minimal when compared to the potential benefits that could assist in meeting the growing needs for water in California.

In 1976, the Bureau of Reclamation established the SCPP as a research-orientated weather modification program in the American River Basin (ARB) of California. Reynolds and Dennis (1986) reviewed the goals of SCPP and the seeding experiments conducted. These experiments demonstrated that aerial seeding produces identifiable "signatures" in both individual convective and widespread stratiform

clouds (Marwitz and Stewart, 1981; Stewart and Marwitz, 1982; Huggins and Rodi, 1985; and Deshler et al., 1989).

Aerial treatment procedures have been used by SCPP researchers to ensure that favored cloud regions were directly seeded at temperatures where nucleation and ice crystal growth would be rapid. However, most large scale operational cloud seeding programs have depended on ground-based AgI generators to deliver seeding material to candidate clouds. Ground-based generators cost less to operate and provide a continuous supply of nucleants during storm periods. During the final year of SCPP, ground-based AgI generators were incorporated into the seeding program to study the effectiveness of ground delivery in conjunction with other research objectives. This paper reports on the results of these studies.

## 2.0 DESIGN

The SCPP ground-based seeding experiment was built around ongoing operational programs and took priority over the concurrent SCPP aerial treatment experiment. Ground seeding operations were not combined with aircraft seeding so that each delivery method could be evaluated separately. This allowed sophisticated equipment and techniques normally utilized for aerial treatment procedures to be used for physical evaluations of the effectiveness of ground releases.

Although shallow orographic clouds may comprise the most seedable conditions (Reynolds and Kuchiauskas, 1988), the seeding criteria used permitted a variety of cloud types to be treated. It has generally been accepted that AgI will not become effective until it reaches cloud regions where the temperature is colder than -5 °C and the cloud is at or above ice saturation. Since these conditions are difficult to forecast in advance, SCPP ground seeding operations were conducted whenever cloud and wind conditions would allow the ground-released AgI to reach cloud and directionally target the study area. This required only that the wind direction below 700 mb be between 170 and 360 degrees and cloud base be less than 1 km above ground as determined from a sounding near the crest of the Sierra Nevada.

The seeding criteria were kept simple so that more days would be likely to qualify for experimentation. However, seeding activities would be suspended if treatment might aggravate threatening weather situations, such as:

- Excess snowpack accumulations
- Rain induced winter flooding
- Severe weather
- Other special circumstances

No suspension criteria were met during the 1986-87 season. Treatment was made by 6-hour time blocks, long enough so that the accumulated seeding effects might be measurable in the precipitation gauges but short enough to obtain more units in a single season. A 2:1 randomization scheme ensured objectivity and provided some nontreated periods for comparison. However, one season was not expected to yield any meaningful results in terms of precipitation increases.

Special flight procedures were designed for two SCPP research aircraft to monitor the horizontal and vertical spread of the ground-released nucleants. In addition, snow samples were collected over a large part of the target to determine if trace quantities of silver accumulated in the snowpack could be detected. These studies were all in an attempt to verify the transport, nucleation, and fallout predictions generated by the SCPP GUIDE model.

## 3.0 OBSERVATIONS AND METHODS FOR SEEDING DECISIONS

For cloud seeding to be effective in producing additional measurable precipitation, the clouds must contain supercooled liquid water (SLW). In addition, the complicated air motions over the mountainous terrain must be understood to develop an effective and reliable seeding strategy that will assure the additional precipitation falls in the desired target area.

A variety of equipment was used to determine the suitability of treating portions of winter storms. The SCPP target area and instrument locations are shown in Figure 1. A weather forecast office in Auburn, California, had the following resources available for the ground seeding experiment:

- Weather maps and prognostic charts from the National Weather Service.
- A minicomputer capable of running the numerical targeting model.
- Animated and hard-copy satellite imagery.
- Hourly weather reports and observations.
- A variety of in situ observations, which were telemetered to the forecast office for near real time display. These included mountaintop meteorological stations that reported temperature, wind conditions, humidity, and icing rate information, and a radiometer located at Kingvale (KGV).
- Precipitation gauge accumulations from the SCPP network.
- Upper air information obtained from serial balloon soundings launched within the project area.

The mountaintop meteorological reporting stations were located throughout the target area as shown in Figure 1. Deiceable anemometers and directional vanes operated in conjunction with temperature and humidity sensors at each site. Rosemount icing rate meters provided direct measurements of SLW passing each site (Henderson and Solak, 1983). SLW content can be computed from the windspeed and the number of deicing "trip" cycles recorded by this device. These measurements proved to be very useful in nowcasting the occurrence of SLW, as well as for postseason stratification of the experiments.

High-resolution precipitation data collected by a network of 16 digital recording precipitation gauges reported to the forecast office each hour the precipitation accumulated within 5-minute increments (Price and Rilling, 1987).

Precipitation data were also collected by gauge networks operated by the Desert Research Institute (DRI), Sacramento Municipal Utility District (SMUD), Pacific Gas and Electric Company (PG&E), and Sacramento County (SC), but were not available in real time. Figure 2 shows the locations of all gauges.

Vertical profiles of wind, temperature, and moisture were derived from two rawinsonde launch sites within the study area (Fig. 1). A new cross-chain Loran atmospheric sounding system (CLASS) rawinsonde system (Lauritsen et al., 1987) was used by SCPP to provide higher resolution in the vertical. This system is not a radiotheodolite but uses Loran (long-range navigation) for positioning information and transmits radio signals back to the launch site. Incoming data are recorded and processed onsite by a minicomputer and can be displayed in real time. Some tracking problems at low elevations were due to weak Loran reception in the mountainous terrain. Balloon flights were made at 3-hour intervals during storms from an upwind location at Lincoln and from KGV (Fig. 1). The latest data served as input to the numerical GUIDE model to determine if the target area might be affected by the ground release of AgI.

The SCPP GUIDE model (Rauber et al, 1988) is a two-dimensional steady-state flow model that incorporates microphysical particle growth and fallout routines. The model was originally developed for aircraft delivery but was recently adapted to estimate the horizontal and vertical dispersion of aerosol plumes (using a Pasquill-Gifford neutral stability dispersion rate) released from the ground. Paired upwind-downwind soundings were used to produce constant mass flow channels over the barrier. Wind components parallel and perpendicular to the barrier are derived from this technique. Vertical motion is computed from the perpendicular wind component and the slope of the mass flow channels. The location in cloud where a sufficient number of nuclei are likely to be effective (-6 °C) is predicted along with the fallout point of a crystal initiated at this location.

Presently, it is difficult to model accurately any events that may occur east of the Sierras because input data is based solely upon soundings upwind of the barrier. Therefore, caution is advised when evaluating plume trajectories downwind of the crest shown in this paper. Comparisons between predicted and observed winds upwind of the barrier have been described by Rauber et al. (1988), but this model has not yet been evaluated and verified for ground seeding; and thus the accuracy of its predictions is unknown. Results of this years operations may help evaluate the ground seeding parameterizations incorporated into the model.

## 4.0 GROUND-BASED SEEDING GENERATORS

A network of 24 ground-based cloud nuclei generators were operated in a coordinated fashion during the SCPP field phase--November 3, 1986, to January 9, 1987. The total network was comprised of four smaller networks belonging to PG&E, SMUD, DRI, and SCPP. These generators had been used in past operational programs except for the SCPP network, which was installed especially for this study. All generators, except PG&E's, burned a 3-percent by weight $AgI-NH_4I-NH_4ClO_4$ in acetone solution ignited by a propane flame. The PG&E generators did not use the $NH_4ClO_4$ additive. Burning this solution released approximately 30 g of AgI per hour from each generator while consuming about a gallon of propane per hour at each site. The SCPP generators were operated manually by local residents while the remaining generators were operated remotely.

Figure 3 shows the location of the generator sites in relation to the SCPP target area, which encompasses the American, Tahoe-Truckee, and Upper Mokelumne River basins. The PG&E, SMUD, and DRI networks had been installed in past years so as to be generally upwind of their respective target areas. The SCPP generators were strategically placed to affect clouds that would eventually pass the KGV area on Interstate Highway 80. SCPP chose these generator locations through the use of the GUIDE model. Mean soundings were constructed from a subset of rawinsonde soundings in which the 700-mb

temperature was less than -5 °C and the wind had a westerly component. Running the mean soundings through the GUIDE model indicated the approximate location for the SCPP generators to affect the KGV area. The final sites chosen were a compromise between the GUIDE model predictions and the availability of residents willing to tend the equipment.

All observations were assembled daily in the forecast office to evaluate the likelihood of conducting seeding experiments. If the conditions were forecast to become favorable within the next 2 hours, an envelope was drawn that contained the randomized seeding decision. If a "no seed" was drawn, ground generators would not be lit and other research activities could commence. If the decision was "seed," then the five generator operators were instructed to ignite the burners for the prescribed 8 hours. Remote control dispensers were ignited by the various agencies per the SCPP forecaster request. This provided 2 hours to allow the ground plumes to disperse horizontally and vertically and a 6-hour time block for treatment effects to be evaluated. Not all generators were lit during each operation. Those predicted by the GUIDE model to miss the target area were not ignited. However, if winds changed later to a more favorable direction, these generators could be lit and run for the remainder of the experimental unit; but no generators were ever stopped early.

## 5.0 PRELIMINARY RESULTS

Each of the 18 randomized case days was analyzed by comparing the timing of SCPP operations with atmospheric temperature and liquid water information, and the accuracy of targeting based on GUIDE model predictions. Each operational period was thus compared to the following:

- Observed temporal variations in mountaintop SLW
- Observed temporal variations in mountaintop temperature
- Observed temporal and spatial variations in precipitation
- GUIDE model predictions of targeting effectiveness
- Timing of the operations with respect to most "seedable" conditions

Seedable conditions were defined as (a) cloud over the barrier with bases less than 1 km above KGV, (b) a westerly wind component, (c) liquid water observed by a mountaintop icing rate meter, and (d) temperature less than -5 °C at Squaw Peak (SQP) (2642 m).

Table 1 summarizes all 18 experiments with respect to seeding status, averaged values of SQP temperature and SLW content, the network averaged precipitation rate, and predicted targeting effectiveness. The timing of each unit in relation to observed SQP SLW is also tabulated, and a qualitative assessment of this is given.

From this table, it can be seen that many experimental units were well timed in relation to the presence of SLW at SQP. However, the GUIDE model predicted poor targeting for many of these cases. Predicted targeting was often fair to poor because of relatively warm temperatures and/or strong southerly wind components. This resulted in either no nucleation or else the predicted fallout trajectories impacted areas downwind of the intended target. Several cases were poorly targeted due to winds becoming northerly or easterly after the unit began. In addition, precipitation during most of the experiments was very light when normalized across the entire SCPP network. For the sake of brevity, only two experimental periods will be detailed in the following section to illustrate the physical plausibility of the GUIDE model predictions. Examples will be shown to illustrate the best targeting case and a marginal case.

### 5.1 Best Targeting Case - January 6, 1987

The best predicted impact on the SCPP target area occurred on January 6, 1987. The SQP temperature (Table 1) averaged -10 °C with a consistent but low average SLW content of 0.02 g $m^{-3}$ for the entire treatment period.

Figure 4 displays the temporal aspects of the meteorological parameters and icing information recorded at SQP and Sierra Ski Ranch (SSR). Temperature, icing, and wind conditions were fairly consistent throughout the experimental unit from 0430 to 1030 (all times G.m.t.).

All generators except S2 were ignited at 0230 and continued to burn until 1030. In Figure 5, showing predicted plume trajectories based on the 0600 Lincoln and KGV soundings, nucleation is depicted as the first asterisk (*) downwind of each generator; and predicted fallout is shown by the second circled asterisk. The crestline is approximately 100 km along the X-axis of the model coordinates. The low-level winds were southwesterly, but aloft turned more westerly to northwesterly. The modeled windspeeds were generally light, ranging from 5 to 15 m $s^{-1}$ throughout the levels reached by the ground plumes. The -5 °C level was near 2000 m m.s.l. so the plumes quickly reached temperature levels where nucleation could take place. Initial fallout was predicted to occur near the target's western boundary. High

elevation generators such as P2 and P3 were shown to nucleate immediately and provide fallout approximately 20 to 30 km downwind of the generators. Plumes from lower elevation sites such as S5 were shown to drift about 30 km before reaching nucleation levels, and fallout was predicted to reach the ground about 10 to 20 km beyond the point of nucleation. The radical wind shift downwind of the crest exemplifies problems with the model in this region.

The results are encouraging in that they are very similar to the effects reported for cold westerly cases by Mooney and Lunn (1969) in the PG&E Lake Almanor studies and by Super et al. (1986) in the Bridger Range in Montana. Such impacts at short distances downwind are plausible during "cold and slow" cases when winds are light and generators are located at high elevations. These model results indicate that seeding cold storms, with low freezing levels, may help to ensure rapid nucleation and short fallout trajectories, which combine for more effective targeting albeit small volume filling.

Figure 6 is a spatial representation of total precipitation recorded during the experimental unit with the GUIDE predicted areas of impact shown as the dashed enclosed area. Treatment effects are not expected to be apparent in this figure. Precipitation amounts ranged from 0.0 to 1.5 mm within the predicted area of effect. Gauges at Blue Canyon and Yuba Gap, upwind of the predicted impact area, recorded the largest precipitation amounts during this time.

### 5.2 Marginal Targeting Case - December 5, 1986

The second experiment, on December 5, 1986, is a typical example of the GUIDE model predicting a marginal impact on the SCPP target area. Figure 7 displays the type of information that was available to the forecast office in near real time from the mountaintop meteorological stations. Some SLW was observed at SQP with temperatures near -5 °C, but no icing was recorded at SSR. For this experiment, all but three generators were lit at 0645; and allowing 2 hours for volume filling, the experimental unit ran from 0845 to 1445.

On the 1200 sounding at KGV (1685 m m.s.l.) wind directions and speeds showed little change with altitude above the inversion located at approximately 650 mb. However, the sounding at Lincoln (1625 m lower) lacked the strong inversion; and windspeeds increased with height. Figure 8 shows the predicted plume trajectories and locations of nucleation and fallout generated from these soundings. Winds were very southerly, and most fallout was predicted to occur north of the target area. Fallout from the low elevation sites impacted approximately 100 km downwind from the ground release points while the high elevation generators showed fallout within about 30 km. Therefore, even with cold temperatures, effective targeting is predicted to be more difficult with low elevation generator sites in this southerly wind case. The GUIDE model frequently predicted such results on other days especially during the early stages of storm development.

Figure 9 presents the spatial view of precipitation during this experimental unit. The GUIDE-predicted areas of impact are shown within the dashed area. Some Sacramento area gauges received more precipitation than many of the higher mountain stations. A temporal display of precipitation (not shown) showed that seeding began with the onset of precipitation. The maximum rates generally occurred during the seeding period, but light precipitation continued for up to 7 hours after the seeding had terminated. The GUIDE model predicted that Castle Valley and Talbot were the only digital gauges in the area that may have been impacted.

## 6.0 AIRCRAFT STUDIES OF NUCLEANT TRANSPORT AND DISPERSION

Aircraft operations traced ground-released nucleants to help verify vertical transport and dispersion and the GUIDE model output. Special flight procedures were devised for each aircraft to measure the transport and diffusion of nucleants during prestorm conditions as well as during actual seeding operations.

An ice nucleus counter developed by the National Center for Atmospheric Research (NCAR) was flown aboard each aircraft to detect the presence of nucleants. The ice nucleus counter (Langer, 1973) is somewhat inexact, especially when used during aircraft survey flights, because of problems associated with the response and relaxation time of the instrument. Tests performed this season with airborne releases of AgI have shown a lag of approximately 20 to 40 seconds for the instrument to respond to the interception of nucleants within the turbulent wake of the seeder aircraft. After leaving the plumes, up to 3 minutes was needed to purge the chamber of nuclei. Therefore, it is difficult to accurately measure plume dimensions when the aircraft is traveling at 90 to 100 m $s^{-1}$. Typically, the aircraft was required to penetrate the plumes from opposite directions after allowing several minutes for the chamber to clear. Unfortunately, this was not always possible when flying

close to the mountain barrier during IFR.

Ice nuclei concentrations are also difficult to quantify because of a loss of nucleants and ice particles to the inside walls of the chamber. Langer (1973) estimates a 10-percent counting efficiency, but Sackiew et al. (1984) report that the NCAR counter may be only 1-percent efficient in quantitatively estimating ice nucleus concentrations. Therefore, the ice concentrations described here may be from 10 to 100 times too low. Using the 10 L $min^{-1}$ sampling rate of the counter as determined for both aircraft, one count would equate to six nuclei $L^{-1}$ active at -20 °C without the factor of 10 to 100 adjustment. For the results shown in the following cases, all the nuclei observed are for an effectivity of -20 °C. These may be reduced two orders of magnitude when considering effectivity at -6 °C.

6.1 Prestorm Test Flights

Flights during prestorm conditions were conducted before the onset of IFR conditions over the barrier but after the arrival of middle and/or upper level clouds from an approaching storm. These flights consisted of a series of profiles normal to the wind direction at 10- to 20-km intervals downwind of a generator (Fig. 10). Each profile was flown at various altitudes starting at a minimum safe altitude above ground level. Usually, the generators sampled were on specific mountain peaks so often it was possible to fly downwind and slightly below the elevation of the generators.

A good example of this flight procedure occurred on November 7, 1986, when a weak shortwave brought middle and high clouds over the ARB. A plume tracing study of generator D5 (Duncan Peak, 2179 m) was initiated while DRI personnel were onsite at the generator to verify its operation. The 2100 KGV sounding (not shown) revealed that the storm consisted mainly of a thin cloud deck based at 2750 m (-8 °C) with a well-mixed atmosphere below. Cloud top was near -17 °C. Winds below cloud veered from southwesterly to northwesterly at cloud base and remained northwesterly through the depth of the cloud. The vertical profile of acoustic sounder winds (not shown) revealed light southwesterly to northwesterly winds up to 2200 m with a mixing depth to at least 2700 m. DRI personnel reported a very light snowfall at D5.

Figure 11a shows a portion of the flight track of the Wyoming aircraft on several north/south passes downwind of the generator at 2200 m elevation with the plume trajectory predicted by the GUIDE model also shown. Since the generator was higher than most of the surrounding terrain, the aircraft was able to begin plume measurements at the same altitude as the generator. Substantial nuclei, 115 to 130 counts per pass (10 $L^{-1}$), were detected during the close-in passes (approximately 2 km downwind). On two additional passes at 2800 m, 11 km downwind of the generator, counts averaged 30 to 50 per pass (near the 6 $L^{-1}$ detectable limit). The approximate plume dimensions as derived from the nuclei counts (after allowing for time lag) are also shown in Figure 11a. The GUIDE model predicted the flow to be slightly north of west while the aircraft measured winds and plume location indicated that the flow was slightly south of west. From these airborne measurements, the plume was estimated to be approximately 2 km wide at a distance of 11 km (10-degree spread). The plume had risen 600 m or an average of 0.3 m $s^{-1}$. In addition, two regions of slightly enhanced ice crystal concentrations (2 to 3 $L^{-1}$ above a background < 1 $L^{-1}$) were measured by the aircraft in an area near the region (assuming plume meander) where nuclei were detected and where the GUIDE model had predicted nucleation to occur. These crystals were of a size and shape consistent with aircraft seeding signatures observed previously in SCPP (small hexagonal plates).

6.2 Instorm Transport and Diffusion Flights

During actual seeding operations, flights were made to determine if the ground-released nucleants were reaching the -6 °C temperature level in sufficient concentrations and in time to cause precipitation within the target area. A series of passes were made by each aircraft at the minimum obstruction clearance altitude (MOCA) to detect nuclei with their onboard NCAR counters. In addition to the MOCA runs, the aircraft would frequently make MOCA descents along the 230-degree radial off the Lake Tahoe (LTA) VOR, which carried them over the middle fork of the American River.

a. December 13, 1986

On December 13, 1986, a randomized ground seeding experiment was conducted while the aircraft performed transport and diffusion studies. All ground generators except S2 were ignited at 1645, and the aircraft were launched at 2320. The 0000 KGV sounding showed the cloud deck to be shallow and stable with southwesterly winds that increased in speed with height. Between 0000 to 0200, the acoustic sounder located at Blue Canyon measured southerly winds at elevations of 1600 to 2300 m with winds increasing to 10 m $s^{-1}$ between 1900 to 2100 m. The mixing depth was calculated at 2000 m.

Figure 11b shows the first flight sequence flown by the aircraft super positioned on the GUIDE predicted ground plumes. Marked on the flight tracks are regions where nuclei were measured. The 30- to 35-second lag has not been accounted for in these representations. What is most apparent is that nuclei were being observed to the west of the SCPP generators and a few to the west of the SMUD generators below 1600 m. Apparently, some of the material was moving downslope especially down the North and Middle Forks of the American River. However, the highest and most continuous nuclei were measured north and east of the SCPP generators and 300 to 400 m above their elevation. Figure 11c shows the continuation of this flight sequence with the aircraft climbing to 1900 m and measuring nuclei within the region anticipated by the GUIDE to contain plumes from the SCPP generators. The GUIDE model predicted the top of the plumes in this region to be 300 m (1000 ft) below the sampling level of the aircraft. Given the plumes are 30 to 40 minutes downwind and 700 to 800 m above the generators, an approximate rise rate of 0.35 m $s^{-1}$ would be required. This is very similar to November 7 and what might be expected due to forced ascent from the slope of the terrain (3 km rise in 100 km; 0.3 m s-1 using a 10 m s-1 upslope wind).

During the final minutes of this flight, the aircraft was sampling between 2200 and 3400 m elevation. The counts were rather sporadic but definitely above background levels. Assuming a background level of three counts in 5 minutes, 21 counts might be expected in 35 minutes. Here 71 counts were measured. The data indicated that some of the nuclei reached levels of supercooled water, but the temperatures were warm enough (-2 to -4 °C) that the AgI could not activate sufficiently.

In summary, this flight in rather stable storm conditions showed nuclei reaching levels of 600 to 1500 m above the generators. Sufficient concentrations (50 to 100 $L^{-1}$ using x 10 factor) appear to be found in the lowest 1000 m above the generators. It is not possible to say much about the GUIDE model on this day other than the plumes appeared to be traveling northeast and that the highest nuclei concentrations were lower down in the cloud. No nucleation was predicted or expected in the ARB based on the fairly warm temperatures observed.

b. December 19, 1986

This day was an example of a much more convective day although the convection was embedded in a stratiform cloud. The sounding from KGV, taken at 2100 near the start of the transport and diffusion study, showed the lower cloud region was neutral to slightly unstable. Saturation was noted above the lower cloud on the sounding. Winds in the lower cloud level were south-southwesterly with winds to 15 m $s^{-1}$ at 3000 m.

The acoustic sounder data (not shown) indicated winds to be southerly to southwesterly at from 7 to 10 m $s^{-1}$ between 1600 to 2200 m. The calculated mixing depth was only 100 m. Between 1600 and 2300, all generators were ignited except B4, B5, and D4. Liquid water values were rather variable but above background during the whole experiment.

The flight sequence was similar to that of December 13 except several passes were made over the crest (Fig. 11d). Substantial counts were noted above background (42 counts) in this flight sequence as seen in Figure 12. Several regions of high ice nuclei counts corresponded with elevated regions of ice crystal concentrations and regions of low liquid water content. The region measured between 2110 and 2115 was associated with a broad region of updrafts. The ice particles noted were very small (300 to 800 m) with very high concentrations (> 150 $L^{-1}$). The temperature as noted on Figure 11d was near -11 °C at this time. This corresponds with other aircraft seeding signatures seen, but it cannot be ruled out that the natural convection was producing these high ice concentrations. More than likely, the source region for these nuclei was the DRI generators.

As the aircraft began its run along the 5,000-ft MOCA at (2130 to 2140), 12 counts were measured or only slightly above background. This run was approximately 10 km west of the SCPP manual generators of which four had been ignited. Flying along the 7,000-ft MOCA from 2140 to 2147 (900 m above the SCPP generators and 1500 m above the SMUD generators), the aircraft entered the predicted plumes from the SMUD and SCPP generators. The plumes were not continuous nor of high concentrations but were significantly above background levels. Individual convective elements were probably lofting the seeding material to the aircraft altitude. As the aircraft flew along the 9,000-ft MOCA (2147 to 2155), 1500 m above the SCPP generators, counts were above background with most counts apparently coming from SCPP's generator B6. Only a few regions of enhanced ice crystal concentrations were noted although ice nuclei and liquid water at temperatures colder than -6 °C were coexisting for a portion of this flight segment.

The research aircraft repeated the flight track along the 6000-ft contour

over the barrier at 2203 observing one region of high ice nuclei counts and high ice crystal concentrations apparently just downwind of generator B3. Again, these crystals were less than 300 m in size, showing the crystals to be fairly new with their size and shape again similar to seeding effects seen in previous aerial seeding experiments. As the aircraft continued its flight along the MOCA, few nuclei were noted.

In summary, this day was the most convective of any transport and diffusion flight this season. Ice nuclei from ground generator releases were noted to be from 1000 to 1500 m above release points in limited regions of the ARB. In several regions where the temperature was colder than -6 °C and liquid water and ice nuclei coexisted, elevated ice crystal concentrations were noted. These crystals were representative of seeding effects observed from aerial seeding experiments. Thus convective processes provided a mechanism to loft seeding material to colder regions of the cloud but only over a limited region of the ARB.

## 7.0 SNOW CHEMISTRY ANALYSIS

The goal of this part of the study was to determine the targeting effectiveness of the coordinated seeding program--a snowpack sampling and chemical analysis program. This would help determine if, when, and where AgI released from the network was reaching the target area. Evidence of seeding effectiveness was to be obtained by measuring the amount of silver in snowfall samples at 15 sites in the project area.

Several snow sampling expeditions were conducted during and after the experimental field season from December 1, 1986, through March 15, 1987. A total of 1,681 individual snow samples were collected for chemical analysis at 14 of the 15 sites shown in Figure 13. Each profile was partitioned into 2-cm increments so that silver and water content could be measured as a function of depth. The profiler cross-sectional area is 200 $cm^2$, giving each partitioned increment a chamber volume of 400 $cm^3$. Each 400-$cm^3$ volume of snow represents a sample for chemical analysis.

A helicopter provided rapid access to the remote sites so individual snow samples had shorter resolved time intervals and, in general, improved quality for chemical analysis. The helicopter allowed rapid transport of the snow samples back to the freezers at the staging area. Transportation time is important because density profiles from each of the sites become easier to relate to one another and samples are less likely to undergo change due to aging or melting.

### 7.1 Laboratory Analyses and Data Processing

The analyses were made in two DRI clean room laboratories. One contains a laminar flow dual-beam flameless atomic absorption spectrophotometer, which is housed in filtered Class 100 air and uses an automated sample injection system for better contaminant control. A clean room sample preparation area is located immediately outside the main clean room but within the positive pressure envelope. The sample preparation area also houses an ion chromatograph for an analysis of major cations (Na, Mg, Ca, K, $NH_4$, etc.) and anions ($SO_4$, $NO_3$, Cl, etc.). The second clean room laboratory is used entirely for rare heavy metal analyses for elements such as Ag, Cs, Rb, and In. This laboratory contains a single-beam flameless atomic absorption spectrophotometer. Each individual snow sample has been analyzed five times by flameless atomic absorption techniques. This number of analyses permits the reduction and computation of a statistical uncertainty in the silver concentration measurements for the individual samples. Blanks and standards are processed continually throughout the laboratory analysis program. The analytical procedures used produce silver concentrations with typical calculated uncertainties of 10 to 20 percent (Warburton, 1977; and Warburton et al., 1968, 1977, 1982).

### 7.2 Results

All the 1681 samples actually collected have been analyzed for silver. Figure 14 shows the average percentage of samples that contain silver in concentrations greater than 4.0 parts per trillion for all samples. This figure is the silver background concentration +2 $\sigma$, hence confidence is high that the samples containing silver greater than this contain a component due to the seeding activity.

The results show that the PG&E program to the south consistently targets well into the more southerly portions of their project area, but these sites are located at the upper ends of valleys into which the seeding aerosols are channeled. These results are quite consistent with earlier results obtained for this area by DRI investigators. The more northerly sampling sites in the PG&E area are not targeted as consistently as the southerly sites even though the predominant wind trajectories across the region are from the west and southwest during seeding.

The other well-targeted area is in the northern Truckee-Tahoe catchment area, which was seeded jointly by DRI and SCPP generators. This consistent targeting also included the basin of the North Fork of the American River. Surprisingly, targeting into the Tahoe Meadows region, northeast of Lake Tahoe was not good. DRI researchers had found this region well-targeted in previous years; perhaps certain, more southerly generators in the DRI network were not always fully operational during the seeding operations. By contrast, the upper regions of the Middle and South Forks of the ARB targeted by SMUD gave consistently poor results. Some seeding generators in this project may need relocation.

## 8. CONCLUSIONS

This 2-month investigation of ground seeding leads to a number of insights into the feasibility of ground seeding operations in the ARB. Unfortunately, the 1986-87 winter field season provided few storms for research so the effectiveness of these operations cannot reasonably be determined. Only suggestions as to predictability of useful seeding periods and on the expected results of the transport and dispersion of ground seeding material can be given.

These preliminary studies indicate that the criteria used this past winter for initiating an experimental unit may have been too broad. On nearly one-third of the ground seeding cases, the temperatures were warmer than -5 °C at elevations that might be expected to be reached by the ground-released nucleants. This may have reduced the accuracy of targeting the seeding effects.

The numerical GUIDE model frequently predicted that the target area may not have been impacted primarily due to high freezing levels, strong southerly wind components, and low elevation generator sites. Nucleants released from the low elevation generator sites were frequently shown to have trajectories parallel to the barrier, i.e. the air moved around the mountain rather than over it. Therefore, nucleation was often delayed; and fallout was usually predicted to impact areas north of the target. Meteorological conditions with low freezing levels and light westerly winds were anticipated to produce the most effective targeting of precipitation in the desired region. These conditions combined to produce fallout predicted to occur a short distance (10 to 30 km) downwind, particularly from the higher elevation generator sites.

Aircraft plume tracing studies began the task of verifying the GUIDE model predictions of ground-released plume trajectories. These limited studies revealed that airborne ice nucleus counters could detect the plumes downwind of the release sites. Although it was difficult to map the horizontal and vertical extent of the plumes, the measurements indicated that the GUIDE model appeared to be providing reasonable estimates of both the horizontal and vertical dispersion of ground released plumes. That is, one can assume a 10- to 15-degree angle of spread and an approximate 0.3 m $s^{-1}$ rise rate of the plume.

As expected, the highest concentrations of nucleants were often observed near the surface; but nucleants above background levels were also observed at heights greater than predicted. In several cases, interesting regions of higher ice crystal concentrations were observed in conjunction with ice nuclei. In one case, this region was close to the location predicted by the GUIDE model. These observations suggest that the GUIDE model may provide a useful predictive and/or diagnostic to the utility of ground seeding. However, many more research flights of this type will be needed for verifying the GUIDE model with direct observations.

Silver sampling indicated a fairly low percentage of silver in snow over most sampling areas. The most favorable regions were the extreme southeast corner and the extreme north end of the target area. Other sampling sites showed almost no silver. These are disturbing results, even if one considers only scavenging, in that the AgI must not have passed over large regions of the target during precipitation events. Much of the AgI may be transported westward or northwestward at low levels, effectively not passing over the barrier.

These results may be specific only to the central Sierra Nevada. In the colder intermountain regions of the west, generators can be placed well above the -5 °C level and thus are not limited by temperature. However this still requires the generators be sited at high elevations to expose the nuclei to the free air flow and ensure transport to the desired cloud regions.

## 9.0 ACKNOWLEDGMENTS

This research was supported by the Bureau of Reclamation. Without the cooperation of PG&E, SMUD, and DRI, this project would not have been possible. The efforts of all participants in the SCPP are greatly appreciated.

## 10.0 REFERENCES


Deshler, T., D.W. Reynolds, and A.W. Huggins, 1989: Physical response of winter orographic clouds over the Central Sierra Nevada Mountains to airborne seeding using dry ice or silver-iodide. Submitted to J. Appl. Meteor.

Elliott, R., and J.O. Rhea, 1984: Comparison of observed and predicted model winds over an orographic barrier. Preprints Ninth Conf. Weather Modification, AMS, Park City, 83-84.

Henderson, T.J., and M.E. Solak, 1983: Supercooled liquid water concentrations in winter orographic clouds from ground-based ice accretion measurements. J. Wea. Mod., 15, No. 1, 64-70.

Huggins, A.W., and A.R. Rodi, 1985: Physical response of convective clouds over the Sierra Nevada to seeding with dry ice. J. Climate Appl. Meteor., 24, 1082-1098.

Langer, G., 1973: Evaluation of NCAR ice nucleus counter. Part I: Basic operations. J. Appl. Meteor., 12, 1000-1011.

Lauritsen, D., Z. Malekmadani, C. Morel, and R. McBeth, 1987: The cross-chain Loran atmospheric sounding system (CLASS). Preprints Sixth Symp. Meteor. Observations and Instrumentation (New Orleans, LA).

Marwitz, J.D., and R.E. Stewart, 1981: Some seeding signatures in Sierra storms. J. Appl. Meteor., 20, 1129-1144.

Mooney, M.L., and G.W. Lunn, 1969: The area of maximum effect resulting from the Lake Almanor randomized cloud seeding experiment. J. Appl. Meteor., 8, 68-74.

Price, G., and R.A. Rilling, 1987: A high resolution, infinite capacity weighing snowgauge for use in remote areas. Preprints Sixth Symp. Meteor. Observations and Instrumentation (New Orleans, LA), 249-252.

Reynolds, D.W., and A.S. Dennis, 1986: A review of the Sierra Cooperative Pilot Project. Bull. Amer. Meteor. Soc., 67, 513-523.

Sackiew, C.M., J.W. Robataille, J.W. Mason, and F.D. Barlow, 1984: Comparison tests of NCAR ice nucleus counters. Preprints Ninth Conf. Weather Modification (Park City, UT), 12-13.

Stewart, R.E., and J.D. Marwitz, 1982: Microphysical effects of seeding wintertime statiform clouds near the Sierra Nevada mountains. J. Appl. Meteor., 21, 874-880.

Super, A.B., and J.A. Heimback, 1984: Evaluation of the Bridger Range winter cloud seeding experiment using control gauges. J. Climate Appl. Meteor., 22, 1989-2011.

Warburton, J.A., 1977: Interrelationships between the physics and chemistry of precipitation. Presented at ICPM Symposium, Joint IAGA/IAMAP Assembly (Seattle, WA).

Warburton, J.A., G.O. Linkletter, and R. Stone, 1982: The use of trace chemistry to estimate seeding effects. Jour. Appl. Meteor., 21, 8, 1089-1110.

Warburton, J.A., M.S. Owens, A.V. Anderson, and R. Stone, 1977: Temporal and spatial distributions of seeding material in a ground-based seeded target area. Proc. Seventh Conference on Inadvertent and Planned Weather Modification (Banff, Canada).

Warburton, J.A., and L.G. Young, 1968: Neutron activation procedures for silver analysis in precipitation, J. Appl. Meteor., 7, 3, 433-448.


Table 1. Summary of SCPP ground-seeding experiments - 1986-87

| Experiment Date | Time | Status | SOP temp. (°C) | SOP SLWC (g m$^{-3}$) | GUIDE-predicted targeting | Unit timing | Area PCP rate timing (mm h$^{-1}$) |
|---|---|---|---|---|---|---|---|
| 861119 | 0800-1400 | Seed | -0.4 | 0.11 | Poor - No nucleation or fallout | Excellent | 0.41 |
| 861121 | 0800-1200 | No seed | -1.7 | 0.06 | Poor - Nucleation east of crest | Good | 1.98 |
| 861129 | 0100-0700 | Seed | -3.2 | 0.00 | Fair - Fallout northeast of target | Too early | 0.17 |
| 861205A | 0245-0645 | No seed | -0.7 | 0.00 | Poor - Fallout far north of target | Poor | 0.00 |
| 861205B | 0845-1445 | Seed | -4.9 | 0.02 | Fair - Fallout in target from high elevation generators | Too early | 0.98 |
| 861206 | 0130-0730 | Seed | -4.3 | 0.01 | Fair - Fallout east of crest | Too late | 0.001 |
| 861213 | 1845-0045 | Seed | -1.7 | 0.03 | Poor - No nucleation | Too early | 0.012 |
| 861218A | 1600-2000 | No seed | -4.3 | 0.12 | Good - Most fallout on crest north of target | Excellent | 0.56 |
| 861218B | 2200-0400 | Seed | -4.3 | 0.07 | Fair - Most fallout east of crest | Excellent | 0.79 |
| 861219 | 1800-2400 | Seed | -4.4 | 0.06 | Good - Fallout on crest, some north of target | Good | 0.49 |
| 861220 | 0500-0900 | No seed | -6.7 | 0.03 | Poor - Easterly wind flow | Good | 0.08 |
| 861222 | 1700-2300 | Seed | -5.0 | 0.05 | Poor - No nucleation | Too early | 1.80 |
| 861223 | 0400-0800 | No Seed | -3.4 | 0.11 | Poor - Northerly wind flow | Excellent | 0.02 |
| 861231 | 1530-2130 | Seed | -4.4 | 0.07 | Good - Fallout near crest, some north of target | Good | 0.26 |
| 870103 | 1530-2130 | Seed | -4.7 | 0.03 | Fair - Fallout east of crest | Excellent | 4.77 |
| 870104A | 0230-0830 | Seed | -8.5 | 0.00 | Good - Short trajectories, most fallout west of target | Good | 0.33 |
| 870104B | 1330-1730 | No seed | -8.8 | 0.02 | Poor - Northerly wind flow | Poor | 0.00 |
| 870106 | 0430-1030 | Seed | -10.0 | 0.02 | Excellent - Fallout in target | Excellent | 0.13 |

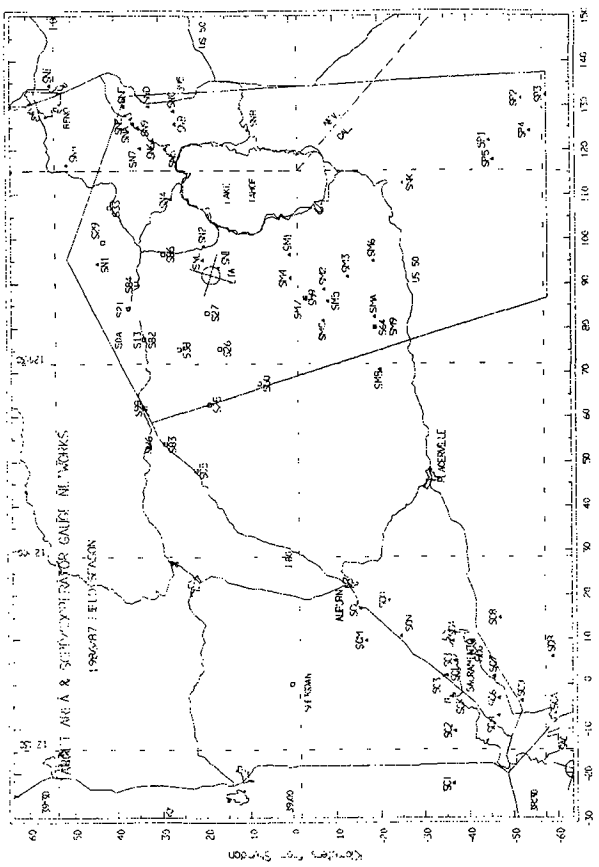

Figure 2. SCPP and cooperator precipitation gauge network for the 1986-87 field season.

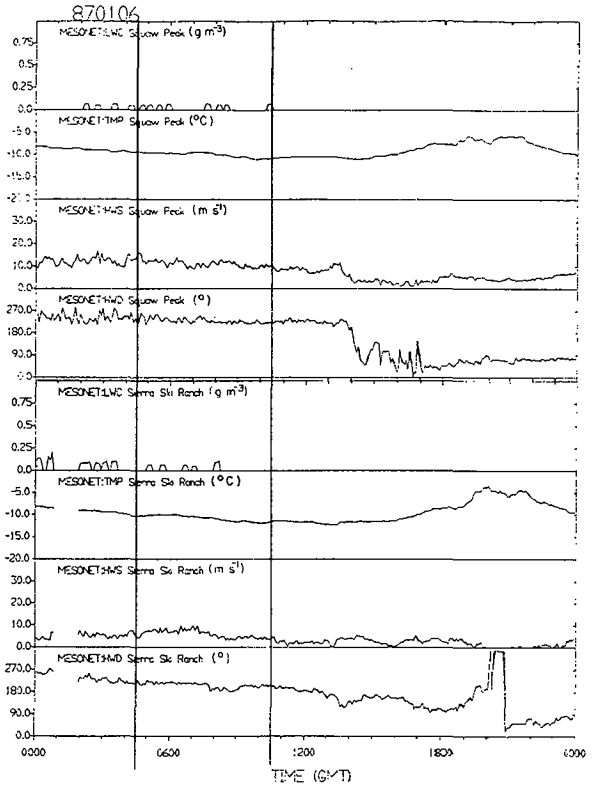


Figure 4. Temporal plot of mountain weather information for January 6, 1987, for two sites--Squaw Peak and Sierra Ski Ranch. For each site, liquid water content (LWC) from a Rosemount icing meter, temperature, and wind direction and speed are displayed from top to bottom. Data are plotted every 5 minutes.

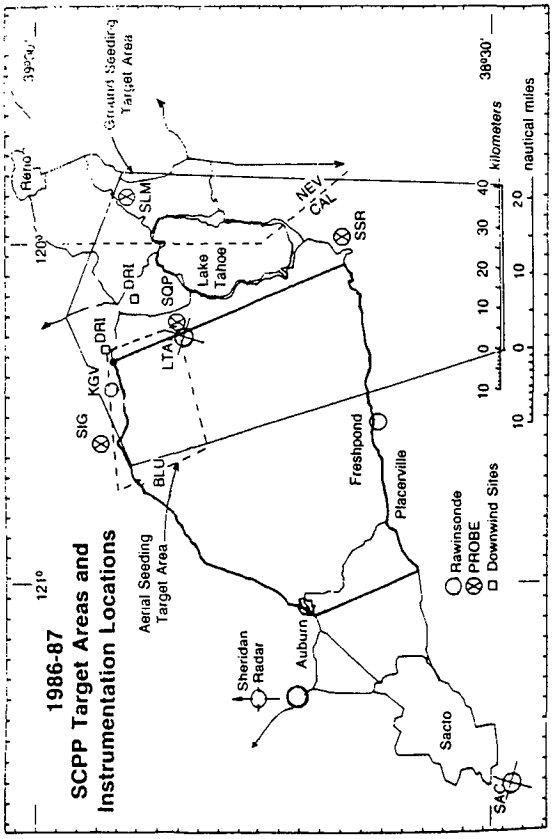


Figure 1. 1986-87 SCPP target areas and instrumentation locations.

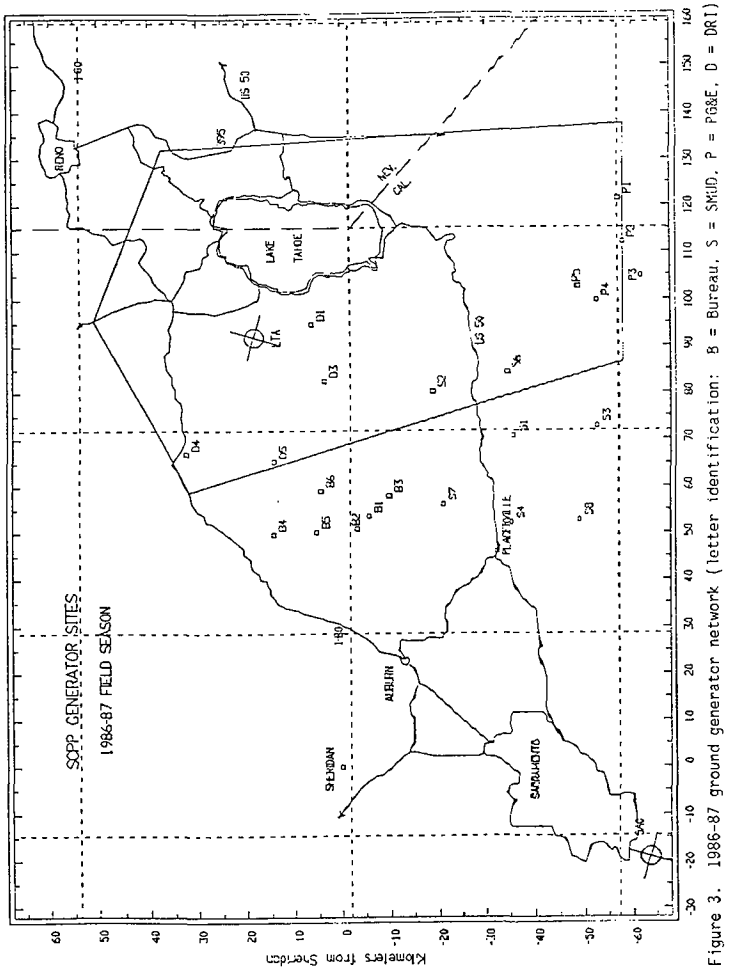


Figure 3. 1986-87 ground generator network (letter identification: B = Bureau, S = SMUD, P = PG&E, D = DRI).

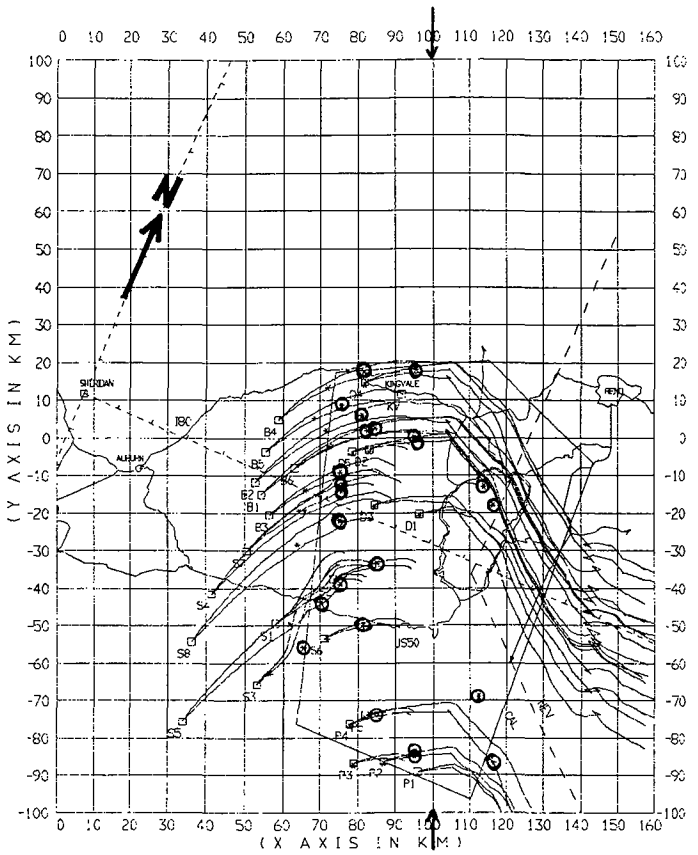


Figure 5. Output from the numerical targeting model (GUIDE) showing seeding plumes superimposed over the target area for January 6, 1987, using the 0600 G.m.t. soundings. The first asterisk denotes the predicted location of nucleation at the -6 °C level, and the second asterisk denotes the fallout point of this crystal.

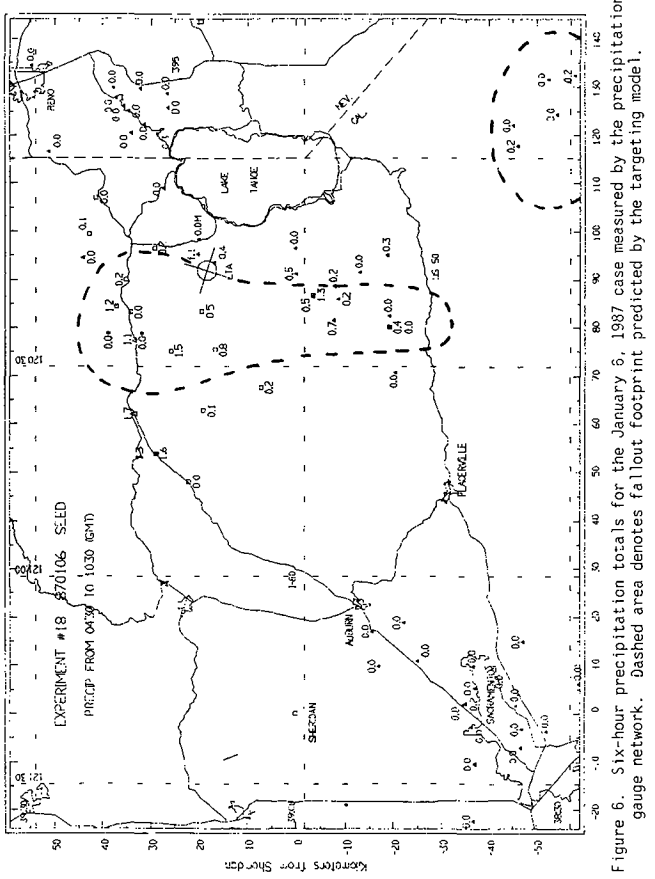


Figure 6. Six-hour precipitation totals for the January 6, 1987 case measured by the precipitation gauge network. Dashed area denotes fallout footprint predicted by the targeting model.

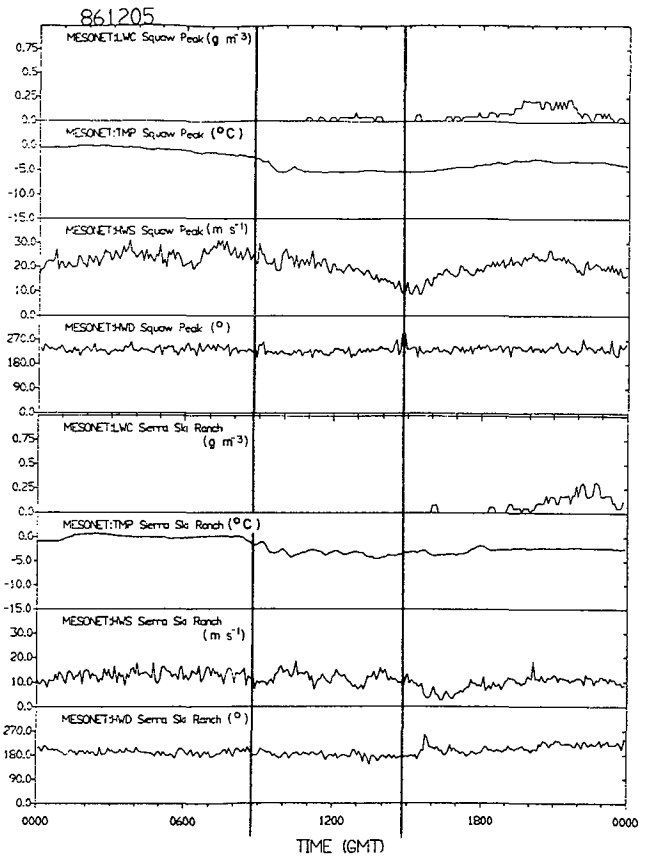


Figure 7. Temporal plot of mountain weather information for December 5, 1986, for two sites--Squaw Peak and Sierra Ski Ranch. For each site, liquid water content (LWC) from a Rosemount icing meter, temperature, and wind direction and speed are displayed from top to bottom. Data are plotted every 5 minutes.

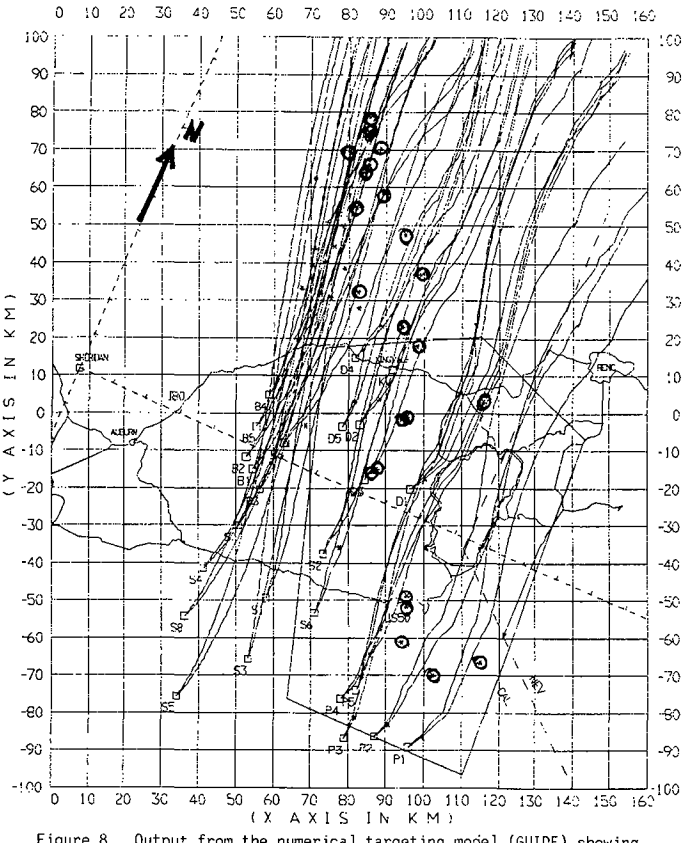


Figure 8. Output from the numerical targeting model (GUIDE) showing seeding plumes superimposed over the target area for December 5, 1986, using the 1200 G.m.t. soundings. The first asterisk denotes the predicted location of nucleation at the -6 °C level, and the second asterisk denotes the fallout point of this crystal.

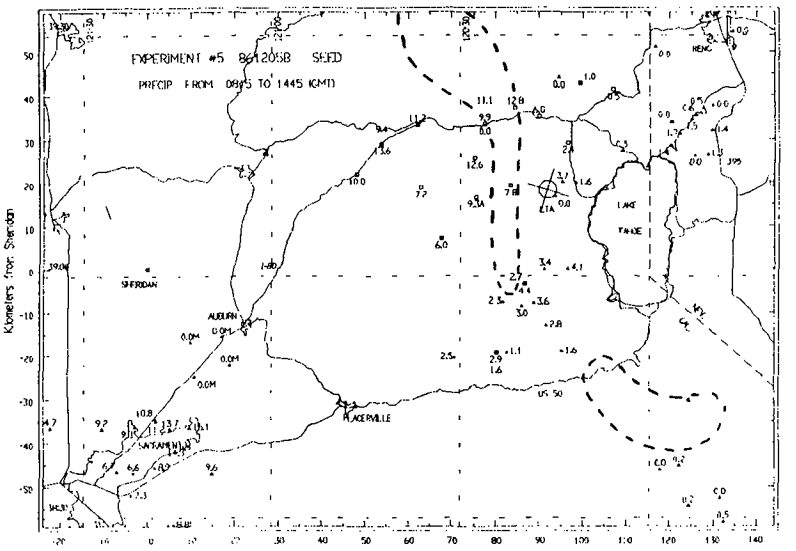


Figure 9. Six-hour precipitation totals for the December 5, 1986 case measured by the precipitation gauge network. Dashed area denotes fallout footprint predicted by the targeting model.

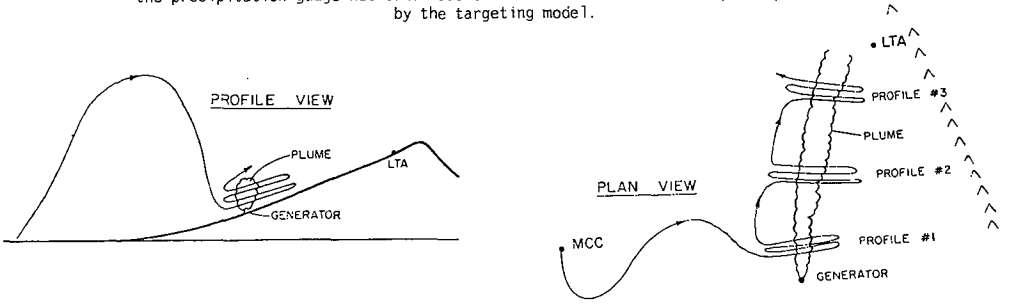


Figure 10. Flight track of the cloud physics or seeder aircraft for tracing ground-released AgI during prestorm conditions.

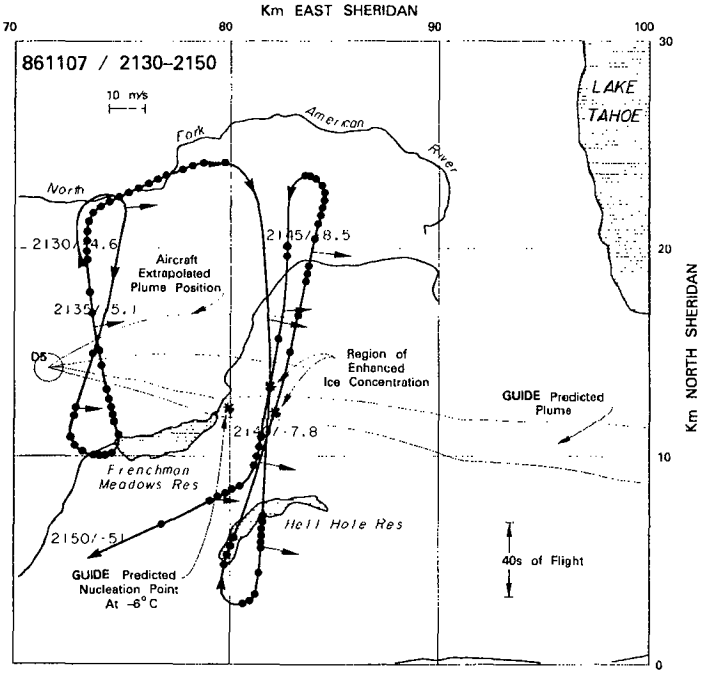


Figure 11a. Cloud physics aircraft flight track for the period 2130-2150 sampling downwind of a DRI generator. The time and temperature along with windspeed and direction (arrows) at flight level are shown periodically along the track. Dark circles along the track indicate locations of ice nuclei counts detected by the nuclei counter. Lag in response time has not been accounted for but can be estimated by noting the scale on the left of the figure showing distance traveled by the aircraft in 40 seconds of flight.

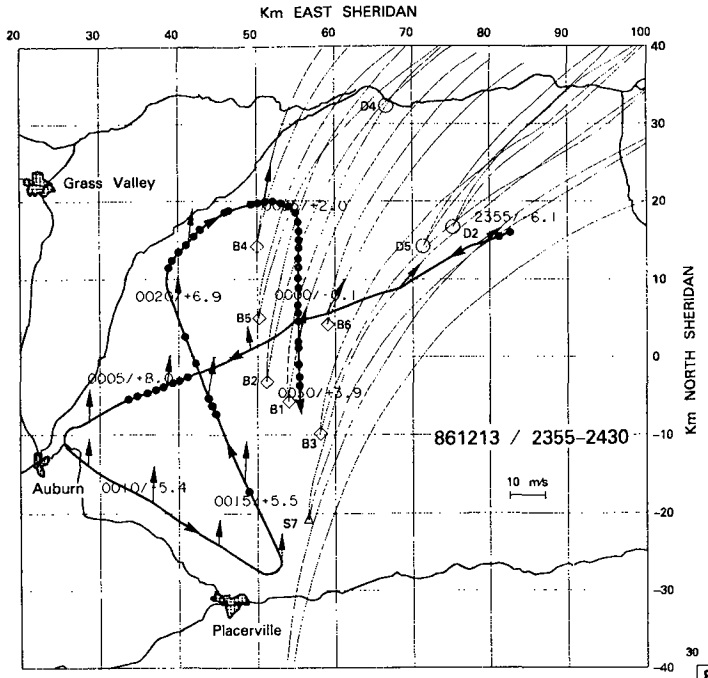


Figure 11b. Same as Figure 11a but for December 13, 1986.

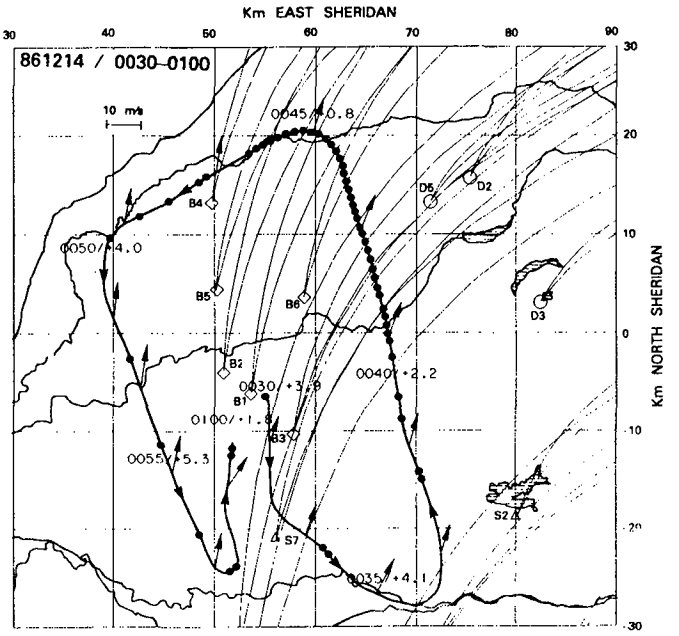


Figure 11c. Continuation of the flight profile from Figure 11a.

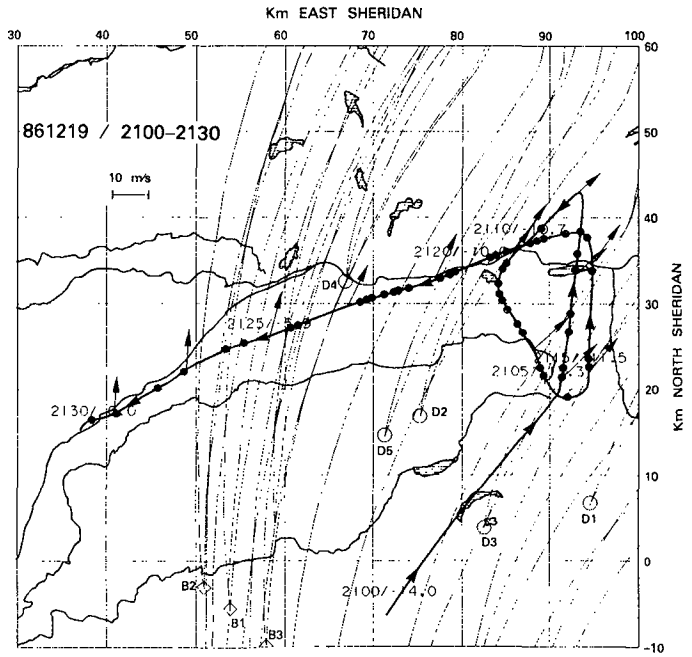


Figure 11d. Same as Figure 11a but for December 19, 1986.

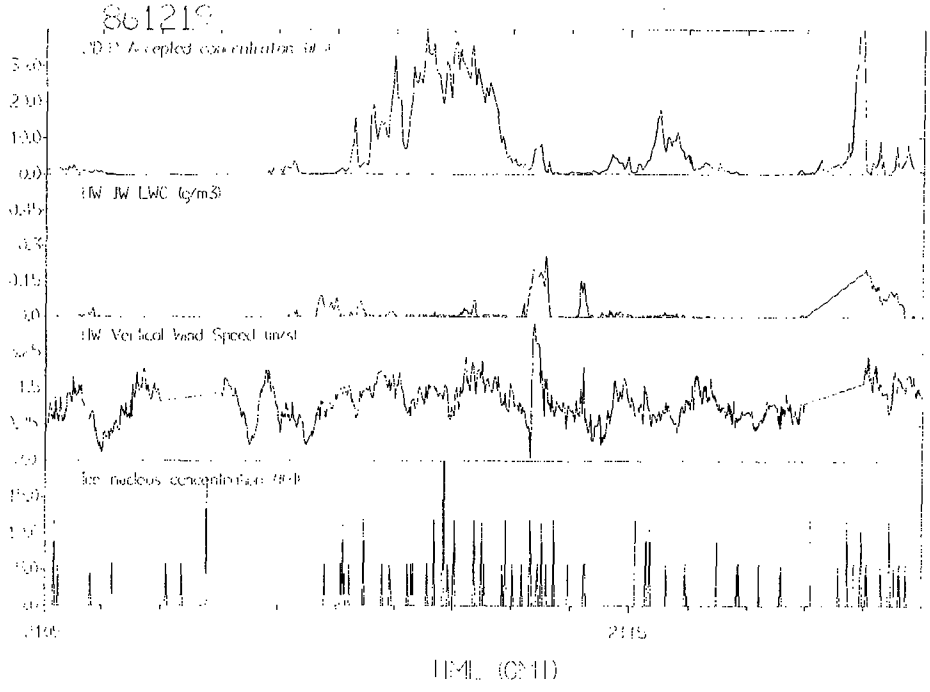


Figure 12. Parameters measured by the cloud physics aircraft as it flew over the crest of the Sierra on December 19, 1986. Top panel is 2D-Pice particle count after reject criteria applied. In the second panel is liquid water as measured by a Johnson-Williams probe. The third panel is aircraft-measured vertical velocity, and the fourth panel is ice nucleus concentrations (see text for further details).

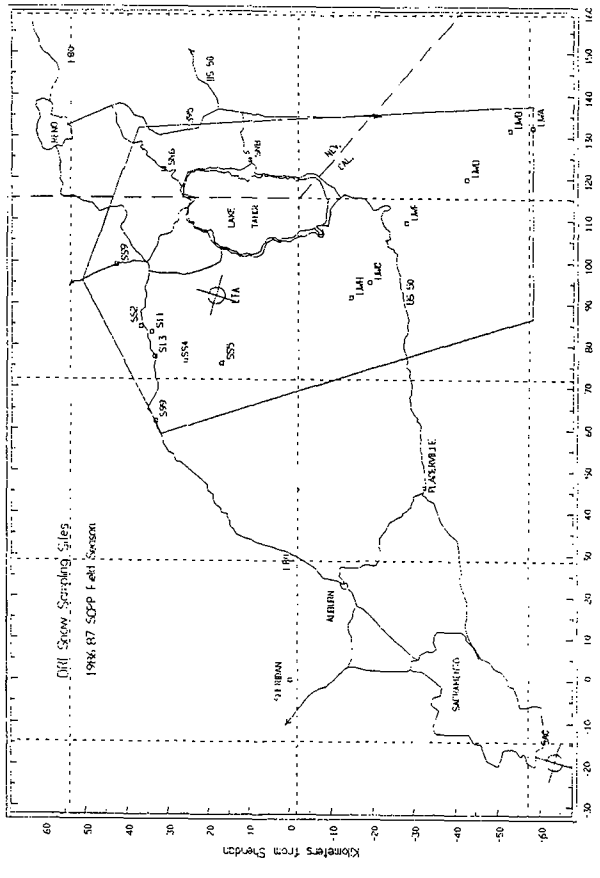


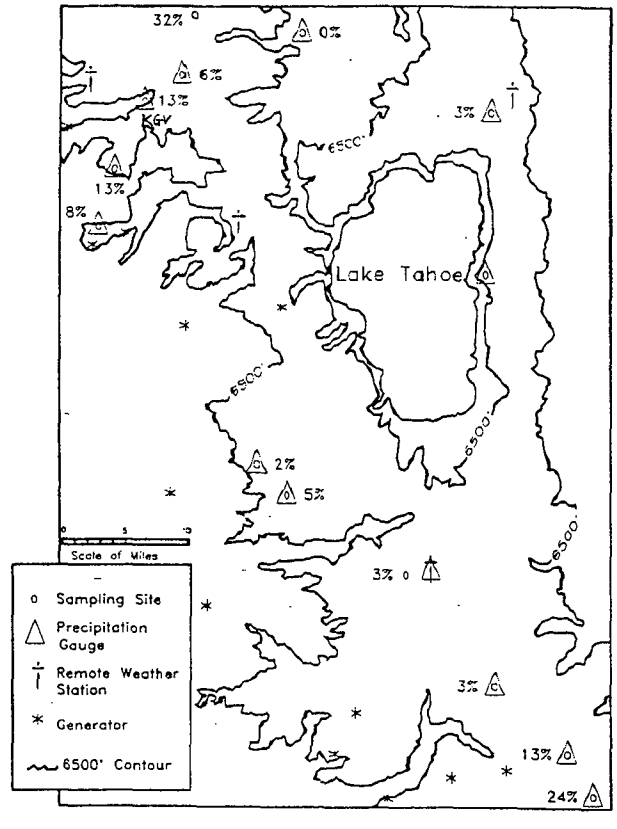


Figure 13. DRI snow chemistry sampling sites for the 1986-87 field season.

# DESIGN OF A GROUND BASED SNOWPACK ENHANCEMENT PROGRAM USING LIQUID PROPANE

David W. Reynolds
Water Augmentation Group
Bureau of Reclamation
Sacramento, CA 94236-0001

Abstract - The design of a winter snowpack augmentation program utilizing liquid propane as the seeding agent is described. The program has been designed utilizing results from the Sierra Cooperative Pilot Project(SCPP). Observations from SCPP showed that the bulk of the supercooled liquid water (SLW) in winter storms over the Sierra occurs within the first kilometer above the barrier at temperatures between 0 and -10°C and in concentrations of 0.05 to 0.2 g/m$^3$. Mountain-top icing stations within the Feather River drainage indicate that icing occurs with a mean temperature near -3°C. These results imply the need for a seeding agent capable of converting the SLW to ice crystals at fairly warm temperatures and be released remotely from the ground. Liquid propane meets these requirements.

The design calls for two 2175 liter tanks of propane at each site. Remote operation will be via radio to an on-site micro-processor. Site seperation will be every two kilometers along the crest of the Sierra above the Middle Fork Feather. Tanks will be flown in by helicopter in the fall and removed early in the spring. Three sites will be used the first year for test purposes. The release rate will be 10 liters/hr per dispenser. Multiple atmospheric soundings, telemetered mountain-top icing data, and a simple diagnostic targeting model will be used for real-time decision making. Initial estimates are that suitable clouds exist from 200 to 400 hours per winter season. Based on propane activitation levels, cloud liquid water content, and crystal growth times, 12,300 m$^3$ per dispenser per hour is possible.

## 1.0 INTRODUCTION

Cloud seeding to increase winter snowpack has been conducted since the early 1950's in several basins in the Sierra Nevada. With the discovery by Drs. Schaefer and Vonnegut that additional ice crystals could be generated in clouds containing supercooled liquid water, an immediate attempt was made to transfer this capability into increasing wintertime snowpacks in the Sierra. This design builds on the assumption that some clouds existing in winter storms over the Sierra Nevada contain insufficient ice-forming nuclei, or that the nuclei are unable to convert cloud condensate, produced by the orographic lift of the barrier, soon enough to remove all the cloud water. Thus that portion of cloud water which exists at temperatures below 0 °C, and is therefore supercooled, is lost to the precipitation process to the lee of the mountain. By proper application of glaciogenic seeding material, an attempt is made to convert this cloud condensate to ice before it passes over the crest. A recent paper by Reynolds (1988) reviews these principles and the current thinking on the feasibility of winter snowpack enhancement. The California Department of Water Resources (DWR) has contracted with the Bureau of Reclamation to design and implement a program to seed the Middle Fork of the Feather River basin in the northern Sierra Nevada to increase runoff to Oroville Reservoir, Fig. 1.. This paper describes the results of this study.

From 1976 through the 1986-87 winter season the Bureau of Reclamation sponsored the Sierra Cooperative Pilot Project (SCPP). The purpose of this program was to further refine when and where to seed clouds in the Sierra Nevada for winter snowpack enhancement and to determine the magnitude of those increases (Reynolds and Dennis, 1986). SCPP achieved two major accomplishments. The first was in the application of observing equipment for determining the spatial and temporal variability of supercooled liquid water in clouds over the Sierra Nevada. The second was developing diagnostic models for determining when and where to seed this supercooled liquid for increasing precipitation within intended target areas. These results were major inputs to the formulation of this design. In addition, several remote meteorological stations providing information on the wind, temperature, and occurrence of rime icing were established in the Feather River basin at high elevation sites. These data provided valuable additional information utilized in this design.

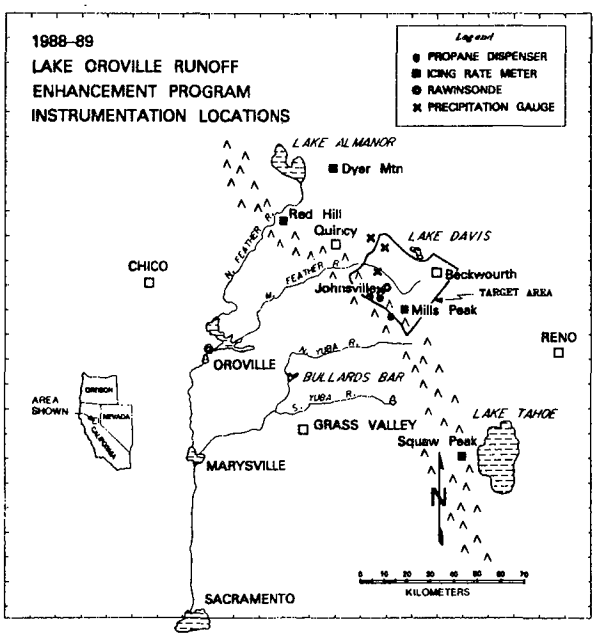


**Figure 1** *Site map and instrumentation locations for the Lake Oroville Runoff Enhancement Program.*

## 2.0 SEEDING HYPOTHESIS

### 2.1 Liquid Water Distributions

As has been mentioned, certain cloud systems which occur within winter storms over the Sierra Nevada are inefficient in removing all the available cloud water before the air passes over the barrier and the cloud water is evaporated. It has been found by the SCPP that this cloud water available for removal by seeding is concentrated in the lowest 1000 m above the barrier, at temperatures between 0 and -10 °C and at concentrations of 0.05-0.2 g/m$^3$. This information was derived by application of a remote sensing device (microwave radiometer) near the crest of the Sierra (Heggli & Rauber, 1988). Further refinement of the occurrence of liquid water at mountain-top level has been made from installation of an icing rate meter positioned at mountain-top. Results of observations from three mountaintop icing stations (see Fig. 1 for locations) are shown in Fig. 2. This shows the cumulative frequency of icing (i.e. supercooled water) atop Squaw Peak in the central Sierra and Dyer Mountain (DMT) and Red Hill (RDH) in the Feather River basin as a function of temperature. Note the distribution for all three stations is skewed to the warmer temperatures with a mode of 0 to -2 °C and a median value of -3 °C. The Squaw Peak data cover two winters, 1985-86 and 1986-87. The DMT and RDH data are from 15 November to 20 January 1986-87.(The temperature sensor on each station failed after 20 Jan.) These data indicate that when supercooled liquid water SLW is present near 2.0 - 2.6 km MSL it is at temperatures slightly below 0 °C, with the occurrence and magnitude of liquid water dropping off at the colder temperatures. Fig. 3 shows the total number of hours of icing at DMT and RDH for 1987-88. The monthly precipitation for the Feather River basin as a percentage of normal is also shown. The figure shows 419 hours of icing at Dyer Mountain and 186 hours at Red Hill from November 21, 1987 to April 30, 1988. Despite this year being a critically dry year, this data indicates substantial time available for seeding.

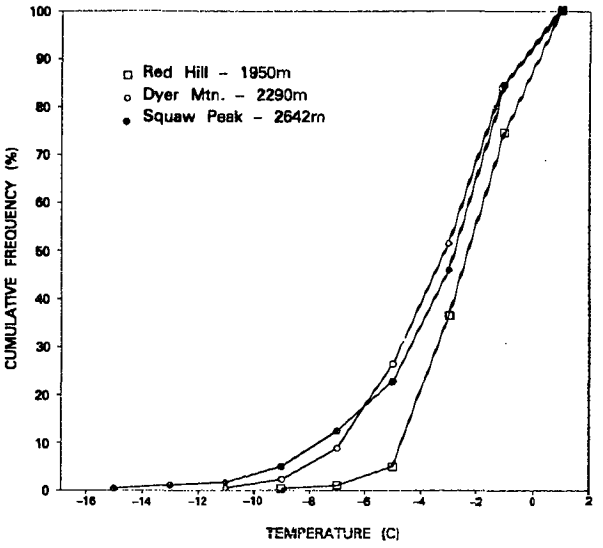


**Figure 2** *Icing occurrence as a function of temperature for three mountain-top locations along the Sierra Nevada.*

### 3.2 Tapping the Available Supercooled Liquid Water

The icing data suggests the need for a seeding agent, active at converting supercooled droplets into ice crystals at temperatures between 0 and -5 °C, thus offering the opportunity for seeding many more events from the surface. Dry ice, or solid $CO_2$, has been shown to be an effective seeding agent at temperatures close to 0 °C and was used extensively on the SCPP. However, the only mechanism for adequate delivery is aerial release. Based on SCPP results, this is not as desirable a delivery mechanism due to limited dispersion within seedlines and difficulties in placing the aircraft within (SLW) regions necessary to adequately target the effects to the desired locations. However, a seeding agent does exist that is effective at producing ice crystals near 0 °C and can be remotely released at a ground site. This agent is liquid propane released as a fine spray. Vardiman et al. (1971) has fully documented the use of propane as a glaciogenic seeding agent for dispersing cold fog. The principle behind this production of ice crystals is that liquid propane, sprayed into the environment as a fine mist, vaporizes and rapidly chills the air to temperatures well below 0 °C. Figure 4

shows the cooling which takes place in the vicinity of the nozzle using a 38 l/hr dispensing rate. As temperatures approach -40 °C (-42 °C is the boiling point of propane) moisture rapidly condenses into many cloud droplets which immediately freeze and grow into tiny ice crystals. This condensation/freezing process is nearly simultaneous. Therefore, in looking at Fig. 4, ice crystal production will occur within 12-14 inches of the release point. Hicks and Vali (1973) and Kumai (1982) have determined through laboratory and field experimentation that the yield from the release of 1 gram of propane is $10^{11}$-$10^{12}$ ice crystals. This activity can be compared to other seeding agents commonly used, Fig. 5.

From the available data given above it is apparent that propane offers a very real potential as a seeding agent for increasing snowpack within the Sierra Nevada. Therefore, the task is to install the most efficient, remotely operated propane dispensing system positioned at altitudes within supercooled clouds and with exposures allowing rapid dispersion of the ice crystals produced.

3.3 Anticipated Effects with Propane

The release of propane within supercooled liquid water clouds at temperatures $\leq$-2 °C is expected to lead to the following results:

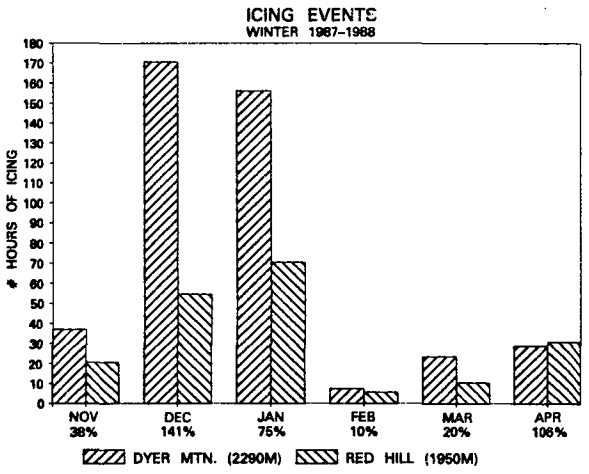


**Figure 3** *Number of hours of icing within the Feather River Drainage for Dyer Mountain and Red Hill for the 1987-1988 winter season. Percentages below the month are the percent of normal precipitation for the Feather River basin.*

Within several feet of the nozzle, a high concentration of very small ice particles (<50 µm) will develop. Due to the turbulent flow at mountaintop levels the plume of ice crystals will disperse horizontally at a rate of 1-2 m s-1 downwind. The small crystals will be lifted into the cloud due to terrain induced vertical motions. These crystals will grow rather slowly at approximatly 0.5 µm/sec and should reach 200-300 µm within 5-10 min. Given these crystals will be compact plates or squatty columns (Hicks and Vali, 1972; Kumai, 1982; Deshler et al., 1987) they will rime rather rapidly in the presence of supercooled water and begin to fallout within the next 5 to 10 min. Given an average wind speed of 10 m/s, the crystals will initially begin to fallout 10 km downwind of the release point. This will vary with liquid water content, wind speed and the height of the underlying terrain. Those crystals that have not reached a size sufficient for fallout will continue downstream. It is anticipated that the bulk of the crystals will have fallen out within 60 min or 36 km downwind, again dependent on wind speed. With dispensing sites near the crest, the descent of air downwind of the crest will accelerate fallout but may also sublimate some of the smaller ice crystals. Therefore, a combination of critical dispenser placement and optimized seeding conditions will be needed to minimize this effect. This will be discussed in the following sections. It is calculated that each dispenser will produce approximately 12,500 $m^3$/hr under suitable cloud conditions.

In conclusion, propane satisfies many critical requirements for effective seeding in Sierra Nevada winter mountain clouds. First, the requirement that it be released in supercooled cloud eliminates the uncertainty of vertical transport to the -5 °C level or colder required by AgI. Liquid water can be confirmed by icing rate observations. [Aircraft seeding in the SCPP was performed almost exclusively to assure direct injection into clouds containing supercooled water]. Ground release assures a continuous source of nuclei during appropriate conditions.

3.4 Proposed Target Areas

Phase I will be a multi-year pilot program to confirm proper dispensing design, release rates, and functional performance under severe wind and rime icing conditions. Three dispensers will be placed on the Sierra crest, southwest of the primary target above 2100 m elevation. (Fig. 1).

A ground microphysics laboratory (Deshler, 1988) will be established at the Johnsville (JVL) ski area, Fig. 1. This ski area is just over 1500 m elevation and is approximately 5 km downwind of the dispensers. Therefore, it should be targeted with the most rapidly falling crystals during lighter wind conditions.

3.5 Propane Dispenser Design and Operation

The propane dispenser and site setup is shown in Fig. 6. The design and

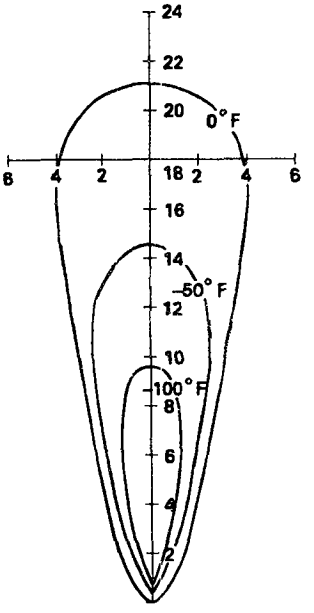


**Figure 4** *Cooling as a function of distance (in.) from the nozzel from release of liquid propane at 38 l/hr. From Vardiman et al. (1971).*

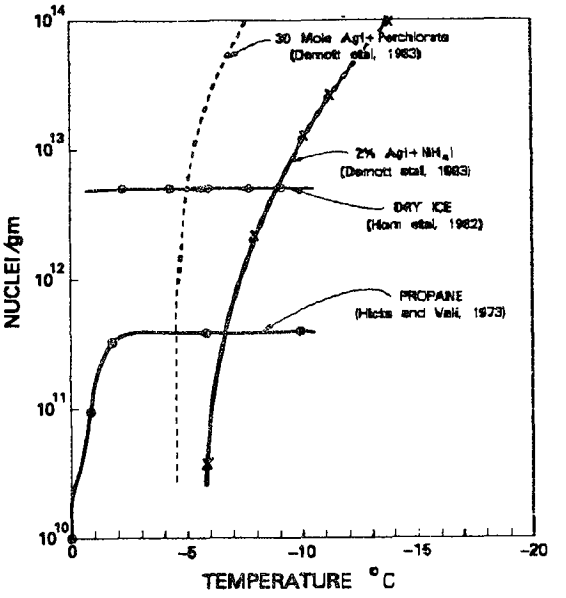


**Figure 5** *Activity spectra of various glaciogenic seeding material as a function of temperature as available from the published literature.*

fabrication of the prototype dispenser was completed by North American Weather Consultants under a Bureau contract. The dispenser is radio controlled via a microwave relay. Both control information and status information is communicated by radio via an on-site microprocessor. Status information includes volume of propane flow, propane tank level and spray temperature to verify actual liquid release (a temperature less than -30 °C verifies liquid spray). Three release nozzles have been mounted but only one is used at a time. If flow ceases, the back-up nozzles can be utilized. Denatured alcohol at a 3 percent by volume solution is added to each tank to minimize nozzle clogging.

Preliminary dispenser release rates have been determined. Using a single nozzle the release rates have been lowered to 11 l /hr from the 38 l/hr now currently used by the Air Force. Dispenser installation will be made in early November upon Forest Service approval and completion of the environmental reporting requirements.

It is envisioned that several different seeding techniques will be used for testing. This includes pulsed seeding (i.e. generator on for 3 hours, then off for 3 hours). Once it is established that the effects of the seeding can be observed at Johnsville, days will be established in which personnel from the Operations Control Center will determine the ON-OFF sequence of the dispensers without notifying the crew at the microphysics laboratory at Johnsville. These procedures should establish the repeatability of the seeding effects.

Phase II of this project (1989-90 winter) will include installation of ten dispensers along the Sierra Crest west and southwest of Johnsville, approximately 10 km upwind. The dispensers will be roughly 2 km apart. Assuming a 15° spread, the ice crystal plumes should be fairly continuous 10 km downstream of the dispensers. Once the effects of the seeding are determined, the statistical design will be implemented. (see Section 6.0).

Phase III would establish dispensing sites along much of the high country within the proposed target area. This would probably not occur until after the third to fifth year of the project to allow testing and evaluation of the proposed project design and allow for reduced seeding trials during wet periods when suspension criteria are invoked (Section 5.0)

## 4.0 SEEDING DECISION MAKING

As has been mentioned, for liquid propane to be an effective seeding agent it must be released within supercooled cloud. This will require knowledge of the presence of supercooled liquid water at the dispensing sites. These observations are being made directly through application of remote mountain icing rate stations. These stations telemeter icing occurrence, temperature, humidity, wind speed, and wind direction back through the California Data Exchange satellite downlink in Sacramento. Several icing stations are required at elevations representative of dispensing site elevations. Two sites have been

established and are shown in Fig. 1. Rawinsonde sites will be located at Oroville and Johnsville. Winds and temperature will be used as input to the numerical targeting model developed as part of the SCPP. (Rauber et al, 1988).

Seeding will commence with the onset of icing. The time of icing onset might be anticipated by determining the timing of cold frontal passage across the dispensing site network. As found by Reynolds and Kuciauskas (1988) and Ryerson (1988), the onset of liquid water occurs quite frequently with or shortly after a surface or upper- level cold frontal passage. Frontal passage is closely associated with a distinct gradient in cloud top temperature as seen on infrared satellite images. Therefore, by monitoring satellite images and icing information, seeding onset time might be estimated. Seeding will be terminated when no icing has occurred for at least 2 hours. Again, satellite images will also help indicate when cloud break-up is occurring to assure conditions suitable for seeding are over.

Rawinsonde data will be monitored to assure targeting within the Feather River basin is expected via model output. This will require periodic launches at six hour intervals. Wind information from the icing stations is used between rawinsonde launches.

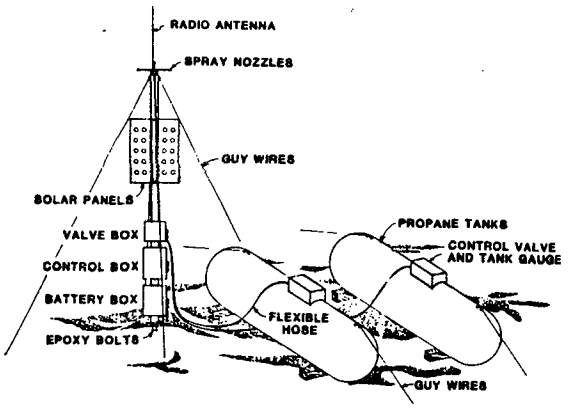


**Figure 6** *Propane dispenser design and example of a typical site set-up on a mountain peak.*

## 5.0 SUSPENSION CRITERIA

Suspension criteria have been developed by the Flood Forecasting Section of the Department of Water Resources based on historical data indicating threshold levels when snowpack or river flow levels begin to cause concern for potential flood generations. The following sections list the criteria to be used.

### 1. Excess Snowpack Water Equivalent

When the water content of the snowpack in the Feather River Basin, as measured at 25 identified snow courses exceeds the accumulation envelope defined by the following percentages of April 1 average amounts on the same date:

| | |
|---|---|
| January 1 | 110% |
| February 1 | 130% |
| March 1 | 150% |
| April 1 | 160% |

### 2. Rain-Induced Winter Floods

Quantitative precipitation forecasts issued by the National Weather Service which would produce excessive runoff in the project area or downstream areas as determined by the Flood Forecasting staff of the Department of Water Resources or these conditions are observed.

a. 60,000 cfs or more inflow to Oroville Reservoir.

b. Whenever Oroville Reservoir is encroached into flood control space and releases are being made over the spillway at Oroville Dam (normally whentotal releases are in excess of about 20,000 cfs.

c. Whenever flood flows or stages are occurring or forecast to occur which exceed flood warning stages on the Feather below Oroville

(1) River stages near Gridley at or over 95 feet.
(2) River stages at Yuba City at or over 65 feet.
(3) River stages at Nicolaus at or over 43 feet.

### 3. Severe Weather

a. Whenever the National Weather Service has issued a flash flood warning for the project area.

### 4. Other Special Circumstances

The DWR Project Manager judges conditions are or may be perceived to be so hazardous as to warrant suspension of seeding. This may include the issuance of avalanche warnings within the project area.

## 6.0 EVALUATION

The evaluation of the snowpack enhancement program will consist of two separate efforts. The first to be emphasized during the first 3-5 years of the program, will require direct physical measurements of the

seeding effects downwind of the dispensing sites (see Section 3.4). It is anticipated that these observations will lay the physical foundation for the second phase of the evaluation. This second phase is not expected to begin until after the full complement of dispensers is in place, probably after the fifth year of the project. This second phase will consist of a statistical analysis of precipitation both within the target area and in areas outside the target area and felt to be untreated. This is called a target/control evaluation method. This will require a high degree of correlation between these two locations. It is anticipated that from historical data available and with subsequent augmentation of the existing precipitation gauge network during years one through five, adequate control gauges can be established. Preliminary studies indicate as high as a .74 correlation coefficient for 3 hourly periods having precipitation between existing target and control sites. The target/control evaluation scheme will be augmented with a three to one randomization scheme. That is for every three storms seeded, one will be left as a control. The 3 to 1 ratio is used to maximize precipitation increases while still providing some control for evaluation purposes. It is envisioned this method will allow a reasonable opportunity to evaluate statistically the impact seeding has on precipitation after the second 5 years of the project.

## 7.0 ACKNOWLEDGEMENTS

This work was supported by the California Department of Water Resources and the Bureau of Reclamation under Cooperative Agreement #B-56392. Mr. Fred Clark, of North American Weather Consultants, provided the design of the propane dispenser.

## 8.0 REFERENCES

Demott,P.J.,W.G. Finnegan, and L.O.Grant,1982: An application of chemical kinectic theory and methodology to characterize the ice nucleating properties of aerosols used for weather modification. J. Clim. Appl. Meteor.,22,1190-1203.

Deshler,T.,1988: Calibration of ice particle measurements at the ground using an aspirated 2D-C. J. Atmos. Oceanic Tech.,5,547-560.

_____,D.W. Reynolds, and J.H. Humphries, 1987: Observations of snow crystal concentration , habit, riming, and aggregation collected at the ground during six fog seeding experiments. Eleventh AMS Conference on Weather Modification, Oct. 6-8, Edmonton, Alberta, Canada. 118-121.

Heggli,M.F. and R.M. Rauber, 1988: The characteristics and evolution of supercooled liquid water in wintertime storms over the Sierra Nevada: A summary of microwave radiometric measurements taken during the Sierra Cooperative Pilot Project. J. Appl. Meteor.,27,989-1015.

Hicks, J.R. and G. Vali, 1973: Ice nucleation in clouds by liquified propane spray. J. Appl.Meteor.,12,1025-1034.

Horn,R.D., W.G. Finnegan, and P.J. Demott,1983: Experimental studies of nucleation of dry ice. J. Appl. Meteor.,21,1567-1570.

Kumai, M., 1982: Formation of ice crystals and dissipation of supercooled fog by artificial nucleation, and variations of crystal habit of early growth stages. J. Appl. Meteor.,21,579-587.

Rauber, R.M., R.D. Elliott, J.O. Rhea, A.W. Huggins, and D.W. Reynolds, 1988: A diagnostic technique for targeting during airborne seeding experiments in wintertime storms over the Sierra Nevada. J. Appl. Meteor., 27, 811-828.

Reynolds, D.W., 1988: A report on winter snowpack augmentation. Bull. Amer Meteor. Soc.,69,1290-1300.

Reynolds,D.W. and A.S. Dennis,1986: A review of the Sierra Cooperative Pilot Project. Bull. Amer. Meteor. Soc.,67,513-523.

_____ and A.P. Kuciauskas,1988: Remote and in-situ observations of Sierra Nevada winter mountain clouds: Relationship between mesoscale structure, precipitation and liquid water. J. Appl. Meteor., 27, 140-156.

Ryerson,C.C.,1988: Atmospheric icing climatologies of two New England Mountains. J. Appl. Meteor.,27,1261-1281.

Vardiman,L.,E.D. Figgins and H.S. Appleman,1971: Operational dissipation of supercooled fog using liquid propane. J. Appl. Meteor., 10, 515-525.

# TEMPORAL VARIATIONS OF CLOUD LIQUID WATER DURING WINTER STORMS OVER THE MOGOLLON RIM OF ARIZONA

Arlin B. Super and Edmond W. Holroyd III
Bureau of Reclamation
Denver CO 80225

Abstract. Several winter storms were observed by various instrumentation systems over the Mogollon Rim of Arizona during early 1987. The storms commonly displayed considerable temporal variability in CLW (cloud liquid water) as monitored by a microwave radiometer. The vertically integrated liquid amounts were often inversely correlated with the height of the cloud tops as measured by radar, suggesting that periods with shallow clouds and warm tops may be the most seedable. However, there were important exceptions to this general rule, associated with strong low-level horizontal winds that presumably produced significant uplift and more condensate than nature could convert to snowfall.

Three storm episodes were selected for illustration of the short-term variability in CLW. It is shown that shallow clouds with abundant liquid often occurred at the beginning and ending phases of a storm, and sometimes in the middle portion as well. However, the timing and duration of the CLW periods would be very difficult to forecast, and limiting seeding operations to just CLW periods would usually be impractical. Rather, seeding would probably need to be continuous throughout most storm episodes because of inability to respond to short-term variations in available liquid water. It is suspected that the situation is similar for other mountain barriers of the West.

## 1. INTRODUCTION

Scientists involved with seeding winter storms over the mountains of the Western United States have long been aware that the storms' temporal variations are often substantial and rapid. Precipitation records or radar cloud top observations are just two indicators of these variations. Yet, in our attempts to understand the processes involved in complex storms, it is often necessary to generalize. References are made to "orographic" storms or "shallow" versus "deep" storms. A storm may be divided into prefrontal and postfrontal phases for ease of comprehension. But a more detailed examination of any storm or phase so designated usually reveals that conditions varied considerably with time and distance and also from storm to storm.

The problem of defining storms or their phases is particularly difficult for randomized seeding experiments, and serious compromises are often made where the experimental unit becomes the 24-hour day or some other rather arbitrary unit. While improvements in instrumentation and knowledge have gradually aided our ability to define portions of storms or cloud systems that are reasonably similar to others, the problem of definition is still difficult, especially if it must be done prior to an episode when a randomized seeding decision is called for. The problem has likely contributed to the limited success of several seeding experiments because quite dissimilar cloud systems may be grouped into the same category for statistical analysis.

This paper illustrates some of this variability in important storm characteristics, specifically over the crestline of the Mogollon Rim of Arizona. In particular, the availability of CLW (cloud liquid water) is addressed. The implications for seeding strategies are also discussed.

## 2. OBSERVATIONS

The most important characteristic of winter storms for the weather modification operator is CLW, especially the portion that is supercooled, because this is the substance that the operator attempts to convert to snowfall. Those storms or portions of storms that naturally convert all CLW to snowfall cannot generally have their snowfall augmented by seeding. (Some limited potential may exist between ice and water saturation that will be ignored here.) CLW has also proven to be one of the most difficult parameters to routinely monitor. Aircraft measurements must be limited to brief (2 to 4 h) portions of the storms

and are usually made at least 600 m above the highest terrain within several kilometers of the flight path. Icing rate meters on towers sample only the lowest portion of the cloud over the particular site, which may not be representative of conditions only a few tens or hundreds of meters higher (Boe and Super, 1986). Yet, recent work has indicated that much, perhaps most, of the CLW in winter orographic storms lies between normal aircraft sampling levels and surface towers (e.g., Holroyd and Super, 1984).

Recently, microwave radiometers have made possible the continuous observation of total CLW along their field of view, which has substantially increased understanding of winter storms over the mountains. Examples of studies using these new instruments, sometimes in conjunction with aircraft measurements, include Holroyd and Super (1984), Rauber et al. (1986), Rauber and Grant (1986), and Boe and Super (1986).

During mid-January to mid-March 1987, a microwave radiometer, a sensitive 5.4-cm radar, and a high-resolution precipitation gauge were collocated at Happy Jack, Arizona, on the crestline of the Mogollon Rim. The crest location is important because CLW passing overhead may be considered excess to that liquid which nature is converting to snowfall. Cloud droplets typically evaporate a short distance downwind in the lee subsidence zone.

The Happy Jack site, located about 55 km south of Flagstaff, and its instrumentation have been described by Super and Boe (1988). Nearly continuous records of vertically integrated CLW, cloud top height and structure, and precipitation rate were obtained through several storm episodes. Three episodes have been selected to illustrate some common features and some differences among the storms, as well as their temporal variability over the observing site.

## 3. STORM VARIABILITY

Examination of the several 1987 storms revealed that their character usually changed considerably with time. The Arizona storms were almost all associated with synoptic scale disturbances. They contained such diverse cloud forms as cirrostratus, altostratus, stratus, orographic stratus or stratocumulus, downwind anvils, and embedded convection. Such clouds can be with or without the presence of CLW or of precipitation.

The presence of high clouds (above 6 km or 20 000 ft m.s.l.), physically connected to lower clouds by particles producing a radar echo, was usually a good indicator that CLW values would be suppressed. Such high clouds will frequently have tops colder than -30°C and therefore may be contoured in typical nighttime satellite infrared images. Analysts with the Sierra Cooperative Pilot Project in California have identified the "cirrus passage" (the advection of the rear edge of a high cirriform cloud band over the project area) as a frequent indicator of the initiation of greater values of CLW in the lower clouds (Reynolds, 1988). But high tops themselves have no effect if the ice particles do not fall into the lower clouds. The same inverse correlation of cloud tops and CLW frequently was apparent in the Mogollon Rim clouds, but there were exceptions in the observations.

In a similar fashion, the presence of high concentrations of ice particles and associated increased precipitation usually precluded the presence of abundant CLW as shown by Rauber et al. (1986). The ice particles rapidly grow at the expense of such CLW and consume it. Such high concentrations are typically associated with periods in which the cloud tops are high. Nucleation of ice particles is commonly thought to be more efficient at the cold temperatures found in high cloud tops, although factors other than temperature may be important (Hobbs and Rangno, 1985).

Figure 1 and two similar figures to follow plot three important storm characteristics on the same time axis for the entire storm episode. The hourly precipitation amounts from the high-resolution gauge are plotted at the bottom of Figure 1. The radiometer vertically integrated CLW, showing three general periods of liquid in the clouds above Happy Jack, is plotted in the middle of the figure. A time-height diagram of echoes from the 5.4-cm Skywater radar is plotted at the top of the figure.

The radar echo plot in Figures 1, 2, and 3 was constructed from RHI (range height indicator) scans made to the north of Happy Jack every 5 minutes. The equivalent radar reflectivity factor was averaged for the 0.1 km by 1.0 degree range bins located within 2.2 to 3.3 km horizontal distance of the radar. This range was chosen to maximize radar sensitivity while minimizing the ground clutter return. Up to four levels of equivalent reflectivity factor are shown on all radar plots: Any values exceeding 0 dBz are shown in black; those between -10 and 0 dBz are gray; the next lighter shading represents -10 to -20 dBz; and the lightest, -25 to -20 dBz, represents the weakest echoes detectable with the particular radar system. While the greater dBz values generally indicate higher precipitation

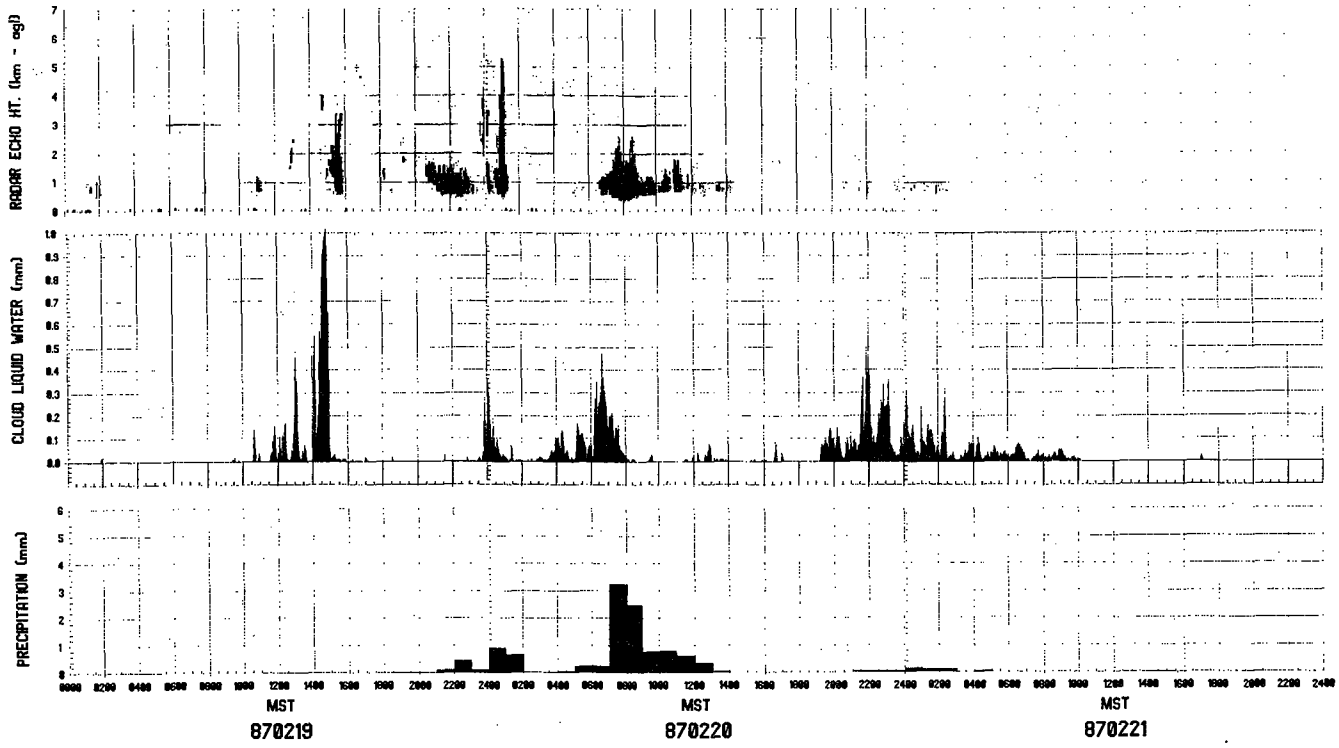


Figure 1. - Time history of precipitation, CLW, and radar echos for February 19-21, 1987.

rates, the relationship can be complex for snow and ice particles, as discussed by Smith (1984).

Figure 1 could also include such variables as temperature, dewpoint, winds, and tower icing rates to show the passages of various synoptic features. Such variables were considered in detailed storm analysis but were omitted from the figures in this paper for the sake of clarity.

The storm episode illustrated in Figure 1 lasted about 48 hours. This episode was chosen for presentation first because it shows wide variations in cloud structure over the storm period. During this storm, a low and trough system over New Mexico retrograded into central Arizona and then resumed a southeastward movement out of the project area.

After the passage of some low cirriform clouds, the episode began with the slow rise of cumulus clouds to the cumulonimbus stage from about 1000 to 1700 [all times l.s.t. (local standard time)] on February 19. Cloud liquid water amounts varied considerably with time, exceeding 1.0 mm at 1445 and then rapidly diminishing to almost zero as the radar echo intensified. The clouds were mostly confined to the higher terrain and therefore appeared to be under mesoscale control, but satellite photos showed enough neighboring clouds to suggest synoptic control.

From about 1700 on February 19 to 0200 on February 20, the clouds were basically stationary debris from earlier convection. This generated a snowfall containing aggregates. Moderate CLW existed for only about 1.5 hours centered near midnight. As the system intensified, CLW amounts increased until almost 0700 on the 20th. Then the high clouds became connected to the lower clouds, and a heavy snowfall consumed the CLW.

After 1200 on February 20, the clouds became towering cumulus until 1800; but the convection was not as tall as on the previous day, and amounts of CLW were quite limited.

At 1800 the low began to pass to the south of the project area as it resumed a southeastward movement. Area winds shifted to being strongly from the northeast. The flow produced a low orographic stratus (upslope) cloud generally confined to the high terrain of the Mogollon Rim. The cloud system produced many hours of CLW and only trace precipitation, suggesting it was very suitable for seeding.

Figure 1 illustrates the general tendency for clouds with tops under 6 km m.s.l. (mean sea level) [3.7 km a.g.l. (above ground level) in the figure], not connected to higher cirriform clouds, to have CLW. It illustrates a case with CLW at both the start and end of an episode as well as within, all of which appeared in low clouds.

An important counterexample to the more typical storm sequence occurred on January 30-31, 1987, as illustrated in Figure 2. (A power outage after 0500 on the 31st interrupted the radar data for about 3 hours. Further, CLW data were interpolated between 1915 and 2115 on the 30th when melting snow on the reflector gave erroneous readings.) The common appearance of an abundance of CLW from a low stratiform cloud at the end of the episode is illustrated well. But the unusual feature is the very strong CLW signal during the night hours when the radar tops were high and the precipitation rates were moderate. Strong flow over the barrier apparently produced much more CLW than could be consumed by the falling ice particles from the deep cloud system. Acoustic sounder winds at 300 m a.g.l. over Happy Jack were about 14 m $s^{-1}$ from the northeast at the time of peak CLW late on the 30th.

An aircraft mission was flown over Happy Jack (elevation 2.3 km m.s.l.) from shortly before 1000 to 1100 on January 31. The King probe on the aircraft measured mean liquid water contents near 0.15 g $m^{-3}$ with peaks as high as 0.7 g $m^{-3}$. Ice particle concentrations averaged less than 0.1 $L^{-1}$ in the upper portions of the layer cloud which had a top at 3.8 km m.s.l. where the temperature was -9°C. The University of Wyoming King Air 200T aircraft, certified for flight into known icing conditions, was unable to stay in the cloud for more than several minutes at a time due to heavy airframe icing. Yet the average radiometer vertically integrated CLW was only 0.2 mm during the aircraft mission. This suggests that aircraft sampling would have been impractical during the higher CLW periods experienced late on the 30th and from 1300 to 1500 on the 31st.

Examination of all 1987 aircraft sampling periods over Happy Jack revealed that the surface radiometer never observed a mean hourly CLW amount greater than 0.22 mm when the aircraft was nearby - essentially the amount present during the January 31 flight. While the vertical distribution of liquid water may vary considerably within and between storms, the heavy icing encountered on that mission suggests that aircraft sampling might

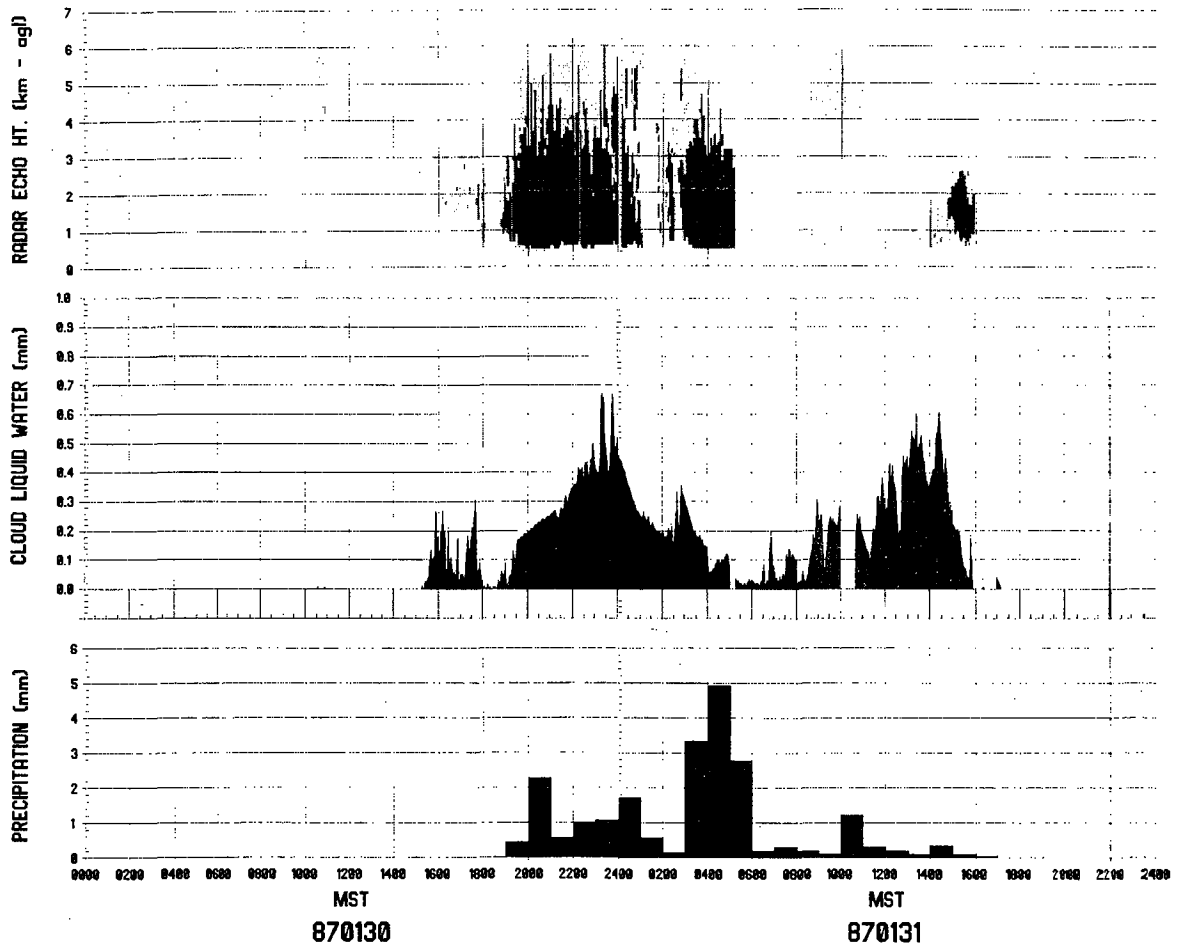


Figure 2. - Time history of precipitation, CLW, and radar echos for January 30-31, 1987.

well be impractical when wetter clouds are present. About 10 percent of all hours with CLW detectable by the radiometer were in excess of 0.2 mm during the 1987 field season. One hour exceeded 0.6 mm. This suggests that aircraft measurements of orographic clouds may underestimate actual liquid water contents for two reasons: (1) the impracticality of flying near the mountainous terrain noted earlier, and (2) the inability to fly in the wetter clouds for more than very brief periods.

The varied character of the storm that brought the largest snowfall to the region in several years is illustrated in Figure 3. The episode began, as usual, with moderate CLW in low clouds. It then changed to high CLW contents from clouds with moderate precipitation and radar tops of a middle height. The presence of light CLW with high radar tops and an extremely high precipitation rate is shown for the daytime hours of February 24. This illustrates that even heavy precipitation may not totally consume the CLW presumably being produced at low levels by the strong winds then present (sometimes exceeding 17 m $s^{-1}$ according to the acoustic sounder). Thereafter, the patterns are similar to those in Figure 1 with high CLW amounts coexisting with shallow clouds.

## 4. DISCUSSION

Several winter storms over the Mogollon Rim of Arizona were investigated during early 1987 using radar, a microwave radiometer, a high-resolution precipitation gauge, and various other observing systems including a cloud physics aircraft for portions of the episodes. These measurements have revealed a number of important features of interest to cloud seeding.

As has been shown in some earlier studies, there was a general tendency for CLW to be present over the crest within shallow clouds, but limited in amount or absent in the presence of deep clouds having cold tops. The beginning and ending portions of the storm episodes frequently had shallow clouds and relatively abundant CLW, suggesting they were suitable for seeding aimed at snowfall augmentation. Additional periods with CLW were in evidence during the middle of some episodes when high clouds became disconnected with lower cloud decks.

Important exceptions to the general rule were found as illustrated in Figure 2. Very abundant CLW existed for many hours during a period of moderate snowfall from deep clouds. Apparently, the strong near-surface winds produced far more uplift and associated condensate than nature could convert to snowfall. Even the heavy snowfall of February 24 (Fig. 3) failed to fully utilize available condensate although CLW amounts were limited to near 0.05 mm in this case.

Another important point emerges from the figures shown. While some periods with abundant CLW were of many hours' duration, others were brief. Further, the transition from periods with abundant CLW to periods with little or none was often very rapid. This suggests that a seeding strategy based on a forecast of suitable conditions will often fail. Even responding to observations of existing conditions would be challenging, especially for airborne seeding with the necessity to

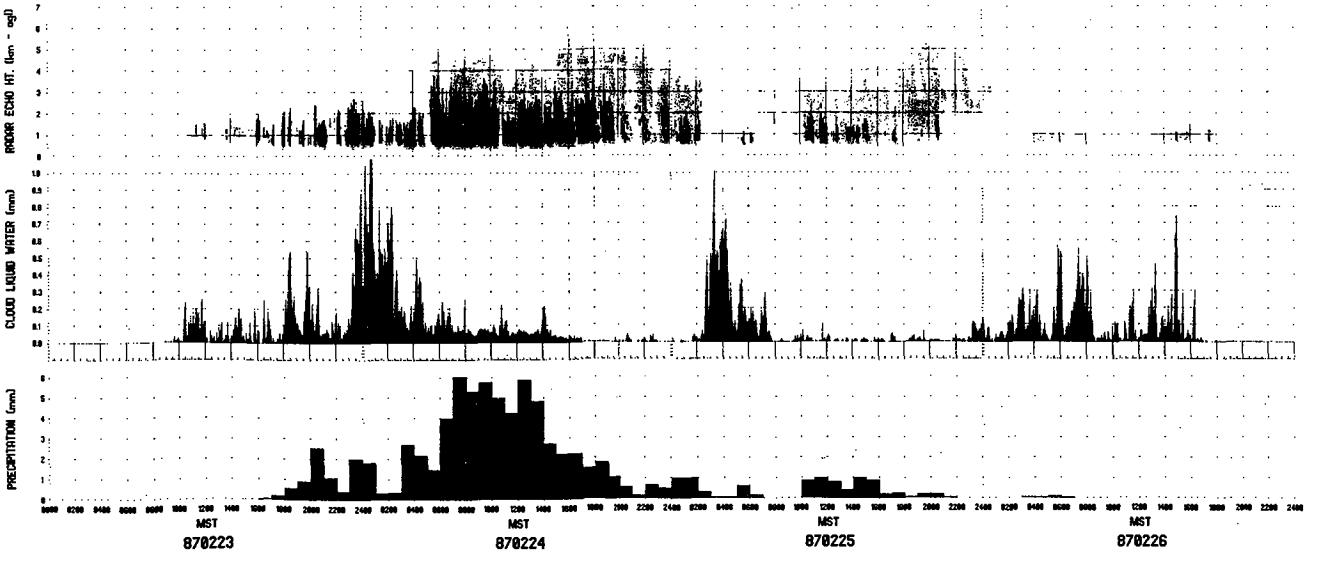


Figure 3. - Time history of precipitation, CLW, and radar echos for February 23-26, 1987.

file flight plans an hour or so before takeoff. The only reasonable approach may be to attempt to seed throughout the storm episode with the assumption that seeding will not significantly decrease snowfall during periods without excess CLW. Fortunately, there is evidence that this assumption may be valid, at least in the northern Rockies (Super, 1986; Super and Heimbach, 1988).

This paper addresses only temporal variability of CLW above a particular observing point. Studies in other regions (e.g., Rauber and Grant, 1986) and aircraft measurements over the Mogollon Rim have demonstrated considerable spatial variability as well. Thus, when the observations above any mountain site indicate abundant CLW, the atmosphere may have no liquid some kilometers away. And, of course, the situation may be reversed a short time later. This further emphasizes the difficulty of attempting to rapidly respond to indications of probable seedability from any practical observing network.

In summary, measurements from several Arizona winter storms have indicated considerable temporal variability in storm characteristics, particularly in the amount of liquid water available. This implies that the seeding potential of the storms also varies markedly with time. Super (1986) suggested that seeding Montana winter storms was highly effective during a small portion of the 6-hour blocks investigated, but had little or no effect for the other periods. That may be partially due to similar variations in CLW. If only limited periods with abundant CLW exist, only those periods have the possibility of substantial snowfall increases when seeded.

Future seeding experiments should routinely monitor the CLW content, preferably with a radiometer. Statistical analysis of randomized experiments should be considerably "sharpened" if experimental periods are partitioned by CLW availability. Physical experiments that attempt to directly detect seeding effects (e.g., Super and Heimbach, 1988) also need to monitor whether CLW is available.

ACKNOWLEDGEMENTS

Jack McPartland directed the field program that obtained the measurements discussed in this paper. Bruce Boe contributed significantly to both data collection and analysis. John Lease provided program direction for the Bureau of Reclamation while Dennis Sundie of the State of Arizona provided important coordination.

This study was jointly supported by the Bureau of Reclamation and the Arizona Department of Water Resources. The U.S. Forest Service provided key ground facilities for the field program.

REFERENCES

Boe, B.A., and A.B. Super, 1986: Wintertime characteristics of supercooled liquid water over the Grand Mesa of western Colorado. J. Weather Mod., 18, 102-107.

Hobbs, P.V., and A.L. Rangno, 1985: Ice particle concentrations in clouds. J. Atmos. Sciences, 42, 2523-2549.

Holroyd, E.W., and A.B. Super, 1984: Winter spatial and temporal variations in supercooled liquid water over the Grand Mesa, Colorado. Preprints Ninth Conf. on Inadvertent and Planned Weather Modification, May 21-23, Park City, UT, 59-60.

Rauber, R.M., and L.O. Grant, 1986: The characteristics and distribution of cloud water over the mountains of northern Colorado during wintertime storms. Part II: Spatial distribution and microphysical characteristics. J. Climate Appl. Meteor., 25, 489-504.

Rauber, R.M., L.O. Grant, D.X. Feng, and J.B. Snider, 1986: The characteristics and distribution of cloud water over the mountains of northern Colorado during wintertime storms. Part I: Temporal variations. J. Climate Appl. Meteor., 25, 468-488.

Reynolds, D.W., 1988: A report on winter snowpack-augmentation. Bull. Amer. Meteor. Soc., 69, 1290-1300.

Smith, P.L., 1984: Equivalent radar reflectivity factors for snow and ice particles. J. Climate Appl. Meteor., 23, 1258-1260.

Super, A.B., 1986: Further exploratory analysis of the Bridger Range winter cloud seeding experiment. J. Climate Appl. Meteor., 25, 1926-1933.

Super, A.B., and B.A. Boe, 1988: Wintertime cloud liquid water observations over the Mogollon Rim of Arizona. J. Weather Mod., 20, 1-8.

Super, A.B., and J.A. Heimbach, 1988: Microphysical effects of wintertime cloud seeding with silver iodide over the Rocky Mountains. Part II: observations over the Bridger Range, Montana. J. Appl. Meteor., 27, 1152-1165.

# AN EFFICIENT, FAST FUNCTIONING NUCLEATING AGENT -- AgI·AgCl-4NaCl[1]

Feng Daxiong
Academy of Meteorological Science
State Meteorological Administration
Western Suburb, Beijing
People's Republic of China

and

William G. Finnegan
Atmospheric Sciences Center
Desert Research Institute
University of Nevada System
Reno, Nevada 89506 U.S.A.

Abstract. A composite ice nucleus aerosol, AgICl-4NaCl, has been generated and characterized for nucleation efficiencies, rates of ice crystal formation, and mechanisms of nucleation, under water saturation and transient supersaturation conditions. The addition of NaCl to the highly efficient contact nucleus, $AgI_{0.8}Cl_{0.2}$, changed the nucleation mechanism to condensation-freezing at water saturation and increased the rates of ice crystal formation dramatically, while retaining the high efficiency of the AgICl nucleus aerosol. Under transient supersaturation conditions, this new aerosol demonstrated improved ice nucleation efficiencies at T > -12 C, and even faster ice crystal formation rates, suggesting a change of nucleation mechanism to forced condensation-freezing. This ice nucleation aerosol should be advantageous for use in weather modification field programs under conditions where low cloud droplet concentrations suggest the use of a condensation-freezing nucleant.

## 1. INTRODUCTION

Since Vonnegut found in 1947, that silver iodide aerosols are effective ice nuclei, AgI has been widely used in weather modification experiments and operations as cold-cloud nucleating agents. When generating AgI, other chemical substances are usually added. For example, when using AgI-acetone solution combustion as a generating method, $NH_4I$, KI or NaI is added as a solubilizer. In AgI pyrotechnics silver iodate $AgIO_3$ is used as an oxidizer, and magnesium, and aluminum as fuels. Even though AgI artificial ice nuclei can be generated by many different ways, they are not pure AgI aerosols because of the existence of other chemical materials. Due to the different properties of the added materials, the ice nucleation mechanisms, the nucleation efficiencies and the nucleation rates will therefore be different.

Vonnegut and Chessin (1971) compared the nucleation efficiencies of pure AgI and AgI·AgBr. Their results showed that pure AgI has a lower nucleation efficiency. They also found that the lattice structure will be closer to that of ice if part of the iodine atoms are replaced by bromine atoms. Sax, et al., (1979) found that some of the Nuclei Engineering, Inc. (NEI) pyrotechnic formulations contained small amounts of chlorine and had aerosol nucleation efficiencies at -10 C, which were one or two orders of magnitude higher than those which did not contain chlorine. They concluded that this increase was caused by the chlorine changing the lattice structure, or introducing active sites on the AgI surface. Later DeMott, et al., (1983) generated AgI·AgCl compound nuclei using an AgI-$NH_4I$-$NH_4ClO_4$-acetone-water burning system. Such nuclei have one order of magnitude higher nucleation efficiencies at -12 C and three orders of magnitude higher efficiency at -6 C than that of pure AgI produced by the AgI-$NH_4I$-acetone system. They also showed that both of these nuclei are contact nuclei, and the nucleation rates are relatively slow. Blumenstein, et al., (1983) showed that the 2AgI-NaI nucleus aerosol is strongly hygroscopic and nucleates by a condensation-freezing nucleation mechanism. Under water-saturation condition, the nucleation rate is very slow and the nucleation efficiency is also low. Under transient supersaturation conditions there is a clear increase of nucleation rate, and the nucleation efficiency also increases at warmer temperatures. Feng and Finnegan (in preparation) studied the T8-1 pyrotechnic aerosols manufactured by different suppliers and concluded that there are big differences in the nucleation mechanisms using the same combination of substances. The pyrotechnics made by the U.S. Navy gave aerosols with lower nucleation efficiencies, but with very high nucleation rates and which were clearly acting as condensation-freezing nuclei. The aerosols from the pyrotechnics made by NEI have a lower nucleation rate and were reacting as contact nuclei. One possible reason is that the materials of different pyrotechnic formulations have different impurities. Therefore, the composition of AgI and different chemical impurities will lead to different nucleation mechanisms, different effectivenesses, and different nucleation rates.

Among various artificial nuclei, AgI·AgCl nuclei have the highest nucleation efficiencies (DeMott, et al., 1983), but they are contact nuclei with low nucleation rates. If hygroscopic material is added, it was thought possible that the nucleation mechanisms would be changed to

---

(1) English translation of "An efficient, fast functioning nucleating agent -- Composite AgI·AgCl-NaCl ice nuclei," originally published in Collected Papers of Meteorological Science and Technology, No. 8 (1985), by the Academy of Meteorological Science, Beijing, PRC.

condensation-freezing. With a careful choice of hygroscopic material, the advantage of the high nucleation efficiency could be retained, and a new high nucleation rate aerosol obtained.

## 2. INSTRUMENTATION AND PROCEDURES

The experiments were conducted in the isothermal cloud chamber of the Department of Atmospheric Sciences, Colorado State University. The cloud produced by the ultrasonic fog generator, was cooled to the chamber temperature before introduction into the chamber. The sizes of the cloud droplets are between 1-16 microns with mean diameter of 7 microns. The liquid water content inside the chamber was maintained at a constant value for each experiment. The values of liquid water content usually chosen were 0.5 g $m^{-3}$ (with corresponding droplet concentration of 2100 $cm^{-3}$) and 1.5 g $m^{-3}$ (4300 droplets $cm^{-3}$). The temperatures at different points of the chamber could be controlled with an accuracy of +- 0.3 C. The aerosols produced by the generator were diluted with ambient air in the wind tunnel. A volume of 4 liters of such diluted air was taken by a sampling syringe then mixed, at fixed ratios, with either pure dry air or saturated air at room temperature. The diluted aerosol samples were then injected into the cloud chamber. The ice crystals produced by the aerosols, fell onto pre-cooled microscope slides. The slides were taken out at certain time intervals (1-3 min.) and the number of ice crystals on the slides counted using a microscope. This process continued until the ice crystal generation ceased. From the cumulative number of ice crystals obtained from each experiment, the nucleation efficiency was calculated. The ice crystal nucleation rate was obtained by counting the number of ice crystals as a function of time. Detailed information about this chamber can be found in Garvey (1975).

In the past, this chamber was used to compare the nucleation efficiencies for various nucleant aerosols and those from different types of generators (DeMott, et al, 1983). In recent years, in cloud simulations and aerosol experiments, the method of chemical kinetics was introduced into the isothermal cloud chamber experiments (DeMott, et al., 1983). By observing the ice crystal nucleation rates changing with time after the aerosols had been introduced into the chamber, the nucleation rate and its relationships with various parameters (such as temperature, droplet concentration, supersaturation ratio, etc.) of the chamber, can be studied and the nucleation mechanisms can be determined. In this way, the nucleation characteristics of various artificial aerosols can be studied. The same methods were used in this experiment.

This experiment was based on the basic composition of AgI·AgCl studied by DeMott, et al., (1983). Sodium chloride (NaCl) was used as the hygroscopic material to add to AgI·AgCl. The reason for this choice is that NaCl will neither form complex compounds nor produce solid solutions with AgI. This addition was achieved by adding sodium perchlorate ($NaClO_4$) to the original solution, e.g., AgI-$NH_4I$-$NH_4ClO_4$-$NaClO_4$-$H_2O$-acetone. Sodium perchlorate is easily soluble in acetone (50 g $NaClO_4$ / 100 g acetone), and is reduced to NaCl during solution combustion. The AgI·AgCl-NaCl aerosols then result from combustion of the total solution.

There were two parts to this experiment. First, the temperature in the chamber was maintained at -10 C while changing the molar ratio between AgI and $NaClO_4$ in the solution in order to determine the optimum composition of AgI and NaCl in the generated aerosol. Secondly, the nucleation efficiencies and rates of this optimum composition were determined between -5 and -20 C.

## 3. EXPERIMENTAL RESULTS

### 3.1 The Best Molar Ratio of AgI to NaCl

In the testing solution, the molar ratio of AgI to $NaClO_4$ was changed from 1:0.5 to 1:5. The aerosols produced by combustion were diluted with dry air or saturated air at room temperature, and were then injected into the chamber at -10 C. In each, the nucleation efficiency was calculated from the total number of ice crystals produced, the rate of formation of AgI and the dilution ratio. The nucleation rate can be expressed in different ways. In this study, the time that 90% of the ice crystals formed (T90), is used as the nucleation rate. Figure 1a shows the AgI nucleation efficiency at different $NaClO_4$ molar concentrations. Figure 1b shows T90 as a function of the $NaClO_4$ concentration. The values for pure AgI in these figures were obtained from the results of DeMott, et al., (1983).

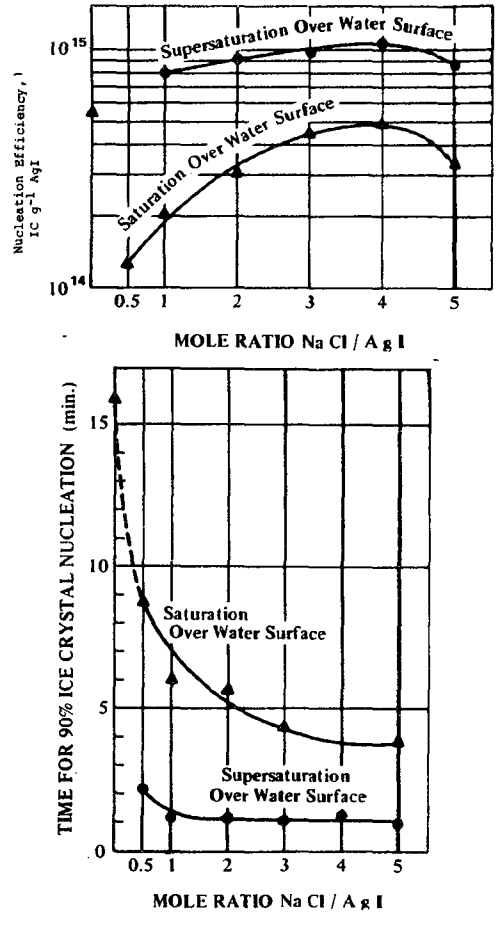


Fig. 1 Nucleation efficiencies (a) and times for 90% ice crystal nucleation (b) as a function of the NaCl/AgI ratios at -10 C.

Figure 1 shows that the highest nucleation efficiency and rate occur when the molar ratio between AgI and $NaClO_4$ was 1:4. At water saturation, the nucleation efficiency reached 4.9 x $10^{14}$ $g^{-1}$ AgI at -10 C, which was very close to the nucleation efficiency of AgI·AgCl, (5.4 x $10^{14}$ $g^{-1}$ AgI), under the same conditions. T90 was 3.8 min. for the composite nuclei, but for AgI·AgCl aerosols T90 was 16 min. When the sample was diluted with saturated air at room temperature, and injected into the chamber, a transient supersaturation was induced in the chamber. The nucleation efficiency reached $10^{15}$ $g^{-1}$ AgI at a molar ratio of 1:4. The nucleation rate increased dramatically with T90 shortening to 1.2 min.

3.2 The Nucleation Efficiency and Nucleation Rate as Functions of Temperature

Aerosols produced by burning the solution with the optimum molar ratio of AgI to $NaClO_4$ at -10 C were tested in the temperature range between -5 C and -20 C. Two sets of results were obtained under both water-saturation and transient supersaturation conditions. These results are shown in Figure 2.

Over the whole temperature range, the AgI·AgCl-4NaCl composite nuclei had very high nucleation efficiencies at water saturation, and they were close to the nucleation efficiency of the AgI·AgCl nuclei. The nucleation efficiency increased dramatically from -5 C to -12 C and reached 2 x $10^{15}$ $g^{-1}$ AgI at -12 C. As the temperature was decreased further to -20 C, the efficiency increase was slight with only a small increase under transient supersaturated conditions. The nucleation efficiency was lower than the values obtained at water-saturation in the temperature range between -5 and -7 C, but it is higher than those for water saturation values between -7 C and -20 C with the largest difference of about a half order of magnitude (see Figure 2a).

The nucleation rate increased with decreasing temperature. At water saturation, T90 was 18 min at -6 C and 1 min at -20 C. The change in nucleation rate with temperature was large when T > -12 C. In the -6 C to -12 C range the nucleation rate, under transient supersaturation conditions, increased much faster than under water-saturation conditions. T90 decreases from 18 min to 2 min at -6 C, but in the lower temperature range (-14 C to -20 C) there was no great difference between the supersaturation and water saturation values (Figure 2b).

3.3 The Nucleation Mechanism

In order to study the changes in the nucleation rate with changes in the concentration of droplets, we performed experiments with liquid water contents of both 0.5 g $m^{-3}$ and 1.5 g $m^{-3}$ at two different temperatures, -8 C and -20 C. The results are shown in Figure 3. The nucleation rate of the composite nuclei does not change with the liquid water content (or the droplet concentration). Therefore, AgI·AgCl-4NaCl nuclei are not contact nuclei. It is shown, from the experiments at both water saturation and supersaturation conditions, that these nuclei are sensitive to water vapor density, and both the nucleation efficiency and the nucleation rates increase greatly under transient supersaturation conditions. These results show that the nuclei are condensation-freezing nuclei.

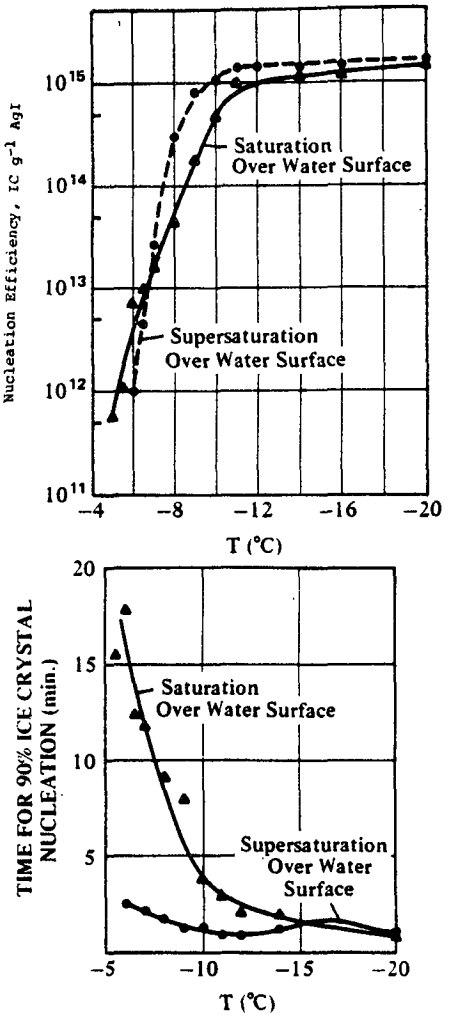


Fig. 2 Nucleation efficiencies (a) and times for 90% ice crystal nucleation (b) of AgI.AgCl-4 NaCl composite nuclei as functions of temperature and humidity.

3.4 Comparison with Other Nuclei

There are many other artificial nuclei generated by acetone solution combustion which have been used for weather modification purposes, but the most popular ones in recent years are AgI, AgI·AgCl, and 2AgI·NaI. The same kinds of studies were then conducted with these three nuclei as with our composite nuclei. Comparison between them are as follows. Some results on AgI and AgI·AgCl nucleus aerosols were obtained from DeMott (1982), and the results on 2AgI·NaI were from Blumenstein, et al., (1983). Their nucleation efficiencies and nucleation rates at -10 C are shown in Figure 4a and 4b, respectively. Figure 4a shows that the nucleation efficiencies of AgI·AgCl-4NaCl and AgI·AgCl nuclei are quite similar. The largest difference occurs at -8 C with AgI·AgCl nuclei two-fold higher than AgI·AgCl-4NaCl. At this time, AgI·AgCl nuclei have the highest nucleation efficiency of all artificial nuclei. This conclusion was drawn from

laboratory experiments where high droplet concentration can promote more rapid contact nucleation of AgI·AgCl nuclei to achieve the higher nucleation efficiencies and rates. In the real atmosphere, the concentration of supercooled droplets is about one order of magnitude smaller than that in the chamber, resulting in much slower nucleation rates for contact nuclei.

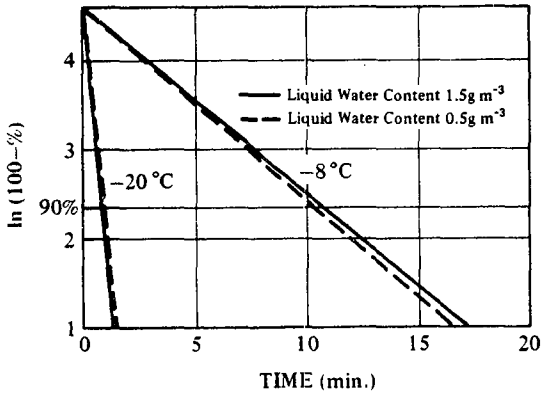


Fig. 3 Rates of depletion of AgI.AgCl-4 NaCl composite nuclei after introduction into the cloud chamber at different liquid water contents.

The AgI·AgCl-4NaCl nuclei are condensation-freezing nuclei, and will retain their nucleation rates, as measured in the chamber, because the nucleation mechanism is independent of droplet concentration. The comparison of AgI·AgCl-4NaCl nuclei with the pure AgI nuclei from AgI-$NH_4$I-acetone solutions shows that the nucleation efficiency of the composite nuclei is one order of magnitude higher at T > -12 C. The nucleation efficiency of AgI·AgCl-4NaCl nuclei was 2-3 orders higher than that of 2AgI·NaI nuclei, and the differences decrease with decreasing temperature. Figure 4b shows that after AgI·AgCl-4NaCl nuclei were injected into the chamber at -10 C, ice crystals were quickly produced, and the production rate decreased rapidly. The nucleation rate of the AgI·AgCl-4NaCl composite nuclei is faster than those measured for the other three kinds of nuclei.

## 4. CONCLUSIONS

As expected, if the hygroscopic material, NaCl, is added to AgI·AgCl aerosols, the nucleation process changes from contact nucleation to condensation-freezing nucleation. These experiments gave the optimum molar ratio of AgI·AgCl to NaCl and resulted in the fast and more efficient composite nuclei, AgI·AgCl-4NaCl. The discovery of these composite nuclei is important in the seeding of cumulus clouds with very strong updrafts and orogaphic clouds with strong horizontal wind speeds, in which high concentrations of ice crystals need to be generated in relatively short time periods. This factor is also important in cold fog dispersion operations.

In these experiments, only the optimum molar ratio of NaCl to AgI·AgCl for maximum efficiencies and rates was determined. Information on the size distributions of the aerosols generated and their chemical components still need further research and analysis. More research is needed on whether the nucleation mechanism of these composite nuclei will change if these nuclei are injected into the lower warm (T > 0 C) parts of clouds before they reach the upper cold (T < 0 C) regions. More experiments are needed on how to generate these kinds of composite nuclei, such as pyrotechnic generation.

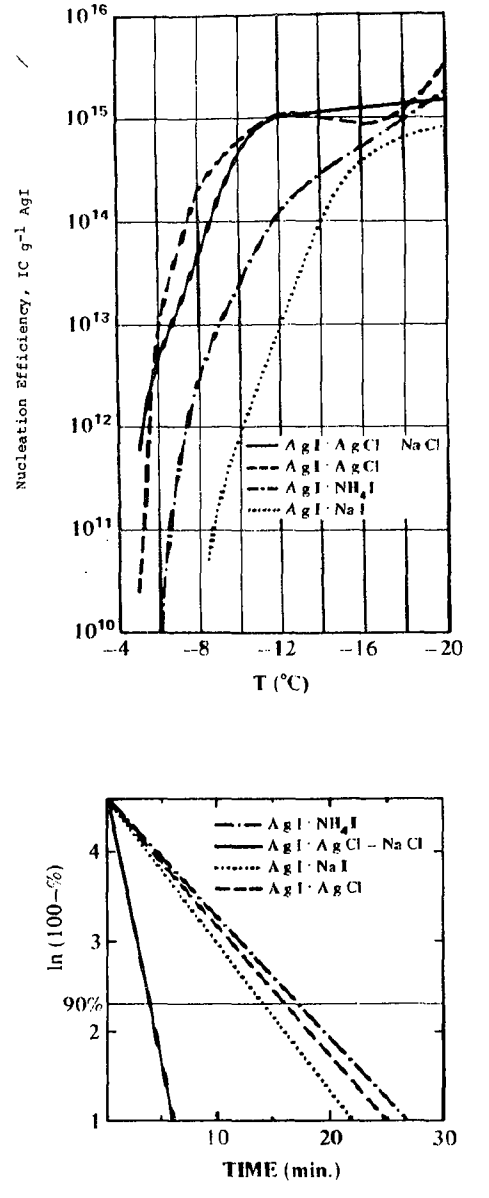


Fig. 4 Comparison of nucleation efficiencies (a) and rates of depletion of nuclei after introduction into the cloud chamber (b) for several different aerosols.


## 5. ACKNOWLEDGEMENTS

We thank Renyi Zhang and Stephen K. Chai for the translation of the original article into English. The experimental work was conducted in the Cloud Simulation and Aerosol Laboratory, Department of Atmospheric Sciences, Colorado State University, Fort Collins, Colorado.

## 6. REFERENCES

Blumenstein, R.R., W.G. Finnegan, and L.O. Grant, 1983: Ice nucleation by silver iodide-sodium iodide: A re-evaluation, J. Wea. Mod., 15, 11-15.

DeMott, P.J., 1982: A characterization of mixed silver iodide-silver chloride ice nuclei, Atmos. Sci. Paper No. 349, Dept. of Atmos. Sci., CSU, Fort Collins, Colorado, 124 pp.

DeMott, P.J., W.G. Finnegan, and L.O. Grant, 1983: An application of chemical kinetic theory and methodology to characterize the ice nucleation properties of aerosols used for weather modification, J. Clim. Appl. Meteor., 22, 1190-1203.

Feng Daxiong and W.G. Finnegan, The analysis of the ice nucleating characteristics of several TB-1 AgI flares (in preparation).

Garvey, D.M., 1975: Testing of cloud seeding materials at the Cloud Simulation and Aerosol Laboratory, 1971-1973, J. Appl. Meteor., 14, 883-890.

Sax, R.I., D.M. Garvey, and F.P. Parungo, 1979: Characteristics of AgI pryotechnic nucleant used in NOAA's Florida Area Cumulus Experiment, J. Appl. Meteor., 18, 195-202.

Vonnegut, B., and H. Chessin, 1971: Ice nucleation by co-precipitated silver iodide and silver bromide, Science, 174, 945-946.

"REVIEWED"

# OBSERVATIONS OF LIQUID WATER PERSISTENCE AND THE DEVELOPMENT OF ICE IN OKLAHOMA CONVECTIVE CLOUDS.

Michael R. Poellot
Department of Atmospheric Sciences
University of North Dakota
Grand Forks, ND 58202

and

John C. Pflaum
Cooperative Institute for
Mesoscale Meteorological Studies
University of Oklahoma
Norman, Oklahoma 73019

Abstract. During late spring of 1986 and September of 1987 the University of North Dakota operated an instrumented aircraft in convective clouds over Oklahoma to help assess the potential for rain increase cloud modification over the state. The Oklahoma Rainfall Enhancement Program seeding plan focuses on seeding growing clouds which contain a persistent region of supercooled liquid water but are lacking in ice crystals. The objectives of this study were to determine the persistence of supercooled liquid water in the sampled clouds and to determine where, when and how the ice phase developed in these clouds. The persistence of supercooled liquid water was examined in terms of cloud top lifetime, defined as the projected time from first penetration to zero liquid water content at the sampling level. Ice particle data were studied in primarily a qualitative sense.

In general, the clouds had high liquid water contents initially, but cloud top lifetimes were relatively short. Liquid water decay rates had a large standard deviation. The development of ice occurred very rapidly in many of the clouds, although there were several missions where ice development was not significant. The ice phase was apparently being enhanced in lower portions of the clouds, perhaps through ingestion of ice from neighboring cells or by ice multiplication.

## 1. INTRODUCTION

As part of the Southwest Cooperative Program the Bureau of Reclamation sponsored two field measurement programs which utilized the University of North Dakota Department of Atmospheric Sciences Citation research aircraft to collect data in convective clouds over Oklahoma. These airborne missions were conducted in cooperation with the Oklahoma Water Resources Board (OWRB) to help assess the potential for rain increase cloud modification over the state. In a technical report (Mathis and Gibeau, 1985) the OWRB and Aeromet, Inc., set forth a plan for a cloud modification project entitled the Oklahoma Rainfall Enhancement Program (OREP). Due to a dearth of knowledge regarding the microphysical properties of clouds over the state, this plan is based largely on the results of studies conducted over portions of west Texas, including the Bureau of Reclamation HIPLEX program (e.g., Jurica et al., 1983; Long, 1980). While it is reasonable to assume that there should be many similarities in the cloud properties over these adjoining areas, significant differences may exist, dictating changes to the OREP plan. It is essential, therefore, that more insight be gained into the nature of Oklahoma clouds prior to the OREP implementation.

The OREP seeding plan focuses on convective clouds which reach above the freezing level and contain supercooled liquid water (SLW). When ice crystals are present and substantial amounts of SLW remain available for a sufficient length of time, ice particles can grow to precipitation size. The latent heat released through the freezing process also contributes to the buoyancy and therefore the dynamics of these clouds. A seeding opportunity may exist in those clouds which contain a persistent region of supercooled water but are lacking in natural ice crystals. The objectives of the analyses performed under this contract were to determine the persistence of SLW in the sampled clouds and to determine where, when and how the ice phase develops in the clouds.

## 2. THE DATA

The data upon which this study is based consist entirely of in situ cloud observations from the UND Citation II research aircraft. There were no supporting radar or mesoscale data collected during the Citation flights. The sampling capabilities of the Citation included measurements of the state parameters, three-dimensional winds and cloud microphysical properties. These measurement systems were supplemented by hand-held 35 mm photographs, side-looking 16 mm time-lapse films (in 1986), forward-looking video (in 1987) and voice notes from the flight scientist. Cloud microphysics probes included Particle Measuring Systems FSSP (2-47 $\mu$m range), 2D-C (31-992 $\mu$m) and 1D-P (300-4500 $\mu$m)

probes, and a Johnson-Williams (JW) liquid water content meter. Most of the data were displayed in real time for interpretation by the flight scientist. This information was used in making operational decisions during data collection missions.

The JW measurements of liquid water content (LWC) were used in this study rather than values derived from FSSP data. During the 1986 study the FSSP instrument was inoperative for all but the first and last missions. In addition, the FSSP seemed to strongly underestimate LWC values in cloud regions where the JW values exceeded 2.8 g $m^{-3}$. The JW values were in reasonable agreement with adiabatic LWCs.

The aircraft was based in Norman, Oklahoma for the periods 27 May - 9 June, 1986, and 8-28 September, 1987. Cloud systems were sampled over the western two-thirds of the state, where average annual precipitation is notably less than in the east. The aircraft was launched whenever potential cloud candidates were observed visually or if conditions appeared favorable from radar or satellite data. Cloud types of interest included isolated cumulus congestus and feeder cells associated with convective complexes. Flights were restricted to daylight hours to facilitate cloud identification and to enhance mission safety.

Favorable weather conditions were encountered during both study periods. In 1986, 77 clouds were sampled two or more times in the course of the ten flight missions, and in 1987 55 clouds were sampled repeatedly on nine flights. Climatologically, this is still a rather limited data set. However, work by Pflaum, et al., (1989), indicates that this cloud activity was representative of these seasonal time periods.

## 3. FLIGHT PROFILES

Cloud sampling legs were flown generally in the vicinity of either the -5°C or -12°C level. Cloud candidates were selected visually based on an appearance of positive vertical growth, a minimum diameter 1 km and a "hard" or sharp boundary at cloud top. The initial penetrations were normally made within about 300-600 m of cloud top shortly after the top rose above the sampling level. The decision to repenetrate a cloud was based primarily on measured parameters from the first pass. The OREP design parameters, which were used as a guideline for this study, call for peak LWC of at least 1.0 g $m^{-3}$, updraft speed of 2.5 m $s^{-1}$ or more and less than 10 $liter^{-1}$ concentration of ice crystals at aircraft penetration levels. Some clouds not meeting these criteria were sampled repeatedly because they were along the path of penetration through other towers or because no other suitable candidates were at hand. Sampling of the cloud continued until the SLW was nearly depleted at the flight level or until operational or safety considerations precluded further measurement.

In the 1986 project an emphasis was placed on sampling at the colder (-12°C) temperatures because the OREP design plan was structured toward a static or microphysical seeding approach. An analysis of the 1986 data set, however, indicated that the SLW probably did not persist in the sampled clouds long enough to enable static seeding to work. It was discovered, though, that there was initially an ample supply of SLW that could perhaps be utilized in a dynamic seeding approach. Thus, the 1987 measurement program focused on sampling at the -5°C level where clouds could be seeded for dynamic effects earlier in their lifetimes.

## 4. PERSISTENCE OF SUPERCOOLED LIQUID WATER

The persistence of SLW was examined in this study in terms of "cloud top" lifetime, as described by Schemenauer and Isaac (1984), hereafter referred to as SI. The lifetime was computed from the mean first pass LWC and a rate of change of LWC. The rate of change, or decay rate (DR), was calculated as the difference between the mean LWC of the first and last sampling passes through a given cloud divided by the time between the midpoints of the passes. The decay rates were assumed to be linear. A cloud top lifetime was thus the projected time from first penetration to 0.0 g $m^{-3}$ LWC at the sampling level. Mean lifetimes for each day and for the whole study period were computed using mean values of first pass LWC and mean decay rates.

### 4.1 Total data set

The mean first pass LWC (LWC1), DR and projected cloud top lifetime of clouds sampled two or more times are given in Table 1a. This does not include data from those cells which were sampled at more than one temperature level. Table 1b contains values for a subset of these clouds which met the first pass OREP design criteria. A large amount of variability is evident from cloud to cloud and from flight to flight. The standard deviation of the DR is nearly equal to the mean, signifying that a wide range of cloud top lifetimes was likely in the study clouds. The distribution of DR, given in Table 2, shows that approximately one third of the cloud samples had DR $\leq$ 0.05 g $m^{-3}$ $min^{-1}$. This potential variability of lifetimes was also evident in the projected lifetimes calculated for each of the individual sampled clouds. Table 3 shows that one fourth of the projected lifetimes were greater than 15 minutes.

Table 1 Daily and total period mean lifetime of clouds

| Date 1986 | a. All Clouds # Cells | Mean Pass 1 LWC ($g\ m^{-3}$) | Mean Decay Rate ($g\ m^{-3}\ min^{-1}$) | Mean Lifetime (min) | b. Clouds Meeting OREP Pass 1 Criteria # Cells | Mean Pass 1 LWC ($g\ m^{-3}\ min^{-1}$) | Mean Decay Rate ($g\ m^{-3}\ min^{-1}$) | Mean Lifetime (min) |
|---|---|---|---|---|---|---|---|---|
| 5/27 | 3 | 0.97 ±.17 | .048 ±.044 | 20 | 2 | 1.07 ±.03 | .063 ±.051 | 17 |
| 5/28 | 5 | 1.46 ±.74 | .061 ±.065 | 24 | 4 | 1.60 ±.77 | .056 ±.074 | 29 |
| 5/31 | 10 | 0.86 ±.17 | .119 ±.078 | 7 | 9 | 0.89 ±.15 | .100 ±.053 | 9 |
| 6/1-1 | 10 | 0.73 ±.38 | .153 ±.108 | 5 | 6 | 0.89 ±.24 | .197 ±.110 | 5 |
| 6/1-2 | 3 | 0.47 ±.30 | .044 ±.028 | 11 | 1 | 0.80 ± - | .062 ±. - | 13 |
| 6/2-1 | 9 | 0.85 ±.44 | .121 ±.077 | 7 | 5 | 1.16 ±.29 | .147 ±.050 | 8 |
| 6/2-2 | 8 | 0.71 ±.29 | .064 ±.075 | 11 | 6 | 0.75 ±.32 | .040 ±.071 | 19 |
| 6/3 | 10 | 0.88 ±.47 | .099 ±.114 | 9 | 4 | 0.98 ±.43 | .086 ±.112 | 11 |
| 6/6 | 13 | 1.00 ±.59 | .129 ±.132 | 8 | 9 | 1.18 ±.64 | .142 ±.156 | 8 |
| 6/9 | 6 | 0.66 ±.11 | .096 ±.055 | 7 | 3 | 0.73 ±.07 | .094 ±.049 | 8 |
| 1986 Total | 77 | 0.87 ±.45 | .106 ±.095 | 8 | 49 | 1.01 ±.49 | .110 ±.101 | 9 |
| | | | Excluding 6/1-1 | | 43 | 1.03 ±.47 | .097 ±.094 | 11 |
| 1987 | | | | | | | | |
| 9/9-1 | 5 | 0.95 ±.49 | .024 ±.059 | 40 | 4 | 1.10 ±.40 | .037 ±.060 | 30 |
| 9/9-2 | 6 | 0.92 ±.34 | .124 ±.105 | 7 | 5 | 1.03 ±.25 | .139 ±.111 | 7 |
| 9/10 | 2 | 0.47 ±.02 | .041 ±.049 | 12 | 1 | .48 | .006 | 80 |
| 9/11 | 7 | 0.69 ±.39 | .062 ±.057 | 11 | 5 | .85 ±.34 | .081 ±.057 | 11 |
| 9/14 | 4 | 0.70 ±.34 | .117 ±.025 | 6 | 2 | .91 ±.42 | .098 ±.018 | 9 |
| 9/15 | 6 | 0.81 ±.31 | .103 ±.093 | 8 | 6 | .81 ±.31 | .103 ±.093 | 8 |
| 9/20-1 | 8 | 0.76 ±.23 | .014 ±.054 | 54 | 6 | .66 ±.16 | .014 ±.063 | 47 |
| 9/20-2 | 7 | 0.50 ±.24 | .056 ±.055 | 9 | 2 | .75 ±.28 | .120 ±.016 | 6 |
| 9/27 | 10 | 0.83 ±.31 | .086 ±.077 | 10 | 10 | .83 ±.31 | .086 ±.077 | 10 |
| 1987 Total | 55 | 0.76 ±.33 | .070 ±.075 | 11 | 41 | .85 ±.30 | .079 ±.080 | 11 |

Table 2. Distribution of calculated LWC decay rates

| Decay Rate ($g\ m^{-3}\ min^{-1}$) | Freq. | Cum. Freq.(%) |
|---|---|---|
| ≤ -.05 | 3 | 2 |
| ≤ 0.00 | 9 | 9 |
| ≤ .05 | 34 | 35 |
| ≤ .10 | 41 | 66 |
| ≤ .15 | 18 | 80 |
| ≤ .20 | 13 | 89 |
| ≤ .25 | 6 | 94 |
| ≤ .30 | 3 | 96 |
| ≤ .35 | 3 | 98 |
| ≤ .40 | 1 | 99 |
| > .40 | 1 | 100 |

Table 3. Distribution of projected cloud top lifetimes

| Lifetime (min) | Freq. | Cum. Freq.(%) |
|---|---|---|
| ≤ 5 | 22 | 18 |
| ≤ 10 | 43 | 54 |
| ≤ 15 | 24 | 74 |
| ≤ 20 | 11 | 83 |
| ≤ 25 | 6 | 88 |
| ≤ 30 | 1 | 89 |
| ≤ 35 | 2 | 91 |
| ≤ 40 | 1 | 92 |
| > 40 | 10 | 100 |

The mean lifetimes are low for most missions, but the variability of LWC and DR means that there were clouds which persisted for significantly longer times. For example, in the 1986 project, the clouds sampled on the first two days clearly seemed to be most suitable for seeding, at least in terms of the persistence of SLW. This is also true for the first flights of 9 and 20 September, 1987. On the other hand, the first flight of 1 June, 1986, found clouds embedded in altostratus that were very short-lived and would likely be poor seeding candidates. Thus, mean values for the 1986 OREP clouds were also computed excluding those samples from 1 June.

The computed values of LWC1, mean DR and cloud top lifetime for the total project are very similar to those reported by SI for clouds sampled in 1977 near Thunder Bay, Ontario: 0.88 ± 0.55 g $m^{-3}$, -0.104±.17 g $m^{-3}$ $min^{-1}$, and 8 min, respectively. SI classified these clouds as having short lifetimes and high LWCs, providing an environment where warm and cold rain processes as well as ice multiplication can occur. They felt that these lifetimes were too short and that, consequently, the clouds would be poor candidates for seeding with silver iodide. However, they did suggest that the use of dry ice would improve their seedability.

Table 4. Data stratified by cloud seedability

| | Cloud Type | # Cells | D | avg. w | avg. LWC | peak LWC |
|---|---|---|---|---|---|---|
| 1986 | S | 5 | 2.1 | 2.2 | 1.37 | 2.2 |
| | SNS | 9 | 1.4 | 2.2 | .98 | 1.5 |
| | NS | 28 | 1.3 | 2.2 | .99 | 1.7 |
| 1987 | S | 10 | 2.8 | 3.9 | .92 | 1.7 |
| | SNS | 21 | 1.8 | 3.8 | .79 | 1.6 |
| | NS | 7 | 1.8 | 5.0 | .97 | 1.7 |

4.2 Stratification by OREP criteria

The 1987 cloud set, as a whole, was somewhat drier than the 1986 set and had a markedly lower decay rate. This gave rise to an average calculated cloud top lifetime that was nearly 40% greater in 1987. When comparing only the OREP clouds, however, the combination of lower LWC1 and lower DR in 1987 produced an average cloud top lifetime similar to that for 1986. Based on this limited set of observations it is not known if the differences in LWC1, DR and lifetime are seasonal in nature or whether they represent a random interannual variability. They do not appear to be the result of a change in emphasis on sampling levels from 1986 to 1987 (see section 4.3).

In an attempt to determine why cloud lifetimes varied markedly from day to day a rather restrictive subset of apparently "seedable" clouds was defined. These were OREP clouds which had projected lifetimes $\geq$ 14 minutes and which developed ice slowly, if at all (no detectable ice before the fourth sampling pass, ~7 minutes from time of first penetration). The first pass characteristics of these seedable clouds are presented in Table 4 as cloud type S. Characteristics of non-seedable clouds which were sampled on days with seedable clouds (type SNS) and characteristics of clouds on days when there were no seedable clouds (NS) are also shown.

The seedable clouds were, on the average, substantially larger than the others. The greater first pass diameter (D) likely promoted the longevity of these clouds by reducing the effects of entrainment. On seedable days, the seedable clouds also had higher LWC than the non-seedable clouds.

Another interesting first-pass characteristic is that the average updraft speed (w) for clouds sampled on seedable days was less than that on non-seedable days. This is in agreement with a more general observation derived from other supporting data that the seedable clouds were found on days or in areas where only weak to moderate convection was occurring. On several of these seedable days atmospheric soundings revealed the presence of a weak mid-level temperature inversion. These observations show that the clouds most suitable for seeding were not associated with strong or severe convective situations. A reason for this may be that the more vigorous clouds reached colder temperatures earlier in their lifetimes and therefore initiated the ice process sooner. It may also be that the stronger updrafts promoted a more rapid recycling of ice within cloud or ingestion of ice from neighboring cells. Entrainment may have also been enhanced by larger updraft velocities.

For most missions in 1986 the mean lifetime of the OREP subset is larger than that of the total cloud set. This indicates that the stratification criteria had a net positive effect on the selection process. However, no such effect was found for the 1987 data set. The fact that the stratification criteria had no effect on the cloud selection process in 1987 but had a net positive effect in 1986 may be due to the nature of the clouds excluded by the screening. In 1986 over 70% of the clouds which did not meet OREP criteria failed due to high ice concentrations. In 1987, the primary reason for excluding clouds (85%) was a low LWC1. The fact that the exclusion of clouds with high initial ice concentrations improved cloud top lifetimes while exclusion of those with lower initial LWC did not, suggests that the ice plays a more significant role in the availability of liquid water.

This postulate is supported by the correlations of the computed cloud top lifetimes with LWC1 and DR. Figures 1a and 1b illustrate these relationships for both years. There was a strong correlation between lifetime and DR, as one would expect, but little or no correlation between lifetime and LWC1. A regression of lifetimes versus LWC1 and DR indicates that approximately 90% of the variance in the lifetimes is explained by the variability of the DR. Thus, the persistence of SLW appears to be more highly dependent on depletion processes such as conversion to ice or entrainment than on the initial liquid water content of the clouds.

4.3 Stratification by temperature and termination type

The clouds in this study were also stratified by penetration temperature and by termination type. Table 5 shows that in 1986 there was little difference in LWC1 or DR between warm and cold cloud penetrations. Temperatures warmer than -10°C were classified as warm. However, in 1987, the cold clouds had a much higher average decay rate. This

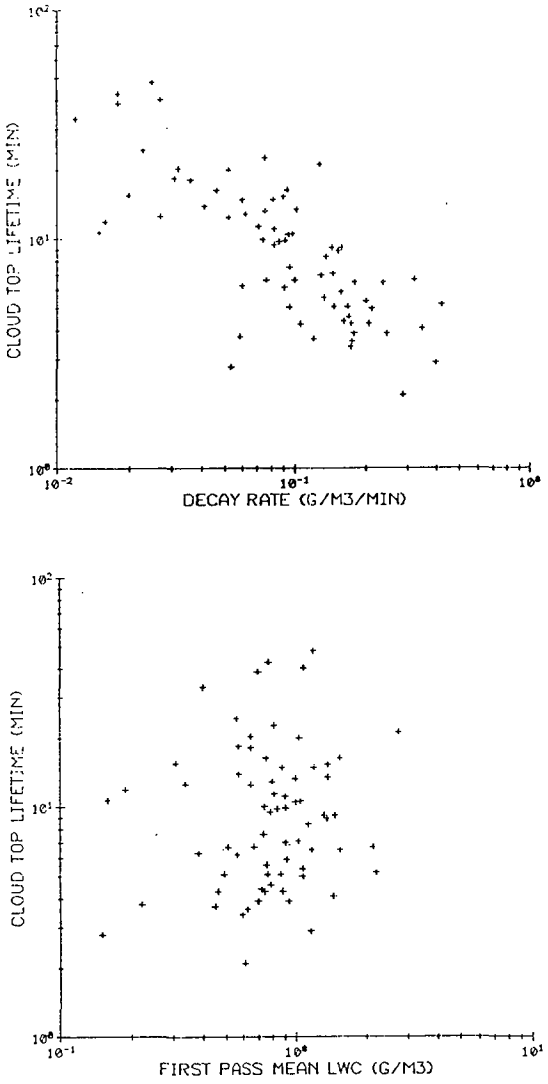


*Fig. 1a. Cloud top lifetime as a function of liquid water decay and as a function of first pass mean liquid water content, for 1986 clouds.*

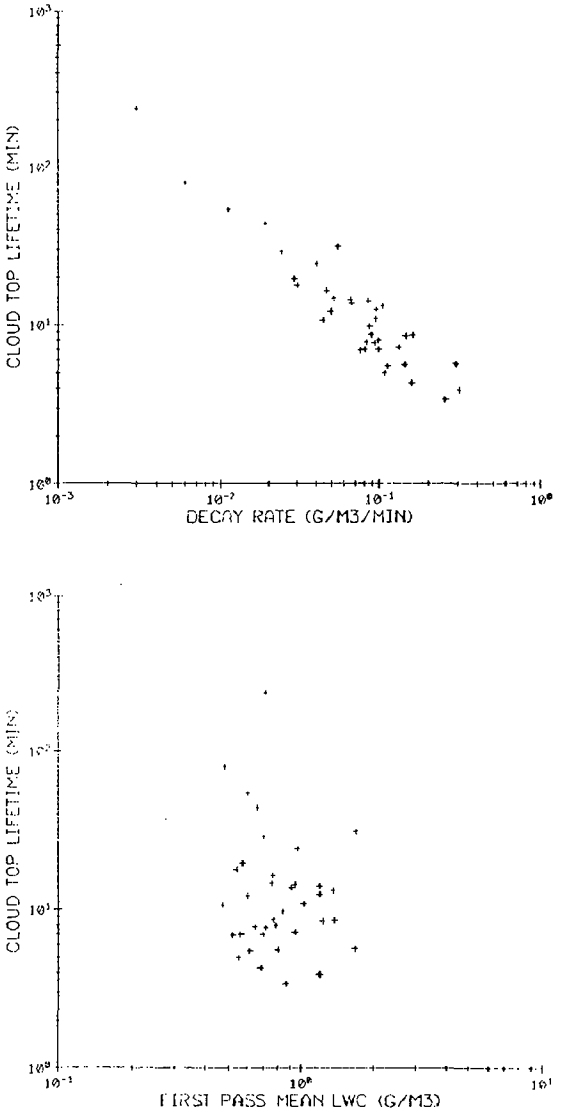


*Fig. 1b. As in Fig. 1a. for 1987 clouds.*

statistic may be biased by the fact that half of the colder penetrations were made on one flight, 9/9-2, which had the highest DR of all 1987 missions.

A comparison of warm and cold samples considering reasons for termination type is presented in Table 6. Termination types may be interpreted as follows:

Dissipation - a loss of liquid water and/or updraft;
Glaciation - peak 2D concentrations > 50 liter$^{-1}$;
Safety - primarily cloud radar reflectivities >40 dBz associated with graupel and/or small hail;
Operations - descents for aircraft de-icing, congested cloud fields, changes in flight tracks to focus on nearby cells.

The 1986 cloud data set showed that the majority (almost 2/3) of the clouds sampled at colder temperatures developed ice compared to only about 1/3 of those sampled at warmer temperatures. The 1987 clouds, however, showed no such preference.

## 5. DEVELOPMENT OF ICE

A second important factor which determines the seedability of clouds is the natural development of ice crystals. For seeding to be effective it must convert the SLW to ice at a faster rate or in a more favorable portion of the cloud than would have occurred naturally. Within the scope of this study the development of ice was examined in primarily a qualitative sense.

The rate at which ice developed, as measured by time from first penetration, varied from flight to flight. On a number of missions, some of the clouds never contained detectable ice particles at flight altitudes and in others it took

Table 5. Data stratified by penetration temperature

| | | Warmer than -10°C | | | Colder than -10°C | | |
|---|---|---|---|---|---|---|---|
| | | Avg. LWC Pass 1 ($gm^{-3}$) | Avg. Decay Rate ($gm^{-3}$ $min^{-1}$) | N | Avg. LWC Pass 1 ($gm^{-3}$) | Avg. Decay Rate ($gm^{-3}$ $min^{-1}$) | N |
| 1986 | All Clouds | .93 | .103 | 42 | .90 | .109 | 35 |
| | OREP Clouds | 1.05 | .104 | 31 | 1.14 | .103 | 18 |
| 1987 | All Clouds | .73 | .060 | 42 | .83 | .101 | 13 |
| | OREP Clouds | .82 | .068 | 32 | .94 | .120 | 9 |

Table 6. Data stratified by termination type and temperature

| | | Dissipation | Glaciation | Safety | Operational |
|---|---|---|---|---|---|
| 1986 | Warm | 55% | 31% | 7% | 7% |
| | Cold | 29% | 49% | 14% | 8% |
| 1987 | Warm | 38% | 12% | 14% | 36% |
| | Cold | 46% | 8% | 23% | 23% |

from five to over 13 minutes before significant concentrations could be detected. By comparison, many missions saw rapid ice development within the candidate clouds. Significant concentrations of ice crystals (10 $\ell^{-1}$) were generally present by the third pass or roughly four minutes after initial penetration. A number of clouds even contained high ice concentrations on the first pass and would not meet the OREP criteria.

There are indications that ice ingestion may have played a significant role in the development of high ice crystal concentrations. Embedded cells were sampled on several occasions and all contained high quantities of ice on the first pass or shortly thereafter. Most of the towers on the first flight of June 1, 1986 were embedded in a sub-freezing altostratus layer. It was also noted that towers which grew up close (within a kilometer) to an older cell tended to develop ice early in their lifetime. These turrets were normally part of a small convective complex and were joined to the mature portion of the system at lower levels. It is possible that ice particles were being ingested at those levels and brought up to cloud top.

Another generalization that may be made concerning ice development is that it seemed to occur primarily low in the cloud, at relatively warm temperatures. This may be inferred from the crystal habits - very few plates or dendritic crystals were observed in any of the cloud turrets. Those are the types of ice particles which would be expected to grow in the -10°C to -20°C temperature range. Instead, there was a preponderance of graupel, columns, frozen drops, and irregular particles (as in Fig. 2) at all sampled temperatures (-5°C to -13°C). This suggests that processes such as ice multiplication (e.g., Mossop, 1976) or ice ingestion from neighboring cells may have been dominant in those clouds which eventually developed detectable ice crystal concentrations.

Data from one of the clouds sampled on May 27 support the possibility of a Hallett - Mossop ice multiplication process. This cumulus congestus was penetrated nine times over a 23 minute period, at temperatures between -5°C and -8°C. The estimated cloud top temperature was no colder than -9°C. During the second pass, at -7°C, the cloud contained relatively high concentrations of both large and small droplets (181 $cm^{-3}$ of diameter >23 $\mu$m and 87 $cm^{-3}$ of diameter <14 $\mu$m) (Fig.3). The ratio of small to large droplet concentrations (0.5) is within the range of values found in clouds in which ice multiplication has been observed (Mossop, 1985). The 2D data (Fig. 2) show round and nearly-round images in passes 4-6, representing liquid and possibly frozen drops up to 1 mm in

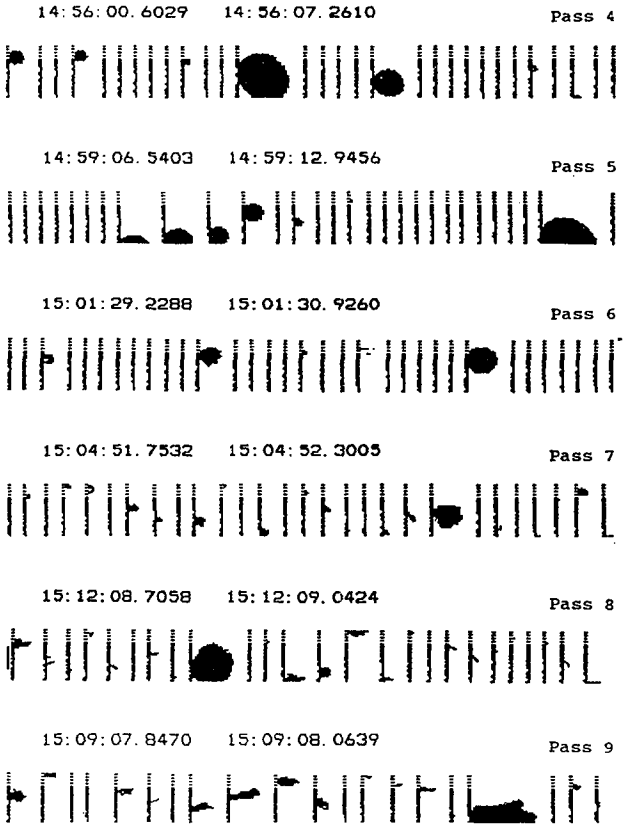


*Fig. 2. 2D images from cloud C on May 27, 1986. Time of initial penetration was 144908. Length of vertical bars corresponds to 1 mm.*

size in concentrations generally <1 $\ell^{-1}$. Ice particles of this size could be active rimers for the production of secondary ice particles. Columns first appeared in pass 7 mixed with irregular and nearly-round particles (up to 37 $\ell^{-1}$). Irregular particles, graupel and columns predominated in passes 8 and 9 (>80 $\ell^{-1}$) as the liquid water content was depleted.

## 6. SUMMARY

The following general characteristics of the sampled cloud water and ice contents were determined:

1. The supercooled liquid water content of the study clouds was observed to decay at a fairly rapid rate. Cloud top lifetimes of 8, 9 and 11 minutes were calculated for all multiple pass clouds and for two select subsets in 1986, and 11 minutes for all clouds in 1987.

2. The liquid water decay rates had a large standard deviation, suggesting that a fair percentage of the clouds may be expected to contain SLW for significantly longer periods of time. The longer-level clouds occurred under conditions of weak to moderate convection.

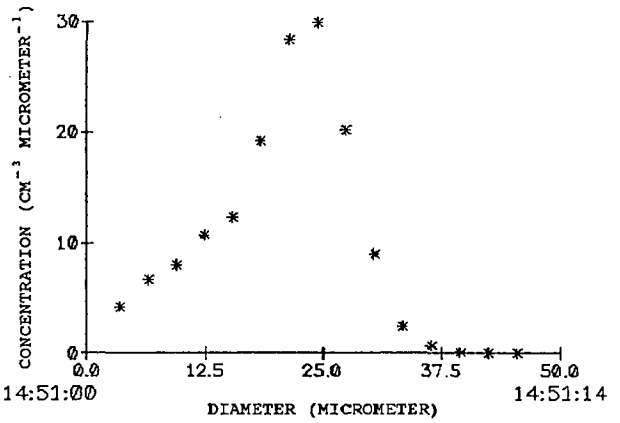


*Fig. 3. FSSP droplet spectrum for cloud C pass 2 on May 27, 1986.*

3. The initial LWCs of the clouds meeting OREP criteria were substantial, with a first pass average of 0.94 g $m^{-3}$.

4. The development of ice occurred very rapidly in many of the clouds, particularly those which grew up close to older towers or were embedded in cold cloud layers. There were several missions, however, where ice development was not significant over the sampled life of the clouds.

5. It appears as though the ice phase is being initiated in lower portions of the clouds. Evidence for this includes a lack of crystal habits normally formed at colder temperatures and the rapid glaciation of towers below the -12°C level.

6. Much of the cloud ice may be the result of ice multiplication and/or ingestion or recirculation from neighboring cells.

## ACKNOWLEDGEMENTS

This work was supported by Bureau of Reclamation Grant No. 4-FC-81-03780 and by the Oklahoma Water Resources Board.

## REFERENCES

Jurica, G.M., C.A. Leary, D.R. Haragan, A. Eddy, H. Johnson, and B. Sladewski, 1983: Summer convective precipitation on the Texas South Plains. Atmospheric Science Group, Texas Tech University and Amos Eddy Inc., Norman, Ok., Texas Department of Water Resources, LP-186.

Long, A.B., 1980: Preliminary cloud microphysics studies for Texas HIPLEX 1979. Department of Meteorology, Texas A & M University for Texas Department of Water Resources, LP-124.

Mathis, M.E. and E.J. Gibeau, 1985: Oklahoma Rainfall Enhancement Program. Oklahoma Water Resources Board and Aeromet Inc., 133 pp.

Mossop, S.C., 1976: Production of secondary ice particles during the growth of graupel by riming. Quart J. Royal Met. Soc., 102, 45-57.

_____, 1985: Secondary ice particle production during rime growth: the effect of drop size distribution and rimer velocity. Quart. J. Royal. Met. Soc., 111, 1113-1124.

Pflaum, J.C., H.L. Johnson, and M.R. Poellot, 1989: Preliminary Investigations of a Dynamic Seeding Strategy for Oklahoma Convective Clouds. J. Wea. Mod., 21.

Schemenauer, R.S. and G.A. Isaac, 1984: The importance of cloud top lifetime in the description of natural cloud characteristics. J. Climate and Appl. Meteor., 23, 267-279.

"REVIEWED"

# PRELIMINARY INVESTIGATIONS OF A DYNAMIC SEEDING STRATEGY FOR OKLAHOMA CONVECTIVE CLOUDS

John C. Pflaum, Cooperative Institute for Mesoscale Meteorological Studies, University of Oklahoma, Norman, OK 73019
Howard L. Johnson, Oklahoma Climatological Survey, University of Oklahoma, Norman, OK 73019
Michael R. Poellot, Department of Atmospheric Sciences, University of North Dakota, Grand Forks, ND 58201

ABSTRACT This article presents some early findings from on-going work investigating the seedability of Oklahoma convective clouds. Using the Great Plains Cloud Model (GPCM), predictions of maximum cloud height were compared for simulations of natural freezing, silver iodide enhanced freezing and dry ice enhanced freezing. Selected soundings were from time periods coinciding with airborne measurements of cloud microphysics which will allow for future evaluation of model realism. Climatological analyses indicated that representative meteorological conditions existed during these time periods. Preliminary indications suggest that opportunities for enhanced cloud growth due to seeding exist on days when cumulus clouds are present over Oklahoma and that a small advantage may result from the use of dry ice as compared to silver iodide.

## I. INTRODUCTION

As part of Oklahoma's overall water resources development strategy, the Oklahoma Water Resources Board (OWRB) has presented a long term plan for utilizing and developing weather modification technology as a tool for water resources management in Oklahoma. This strategy is referred to as the Oklahoma Rainfall Enhancement Program (OREP). OREP takes the approach of utilizing today's best available cloud seeding technology, while at the same time remaining flexible enough to quickly incorporate advances in the technology.

The preliminary OREP seeding hypothesis was based on the static seeding concept as developed in HIPLEX (Bureau of Reclamation, 1979) and partially verified by Cooper and Lawson (1984) in Montana. Static seeding presumes that precipitation in seeded clouds occurs via initial diffusional growth of ice crystals to sizes where riming can commence, followed by subsequent evolution of the crystals into graupel. An increase in the total rainfall amount is expected through an increase in the average ice concentration to about 10 per liter, a concentration expected to be more efficient than the natural ice concentrations in converting condensate to precipitation. In addition, it is expected that the injection of ice into the cloud early in its lifetime will lead to earlier precipitation development, and to development of precipitation in some clouds that would not precipitate naturally (Mathis and Gibeau, 1985).

In contrast to this static approach, the design of the Southwest Cooperative Program Rainfall Enhancement Experiment for stimulating rainfall in West Texas, suggested a dynamic seeding approach (Jurica and Woodley, 1985). The conceptual model guiding the experiment invokes a chain of events beginning with the direct injection of an ice nucleant into supercooled updraft regions of convective cells. This on-top injection of the nucleant is expected to produce extensive and rapid glaciation of the updraft, resulting in release of latent heat of fusion, producing an increase in buoyancy and invigorating the cells' internal circulations, including downdrafts. The model predicts that seeded cells will grow taller, produce higher rain rates, last longer and produce more total rainfall. The enhanced downdrafts beneath the cells are expected to produce regions of enhanced convergence at the interface between downdraft outflows and the ambient flow which, in turn, will invigorate existing cells and/or produce new ones. This sequence of events is predicted to lead ultimately to a larger cloud system that lasts longer and produces more rainfall. This West Texas conceptual model is based in part on the FACE program (Florida Area Cumulus Experiment) which had a similar conceptual model and which produced increases in excess of 100% in rainfall on the scale of convective cells (Jurica and Woodley, 1985).

The results from the first year of the Southwest Cooperative Program, 1986, suggest that rainfall from the small meso-scale convective systems was increased due to silver iodide seeding suitable to produce dynamic effects. The apparent increases in rainfall, amounting to over 100%, were due to an increase in cell number, to an increase in mean cell height, and to an increase in total cluster area within the seeded systems. These apparent effects were consistent with an alteration and invigoration of the dynamics of the convective cells contained within the convective systems (Woodley et al., 1987).

Additional results from 1987 suggest similar trends with a positive effect of AgI treatment on cell duration, maximum reflectivity, area, rain rate and rain volume. The largest effect was on mean total cell rainfall which increased between 50 and 146% (Woodley and Rosenfield, 1988).

In an effort to evaluate potential opportunities for dynamic seeding in Oklahoma, Johnson (1982) prepared an analysis of area rawinsondes for the five year period 1976-1980. The "dynamic seedability" was evaluated using the Great Plains Cloud Model - GPCM (Hirsch, 1971). This one-dimensional, steady-state model uses temperature, humidity, and wind data from a specified rawinsonde observation to predict the values of various dynamical and microphysical parameters in a resultant cumulus cloud. Of primary interest is the additional height of cloud development present when glaciation is allowed to occur in warmer portions of the cloud (thus simulating a seeding effect), and this height change is synonomous with the term "dynamic seedability". The conclusions from this study were that there is a likelihood of dynamic seeding opportunities on most days, somewhere in western Oklahoma, during the summer months. Such findings for Oklahoma were consistent with those of Matthews (1981) who demonstrated that dynamic seeding opportunities appeared to exist in Montana, Kansas and Texas during the summer months of 1975-1977.

## 2. DYNAMIC SEEDABILITIES

As part of the continuing effort to develop the basis for a scientifically sound weather modification program in Oklahoma, the University of North Dakota Citation cloud physics aircraft research team came to Oklahoma to collect microphysical data for analysis. Data were collected during spring (May 27 through June 9) 1986 and late summer (September 9 through September 28) of 1987 at the sites shown in Fig. 1. The results of analyses of the 1986 sampling effort are reported in Poellot (1986) and summarized in Mathis (1987). The results from the 1987 sampling effort are reported in Poellot (1988) and Pflaum (1988). The analyses indicate that Oklahoma convective clouds appear to develop precipitation initially through a warm rain process. As continued vertical development occurs and the clouds reach lower temperatures, the drops freeze, subsequently evolving into graupel. The data also indicated that supercooled liquid water does not persist long enough to enable static seeding to work (see companion article in this journal by Poellot and Pflaum). However, an ample supply of supercooled liquid water exists initially, suggesting that a dynamic seeding approach might be more appropriate.

As a first step toward investigating this possibility, the GPCM was applied to soundings for the days during which the Citation was collecting data. This was done for two purposes: 1) To evaluate the dynamic seedability on days when it was known that seeding candidates

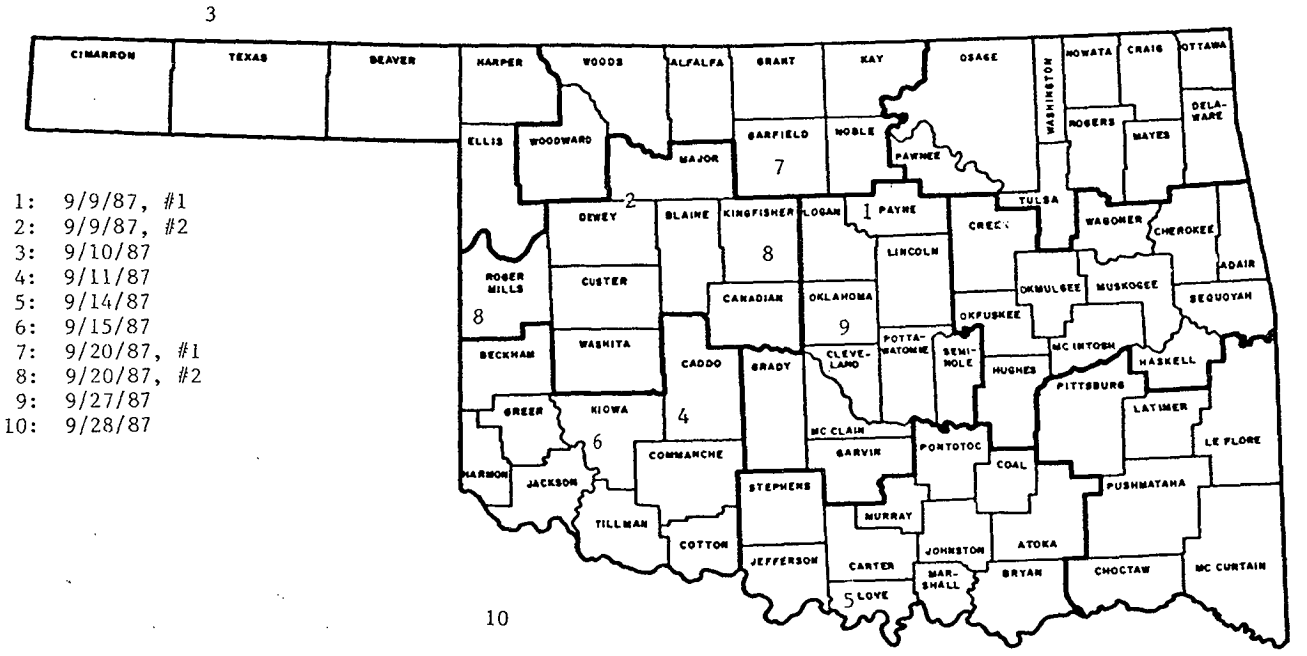


Figure 1: Flight Locations and Dates

existed, and 2) to compare the dynamic seedability of two hypothetical seeding treatments. Tables 1.1 - 1.12 represent compilations of the model predicted seedabilities (km) for various cloud radii. In the "natural cloud", the conversion to ice is effected linearly between -20 °C to -40 °C. In test one, designed to simulate seeding with AgI, the conversion to ice was shifted to warmer regions of the cloud and effected linearly between -5 and -25 °C. In test two, designed to simulate seeding with dry ice, the conversion of ice was shifted to even higher temperatures, and effected linearly between 0 and -15 °C. The abbreviations, OKC, AMA, and DDC stand for Oklahoma City, Amarillo and Dodge City, respectively. National Weather Service soundings for these 3 sites were used as input to the model. The letter M indicates that sounding data was missing.

It is seen that on days when convection existed: 5/27, 28, 31, 6/1, 2, 3, 6, 9, 1986; 9/9, 10, 11, 14, 15, 20, 27, 28, 1987, and sounding data was available, the opportunity for enhanced vertical development was present at least at one of the stations, often at all three. Enhancement of greater than 1 km was generally present for clouds of at least one size category.

The effects of changing the ice conversion temperature were relatively small but general trends were as follows:

a. When dynamic seedability was demonstrated in test 1, it was present in test 2 at a slightly enhanced value. However, it was not uncommon for small negative variations to occur as well.

b. When more substantial positive changes occurred from test 1 to test 2, they usually took the form of an expansion of effects to neighboring cloud sizes rather than any initiation of effects where none existed for test 1. There were two cases where test 2 produced a significant reduction as compared to test 1.

c. Spring days were slightly more responsive than fall days to the simulated seeding, a trend also noted by Johnson (1982).

In summary, according to GPCM predictions, opportunities existed for positive dynamic seeding effects on days when convection was present during the Spring of 1986 and Fall of 1987. In addition, the model suggested that a small advantage may result from dry ice seeding as compared to silver iodide seeding.

## 3. CLIMATOLOGICAL REPRESENTATIVENESS OF THE DATA COLLECTION PERIODS

In light of the short sampling periods and the lack of any historical record of cloud physics information in Oklahoma, a climatological perspective was needed for the observations and GPCM predictions. The following is an attempt to provide such a perspective.

### 3.1 The Spring Period (May 27-June 9, 1986)

The Spring thunderstorm season in Oklahoma is the period of greatest rainfall for the State. The transition from winter to summer is nearly complete by the end of May. Severe thunderstorms that develop in response to the interaction between transient disturbances in the jet stream and the warm moist air which dominates the State's surface weather, frequently spawn tornadoes, strong winds, and hail. Those same thunderstorms also produce locally heavy rains which supply water to the ripening wheat crop and runoff water into the lakes and ponds. The spring storm season then is a good time to find rain clouds in Oklahoma and to study their characteristics.

Clouds were sampled on 9 of the 14 days during the Spring 1986 sampling period. The aircraft was down for repairs on two additional days, one of which was marked by heavy rains in Norman (Poellot, 1986). Rainfall was reported within the western two-thirds of Oklahoma on each day of the sampling period (OCS, 1986a and OCS, 1986b). Eddy (1982) found that rain-producing clouds are normally present in western Oklahoma on 95% of the days in spring and summer. The reported frequency of raindays is not atypical for a short period of time, but the wide-spread nature of the rain in the 1986 period was.

A persistent upper-level low pressure area lingered to the west of the State throughout the observational period. Frontal activity was generally weak, but the environment was favorable for the development of showers and thunderstorms in response to the small-scale disturbances which frequently are embedded in the wind flows that dominated the period. Since no fronts of any significance passed through the State, ample moisture was available to support convective activity. The study period was a wetter-than-normal two week interval, but not a period that could be characterized as an extremely wet period.

The atmosphere during the observational period tended to be cooler (by 3 °C at 850 mb and 700 mb and by 1 °C at 500 mb at Oklahoma City) than normal. The basic low-level moisture measures indicate that greater than normal moisture was available during the period. The stability, as measured by the Lifted Index and the Total Totals was near normal throughout the period. The K-index tended to be higher than normal, a reflection of the depth of the available moisture. Table 2 is a summary of the moisture and stability parameters during the field project.

The clouds sampled during the 1986 field period were found in an airmass that was generally unstable though not of the extreme instability associated with spring outbreaks of severe weather in western and central Oklahoma. A more normal two-week period would likely have resulted in, at least, one or two

Table 4.1
**Dynamic Seedability (Km): OKC**
**Test I**

| Date 1986 | Time (GMT) | Cloud radius (km) 0.5 | 1.0 | 1.5 | 2.0 | 3.0 | 10.0 |
|---|---|---|---|---|---|---|---|
| 5/27 | 00 | 0.0 | 0.0 | 0.0 | 0.0 | 0.0 | 0.0 |
| 5/27 | 12 | 0.0 | 0.0 | 0.0 | 0.0 | 0.0 | 2.8 |
| 5/28 | 00 | 0.0 | 0.0 | 0.0 | 0.0 | 0.0 | 0.0 |
| 5/28 | 12 | 0.0 | 0.1 | 3.6 | 0.0 | 0.0 | 0.3 |
| 5/29 | 00 | 0.0 | 0.0 | 0.3 | 0.5 | 1.0 | 0.7 |
| 5/29 | 12 | M | M | M | M | M | M |
| 5/30 | 00 | 0.0 | 0.0 | 0.2 | 4.3 | 4.4 | 1.4 |
| 5/30 | 12 | 1.2 | 2.4 | 0.3 | 0.3 | 0.0 | 0.7 |
| 5/31 | 00 | 0.0 | 0.2 | 5.2 | 0.0 | 0.3 | 0.7 |
| 5/31 | 12 | M | M | M | M | M | M |
| 6/1 | 00 | 0.0 | 3.3 | 0.7 | 0.5 | 0.3 | 1.0 |
| 6/1 | 12 | 0.0 | 3.5 | 3.2 | 0.6 | 0.3 | 6.6 |
| 6/2 | 00 | 0.9 | 1.8 | 0.8 | 0.3 | 0.4 | 0.4 |
| 6/2 | 12 | 0.5 | 1.2 | 2.0 | 3.9 | 0.0 | 0.4 |
| 6/3 | 00 | 0.0 | 4.3 | 0.0 | 0.3 | 0.0 | 0.5 |
| 6/3 | 12 | 0.0 | 0.2 | 4.1 | 0.3 | 0.4 | 0.5 |
| 6/4 | 00 | 0.0 | 0.0 | 0.0 | 5.5 | 5.5 | 0.4 |
| 6/4 | 12 | M | M | M | M | M | M |
| 6/5 | 00 | 0.0 | 0.0 | 0.0 | 0.0 | 0.0 | 0.0 |
| 6/5 | 12 | 0.0 | 0.2 | 0.3 | 0.5 | 6.2 | 0.4 |
| 6/6 | 00 | M | M | M | M | M | M |
| 6/6 | 12 | M | M | M | M | M | M |
| 6/7 | 00 | 0.0 | 0.0 | 0.0 | 0.0 | 0.0 | 0.0 |
| 6/7 | 12 | 0.0 | 0.0 | 0.0 | 0.0 | 0.0 | 0.0 |
| 6/8 | 00 | M | M | M | M | M | M |
| 6/8 | 12 | M | M | M | M | M | M |
| 6/9 | 00 | 0.0 | 0.0 | 0.0 | 0.0 | 0.0 | 0.0 |
| 6/9 | 12 | 0.0 | 0.0 | 3.9 | 4.0 | 0.3 | 0.8 |

Table 4.2
**Dynamic Seedability (Km): OKC**
**Test 2**

| Date 1986 | Time (GMT) | Cloud radius (km) 0.5 | 1.0 | 1.5 | 2.0 | 3.0 | 10.0 |
|---|---|---|---|---|---|---|---|
| 5/27 | 00 | 0.0 | 0.0 | 0.0 | 0.0 | 0.0 | 0.0 |
| 5/27 | 12 | 0.0 | 0.0 | 0.0 | 0.0 | 0.0 | 2.8 |
| 5/28 | 00 | 0.0 | 0.0 | 0.0 | 0.0 | 0.0 | 0.0 |
| 5/28 | 12 | 0.0 | 0.3 | 3.4 | 0.0 | 0.0 | 0.5 |
| 5/29 | 00 | 0.0 | 0.2 | 0.5 | 0.7 | 1.0 | 0.7 |
| 5/29 | 12 | M | M | M | M | M | M |
| 5/30 | 00 | 0.0 | 0.0 | 4.0 | 4.1 | 4.4 | 1.7 |
| 5/30 | 12 | 1.4 | 2.4 | 0.3 | 0.3 | 0.0 | 0.7 |
| 5/31 | 00 | 0.0 | 4.8 | 5.2 | 0.0 | 0.3 | 0.7 |
| 5/31 | 12 | M | M | M | M | M | M |
| 6/1 | 00 | 3.3 | 3.3 | 0.7 | 0.5 | 0.3 | 1.0 |
| 6/1 | 12 | 0.0 | 3.5 | 3.2 | 0.6 | 0.3 | 7.0 |
| 6/2 | 00 | 1.1 | 1.8 | 0.9 | 0.3 | 0.4 | 0.9 |
| 6/2 | 12 | 1.3 | 1.4 | 2.2 | 3.9 | 0.0 | 0.7 |
| 6/3 | 00 | 0.0 | 4.0 | 0.0 | 0.3 | 0.0 | 0.5 |
| 6/3 | 12 | 0.0 | 1.9 | 4.1 | 0.3 | 0.4 | 0.5 |
| 6/4 | 00 | 0.0 | 0.0 | 0.0 | 5.2 | 5.5 | 0.8 |
| 6/4 | 12 | M | M | M | M | M | M |
| 6/5 | 00 | 0.0 | 0.0 | 0.0 | 0.0 | 0.0 | 0.0 |
| 6/5 | 12 | 0.0 | 0.5 | 0.5 | 1.7 | 6.2 | 0.8 |
| 6/6 | 00 | M | M | M | M | M | M |
| 6/6 | 12 | M | M | M | M | M | M |
| 6/7 | 00 | 0.0 | 0.0 | 0.0 | 0.0 | 0.0 | 0.0 |
| 6/7 | 12 | 0.0 | 0.0 | 0.0 | 1.9 | 3.5 | 0.0 |
| 6/8 | 00 | M | M | M | M | M | M |
| 6/8 | 12 | M | M | M | M | M | M |
| 6/9 | 00 | 0.0 | 0.0 | 3.4 | 4.0 | 0.3 | 0.8 |

Table 4.3
**Dynamic Seedability (Km): OKC**
**Test I**

| Date 1987 | Time (GMT) | Cloud radius (km) 0.5 | 1.0 | 1.5 | 2.0 | 3.0 | 10.0 |
|---|---|---|---|---|---|---|---|
| 9/9 | 00 | 0.2 | 0.5 | 1.0 | 0.0 | 0.3 | 0.4 |
| 9/9 | 12 | 0.2 | 1.5 | 0.3 | 0.0 | 0.0 | 0.0 |
| 9/10 | 00 | 0.2 | 0.3 | 2.2 | 0.5 | 0.3 | 0.7 |
| 9/10 | 12 | 0.0 | 0.0 | 0.7 | 0.6 | 0.3 | 0.4 |
| 9/11 | 00 | 0.0 | 0.7 | 1.0 | 0.5 | 0.3 | 0.8 |
| 9/11 | 12 | 0.0 | 0.0 | 0.0 | 0.0 | 0.0 | 0.0 |
| 9/12 | 00 | M | M | M | M | M | M |
| 9/12 | 12 | M | M | M | M | M | M |
| 9/13 | 00 | M | M | M | M | M | M |
| 9/13 | 12 | M | M | M | M | M | M |
| 9/14 | 00 | M | M | M | M | M | M |
| 9/14 | 12 | M | M | M | M | M | M |
| 9/15 | 00 | 0.0 | 0.0 | 0.0 | 0.4 | 0.0 | 0.0 |
| 9/15 | 12 | 0.0 | 0.7 | 1.0 | 1.0 | 0.0 | 0.5 |
| 9/16 | 00 | 0.2 | 0.2 | 0.4 | 0.4 | 0.5 | 0.4 |
| 9/16 | 12 | 0.0 | 0.0 | 0.0 | 5.4 | 0.3 | 0.3 |
| 9/17 | 00 | 0.0 | 0.0 | 4.0 | 0.3 | 0.3 | 0.4 |
| 9/17 | 12 | 0.0 | 0.5 | 0.0 | 0.0 | 0.0 | 0.4 |
| 9/18 | 00 | 0.2 | 0.8 | 0.2 | 0.3 | 0.3 | 0.5 |
| 9/18 | 12 | 0.0 | 0.0 | 0.0 | 0.0 | 0.0 | 0.0 |
| 9/19 | 00 | 0.0 | 0.0 | 0.0 | 0.0 | 0.0 | 0.0 |
| 9/19 | 12 | 0.0 | 0.0 | 0.0 | 0.0 | 0.0 | 0.6 |
| 9/20 | 00 | 0.6 | 1.1 | 0.2 | 0.3 | 0.0 | 0.7 |
| 9/20 | 12 | M | M | M | M | M | M |
| 9/21 | 00 | 2.0 | 0.5 | 0.3 | 1.4 | 0.0 | 3.1 |
| 9/21 | 12 | 0.0 | 0.2 | 0.8 | 1.4 | 0.4 | 0.6 |
| 9/22 | 00 | 0.0 | 0.0 | 0.0 | 0.0 | 0.0 | 0.2 |
| 9/22 | 12 | 0.0 | 0.0 | 0.0 | 0.0 | 0.0 | 0.0 |
| 9/23 | 00 | 0.0 | 0.0 | 0.2 | 2.7 | 1.1 | 1.2 |
| 9/23 | 12 | 0.0 | 0.0 | 0.0 | 0.0 | 4.8 | 3.7 |
| 9/24 | 00 | 0.2 | 1.2 | 0.8 | 0.6 | 0.3 | 0.4 |
| 9/24 | 12 | 0.0 | 0.8 | 1.2 | 0.3 | 0.3 | 0.8 |
| 9/25 | 00 | 0.0 | 0.0 | 2.0 | 2.4 | 0.6 | 1.0 |
| 9/25 | 12 | 0.0 | 0.7 | 0.7 | 0.6 | 0.3 | 0.4 |
| 9/26 | 00 | 0.0 | 0.5 | 0.5 | 0.5 | 0.3 | 0.8 |
| 9/26 | 12 | 0.0 | 2.7 | 0.5 | 0.5 | 0.3 | 0.4 |
| 9/27 | 00 | M | M | M | M | M | M |
| 9/27 | 12 | M | M | M | M | M | M |
| 9/28 | 00 | M | M | M | M | M | M |
| 9/28 | 12 | M | M | M | M | M | M |

Table 4.4
**Dynamic Seedability (Km): OKC**
**Test 2**

| Date 1987 | Time (GMT) | Cloud radius (km) 0.5 | 1.0 | 1.5 | 2.0 | 3.0 | 10.0 |
|---|---|---|---|---|---|---|---|
| 9/9 | 00 | 0.5 | 0.5 | 1.0 | 0.0 | 0.3 | 0.4 |
| 9/9 | 12 | 1.3 | 1.5 | 0.3 | 0.0 | 0.0 | 0.4 |
| 9/10 | 00 | 0.6 | 0.7 | 2.2 | 0.5 | 0.3 | 0.7 |
| 9/10 | 12 | 0.0 | 0.2 | 1.2 | 0.8 | 0.3 | 0.8 |
| 9/11 | 00 | 0.2 | 0.7 | 1.0 | 0.5 | 0.3 | 0.8 |
| 9/11 | 12 | 0.0 | 0.0 | 0.0 | 0.0 | 0.0 | 0.0 |
| 9/12 | 00 | M | M | M | M | M | M |
| 9/12 | 12 | M | M | M | M | M | M |
| 9/13 | 00 | M | M | M | M | M | M |
| 9/13 | 12 | M | M | M | M | M | M |
| 9/14 | 00 | M | M | M | M | M | M |
| 9/14 | 12 | M | M | M | M | M | M |
| 9/15 | 00 | 0.0 | 5.7 | 0.0 | 0.4 | 0.0 | 0.0 |
| 9/15 | 12 | 0.0 | 0.7 | 1.3 | 1.0 | 0.0 | 0.5 |
| 9/16 | 00 | 0.2 | 0.4 | 0.6 | 0.7 | 0.5 | 0.8 |
| 9/16 | 12 | 0.0 | 0.0 | 0.0 | 5.4 | 0.0 | 0.3 |
| 9/17 | 00 | 0.0 | 0.2 | 3.8 | 0.3 | 0.3 | 0.8 |
| 9/17 | 12 | 0.2 | 0.9 | 0.0 | 0.0 | 0.0 | 0.4 |
| 9/18 | 00 | 0.5 | 0.8 | 0.2 | 0.3 | 0.3 | 0.5 |
| 9/18 | 12 | 0.0 | 0.0 | 0.0 | 0.0 | 0.0 | 0.0 |
| 9/19 | 00 | 0.0 | 0.0 | 0.0 | 0.0 | 0.0 | 0.0 |
| 9/19 | 12 | 0.0 | 0.0 | 0.0 | 0.0 | 0.0 | 0.9 |
| 9/20 | 00 | 0.6 | 1.3 | 0.2 | 0.3 | 0.3 | 0.6 |
| 9/20 | 12 | M | M | M | M | M | M |
| 9/21 | 00 | M | M | M | M | M | M |
| 9/21 | 12 | 0.1 | 0.5 | 1.1 | 1.4 | 0.6 | 0.6 |
| 9/22 | 00 | 0.0 | 0.0 | 0.0 | 0.0 | 0.6 | 0.5 |
| 9/22 | 12 | 0.0 | 0.0 | 0.0 | 0.0 | 0.0 | 0.0 |
| 9/23 | 00 | 0.0 | 0.1 | 2.9 | 2.7 | 1.1 | 1.2 |
| 9/23 | 12 | 0.0 | 0.0 | 0.0 | 0.0 | 4.8 | 3.7 |
| 9/24 | 00 | 0.4 | 1.4 | 0.8 | 0.6 | 0.3 | 0.9 |
| 9/24 | 12 | 0.0 | 1.0 | 1.2 | 0.6 | 0.3 | 0.9 |
| 9/25 | 00 | 0.0 | 0.0 | 2.0 | 2.7 | 0.6 | 1.0 |
| 9/25 | 12 | 1.8 | 0.9 | 0.7 | 0.6 | 0.3 | 0.8 |
| 9/26 | 00 | 0.0 | 0.9 | 0.5 | 0.5 | 0.3 | 0.8 |
| 9/26 | 12 | 0.0 | 2.5 | 0.7 | 0.5 | 0.3 | 0.4 |
| 9/27 | 00 | M | M | M | M | M | M |
| 9/27 | 12 | M | M | M | M | M | M |
| 9/28 | 00 | M | M | M | M | M | M |
| 9/28 | 12 | M | M | M | M | M | M |

Table 4.5
**Dynamic Seedability (Km): AMA**
**Test I**

| Date 1986 | Time (GMT) | Cloud radius (km) 0.5 | 1.0 | 1.5 | 2.0 | 3.0 | 10.0 |
|---|---|---|---|---|---|---|---|
| 5/27 | 00 | 0.0 | 0.0 | 0.1 | 0.0 | 3.2 | 3.5 |
| 5/27 | 12 | 0.0 | 0.0 | 0.0 | 0.0 | 0.0 | 0.0 |
| 5/28 | 00 | 0.0 | 0.0 | 0.0 | 0.0 | 0.0 | 0.0 |
| 5/28 | 12 | 0.0 | 0.0 | 0.0 | 0.0 | 0.0 | 0.0 |
| 5/29 | 00 | 0.0 | 0.0 | 0.1 | 0.0 | 0.2 | 0.5 |
| 5/29 | 12 | 0.0 | 0.0 | 0.0 | 0.0 | 0.0 | 0.0 |
| 5/30 | 00 | 0.0 | 0.0 | 0.3 | 1.5 | 2.0 | 1.5 |
| 5/30 | 12 | 0.0 | 0.0 | 0.0 | 0.2 | 0.2 | 0.8 |
| 5/31 | 00 | 0.0 | 0.0 | 0.3 | 1.2 | 2.7 | 0.6 |
| 5/31 | 12 | 0.0 | 0.0 | 0.0 | 0.0 | 6.5 | 5.9 |
| 6/1 | 00 | M | M | M | M | M | M |
| 6/1 | 12 | 0.0 | 0.3 | 0.9 | 1.7 | 3.6 | 0.6 |
| 6/2 | 00 | 0.0 | 1.2 | 4.3 | 0.0 | 0.0 | 0.4 |
| 6/2 | 12 | 2.9 | 0.7 | 0.3 | 0.0 | 0.0 | 0.3 |
| 6/3 | 00 | 0.0 | 0.0 | 0.2 | 0.0 | 0.2 | 5.2 |
| 6/3 | 12 | 0.0 | 2.3 | 0.0 | 0.0 | 0.3 | 0.4 |
| 6/4 | 00 | 0.0 | 2.6 | 0.0 | 0.0 | 0.0 | 0.7 |
| 6/4 | 12 | M | M | M | M | M | M |
| 6/5 | 00 | 0.0 | 0.0 | 0.0 | 0.0 | 0.0 | 0.0 |
| 6/5 | 12 | 0.0 | 0.0 | 5.5 | 0.3 | 0.0 | 0.4 |
| 6/6 | 00 | M | M | M | M | M | M |
| 6/6 | 12 | M | M | M | M | M | M |
| 6/7 | 00 | 0.9 | 0.0 | 0.3 | 0.0 | 0.0 | 0.4 |
| 6/7 | 12 | 0.7 | 0.7 | 0.3 | 0.6 | 0.4 | 0.8 |
| 6/8 | 00 | M | M | M | M | M | M |
| 6/8 | 12 | M | M | M | M | M | M |
| 6/9 | 00 | 0.2 | 2.6 | 2.6 | 2.8 | 3.0 | 2.8 |
| 6/9 | 12 | 0.0 | 0.4 | 1.0 | 1.6 | 0.3 | 0.8 |

Table 4.6
**Dynamic Seedability (Km): AMA**
**Test 2**

| Date 1986 | Time (GMT) | Cloud radius (km) 0.5 | 1.0 | 1.5 | 2.0 | 3.0 | 10.0 |
|---|---|---|---|---|---|---|---|
| 5/27 | 00 | 0.0 | 0.0 | 0.7 | 2.8 | 3.2 | 3.7 |
| 5/27 | 12 | 0.0 | 0.0 | 0.0 | 0.0 | 0.0 | 0.0 |
| 5/28 | 00 | 0.0 | 0.0 | 0.0 | 0.0 | 0.0 | 0.0 |
| 5/28 | 12 | 0.0 | 0.0 | 0.0 | 0.0 | 0.1 | 0.1 |
| 5/29 | 00 | 0.0 | 0.4 | 0.4 | 0.6 | 0.8 | 1.1 |
| 5/29 | 12 | 0.0 | 0.0 | 0.0 | 0.0 | 0.0 | 0.0 |
| 5/30 | 00 | 0.0 | 0.1 | 0.9 | 1.7 | 2.0 | 1.5 |
| 5/30 | 12 | 0.0 | 0.1 | 0.1 | 0.3 | 0.9 | 2.4 |
| 5/31 | 00 | 0.0 | 0.2 | 0.8 | 1.4 | 2.7 | 0.9 |
| 5/31 | 12 | 0.0 | 0.0 | 0.0 | 5.4 | 6.5 | 6.2 |
| 6/1 | 00 | M | M | M | M | M | M |
| 6/1 | 12 | 0.2 | 0.6 | 1.2 | 2.3 | 3.6 | 0.6 |
| 6/2 | 00 | 0.5 | 1.4 | 4.0 | 0.0 | 0.0 | 0.4 |
| 6/2 | 12 | 2.5 | 0.7 | 0.3 | 0.0 | 0.0 | 0.7 |
| 6/3 | 00 | 0.0 | 0.2 | 0.3 | 0.2 | 6.1 | 5.8 |
| 6/3 | 12 | 0.0 | 2.2 | 0.0 | 0.0 | 0.3 | 0.4 |
| 6/4 | 00 | 0.0 | 2.4 | 0.0 | 0.0 | 0.0 | 0.7 |
| 6/4 | 12 | M | M | M | M | M | M |
| 6/5 | 00 | 0.0 | 0.0 | 0.0 | 0.0 | 0.0 | 0.0 |
| 6/5 | 12 | 0.0 | 5.4 | 5.5 | 0.3 | 0.0 | 0.4 |
| 6/6 | 00 | M | M | M | M | M | M |
| 6/6 | 12 | M | M | M | M | M | M |
| 6/7 | 00 | 1.1 | 0.0 | 0.3 | 0.0 | 0.0 | 0.4 |
| 6/7 | 12 | 0.9 | 0.7 | 0.3 | 0.6 | 0.4 | 0.8 |
| 6/8 | 00 | M | M | M | M | M | M |
| 6/8 | 12 | M | M | M | M | M | M |
| 6/9 | 00 | 1.7 | 2.4 | 2.6 | 2.8 | 3.0 | 3.1 |
| 6/9 | 12 | 0.0 | 0.7 | 1.2 | 1.6 | 0.3 | 0.8 |

Table 4.7
**Dynamic Seedability (Km): AMA**
**Test 1**

| Date 1987 | Time (GMT) | Cloud radius (km) 0.5 | 1.0 | 1.5 | 2.0 | 3.0 | 10.0 |
|---|---|---|---|---|---|---|---|
| 9/9 | 00 | 0.0 | 0.3 | 0.4 | 0.8 | 1.2 | 0.4 |
| 9/9 | 12 | 0.2 | 0.7 | 2.0 | 0.8 | 0.3 | 0.4 |
| 9/10 | 00 | 1.5 | 0.6 | 0.6 | 0.7 | 0.6 | 0.7 |
| 9/10 | 12 | 0.2 | 0.6 | 0.2 | 0.3 | 0.0 | 0.4 |
| 9/11 | 00 | 1.2 | 0.5 | 0.3 | 0.0 | 0.3 | 0.4 |
| 9/11 | 12 | 5.1 | 0.3 | 0.0 | 0.0 | 0.0 | 0.3 |
| 9/12 | 00 | M | M | M | M | M | M |
| 9/12 | 12 | M | M | M | M | M | M |
| 9/13 | 00 | M | M | M | M | M | M |
| 9/13 | 12 | M | M | M | M | M | M |
| 9/14 | 00 | M | M | M | M | M | M |
| 9/14 | 12 | M | M | M | M | M | M |
| 9/15 | 00 | 0.0 | 0.2 | 0.4 | 0.8 | 1.5 | 0.8 |
| 9/15 | 12 | 0.3 | 0.2 | 0.4 | 0.2 | 0.2 | 0.8 |
| 9/16 | 00 | 0.0 | 0.0 | 0.0 | 0.0 | 3.3 | 2.6 |
| 9/16 | 12 | 0.0 | 0.0 | 3.7 | 3.6 | 3.5 | 0.9 |
| 9/17 | 00 | 0.0 | 0.2 | 0.0 | 0.2 | 0.2 | 0.2 |
| 9/17 | 12 | 0.4 | 0.5 | 0.3 | 0.0 | 0.0 | 0.4 |
| 9/18 | 00 | 0.6 | 1.1 | 0.3 | 0.0 | 0.0 | 0.5 |
| 9/18 | 12 | 0.2 | 0.5 | 0.9 | 1.5 | 5.1 | 4.5 |
| 9/19 | 00 | 0.0 | 0.0 | 0.0 | 0.0 | 0.0 | 0.0 |
| 9/19 | 12 | 0.0 | 0.2 | 0.3 | 0.0 | 0.0 | 0.4 |
| 9/20 | 00 | 0.0 | 0.0 | 0.3 | 0.0 | 0.3 | 0.4 |
| 9/20 | 12 | M | M | M | M | M | M |
| 9/21 | 00 | M | M | M | M | M | M |
| 9/21 | 12 | 0.0 | 0.3 | 0.8 | 1.3 | 0.2 | 0.6 |
| 9/22 | 00 | 0.0 | 1.4 | 1.2 | 1.1 | 0.6 | 1.3 |
| 9/22 | 12 | 0.1 | 1.2 | 0.2 | 0.0 | 0.2 | 0.6 |
| 9/23 | 00 | 0.0 | 0.0 | 0.0 | 0.0 | 0.0 | 2.8 |
| 9/23 | 12 | 0.0 | 0.2 | 3.3 | 3.7 | 0.3 | 0.7 |
| 9/24 | 00 | 0.2 | 2.3 | 0.3 | 0.3 | 0.0 | 0.4 |
| 9/24 | 12 | 0.5 | 1.4 | 2.2 | 0.5 | 0.6 | 1.0 |
| 9/25 | 00 | 0.2 | 1.8 | 0.3 | 0.3 | 0.3 | 0.8 |
| 9/25 | 12 | 0.5 | 2.9 | 0.3 | 0.3 | 0.3 | 0.4 |
| 2/26 | 00 | 0.0 | 2.8 | 1.2 | 0.6 | 0.3 | 0.4 |
| 2/26 | 12 | 0.8 | 0.0 | 0.0 | 0.0 | 0.0 | 0.4 |
| 9/27 | 00 | M | M | M | M | M | M |
| 9/27 | 12 | M | M | M | M | M | M |
| 9/28 | 00 | M | M | M | M | M | M |
| 9/28 | 12 | M | M | M | M | M | M |

Table 4.8
**Dynamic Seedability (Km): AMA**
**Test 2**

| Date 1987 | Time (GMT) | Cloud radius (km) 0.5 | 1.0 | 1.5 | 2.0 | 3.0 | 10.0 |
|---|---|---|---|---|---|---|---|
| 9/9 | 00 | 0.0 | 0.3 | 0.5 | 1.0 | 1.2 | 0.4 |
| 9/9 | 12 | 0.4 | 0.9 | 2.2 | 1.1 | 0.3 | 0.4 |
| 9/10 | 00 | 1.5 | 0.6 | 0.6 | 0.7 | 0.6 | 0.7 |
| 9/10 | 12 | 0.2 | 0.6 | 0.2 | 0.3 | 0.0 | 0.4 |
| 9/11 | 00 | 1.1 | 0.5 | 0.3 | 0.0 | 0.3 | 0.4 |
| 9/11 | 12 | 4.8 | 0.3 | 0.0 | 0.0 | 0.0 | 0.7 |
| 9/12 | 00 | M | M | M | M | M | M |
| 9/12 | 12 | M | M | M | M | M | M |
| 9/13 | 00 | M | M | M | M | M | M |
| 9/13 | 12 | M | M | M | M | M | M |
| 9/14 | 00 | M | M | M | M | M | M |
| 9/14 | 12 | M | M | M | M | M | M |
| 9/15 | 00 | 0.0 | 0.3 | 0.5 | 1.0 | 1.7 | 0.8 |
| 9/15 | 12 | 0.5 | 0.2 | 0.4 | 0.2 | 0.2 | 1.1 |
| 9/16 | 00 | 0.0 | 0.1 | 2.3 | 2.6 | 3.3 | 2.6 |
| 9/16 | 12 | 0.0 | 0.5 | 1.9 | 3.6 | 3.5 | 0.9 |
| 9/17 | 00 | 0.0 | 0.2 | 0.2 | 0.3 | 0.3 | 0.5 |
| 9/17 | 12 | 0.5 | 0.5 | 0.3 | 0.0 | 0.0 | 0.4 |
| 9/18 | 00 | 0.6 | 1.1 | 0.3 | 0.0 | 0.0 | 0.5 |
| 9/18 | 12 | 0.3 | 1.1 | 1.4 | 2.8 | 5.1 | 4.5 |
| 9/19 | 00 | 0.0 | 0.0 | 0.0 | 0.0 | 0.0 | 0.0 |
| 9/19 | 12 | 0.0 | 0.2 | 0.3 | 0.0 | 0.0 | 0.4 |
| 9/20 | 00 | 0.0 | 0.0 | 0.3 | 0.0 | 0.3 | 0.4 |
| 9/20 | 12 | M | M | M | M | M | M |
| 9/21 | 00 | M | M | M | M | M | M |
| 9/21 | 12 | 0.0 | 0.6 | 1.1 | 1.5 | 0.2 | 0.8 |
| 9/22 | 00 | 0.0 | 1.1 | 1.4 | 1.1 | 0.6 | 1.3 |
| 9/22 | 12 | 0.1 | 1.4 | 0.2 | 0.0 | 0.2 | 0.6 |
| 9/23 | 00 | 0.0 | 0.0 | 0.0 | 0.0 | 0.0 | 3.1 |
| 9/23 | 12 | 0.0 | 1.3 | 3.3 | 3.7 | 0.3 | 0.7 |
| 9/24 | 00 | 1.0 | 2.3 | 0.3 | 0.3 | 0.0 | 0.4 |
| 9/24 | 12 | 0.7 | 1.6 | 2.2 | 0.5 | 0.6 | 1.0 |
| 9/25 | 00 | 0.4 | 1.8 | 0.3 | 0.3 | 0.3 | 0.8 |
| 9/25 | 12 | 0.9 | 2.9 | 0.3 | 0.3 | 0.3 | 0.4 |
| 9/26 | 00 | 0.0 | 2.8 | 1.2 | 0.6 | 0.3 | 0.4 |
| 9/26 | 12 | 0.0 | 0.0 | 0.0 | 0.0 | 0.0 | 0.4 |
| 9/27 | 00 | M | M | M | M | M | M |
| 9/27 | 12 | M | M | M | M | M | M |
| 9/28 | 00 | M | M | M | M | M | M |
| 9/28 | 12 | M | M | M | M | M | M |

Table 4.9
**Dynamic Seedability (Km): DDC**
**Test 1**

| Date 1986 | Time (GMT) | Cloud radius (km) O.5 | 1.0 | 1.5 | 2.0 | 3.0 | 10.0 |
|---|---|---|---|---|---|---|---|
| 5/27 | 00 | 0.0 | 0.1 | 0.1 | 3.9 | 3.8 | 3.1 |
| 5/27 | 12 | 1.3 | 0.0 | 0.2 | 0.0 | 0.0 | 0.5 |
| 5/28 | 00 | 0.0 | 0.0 | 0.0 | 0.0 | 0.0 | 0.0 |
| 5/28 | 12 | 0.0 | 0.0 | 0.0 | 5.7 | 5.7 | 1.4 |
| 5/29 | 00 | 0.0 | 0.0 | 0.3 | 0.5 | 4.2 | 0.5 |
| 5/29 | 12 | 0.0 | 0.0 | 0.0 | 0.0 | 0.0 | 0.0 |
| 5/30 | 00 | 0.0 | 0.0 | 0.3 | 0.8 | 3.0 | 1.1 |
| 5/30 | 12 | 0.0 | 0.2 | 1.0 | 1.8 | 0.9 | 1.4 |
| 5/31 | 00 | 0.0 | 0.0 | 0.0 | 0.0 | 0.2 | 0.2 |
| 5/31 | 12 | 0.0 | 0.0 | 0.5 | 0.5 | 2.6 | 1.2 |
| 6/1 | 00 | 0.3 | 1.3 | 1.8 | 0.5 | 0.0 | 0.4 |
| 6/1 | 12 | 0.0 | 0.0 | 1.6 | 0.3 | 0.0 | 0.4 |
| 6/2 | 00 | 0.0 | 0.0 | 0.0 | 0.0 | 0.0 | 0.4 |
| 6/2 | 12 | 0.2 | 0.2 | 0.0 | 0.0 | 0.2 | 0.7 |
| 6/3 | 00 | 0.0 | 0.8 | 1.4 | 3.9 | 0.0 | 0.4 |
| 6/3 | 12 | 0.0 | 1.1 | 1.4 | 4.6 | 4.7 | 0.7 |
| 6/4 | 00 | 0.0 | 6.1 | 0.3 | 0.4 | 0.0 | 0.5 |
| 6/4 | 12 | M | M | M | M | M | M |
| 6/5 | 00 | 0.4 | 0.3 | 0.0 | 0.4 | 0.0 | 0.0 |
| 6/5 | 12 | 0.3 | 0.7 | 1.7 | 1.0 | 0.3 | 0.4 |
| 6/6 | 00 | M | M | M | M | M | M |
| 6/6 | 12 | M | M | M | M | M | M |
| 6/7 | 00 | 3.8 | 0.3 | 0.0 | 0.0 | 0.0 | 0.5 |
| 6/7 | 12 | 0.4 | 0.9 | 0.5 | 0.3 | 0.3 | 0.8 |
| 6/8 | 00 | M | M | M | M | M | M |
| 6/8 | 12 | M | M | M | M | M | M |
| 6/9 | 00 | 0.2 | 1.2 | 1.2 | 1.1 | 1.1 | 1.3 |
| 6/9 | 12 | 0.0 | 0.2 | 1.7 | 2.2 | 0.3 | 1.0 |

Table 4.10
**Dynamic Seedability (Km): DDC**
**Test 2**

| Date 1986 | Time (GMT) | Cloud radius (km) O.5 | 1.0 | 1.5 | 2.0 | 3.0 | 10.0 |
|---|---|---|---|---|---|---|---|
| 5/27 | 00 | 0.0 | 3.4 | 3.5 | 3.7 | 3.8 | 3.5 |
| 5/27 | 12 | 1.3 | 0.0 | 0.2 | 0.0 | 0.0 | 0.5 |
| 5/28 | 00 | 0.0 | 0.0 | 0.0 | 0.0 | 0.0 | 0.0 |
| 5/28 | 12 | 0.0 | 0.0 | 0.0 | 5.7 | 5.7 | 5.1 |
| 5/29 | 00 | 0.0 | 0.0 | 0.6 | 1.4 | 4.0 | 0.5 |
| 5/29 | 12 | 0.0 | 0.0 | 0.0 | 0.0 | 0.0 | 0.0 |
| 5/30 | 00 | 0.1 | 0.3 | 0.8 | 1.7 | 3.2 | 1.1 |
| 5/30 | 12 | 0.0 | 0.5 | 1.4 | 1.8 | 0.9 | 1.4 |
| 5/31 | 00 | 0.0 | 0.1 | 0.2 | 0.2 | 0.3 | 0.5 |
| 5/31 | 12 | 0.1 | 0.3 | 0.6 | 0.9 | 2.8 | 1.2 |
| 6/1 | 00 | 0.7 | 1.5 | 1.8 | 0.5 | 0.0 | 0.4 |
| 6/1 | 12 | 0.0 | 0.0 | 1.4 | 0.0 | 0.0 | 0.4 |
| 6/2 | 00 | 0.0 | 0.0 | 0.0 | 0.0 | 0.0 | 0.7 |
| 6/2 | 12 | 0.3 | 0.2 | 0.0 | 0.0 | 0.2 | 0.7 |
| 6/3 | 00 | 0.0 | 1.1 | 1.6 | 3.6 | 0.0 | 0.4 |
| 6/3 | 12 | 0.0 | 1.1 | 1.6 | 4.0 | 4.7 | 0.7 |
| 6/4 | 00 | 0.0 | 6.1 | 0.3 | 0.4 | 0.0 | 0.5 |
| 6/4 | 12 | M | M | M | M | M | M |
| 6/5 | 00 | 0.6 | 0.3 | 0.0 | 0.4 | 0.0 | 0.0 |
| 6/5 | 12 | 0.5 | 0.9 | 1.7 | 1.0 | 0.3 | 0.4 |
| 6/6 | 00 | M | M | M | M | M | M |
| 6/6 | 12 | M | M | M | M | M | M |
| 6/7 | 00 | 2.0 | 0.3 | 0.0 | 0.0 | 0.0 | 0.5 |
| 6/7 | 12 | 0.6 | 1.1 | 0.8 | 0.6 | 0.3 | 0.8 |
| 6/8 | 00 | M | M | M | M | M | M |
| 6/8 | 12 | M | M | M | M | M | M |
| 6/9 | 00 | 0.7 | 1.2 | 1.2 | 1.2 | 1.3 | 1.5 |
| 6/9 | 12 | 0.0 | 0.7 | 1.9 | 2.2 | 0.6 | 1.0 |

Table 4.11
**Dynamic Seedability (Km): DDC**
**Test 1**

| Date 1987 | Time (GMT) | Cloud radius (km) O.5 | 1.0 | 1.5 | 2.0 | 3.0 | 10.0 |
|---|---|---|---|---|---|---|---|
| 9/9 | 00 | 0.2 | 0.2 | 0.0 | 0.3 | 0.3 | 0.4 |
| 9/9 | 12 | 0.3 | 0.9 | 0.5 | 0.3 | 0.0 | 0.0 |
| 9/10 | 00 | 0.7 | 0.3 | 0.0 | 0.3 | 0.0 | 0.4 |
| 9/10 | 12 | 2.6 | 0.0 | 0.3 | 0.0 | 0.0 | 0.0 |
| 9/11 | 00 | 3.9 | 0.0 | 0.0 | 0.0 | 0.3 | 0.4 |
| 9/11 | 12 | 1.3 | 2.2 | 0.3 | 0.0 | 0.0 | 0.4 |
| 9/12 | 00 | M | M | M | M | M | M |
| 9/12 | 12 | M | M | M | M | M | M |
| 9/13 | 00 | M | M | M | M | M | M |
| 9/13 | 12 | M | M | M | M | M | M |
| 9/14 | 00 | M | M | M | M | M | M |
| 9/14 | 12 | M | M | M | M | M | M |
| 9/15 | 00 | 0.7 | 1.1 | 0.5 | 0.3 | 0.0 | 0.8 |
| 9/15 | 12 | 0.4 | 0.2 | 0.2 | 0.2 | 0.3 | 0.7 |
| 9/16 | 00 | 0.5 | 1.2 | 0.2 | 0.2 | 0.3 | 0.3 |
| 9/16 | 12 | M | M | M | M | M | M |
| 9/17 | 00 | 0.0 | 0.0 | 0.0 | 0.0 | 0.0 | 0.5 |
| 9/17 | 12 | 0.7 | 0.6 | 0.2 | 0.3 | 0.3 | 0.4 |
| 9/18 | 00 | 0.6 | 0.2 | 0.2 | 0.0 | 0.0 | 0.4 |
| 9/18 | 12 | 0.0 | 0.0 | 0.0 | 0.0 | 0.0 | 0.0 |
| 9/19 | 00 | 0.0 | 0.0 | 0.0 | 0.0 | 0.2 | 3.2 |
| 9/19 | 12 | 1.2 | 0.7 | 0.4 | 0.2 | 0.0 | 0.4 |
| 9/20 | 00 | 0.5 | 0.4 | 0.4 | 0.2 | 0.3 | 0.7 |
| 9/20 | 12 | M | M | M | M | M | M |
| 9/21 | 00 | M | M | M | M | M | M |
| 9/21 | 12 | 0.0 | 0.1 | 0.1 | 0.3 | 0.5 | 0.6 |
| 9/22 | 00 | 0.1 | 0.9 | 1.1 | 1.1 | 1.3 | 1.4 |
| 9/22 | 12 | 0.0 | 0.0 | 0.0 | 0.0 | 0.0 | 0.0 |
| 9/23 | 00 | 0.0 | 0.0 | 0.0 | 0.0 | 0.0 | 0.9 |
| 9/23 | 12 | 0.0 | 0.0 | 0.0 | 0.0 | 0.0 | 0.0 |
| 9/24 | 00 | 0.0 | 0.6 | 2.1 | 0.3 | 0.0 | 0.5 |
| 9/24 | 12 | 0.0 | 0.0 | 0.0 | 0.0 | 0.0 | 0.8 |
| 9/25 | 00 | 0.2 | 0.8 | 1.4 | 0.5 | 0.3 | 0.8 |
| 9/25 | 12 | 0.0 | 0.0 | 0.0 | 0.0 | 0.0 | 0.0 |
| 9/26 | 00 | 0.4 | 1.2 | 0.7 | 0.5 | 0.3 | 1.0 |
| 9/26 | 12 | 3.5 | 0.3 | 0.3 | 0.0 | 0.0 | 0.4 |
| 9/27 | 00 | M | M | M | M | M | M |
| 9/27 | 12 | M | M | M | M | M | M |
| 9/28 | 00 | M | M | M | M | M | M |
| 9/28 | 12 | M | M | M | M | M | M |

Table 4.12
**Dynamic Seedability (Km): DDC**
**Test 2**

| Date 1987 | Time (GMT) | Cloud radius (km) O.5 | 1.0 | 1.5 | 2.0 | 3.0 | 10.0 |
|---|---|---|---|---|---|---|---|
| 9/9 | 00 | 0.5 | 0.2 | 0.0 | 0.3 | 0.3 | 0.4 |
| 9/9 | 12 | 0.5 | 0.9 | 0.5 | 0.3 | 0.3 | 0.0 |
| 9/10 | 00 | 0.7 | 0.5 | 0.0 | 0.3 | 0.0 | 0.4 |
| 9/10 | 12 | 2.2 | 0.0 | 0.3 | 0.0 | 0.0 | 0.5 |
| 9/11 | 00 | 3.9 | 0.0 | 0.0 | 0.0 | 0.3 | 0.4 |
| 9/11 | 12 | 1.3 | 2.2 | 0.3 | 0.0 | 0.0 | 0.4 |
| 9/12 | 00 | M | M | M | M | M | M |
| 9/12 | 12 | M | M | M | M | M | M |
| 9/13 | 00 | M | M | M | M | M | M |
| 9/13 | 12 | M | M | M | M | M | M |
| 9/14 | 00 | M | M | M | M | M | M |
| 9/14 | 12 | M | M | M | M | M | M |
| 9/15 | 00 | 0.9 | 1.4 | 0.5 | 0.3 | 0.0 | 0.8 |
| 9/15 | 12 | 0.4 | 0.4 | 0.2 | 0.2 | 0.3 | 0.7 |
| 9/16 | 00 | 0.7 | 1.4 | 0.2 | 0.2 | 0.3 | 0.6 |
| 9/16 | 12 | M | M | M | M | M | M |
| 9/17 | 00 | 0.0 | 0.0 | 0.0 | 0.0 | 0.0 | 0.5 |
| 9/17 | 12 | 0.6 | 0.6 | 0.5 | 0.3 | 0.3 | 0.4 |
| 9/18 | 00 | 0.5 | 0.2 | 0.2 | 0.0 | 0.0 | 0.4 |
| 9/18 | 12 | 0.0 | 0.0 | 0.0 | 0.0 | 0.0 | 0.0 |
| 9/19 | 00 | 0.0 | 0.1 | 0.2 | 0.2 | 0.3 | 3.6 |
| 9/19 | 12 | 1.2 | 0.9 | 0.4 | 0.2 | 0.3 | 0.4 |
| 9/20 | 00 | 0.5 | 0.4 | 0.4 | 0.5 | 0.3 | 0.7 |
| 9/20 | 12 | M | M | M | M | M | M |
| 9/21 | 00 | M | M | M | M | M | M |
| 9/21 | 12 | 0.1 | 0.3 | 0.3 | 0.5 | 0.6 | 1.0 |
| 9/22 | 00 | 0.6 | 1.1 | 1.3 | 1.3 | 1.5 | 1.6 |
| 9/22 | 12 | 0.0 | 0.0 | 0.0 | 0.0 | 0.0 | 0.0 |
| 9/23 | 00 | 0.0 | 0.0 | 0.2 | 0.3 | 5.0 | 1.2 |
| 9/23 | 12 | 0.0 | 0.0 | 0.0 | 0.0 | 0.0 | 0.0 |
| 9/24 | 00 | 0.0 | 0.8 | 2.4 | 0.3 | 0.4 | 0.5 |
| 9/24 | 12 | 0.0 | 0.0 | 0.0 | 0.0 | 0.0 | 0.8 |
| 9/25 | 00 | 0.2 | 0.8 | 1.6 | 0.5 | 0.6 | 0.8 |
| 9/25 | 12 | 0.0 | 0.0 | 0.0 | 0.0 | 0.0 | 0.0 |
| 9/26 | 00 | 0.4 | 1.2 | 0.7 | 0.5 | 0.3 | 1.0 |
| 9/26 | 12 | 3.2 | 0.0 | 0.3 | 0.0 | 0.0 | 0.4 |
| 9/27 | 00 | M | M | M | M | M | M |
| 9/27 | 12 | M | M | M | M | M | M |
| 9/28 | 00 | M | M | M | M | M | M |
| 9/28 | 12 | M | M | M | M | M | M |

major systems which produced severe thunderstorms. Those major systems would then be followed by 2 or 3 days of quiescence. The clouds encountered were probably different from the seasonal norms in that they grew with less explosiveness, grew in a deeper moisture field, and were more numerous than would be considered typical. The sampling period was representative of a relatively moist mid-spring period.

3.2 The Late Summer Period (September 9-28, 1987)

Summer in Oklahoma dies hard, but in normal times the oppressive heat of August gives way to a milder September. The jet stream typically begins to work its way southward during September, bringing with it an occasional surface frontal system. Rainfall in Oklahoma generally increases during the transition from summer to fall. Overall rainfall is not normally as great in the fall as during the spring storm season. Rainfall is sometimes increased dramatically by remnants of tropical disturbances, either from the Gulf of Mexico or from the Pacific Ocean via Mexico, which occasionally enter Oklahoma as they become incorporated into the mid-latitudinal weather systems.

Western portions of Oklahoma received near normal rainfall during the first half of the sampling period, but the last half was much wetter than normal. By the end of the month total precipitation in each of the six climate divisions in the western two-thirds of the State was 1 to 2 inches above the monthly norm (NOAA, 1987). Rainfall was reported somewhere in the experimental area on every day from the 6th through the 22nd. Significant storm systems moved across the State on the 9th, the 14th and 15th, the 18th and on the 27th of the month (OCS, 1987).

The Oklahoma City 1200 GMT rawinsonde observations are summarized in Table 3. The average soundings were somewhat cooler and more stable than normal, although individual events differed greatly from those means. Available moisture averaged less than normal. The events that produced the greater-than-average rainfall differed little from those typically observed in September. The frequency of rainfall events of interest to the sampling effort was greater than normal. Rain-producing storms that were sampled were probably similar in nature, though greater in number than would be expected in a typical September.

In summary, a few differences existed between historical means and the clouds sampled in Spring 1986 and Fall 1987. However, these differences were small and it is probable that observed microphysical characteristics and predicted dynamic seedabilities can be considered representative of an "average" spring and fall in Oklahoma.

## 4. SUMMARY

Oklahoma convective clouds, observed during the periods May 27 - June 9, 1986 and September 9-28, 1987, appear to be representative of clouds typically encountered during these seasonal time periods. The GPCM, initiated with soundings from Oklahoma City, Amarillo and Dodge City, indicated some opportunity for dynamic seedability on all days when convection was observed. Comparison of model runs simulating silver iodide seeding and dry ice seeding suggested a small advantage to the dry ice. Further studies will be done to check the model's realism by comparing predicted water content values to in-situ cloud microphysical measurements. Stratification of response variables to predicted natural cloud height will also be examined.

The microphysical mechanisms observed in Oklahoma convective clouds suggest that the initial development of precipitation occurs via collision-coalescence. This sequence is similar to that previously identified in the clouds from the Texas HIPLEX region. Additionally, the observed Oklahoma clouds contained supercooled water in amounts equal to or greater than the amounts reported for Texas HIPLEX clouds.

In view of the growing evidence suggesting increased rainfall in Texas HIPLEX as the result of a dynamic seeding approach, further investigation of this strategy for Oklahoma clouds seems warranted.

## 5. ACKNOWLEDGEMENTS

The authors are indebted to the Bureau of Reclamation and the Oklahoma Water Resources Board for providing support for this work. The authors would also like to thank Sana Bahouth for her assistance in manuscript preparation.

## 6. REFERENCES

Bureau of Reclamation, 1979: The design of HIPLEX-1, High Plains Cooperative Program, U.S. Department of Interior, Bureau of Reclamation, 271 pp.

Cooper, W. A. and P. R. Lawson, 1984: Physical interpretation of results from the HIPLEX-1 experiment, Climate and Appl. Meteor., 23, 523-540.

Eddy, A., 1982: "A rainfall climatology for Oklahoma", Operational Weather Modification, Vol. 5, Oklahoma Climatological Survey, Norman, OK. 120 pp.

Hirsch, J. H. 1971: Computer modeling of cumulus clouds during Project Cloud Catcher. Report 71-7, Institute of Atmospheric Sciences, South Dakota School of Mines and Technology, Rapid City, SD. 61 pp.

Johnson, H. L., 1982: "A climatology of convective instability and cloud model output", Operational Weather Modification, Vol. 7, Oklahoma Climatological Survey, Norman, OK. 125 pp.

Jurica, G. M. and W. L. Woodley, 1985: The design of the Southwest Cooperative Program rainfall enchancement experiment. Texas Water Commission, Austin, TX. 140 pp.

Mathis, M. E., 1987: Southwest Cooperative Program 1986: Oklahoma field project, Final Report, Oklahoma Water Resources Board, Oklahoma City, OK. 93 pp.

Mathis, M. E. and E. J. Gibeau: Oklahoma rainfall enhancement program. Oklahoma Water Resources Board and Aeromet, Inc., Oklahoma City, OK. 124 pp.

Matthews, D. A., 1981: Natural variability of thermodynamic features affecting convective cloud growth and dynamic seeding: A comparative summary of three High Plain sites from 1975 to 1977. J. Appl. Meteor., 20, 971-996.

NOAA, 1987: Climatological data: Oklahoma, September 1987, Volume 96, No. 9, National Climatic Data Center, Asheville, NC. 30 pp.

OCS, 1986a: Oklahoma climate summary May 1986, Oklahoma Climatological Survey, Norman, OK. 16pp.

___, 1986b: Oklahoma climate summary June 1986, Oklahoma Climatological Survey, Norman, OK. 19pp.

___, 1987: Oklahoma climate summary September1987, Oklahoma Climatological Survey, Norman, OK. 17pp.

Pflaum, J. C., 1988: Microphysical studies of Oklahoma clouds. Final report to the Oklahoma Water Resources Board. CIMMS Report No. 86. Univ. of Oklahoma, Norman, OK. 67 pp.

Poellot, M. R., 1986: Persistence of supercooled liquid water and the development of ice in Oklahoma convective clouds. Univ. of North Dakota, AS-86-1. 38 pp.

_____, 1988: Weather modification pilot training and weather modification research. Supplemental final report to U. S. Bureau of Reclamation. Univ. of North Dakota, Grand Forks, ND. 37 pp.

Simpson, J., 1976: Precipitation augmentation from cumulus clouds and systems: Scientific and technological foundations. Adv. in Geophysics, Vol. 19, Academic Press, 1-72.

Woodley, W. L. and D. Rosenfeld, 1988: Assessment of the effect of treatment in SWCP. Woodley Weather Consultants, Boulder, CO. 388 pp.

_____, A. Gagin and D. Rosenfeld, 1987: Assessment of seeding effects in the SWCP of 1986. Final report. Woodley Weather Consultants, Boulder, CO. 44 pp.

Table 2. Comparison of May 27-June 9, 1986 OKC Rawinsonde Parameters to Historical Data (1976-1987)

| | Historical | | 1986 | | |
|---|---|---|---|---|---|
| Parameter | mean | st. dev. | mean | min | max |
| Freezing level (km) | 4.17 | 0.51 | 3.85 | 2.71 | 4.67 |
| -5C isotherm (km) | 4.92 | 0.50 | 4.79 | 3.56 | 5.63 |
| -10C isotherm (km) | 5.59 | 0.53 | 5.64 | 4.31 | 6.58 |
| CCL Height (km) | 2.56 | 1.03 | 3.51 | 3.17 | 4.17 |
| CCL Temperature (°C) | 10.71 | 5.30 | 12.96 | 5.66 | 17.89 |
| Precip Water (cm) | 2.84 | 0.73 | 3.28 | 1.84 | 3.95 |
| Mixing Ratio (g/kg) | 10.74 | 2.87 | 11.70 | 7.36 | 14.63 |
| Lifted Index | 0.40 | 5.20 | 0.40 | -1.30 | 3.10 |
| K-Index | 24.50 | 11.90 | 32.50 | 27.30 | 36.50 |
| SWEAT Index | 219.70 | 124.30 | 173.40 | 104.60 | 232.00 |
| Total Totals Index | 46.30 | 8.50 | 46.40 | 42.90 | 50.50 |
| T at 850 mb (°C) | 16.70 | 5.20 | 13.20 | 6.60 | 17.40 |
| TD at 850 mb (°C) | 8.80 | 5.50 | 10.80 | 4.00 | 16.10 |
| T-TD at 850 mb (°C) | 8.00 | 5.30 | 2.40 | 0.70 | 7.00 |
| T at 700 mb (°C) | 7.40 | 3.70 | 4.20 | -1.90 | 8.00 |
| TD at 700 mb (°C) | -3.90 | 7.70 | 1.40 | -5.50 | 5.40 |
| T-TD at 700 mb (°C) | 11.30 | 8.40 | 2.80 | 0.20 | 6.00 |
| T at 500 mb (°C) | -10.50 | 2.30 | -11.10 | -18.90 | -10.30 |

Table 3. Comparison of September 1987 OKC Rawinsonde Parameters to Historical Data (1976-1987)

| | Historical | | 1987 | | |
|---|---|---|---|---|---|
| Parameter | mean | st. dev. | mean | min | max |
| Freezing level (km) | 4.32 | 0.53 | 4.06 | 3.25 | 4.61 |
| -5C isotherm (km) | 5.16 | 0.41 | 4.99 | 4.28 | 5.35 |
| -10C isotherm (km) | 5.88 | 0.42 | 5.75 | 4.98 | 6.21 |
| CCL Height (km) | 2.97 | 1.13 | 4.47 | 1.81 | 5.86 |
| CCL Temperature (°C) | 9.88 | 6.46 | 6.34 | -4.42 | 15.46 |
| Precip Water (cm) | 2.97 | 0.93 | 2.33 | 0.99 | 3.94 |
| Mixing Ratio (g/kg) | 10.54 | 3.18 | 8.85 | 4.82 | 13.18 |
| Lifted Index | 2.00 | 5.80 | 3.60 | -3.80 | 11.30 |
| K-Index | 23.50 | 14.00 | 19.20 | -10.10 | 37.50 |
| SWEAT Index | 191.70 | 92.70 | 145.30 | 21.30 | 266.60 |
| Total Totals Index | 43.60 | 8.20 | 42.60 | 23.00 | 53.80 |
| T at 850 mb (°C) | 16.90 | 4.20 | 15.80 | 8.60 | 19.80 |
| TD at 850 mb (°C) | 8.70 | 6.90 | 5.50 | -15.80 | 14.20 |
| T-TD at 850 mb (°C) | 8.30 | 6.30 | 10.30 | 0.80 | 30.00 |
| T at 700 mb (°C) | 7.50 | 2.80 | 5.40 | 0.60 | 8.80 |
| TD at 700 mb (°C) | -3.50 | 9.00 | -7.30 | -24.60 | 4.20 |
| T-TD at 700 mb (°C) | 11.00 | 9.00 | 12.70 | 1.20 | 30.00 |
| T at 500 mb (°C) | -9.10 | 2.40 | -10.70 | -15.70 | -7.70 |

# PROJECTION ONTO GROUND RAINFALL DISTRIBUTIONS OF EFFECTS OF SEEDING CONVECTIVE CLOUDCELLS

Arie Ben-Zvi
Israel hydrological Service
P.O.Box 6381, Jerusalem 91063, ISRAEL

Abstract. Observed changes in the ground distributions of rainfall in the first and Second Israeli cloud seeding experiments are related to observed changes in cloud cell size and rainwater volume, rate and duration. The ground information is recorded by standard stations under static seeding experimentation in Israel, while the cloud information is of a radar records under dynamic seeding experimentation in Florida. The increase in the ground rainfall intensity seems to follow the increase in cloud cell depth. The increase in the ground rainfall duration, frequency and spatial correlation is suggested to be related to the increase in the cloud size and rainwater content, and to the kinematics of its motion. The well known increase in the ground rainfall depth (Gagin and Neumann, 1974)

## 1. INTRODUCTION

Static cloud seeding experiments in Israel, 1960 to 1967 and 1969 to 1975, apparently caused an average increase of 13 to 15 percent, significant within 5%, in the daily depth of precipitation over the target area (Gagin and Neumann, 1974, 1981). Further analyses of ground data reveal increases in the spatial correlation of daily depth of precipitation (Sharon, 1978; Ben-Zvi, 1988), in the daily duration of the rainfall (Gagin and Gabriel, 1987), in the number of rainfall events per day (Gagin and Gabriel, 1987), and in the rainfall intensity (Ben-Zvi, 1988).

The dynamic cloud seeding experiment brought increases in the precipitation echo for the top height of the convective cells, for the area covered by the cells, and in the radar derived rainfall volume, rate and duration (Gagin et al., 1986). The main results of the two modes of experimentation have been been summarized by Gagin (1986). The present work provides another link between the results of the two modes of seeding.

## 2. RAINFALL INTENSITY

Based upon vertically pointing radar data of cloud depths, and upon ground data of raindrop characteristics, Gagin (1980) has derived regression formulas relating rainfall intensity to cloud depth. In these formulas, the maximal and the temporally averaged rainfall intensity from a passing raincloud, increase monotonously with the maximal cloud depth.

Having analysed raingage charts, of ten stations for the Second Israeli Rainfall Enhancement Experiment, Gagin and Gabriel (1987) found no apparent effect on the distribution of the daily rainfall intensity. Yet, from their mean daily depth and duration of rainfall, one can compute totals for the entire experiment and obtain the overall mean intensity for the different series in the experiment. These are (in mm/h): 3.99 for the seeded target, 3.32 for the unseeded target, 5.29 for the "seeded" control, and 4.68 for the "unseeded" control. The overall mean intensity for the seeded rainfall at the target is 1.20 times higher than that for the unseeded rainfall. The ratio of the overall mean intensities for the corresponding days at the control is only 1.13. This indicates, although without any computable statistical significance, that the cloud seeding contributes also to the rainfall intensity.

From an independent analysis of charts of four of those raingages, Ben-Zvi (1988) obtained some additional conclusions. A summation of the rainfall depth, according to the instantaneous intensity, reveals that its distribution is changed. The share of the intense rainfall depth ( >20 mm/h) increased from 11 to 17 percent, while the share of the depth falling at low intrensity ( <5 mm/h) decreased from 63 to 54 percent. At the same time, the distribution of the rainfall depth at the control is the same for the "seeded" and the "unseeded" states.

From an analysis of radar data on clouds in the FACE-2 dynamic seeding experiment, Gagin et al. (1986) concluded that cells exposed to a high dosage of AgI in their early stages, grow larger and yield more rainwater. On the average, these cells are 20 percent taller, and their areas are 50 percent larger, than those of the corresponding sand-treated cells. The average rainwater yield of those cells is 2.6 times higher than that of the corresponding sand-treated cells. On the average, the maximal rainfall rate for the early and high dosage AgI treated cells is 2.0 times higher, and the duration of the rainfall at their bases is 1.8 times longer than those for the corresponding sand-treated cells. These figures are statistically significant

within 2%. Cells which are exposed to a lower dosage, or are treated at a later stage of their lives, are considerably less affected.

The data published by Gagin et al. (1986) provide for two estimates of the mean rainfall intensity at the cloud base:

$$R_m = RVR_{max} / A_{max} \quad (1)$$

$$R_a = RV / (DUR \cdot A_{max}) \quad (2)$$

in which $R_m$ and $R_a$ are "maximal" and "averaged" intensities at the cloud base, $RVR_{max}$ is the maximal rainfall rate at the cloud base, $A_{max}$ is the maximal cell area, RV is the rain volume which the cell yields, and DUR is the rainfall duration at the cloud base. It should be noted here that since $A_{max}$ does not last for the entire DUR, and as it does not necessarily appear simultaneously with $RVR_{max}$, both estimates for $R_m$ and $R_a$ are downwardsly biased. We assume that the bias inflicted on the estimates for the AgI treated cells is similar to that for the sand treated cells.

For the early and the high dosage AgI treated cells, $R_m$ is 9.8 mm/h, and $R_a$ is 5.6 mm/h; while for the corresponding sand treated cells they are, respectively, 8.1 and 4.6 mm/h. The estimates for these AgI treated cells are 1.21 times higher than those for the sand treated cells. This ratio is equal to the single ratio of the maximal cloud depths (Gagin, 1986).

The simultaneous increase in the cloud depth and in its rainfall intensity is consistent with the conclusion of Gagin (1980), although the numerical value is different. This difference is attributed to the differences in the observation and the seeding methodologies, and to the differences in the rain processes between the sites.

The seeming inagreement between our positive results, about the rainfall intensity, and the inconclusive results of Gagin and Gabriel (1987), stems from the difference between the definitions of the discussed intensity. Gagin and Gabriel (1987) compared statistics of mean daily intensities, while we compare the distribution of the depth according to the instantaneous intensity. The relation between these two variables is not linear. For example, an addition of a few days of low depth and intensity might affect their statistics, but would contribute little to ours. Therefore, the different conclusions are not necessarily contradictory.

## 3. FRQUENCY AND DURATION

Gagin and Gabriel (1987) observed that the number of rainfall events on seeded days is larger than that on unseeded days. Gagin et al. (1986) observed that early treatment with a high dosage of AgI causes an extension of the area and the duration of raincells. These two observations are linked here to each other.

The convective raincells are small and short lived. Wind moves them with respect to the ground. The tracks and the birth points of the cells have strong random components with respect to the ground. As a result, the rain traces of cells cover small and randomly located areas. The integrated trace of a large number of individual cells forms a stable pattern, as is shown in rainfall maps.

In considerating an individual cell, the extension of the cell area results in an extension of its trace area. Records of raingages which are located at the extended area include events which reach them only due to the effect of the seeding. Owing to the random locations of the traces, additional events would be recorded by every raingage in the target area. Thus, the extension of the cell areas causes an increase in the number of events detected by the raingages.

In case that two adjacent cells are united by the extension of their areas, their traces are united too. If the individual traces had a certain overlapping area, a raingage located at that particular area would have counted only the united event, rather the two individual ones. We believe that this effect is considerably smaller than the effect of the extension of the cell areas.

We should note here that cell area may be extended by linear extensions in all horizontal directions. Components in the direction of cell motion contribute to the lengthening the ground trace, while components in the perpendicular directions contribute to widening it. Trace lengthening results in an extension of the rainfall duration at the front and the back edges of the trace. By that, the effect of the extension of the cell area is mixed with the effect of the extension of the rainfall duration from the cloud.

The extension of the rainfall at cloud base results in an extension of the duration at ground points which would have recorded the entire duration of the unseeded cloud rainfall. It also results in an additional lengthening of the rainfall trace, and by that to another increase in the number of events recorded by gages located at the extended area.

We conclude that extension of cell area provides an explanation for the increase in the ground rainfall duration as well as for that in the number rain events (Gagin and Gabriel, 1987). Yet, it does not contradict their explanation about initiation of rainfall from clouds which would not have rained otherwise.

A third possible explanation considers the evaporation from the rainshaft on its way from the cloud base to ground. If evaporation rate is higher at the edges of the shaft, the size of the ground trace is reduced with respect to the projection of the moving cloud base, and a number of small and low intensity events do not reach the ground. As the seeding extends the rain volume and intensity (Gagin et al., 1986), it results in a smaller reduction of the trace area and of the number of events which reach the ground. In other words, the increase in the raincell intensity and volume may cause an indirect increase in the ground trace area and in the number of recorded events. This conclusion, and the assumptions leading to it, still need verification.

We conclude that the extension of cell area and its rainfall duration (Gagin et al., 1986) causes an increase in the trace area of the cell. As a result, the probability of simultaneous recording of the same event by different raingages is enhanced, and it causes an increase in the spatial correlation of the rainfall depth, as it is observed by Sharon (1978) and by Ben-Zvi (1988).

## 4. CONCLUSIONS

A link is provided here between changes observed in dynamically seeded raincells and changes observed in ground traces of statically seeded clouds. The increase in the intensity, duration, frequency and spatial correlation of the ground rainfall seems as being explained by the increase in raincell size, and rainwater volume, rate and duration from the cloud. The quantitative rate of the changes may differ from one experiment to another due to differences in the rain processes, the seeding modes, the measurement methodologies, and the dilution of the intensive effect of the dynamic seeding of suitable clouds by a static seeding of presumably all the clouds which cross a predetermined line. Yet, the trends observed on the ground seem consitent with those observed on the cloud cells.

Changes are observed in the depth, duration, intensity, number of events, depth and duration per event, and the spatial correlation of rainfall depth at the ground level. These variables encompass all the components of the rainfall volume at the target area. They all have positive effects on the generation process of hydrologic water.

## 5. REFERENCES


Ben-Zvi, A., 1988: Enhancement of runoff from a small watershed by cloud seeding, J. Hydrol. 101, pp. 291-303.

Gagin, A., 1980: The relation between the depth of cumuliform clouds and their raindrop characteristics, J. Rech. Atmos. 14, pp. 409-422.

Gagin, A., 1986: Evaluation of "static" and "dynamic" seeding concepts through analyses of Israel II and FACE-2 experimemnts, in R.R. Braham Jr. (ed): Precipitation Enhancement - A Scientific Challenge, Met. Monograph v. 21, Am. Met. Soc., pp. 63-76.

Gagin, A. and K.R. Gabriel, 1987: Analysis of recording raingage data for the Israeli II experiment; pt. I: effect of cloud seeding on the components of daily rainfall, J. Clim. Appl. Meteo. 26, pp. 913-921.

Gagin, A. and J. Neumann, 1974: Rain stimulation and cloud physics in Israel, in W.N. Hess (ed): Weather And Climate Modification, Willey N.Y., pp. 454-494.

Gagin, A. and J. Neumann, 1981: The second Israeli radomized cloud seeding experiment: evaluation of the results, J. Appl. Meteo. 20, pp. 1301-1311.

Gagin, A., D. Rosenfeld, W.L. Woodley and R.E. Lopez, 1986: Results of seeding for dynamic effects on raincells properties in FACE-2, J. Clim. Appl. Meteo. 25, pp. 3-13.

Sharon, D., 1978: Rainfall fields in Israel and Jordan and the effect of cloud seeding on them, J. Appl. Meteo. 17, pp. 40-48.

# HAIL GROWTH PROCESSES IN AN ALBERTA HAILSTORM

Dennis J. Musil and Paul L. Smith
Institute of Atmospheric Sciences
South Dakota School of Mines and Technology
501 East St. Joseph Street
Rapid City, South Dakota 57701-3995

Abstract. A series of observations inside an Alberta hailstorm was made with the T-28 armored research aircraft during the summer of 1985, as part of the Alberta Hail Project. An analysis of some of the characteristics of the hail size distributions in relation to other T-28 measurements showed many features similar to past T-28 observations. Most of the hail observed was falling through the -17°C penetration level, even in the updrafts. A preliminary assessment of the hail growth mechanisms in this storm shows that most of the hailstones were in a dry growth regime at the penetration level, but likely in wet growth lower down in the storm. Recirculation of hydrometeors probably played a significant role in the hail development.

## 1. INTRODUCTION

Past studies of cloud turrets (feeder clouds or new growth) surrounding Alberta hailstorms and of the accompanying hailfall distribution patterns on the ground suggest that the turrets represent a major source of hailstone embryos for the storms (e.g., Krauss and Marwitz, 1984). If the feeder clouds are the major source of embryos for a natural hailstorm, then it follows that a seeding treatment designed to intervene in the hail process should be applied to that cloud region. This was the basis for hailstorm seeding experiments during the last few years of the Alberta Hail Project (English, 1986; Humphries et al., 1987).

Accordingly, controlled cloud seeding experiments involving three aircraft, radar, and ground-based sampling systems were conducted in the summer of 1985 in an attempt to confirm whether the clouds in the new growth zone are the major source of embryos, as well as to document the effects of seeding with an ice nucleant in those clouds. Plans called for cloud physics measurements by a Conquest research aircraft to identify and follow the initial growth and movement of ensembles of precipitation particles originating in the new growth zone. The armored T-28 research aircraft (Johnson and Smith, 1980) was to document the continued growth of the particles into hailstones by penetrating through the feeder clouds and on into the main part of the hailstorm. The radar observations and time-resolved hailstone samples collected at the ground would provide further information about the evolution of the hailstones. The magnetic-particle tracer technique described by Knight et al. (1986) was also tried in an effort to obtain further information about hailstone embryo sources and trajectories.

A storm which occurred on 11 July 1985 provided the best data for a detailed analysis effort. Unfortunately, funds supporting the Alberta Hail Project were sharply cut not long after the end of the 1985 season, so no such analysis effort could be completed. Nevertheless, the four penetrations made by the T-28 provided a data set which permits a preliminary assessment of the hail growth processes in this storm. The purpose of this paper is to describe some of the measurements by the T-28 in the context of inferences about the hail growth mechanisms. Oleskiw and English (1986) have also discussed this storm.

## 2. BRIEF DESCRIPTION OF THE STORM

A representative sounding and hodograph from Red Deer, Alberta, are shown in Fig. 1. Cloud base conditions are estimated to be near the LCL, at a temperature of about +8°C and corresponding to a potential wet bulb temperature of 20°C.

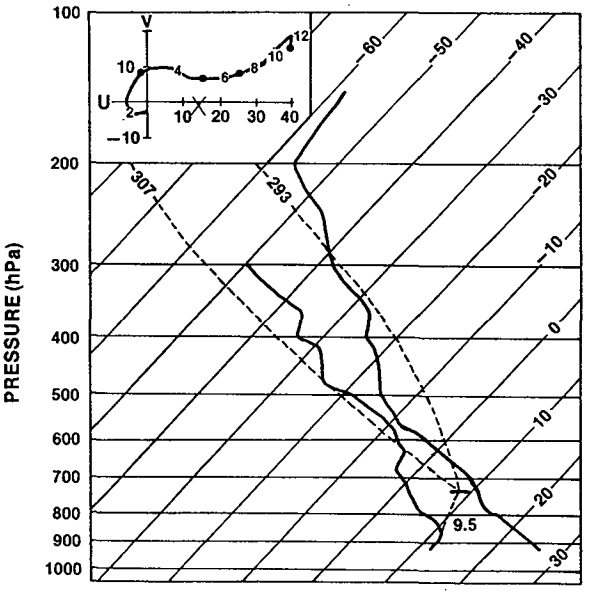


Fig. 1: Rawinsonde from Red Deer, Alberta at 2000 MDT on 11 July 1985 plotted on skew T-log P diagram. The LCL is located near +8°C and 735 hPa and is associated with a wet-bulb potential temperature of 20°C. The hodograph shown in the inset (wind components in m/s, heights in km) was derived from winds taken four hours earlier than the sounding plotted because of missing wind data at the later time. The storm motion is indicated by the X.

This indicates some negative thermal buoyancy in the updraft region at cloud base, with the level of free convection located near the 655 hPa level. The environmental wind shear from the estimated cloud base to the indicated top of the positive energy area was about 5.5 x $10^{-3}$ $s^{-1}$, while the sub-cloud environmental winds were weak and veered about 150° below the LCL. The hodograph is quite similar to that shown by Krauss and Marwitz (1984), except that the wind shear is somewhat stronger in this case.

The storm of interest formed well north of Red Deer and initially moved in a southerly direction, but then during the mature stage followed a path from west to east while producing up to walnut-sized hail. Its movement at about 14 m $s^{-1}$ was well to the right of the mid-level winds, and it laid down a continuous hailswath over 200 km long. The storm was under study by project aircraft for over three hours, long enough for four different seeding treatments (including a placebo) to be applied in a randomized sequence (Oleskiw and English, 1986). Although the radar data have not been analyzed in great detail, the echo tops were around 11 km and the storm persistently had maximum reflectivity values >60 dBZ during the time of the research mission. A low elevation angle PPI representation of the storm near the time of the first T-28 penetration is shown in Fig. 2. It was fairly isolated with no visually distinct feeder clouds associated with the storm, according to personnel in the research aircraft. However, there were persistent cumulus towers growing on the south and west sides of the main storm, near the cloud-base feed-in area. Some of these towers extended 5-10 km from the parent cell and might be classified as feeder cells, although

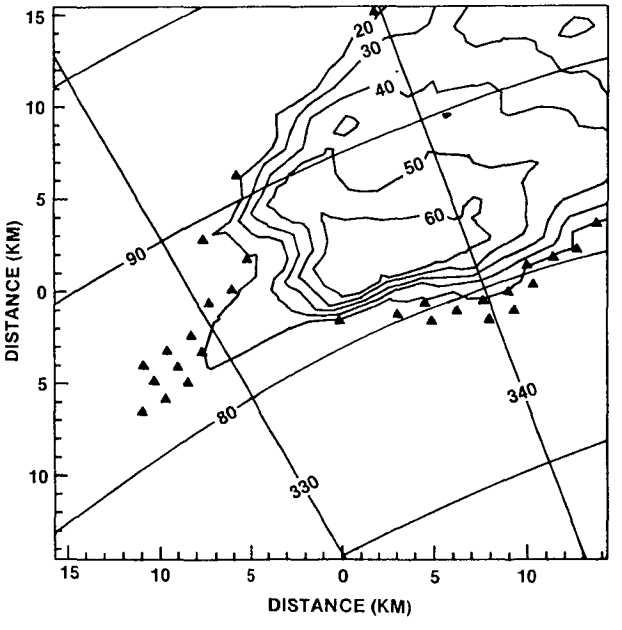


Fig. 2: Plan position indicator plot at 0.9° from the S-band Alberta radar near the time of the first T-28 penetration. Contours of equivalent radar reflectivity (dBZ) are labeled and the triangles represent reflectivities 15-20 dBZ. The tic marks on the axes are at 1-km intervals from the center of the plot located at 335°/83 km.

further analysis is required to verify that. The storm can best be classified as having very weak evolution (Foote and Frank, 1983), and probably had enough features to be called a "supercell."

## 3. SUMMARY OF T-28 PENETRATIONS

The T-28 made four penetrations of this storm; Table 1 shows the times of the penetrations and some of the pertinent observations from each. There was a break of approximately 30 minutes in the penetration sequence because of heavy icing encountered during the first two penetrations. The penetrations were all made at roughly the same average temperature of about -17°C, which corresponds to an altitude of about 6.2 km MSL.

TABLE 1

Summary of T-28 Penetration Data from 11 July 1985.
(Values are maxima/minima observed for each penetration)

| Pen | TIMES In (MDT) | TIMES Out (MDT) | L (km) | $\theta_e$ (K) | VERTICAL DRAFTS U (m/s) | VERTICAL DRAFTS D (m/s) | LWC (g/m³) | TURB ($cm^{2/3}$) | HAIL $N_T$ ($m^{-3}$) | HAIL $W_H$* ($g/m^3$) |
|---|---|---|---|---|---|---|---|---|---|---|
| 1 | 182942 | 183243 | 18.1 | 331 | 15 | -10 | 2.4 | 15 | 8 | 12 |
| 2 | 183746 | 184135 | 22.9 | 329 | 6 | -11 | 2.0 | 12 | 39 | 12 |
| 3 | 191421 | 191723 | 18.2 | 328 | 13 | -13 | 3.0 | 11 | 9 | 9 |
| 4 | 192040 | 192303 | 14.3 | 328 | 16 | -21 | 2.9 | 10 | 11 | 5 |

*Based on an assumed density of 0.9 g $cm^{-3}$.

The Conquest also made numerous penetrations about 1.5 km below the T-28, through low-reflectivity regions along the south side of the storm (Oleskiw and English, 1986). The initial seeding treatment (using dry ice at a "low" rate of 100 g $km^{-1}$) began at 1838, during the second T-28 penetration of the storm. The second treatment (using dry ice at a "high" rate of 1 kg $km^{-1}$) began at 1922, during the final T-28 penetration. Because of this timing, the T-28 observations can add little to the Oleskiw and English discussion of the seeding experiments, except for a more complete description of the storm initial conditions.

The largest observed hailstone sizes were >4 cm on each T-28 penetration. Both the temperatures and equivalent potential temperatures ($\theta_e$ ~ 330 K) were several degrees lower than would be expected from an adiabatic ascent. This is in fairly good agreement with the cloud liquid water concentrations (LWC); the peaks tended to be about 60-70% of adiabatic, according to measurements from a Forward Scattering Spectrometer Probe (FSSP) carried on the T-28. A substantial amount of mixing may have occurred, because there were no distinct regions of high equivalent potential temperatures in the updrafts as are often found in other T-28 observations (e.g., Musil et al., 1986).

The lengths of the penetrations (L), the peak vertical wind velocities, and the turbulence values are quite typical of other T-28 penetrations in active hailstorms. The vertical velocities were similar on all penetrations, except that the updrafts were weaker on Penetration 2. The hailstone number ($N_T$) and

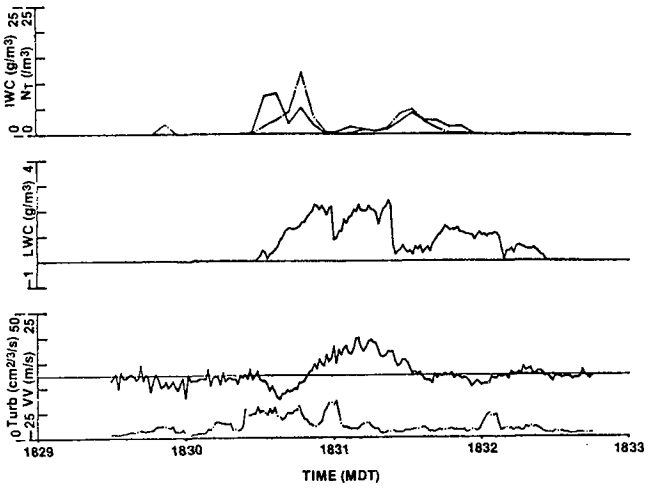


Fig. 3: Plot of T-28 data for Penetration 1 on 11 July 1985, made from southeast to northwest. Upper panel: Equivalent hail mass concentration - g $m^{-3}$ (dash-dot), hailstone number concentration - $m^{-3}$ (solid); middle panel: FSSP liquid water concentration - g $m^{-3}$; lower panel: Kopp vertical wind velocity - m $s^{-1}$ (solid), turbulence - $cm^{2/3}$ $s^{-1}$ (dash-dot). The time scale can be converted to an approximate distance scale using the nominal T-28 flight speed of 6 km/min.

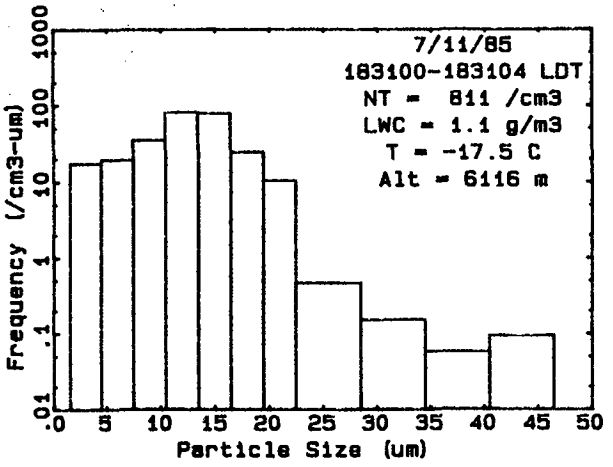


Fig. 4: Typical cloud droplet size distribution from an FSSP, observed near the middle of the updraft region shown in Fig. 3. Inset shows total droplet concentration (NT), LWC, temperature (T), and altitude (ALT).

mass ($W_H$) concentrations represent maxima obtained over 5-s time periods for each penetration. Penetration 2, at a time when the updrafts were relatively weak, exhibited the largest hail amounts; there was also a substantial amount of cloud water in the downdraft region on that penetration.

Figure 3 shows a sample plot of several variables for Penetration 1, which is mostly typical of the other penetrations. Included are plots of the 5-s hail mass and number concentrations along with FSSP cloud water concentration, vertical wind, and turbulence at 1-s intervals. The LWC peaks exceed 2 g $m^{-3}$ through most of the updraft; the Conquest observed similar values at a lower altitude (4.6 km). The turbulent eddy dissipation rate exceeded 10 $cm^{2/3}$ $s^{-1}$ over a substantial portion of the penetration. The radar data have not been analyzed with specific regard to the T-28 penetrations, so the exact orientation of these observations with respect to the reflectivity structure as shown by Oleskiw and English (1986) is not known.

Figure 4 shows a typical cloud droplet size distribution averaged over a 5-s time period near the middle of the updraft region shown in Fig. 3. The presence of large droplets is unusual in High Plains thunderstorms, but was quite common in this storm.

## 4. HAIL OBSERVATIONS

A detailed analysis of the T-28 data gathered on 11 July was accomplished. Of special interest are the observations of hailstones from the Institute of Atmospheric Sciences (IAS) laser shadowgraph hail spectrometer (Jansen, 1981). This instrument operates on the same basic principles as the probes described by Knollenberg (1981) and provides both "one-dimensional" particle size distributions and two-dimensional images (see Appendix).

### 4.1 Hailstone Size Distributions

The size distributions from the 1-D portion of the hail spectrometer have been summarized for each penetration on 11 July (Fig. 5) for the times when hail was present during the penetration. In Penetration 1 (Fig. 5A), reasonable images up to about 4 cm in size were also observed so that one can be confident that particles that large were present. Some of the 4-and 5-cm hailstone counts could be questionable due to the broken-up nature of some of the very large particle images; however, a "slow-particle detection" feature in the 1-D channel is designed to reject such events. In any event, the total concentrations of hailstones are not affected very much by the counts of large stones (because the high concentrations of small stones dominate that calculation).

The hailstones do not conform exactly to exponential size distributions, which would appear as straight lines on these semi-log plots. However, the pronounced kink at about 1.5 cm diameter noted in the plots by Smith and Jansen (1982) is not evident here. No attempt was made to fit any curve to the distributions.

The times shown in the insets of Fig. 5 indicate the times when hail was observed during each penetration. The hail was continuous during that entire period, although the concentrations fluctuated a great deal within the interval. The time interval in Fig. 5A corresponds to a hail region approximately 9 km across, which is a relatively large region of continuous hail in comparison to past T-28 observations. The hail regions on subsequent penetrations were even wider.

The largest region of hail, about 14 km across, occurred during Penetration 3 (Fig. 5C), although more hailstones were found in Penetration 2. Thus, the average total number

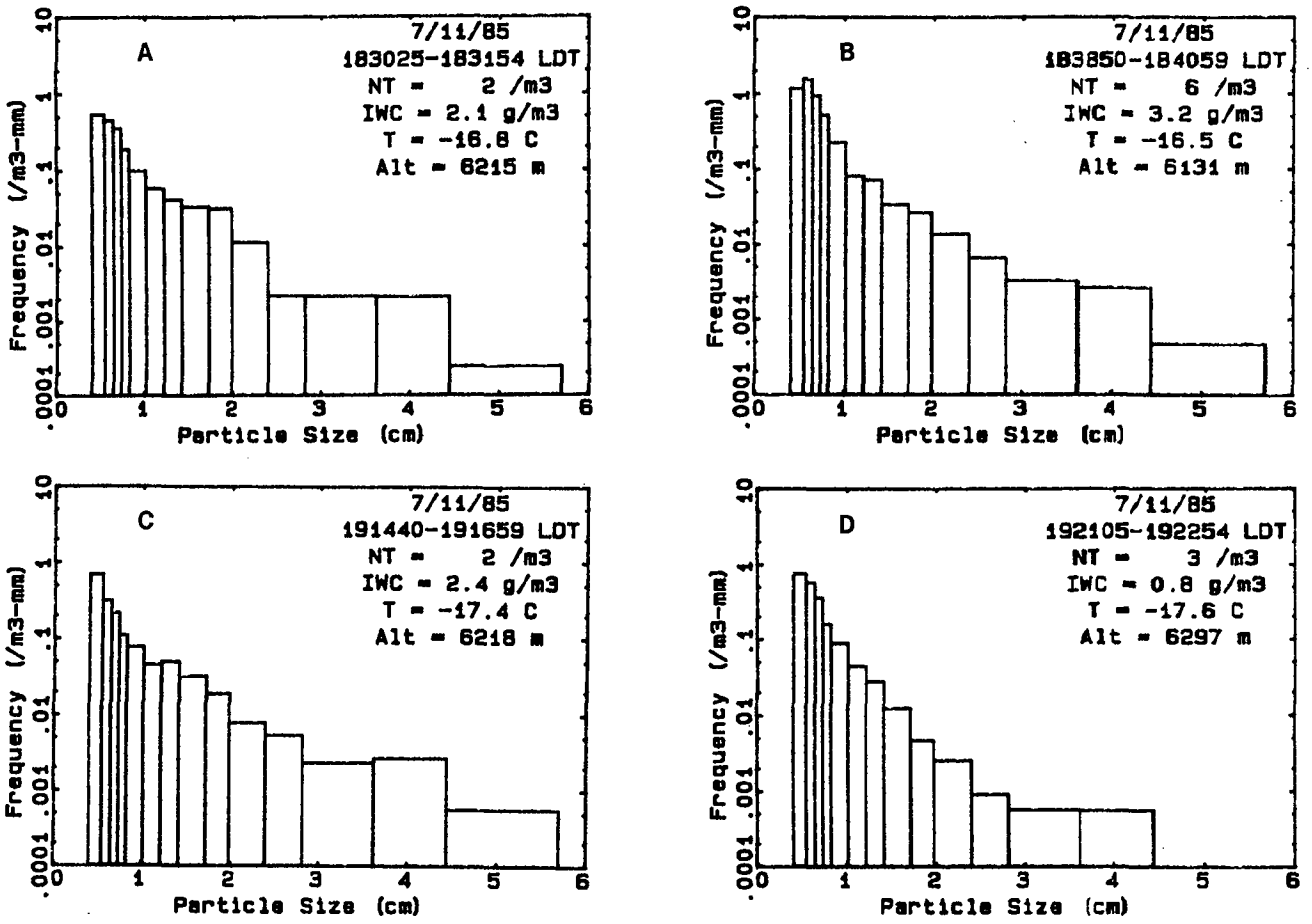


Fig. 5: Composite hailstone size distribution for each penetration on 11 July 1985 from 1-D operation of hail spectrometer. Inset indicates time when hail was observed and averages for total concentration ($N_T$), equivalent hail mass concentration (IWC), temperature (T), and altitude (ALT) for that period. Ordinate has units of $m^{-3}$ $mm^{-1}$ of size interval. A, B, C, D correspond to penetrations 1-4, respectively.

concentration ($N_T$) and equivalent ice mass concentration (IWC) were greatest in Penetration 2. No specific physical reasons for the higher values are known, but the flight track for Penetration 2 carried the aircraft through higher reflectivity regions north and east of the strong updraft region. The coexistence of significant hail and supercooled cloud water in a moderate downdraft on that penetration may have signified an enhanced growth environment at the time. Penetrations 3 and 4 had size distributions that were more similar to those found in Penetration 1.

The mass concentrations were calculated assuming that the particles had a density of 0.9 g $cm^{-3}$, leading to average IWC values ranging between about 1-3 g $m^{-3}$. These mass concentrations are somewhat higher than those found by other investigators (e.g., Heymsfield, 1978). On the average, Heymsfield's calculations result in hailstone masses 20-30% lower than those obtained assuming a constant density of 0.9. The differences are even greater for the smaller sizes, where Heymsfield's method may be more correct because the observed densities there are typically lower than 0.9 g $cm^{-3}$ (Knight and Heymsfield, 1983).

4.2 Hail Locations

Hailstone size distributions were also determined for 5-s time periods for each penetration. From these distributions, values of $N_T$ and IWC have been calculated as a function of time (see Fig. 3) to permit an analysis of the locations of the hail in relation to some of the other T-28 measurements. The observed locations of the hail may be related partly to the path of the T-28 through the storm, because the penetrations did not pass through exactly the same portion of the storm in each case.

In Penetration 1, the largest amounts of hail were found near the edges of the updraft region and in the adjacent downdraft regions. This is similar to the common situation in other hailstorms of the High Plains (e.g., Sand, 1976). There was some hail throughout nearly the entire LWC region, which in turn extended well beyond the updraft. The subsequent penetrations tended not to show larger amounts of hail near the updraft edges, but the coexistence of hail and supercooled cloud water was typical of all the penetrations. On Penetration 2, most of the hail was in a downdraft containing up to 2 g $m^{-3}$ of cloud liquid.

5. HAIL GROWTH PROCESSES

The observations discussed in the foregoing section indicate that the hailstones encountered were still growing, because they were predominantly found in regions with supercooled cloud water. In fact, when one compares the mass of

hail which was accreting cloud liquid to the total mass of hail found in each penetration, nearly 100% of the hail was still in a favorable growth environment when encountered by the T-28.

5.1 Hailstone Motions

No Doppler data were available in this project, so it was only possible to study hailstone trajectories in this storm by examining the fine-scale reflectivity patterns (as in Oleskiw and English, 1986). Their findings suggest parcel trajectories that would carry particles from cumulus turrets on the south edge of the storm right through the regions of the storm penetrated by the T-28. However, information about the vertical motions is limited.

A simple comparison of hailstone terminal velocities ($V_t$) with the vertical winds from the T-28 measurements provides useful information about vertical hailstone motions in the cloud. The comparison was accomplished by determining which of the observed hailstones were rising or falling in the vertical-wind environment measured by the T-28. Figure 6 shows a plot of the largest hail size observed in each 5-s time period during Penetration 1, as well as the maximum-sized hailstone that would just be balanced in the vertical wind field at that time. Whenever the "balance" curve (dashed) exceeds the maximum hail size observed, all the observed hail is rising in the updraft; when it is below the maximum-size curve, only the hailstones smaller than the sizes indicated by the "balance" curve are rising. In all other locations, all the hail is descending in downdraft air. Overall, the region of rising hail (which, of course, is located in the updraft region - compare with Fig. 3) is very small compared to the total amount of observed hail. However, even in the updraft region there are hailstones which are descending, except for a small region near 1831 MDT in the plot.

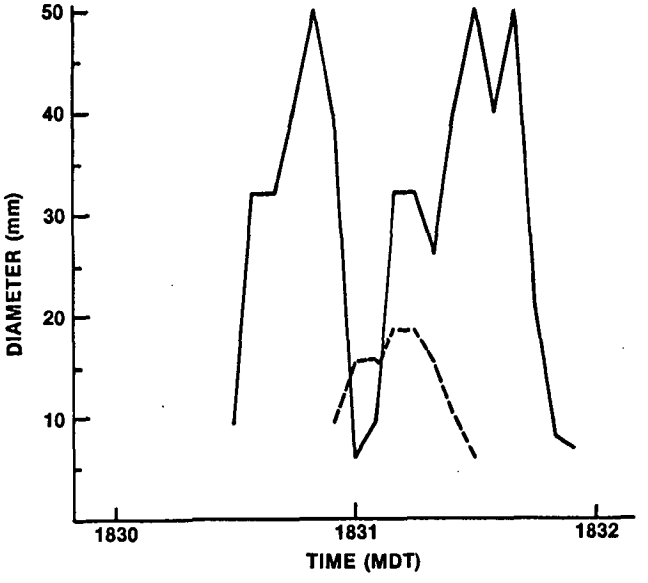


Fig. 6: Distribution of hail sizes vs. time for 5-s time periods for Penetration 1 on 11 July 1985. Solid line shows maximum-sized hail, while dashed line shows maximum-sized hail that would just be balanced in the observed updrafts.

In terms of mass of hail, the amount rising was small for all the penetrations, ranging from <1% on Penetration 2 to a maximum of about 20% on Penetration 4. In other words, while most of the hail was growing when observed (because of its coexistence with cloud liquid water), most of it was also descending, even in the updrafts at the T-28 penetration altitudes.

The comparisons in the preceding paragraphs should be considered estimates because in comparing calculated terminal velocities and vertical winds from the T-28 data, we are dealing with quantities involving substantial uncertainties. Knight and Heymsfield (1983) made calculations of $V_t$ for hailstones falling near the ground and Heymsfield (1978) developed a set of empirical equations for various types and sizes of hydrometeors. Some models of particle growth have used a variable-density technique for dealing with particle terminal velocities in Doppler flow fields (e.g., Heymsfield, 1982; Foote, 1984). Other numerical investigations (Musil, 1970; Dennis and Musil, 1973; Nelson, 1983) have assumed a hailstone density of about 0.9 g $cm^{-3}$ for calculating terminal velocities for hailstones greater than 1 cm diameter. This results in terminal velocities substantially greater than those reported by the other investigators. However, precise calculations are not possible because little is known about the terminal velocities of actual hailstones in atmospheric free fall, especially at mid-storm levels. Because at least some observations tend to show lower terminal velocities, especially for the smaller hydrometeors, and knowledge of the subject is limited anyway, we used the Heymsfield (1978) empirical equations for estimating $V_t$. This contrasts with the assumption of a fixed density used in calculating the hail mass concentrations, and is intended to produce conservative estimates of the terminal velocities. If a hailstone density of 0.9 g $cm^{-3}$ had been assumed, the regions of rising hail would have been even smaller than shown in Fig. 6. Kopp (1985) discusses the uncertainties in the vertical-wind calculations.

Although the hailstones found in downdraft regions will continue to grow as long as they coexist with supercooled liquid water, the hail (along with the smaller ice hydrometeors) will likely deplete the liquid rather quickly in those regions. Depletion calculations have not been made with this data set, but the depletion equations used by Heymsfield and Musil (1982) suggest that it could be accomplished in something of the order of two minutes in the downdraft regions. Evaporation effects are unknown, but would only accomplish the depletion faster.

Most of the hailstones in the downdraft regions therefore were probably nearing the end of their growth cycle, as the updraft appeared to be essentially vertical. Those found in or at the edges of the updraft regions would have the best opportunity to continue growing because there was an ample supply of cloud liquid that was continually being replenished. There is a strong suggestion in these data that a substantial amount of hail growth had occurred at altitudes above the T-28 since many hailstones were already very large when observed by the T-28.

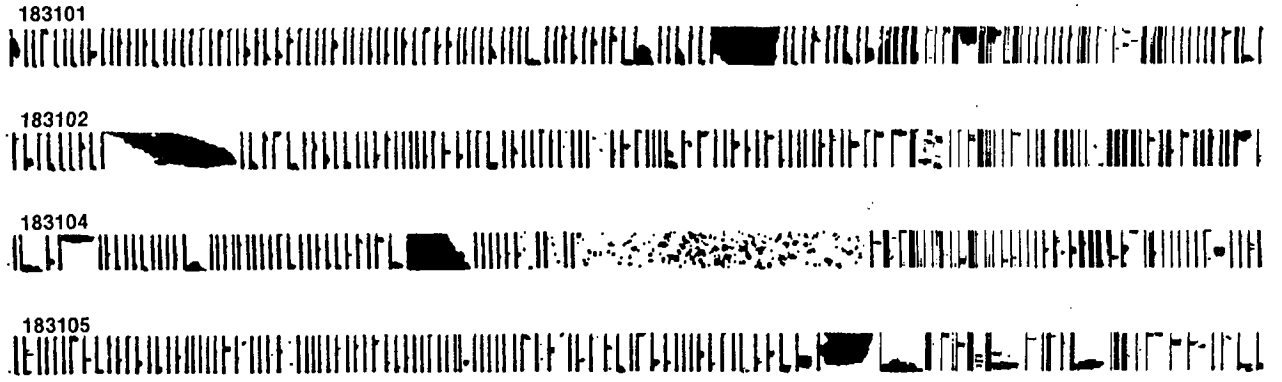


Fig. 7: Sample of 2D-C images near the middle of the updraft region (~ 1831 MDT) shown in Fig. 3. Vertical bars approximately 1 mm long.

5.2 Hailstone Growth Regime and Embryo Sources

The growth modes of the hailstones observed in this storm were investigated by computing the wet and dry growth rates for a wide variety of hailstone sizes, cloud liquid water concentrations, and temperatures. The calculations of dry and wet growth regimes follow the work by Musil (1970) and Dennis and Musil (1973). Small ice particles were also considered in these calculations and were found to be an important factor. A sample of the particles measured with a 2D-C probe near the middle of the updraft region in Fig. 3 is shown in Fig. 7. They range from hundreds of micrometers to several millimeters in size. The related mass concentrations are unknown, but 1 g $m^{-3}$ was taken as a typical value (Knight and Squires, 1982) for the growth-regime investigation. The presence of small ice particles allows the hailstones to remain in a dry growth regime somewhat longer than would otherwise be, because the accreted ice tends to keep the hailstones cooler.

Figure 8 is a sample plot showing the boundaries between dry and wet growth regimes for conditions near those found on 11 July. The area to the left of each curve indicates the dry growth region and the area to the right, the wet growth region for the corresponding conditions. The dashed line outlines the approximate region of the bulk of the hailstone observations on 11 July.

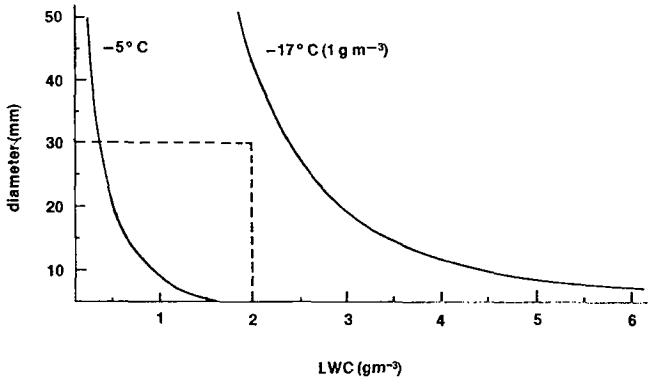


Fig. 8: Plot showing boundary between regions of dry and wet growth of hailstones, for temperatures of -17°C with an IWC of 1 g $m^{-3}$ and -5°C with no ice. Dry growth region is to left of boundary, wet growth region to right. Area enclosed by dashed line defines approximate region of most of the hailstone observations with the T-28 on 11 July 1985.

The vast majority of the observed hailstones fall within the dry growth regime, which is not surprising considering the low temperatures of the T-28 penetrations. As the hailstones fall, however, they likely increase somewhat in size and the dry/wet growth boundary also moves to the left (as suggested by the curve for -5°C in Fig. 8). Thus, lower in the cloud, the wet growth process should be active, and could produce raindrops by shedding. As descending hailstones were found in the updraft regions, the shed drops could provide a source of frozen-drop embryos for subsequent hailstone development. This has been noted as a significant embryo source in at least some High Plains hailstorms (e.g., Rasmussen and Heymsfield, 1987).

The present calculations cannot say anything about the possible development of embryos in other regions of the cloud. The observations reported by Oleskiw and English (1986) showed embryo-size ice particles appearing lower down in cumulus turrets on the southern edge of the storm. Millimeter-sized particles appeared so quickly that it seems likely they were generated in a different part of the storm. The observed storm-relative winds and the fine-scale reflectivity pattern analysis showed that these particles could be transported into the main part of the storm to act as hail embryos. This and the shedding process could therefore provide a combination of graupel and frozen-drop embryos, through recirculation processes which cannot yet be specified in detail.

Frozen-drop embryos could also result from the melting of hail once it has fallen below the melting level, with recirculation of the resulting drops into the updraft (e.g., Heymsfield and Ljelmfelt, 1984). It is not known whether the embryos in this storm were predominantly graupel or frozen drops; both types have been found in hailstones from other Alberta storms (Knight, 1981). However, it appears that some type of recirculation mechanism must be involved in either case, since it is unlikely that much of the hail observed by the T-28 could be developed in a single simple up-and-down trajectory.

Further investigation of the embryo question is necessary and it is planned to explore this with the aid of comparisons of T-28 and other observations with numerical cloud model output. The approach will be similar to that accomplished by Kubesh et al. (1988) for a storm in southeastern Montana.

## 6. SUMMARY OF RESULTS

The data gathered by the T-28 on 11 July 1985 provided valuable in situ observations from an isolated Alberta hailstorm. This permitted an analysis of some of the characteristics of the hailstone distributions in this storm in relation to other T-28 measurements. These characteristics, as well as the vertical winds and cloud LWC, were generally similar to past observations by the T-28 in other High Plains storms. However, hail was observed over larger regions of each penetration on 11 July than is usual in other locations where the T-28 has operated. The data also included the first 2-D images of hailstones from the hail spectrometer in flight.

Even though the analysis of the data is incomplete, a preliminary assessment of the hail growth mechanisms in this storm has been made. The hail was almost always found in relatively high concentrations of supercooled cloud water, on the order of 1-2 g $m^{-3}$, indicating that the hail was still growing at the time of observation. Most of the observed hailstones at the -17°C level were growing in a dry growth regime, as well as descending in the cloud. A wet growth process was likely active lower in the storm. There are strong indications that the hail achieved a substantial portion of its growth above the T-28 altitudes. Recirculation of particles probably played a significant role in the hail mechanism because it is unlikely that the hail sizes observed by the T-28 could have resulted from a single trip through the cloud. It is not known what role the cumulus towers to the southwest may have played in providing hail embryos for this storm.

Additional work is necessary to combine the FSSP, 2D-C probe, foil impactor, and hail spectrometer data in order to examine the total hydrometeor spectra measured by the T-28 in this storm. Further information about the hail mechanism could then be obtained by making comparisons between the aircraft observations and the results of 2D time-dependent model simulations for both bulk water and hail-category microphysics (e.g., Farley, 1987). Detailed analysis of the radar history of this storm would also aid in such an investigation.

Acknowledgments. This work was supported by the Alberta Research Council under Contract No. IAS 102.00.85 and by the National Science Foundation under Grant No. ATM-8409407 and Cooperative Agreement No. ATM-8620145. The work of G. N. Johnson in the development of the imaging system for the hail spectrometer is acknowledged.

## 7. REFERENCES

Dennis, A. S., and D. J. Musil, 1973. Calculations of hailstone growth and trajectories in a simple cloud model. J. Atmos. Sci., 30:278-288.

English, M., 1986. The testing of hail suppression hypotheses by the Alberta Hail Project. Preprints 10th Conf. Wea. Modif., Arlington, VA, Amer. Meteor. Soc., 72-76.

Farley, R. D., 1987. Numerical modeling of hailstorms and hailstone growth. Part III: Simulation of an Alberta hailstorm -- natural and seeded cases. J. Climate Appl. Meteor., 26:789-812.

Foote, G. B., 1984: A study of hail growth utilizing observed storm conditions. J. Climate Appl. Meteor., 23:84-101.

_____, and H. W. Frank, 1983. Case study of a hailstorm in Colorado. Part III. Airflow from triple-Doppler measurements. J. Atmos. Sci., 40:686-707.

Heymsfield, A. J., 1978. The characteristics of graupel particles in northeastern Colorado cumulus congestus clouds. J. Atmos. Sci., 35:284-295.

_____, 1982. A comparative study of the rates of development of potential graupel and hail embryos in High Plains storms. J. Atmos. Sci., 39:2867-2897.

_____, and M. R. Hjelmfelt, 1984. Processes of hydrometeor development in Oklahoma convective clouds. J. Atmos. Sci., 41:2811-2835.

_____, and D. J. Musil, 1982. Case study of a hailstorm in Colorado. Part II: Particle growth processes at mid-levels as deduced from the in-situ measurements. J. Atmos. Sci., 39:2847-2866.

Humphries, R. G., M. English and J. Renick, 1987. Weather modification in Alberta. J. Wea. Modif., 19:13-24.

Jansen, D. C., 1981. An analysis of airborne hail spectrometer data. M.S. Thesis, Department of Meteorology, South Dakota School of Mines and Technology, Rapid City, SD. 83 pp.

Johnson, G. N., and P. L. Smith, Jr., 1980. Meteorological instrumentation system on the T-28 thunderstorm research aircraft. Bull. Amer. Meteor. Soc., 61:972-979.

Knight, C. A., and P. Squires (eds.), 1982. Hailstorms of the Central High Plains. Vol. I: The National Hail Research Experiment. Colorado Associated University Press, Boulder, Colorado. 282 pp.

Knight, N. C., 1981. The climatology of hailstone embryos. J. Appl. Meteor., 20:750-755.

_____, and A. J. Heymsfield, 1983. Measurement and interpretation of hailstone density and terminal velocity. J. Atmos. Sci., 40:1510-1516.

_____, A. J. Weinheimer and M. B. Steiner, 1986. The use of powdered iron as a tracer in hailstorm research. Preprints Joint Sessions 23rd Conf. Radar Meteor. and Conf. Cloud Physics, Snowmass, CO, Amer. Meteor. Soc., JP1-JP2.

Knollenberg, R. G., 1981. Techniques for probing cloud microstructure. In Clouds, Their Formation, Optical Properties, and Effects. (P. V. Hobbs and A. Deepak, eds.). Academic Press, NY. 497 pp.

Krauss, T. W., and J. D. Marwitz, 1984. Precipitation processes within an Alberta supercell hailstorm. J. Atmos. Sci., 41:1025-1034.

Kubesh, R. J., D. J. Musil, R. D. Farley and H. D. Orville, 1988. The 1 August 1981 CCOPE storm: Observations and modeling results. J. Appl. Meteor., 27:216-243.

Musil, D. J., 1970. Computer modeling of hailstone growth in feeder clouds. J. Atmos. Sci., 27:474-482. [Reply: J. Atmos. Sci., 28:294-295]; [Corrigendum: J. Atmos Sci., 29:225].

_____, A. J. Heymsfield and P. L. Smith, 1986. Microphysical characteristics of a well-developed weak echo region in a High Plains supercell thunderstorm. J. Climate Appl. Meteor., 25:1037-1051.

Nelson, S. P., 1983. The influence of storm flow structure on hail growth. J. Atmos. Sci., 40:1965-1983.

Oleskiw, M. M., and M. English, 1986. A comparison of several seeding treatments on growing towers within Alberta hailstorms. Preprints 10th Conf. Wea. Modif., Arlington, VA, Amer. Meteor. Soc., 84-89.

Rasmussen, R. M., and A. J. Heymsfield, 1987. Melting and shedding of graupel and hail. Part III: Investigation of the role of shed drops as hail embryos in the 1 August CCOPE severe storm. J. Atmos. Sci., 44:2783-2803.

Sand, W. R., 1976. Observations in hailstorms using the T-28 aircraft system. J. Appl. Meteor., 15:641-650.

Smith, P. L., and D. C. Jansen, 1982. Observations inside SESAME thunderstorms with an airborne hail spectrometer. Preprints 12th Conf. Severe Local Storms, San Antonio, TX, Amer. Meteor. Soc., 16-19.

_____, D. J. Musil and D. C. Jansen, 1980. Observations of anomalous large particles inside Colorado and Oklahoma thunderstorms. Proc. VIII Intnl. Conf. Cloud Physics, Clermont-Ferrand, France, 295-298.

## APPENDIX: IMAGING CAPABILITY IN THE HAIL SPECTROMETER

For many years, the hail spectrometer aboard the T-28 has provided one-dimensional size data, with 14 size categories ranging from about 0.5-5 cm in diameter. Although these data have been useful and of apparent good quality, there have often been questions about the very large particles observed during the T-28 penetrations (Smith et al., 1980). The possibility of contamination due to ice fragments shedding from leading edges of the aircraft wing or the forward portion of the spectrometer could not readily be discounted.

To help resolve these questions, an imaging system working in conjunction with the 1-D categorization scheme was developed. The imager scans the array of 64 laser-illuminated phototransistors every 10 μs whenever a shadow is present in the array, thereby producing an image slice for about every millimeter of aircraft travel. (Only every other sensor in the 1-D array is scanned, so the image resolution across the array is about 1.8 mm.) The resultant 64-bit slice is compressed into a 16-bit word and stored in a buffer prior to being recorded on magnetic tape.

During the summer of 1985, images of significant hail encounters were obtained for the first time. Several buffers of images from the hail spectrometer during Penetration 1 (~1831 MDT) on 11 July are shown in Fig. A1. Good images are readily apparent, some as large as 2-3 cm in diameter. Also evident are some extremely large images which may be a result of shedding from the forward portion of the hail spectrometer. Most of these appear to be causing a data overflow problem, so that the images appear partially broken up. A "slow-particle detection" feature in the 1-D channel should reject such images from being counted. A weak intermittent detector is also evident, as indicated by the nearly continuous signal occurring at times near the middle of some buffers.

Generally, the spectrometer performed well in Alberta, but image data of consistently usable quality were not obtained. Many of the characteristics of hailstone size distributions are adequately represented by the 1-D portion of the hail spectrometer data. Following these initial observations, modifications have been made to the hail spectrometer imaging electronics, but no flight tests in sizable hail have yet been made.

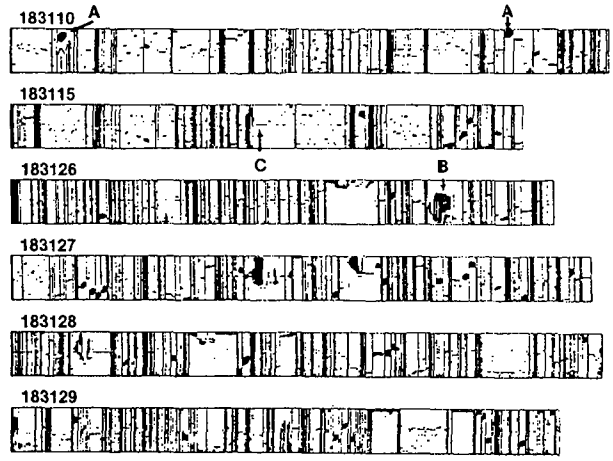


Fig. A1: Dump of several image buffers from hail spectrometer between 183110-183129 MDT on 11 July 1985. Width of array (vertical bars) about 12 cm. (A) Image > 3 cm diameter; (B) Shed broken-up image; (C) Weak intermittent diode malfunction.

# ON THE OPTIMAL LENGTH OF THE HAIL SUPPRESSION SEASON

N.M.Aleksić, N.Djordjević and J.Mališić

Summary. The length of a hail suppression season should depend on the climatology of the hail occurrence. We use hail occurrence data for a large number of stations and a 19-year record of seeding activities in order to show that the hail suppression season in Serbia has the proper starting date, but that there is a strong possibility that a season could end earlier.

## 1. INTRODUCTION

In order to obtain the optimal length of a hail suppression season, hystorical data ought to be examined. The opening and the closing of the season should depend on the hail climatology over the protected areas.

Currently, the hail suppression season in Serbia starts on 15 April and continues until 15 October. These dates being rather arbitrary, we were interested in determining if the season could be shortened. We were primarily interested in the following three fortnight periods: the end of April, the end of September and the beginning of October.

Available data consisted of the yearly records of graupel and hail occurrences from the 95 meteorological stations in Serbia. Sample sizes ranged from 21 to 44 years, most of them from 30 to 40 years. We have used these records to estimate point and areal probabilities of the hail occurrences.

In addition, we have analyzed seeding records from the 19 seasons of hail suppression that have been conducted in Serbia.

## 2. POINT HAIL OCCURRENCE

For each fortnight period, for each station, we have estimated the probabilities of the occurrence of hail days. As the estimate of the probability, we have used relative frequency $p=m/n$, where $m$ is the number of years with at least one hail day observed in a given fortnight period and $n$ is the sample size in years.

A summary of the analysis is given in the Table 1. The first column of this table defines a fortnight period. The next five columns give the number of stations with a hail occurrence probability in a given interval. The last column shows the hail probability averaged over all the stations.

For the beginning fortnight of the season, most of the point probabilities are below 0.1. Since the occurrence of at least one hail day is a binomial type variable, its recurrence interval is simply the inverse value of the probability. Thus, for the average probability of 0.082 at the end of the April, the average return period is 12.2 years. For the end of September, the average return period is 83.3 years, and for the last fortnight of the season it reaches even 200 years.

## 3. AREAL HAIL OCCURRENCE

Generally, the probabilities of hail occurrence are higher over an area than for any given point inside it. The hail suppression system is supposed to protect the area, and this was the reason that the second step of the analysis was to estimate the areal hail probabilities.

For each year in the period 1941-1983 and for the same fortnight periods we have calculated the fraction of the stations experiencing hail. The probabilities of the hail occurrence somewhere in the area are estimated as the ratio of the number of years with recorded hail to the total number of years.

Results are summarized in the Table 2. The first column of this table defines the fortnight period and the second contains the areal hail probabilities. The third column gives the return periods of the hail occurrence and the fourth shows the mean annual fraction of stations recording hail, averaged over the years with hail

Table 2 shows that the return period of the hail in the first half of October is larger than 5 years and that hail affects only some 2% of the stations. On the other hand, in the second half of the April, hail occurs almost every year, and affects almost 10% of the stations.

Table 1. Summary of point data analysis

| Period | Number of stations with a $p$ in the interval | | | | | Average $p$ |
|---|---|---|---|---|---|---|
| | .00-.05 | .05-.10 | .10-.15 | .15-.20 | .20 | |
| 16.-30.Apr | 35 | 30 | 13 | 7 | 10 | 0.082 |
| 16.-30.Sep | 89 | 6 | 0 | 0 | 0 | 0.012 |
| 1.-15.Oct | 93 | 2 | 0 | 0 | 0 | 0.005 |

Table 2. Summary of the areal analysis

| Period | Probability of hail occurrence | Return period of hail occurrence (years) | Mean fraction (%) of stations with hail occurrence |
|---|---|---|---|
| 16.-30.Apr. | 0.88 | 1.1 | 9 |
| 16.-30.Sep. | 0.37 | 2.7 | 3 |
| 1.-15.Oct. | 0.19 | 5.4 | 2 |

4. SEEDING RECORDS

The most direct way to see whether the season should be shortened or not is, of course, to look into the seeding records. If they show a virtual absence of seeding during a particular period, the answer is straightforward.

In this particular case we had at our disposal seeding records from 1967 to 1986 (except for the 1979). The summary of these records is given in Table 3. The first column of the table defines the period, the second shows the number of years with seeding, and third gives the total number of seeding days over all the seasons. The fourth column gives the total rocket expenditure, which can be used as a rough measure of the hail process intensity.

Table 3. Summary of seeding data

| Period | Number of years with seeding | Number of days with seeding | Total expenditure of rockets |
|---|---|---|---|
| 15.-30.Apr. | 13 | 46 | 4098 |
| 15.-30.Sep. | 13 | 34 | 1416 |
| 1.-15.Oct. | 8 | 10 | 195 |

The most striking feature of this table is that for the 19 seasons there were only 10 seeding days in October, with the 195 rockets used. For the comparison, total number of seeding days over all the seasons was 1190 with 182,348 rockets used.

5. CONCLUSION

The simple analysis described above has shown that risk of hail in the first half of the October is truly marginal. Low probabilities of hail occurrence are underlined by the *de facto* absence of seeding. This clearly points toward an earlier closing date of the season.

Data for the beginning of the hail suppression season seem to confirm its opening date.

Concerning the end of September, the authors feel that additional subregional analysis is needed to see whether the hail affects all of the protected teritory or only some of its parts. If the latter is true, there is possibility of keeping only part of the suppression system active, which would reduce its overall cost.

ACKNOWLEDGEMENT

The authors appreciate help provided by Mrs. Nada Pavlović, Mr. Slobodan Golubović and Mrs. Verica Vesić. Mrs. Ljubica Radoja has graciously typed the manuscript.

# EFFECTIVENESS OF HAIL CONTROL IN SERBIA

Djuro Radinović
Faculty of Natural and Mathematical Sciences
11001 Belgrade, Yugoslavia

Abstract. The artificial modification of hail formation in the SR of Serbia has been organized and operating according to principles similar to those developed in the U.S.S.R. The hail control system in Serbia covers about 4 million hectares of agricultural surface, which is one of the largest connected areas protected by such a system in the world.

After a period of 17 years of continuous operation an evaluation of its effectiveness has been made. This evaluation is based on the statistics of the size of hail-swept areas, percentage of the damaged crops and the frequencies of hail occurrences observed in the regular network of meteorological stations.

The size reduction of hail-swept areas in protected territory show a decrease of an estimated 63% when compared to unprotected territory. A 22% reduction in hail frequency is suggested by the data analysis according to observations at meteorological stations.

## 1. INTRODUCTION

Almost a quarter of a century ago Russian scientists (Karcivadze, 1964; Fedorov, 1965; Gajvoronskij and Seregin, 1965; Sulakvelidze, 1967) reported some very promising results from their hail control operations. These results were not based on the present day knowledge of the physics and dynamics of clouds, but on the hypothesis of the competition of nuclei of crystalization, which are generally deficient in hailstorm clouds. For that reason, many specialists in cloud physics and weather modification in other countries were sceptical about the results reported by Soviet scientists.

In order to prove the real efficasy of the Soviet hail control operating method, several hail suppression field experiments were organized; i.e. the National Hail Research Experiment in Colorado and Grossversuch in Switzerland. These randomized experiments did not show any significant hail control results (Knight et al. 1979; Federer et al. 1986). However, the methodology and the seeding technique used in the NHRE and the size of target area in Grossversuch were not the same as those applied in the U.S.S.R.

On the other hand, the Soviet sciences have constantly reported very optimistic results from their hail control operations (Izrael, 1983; Sedunov, 1986). So, a dilemma on a hail control problem, which is of a great scientific and economic value, remains. The aim of this paper is to contribute to the solution of this problem.

## 2. METHODOLOGY OF HAIL CONTROL IN SERBIA

The hail control system, developed in the U.S.S.R. and applied in Serbia, had four basic components (Radinović, 1972).

1) Determination (by radar) of the place of initiation of hail formation and growth in cloud;

2) Selection of reagent, which causes crystallization and freezing of supercooled drops in clouds;

3) Timely delivery of the reagent into the hail formation zone in the cloud; and

4) Evaluation of the results of the action.

Determination of the position of the growth zone in clouds, in the beginning of the hail control operations (1969-1977), had been made by Soviet radar, MRL-1, on wave length of 3.2 cm, and by military radars, 3MK-7, of wave length 10.0 cm. During the period 1978-1980 eight military radars were replaced by Japanese meteorological radars, RC-34A, of wave length 10.0 cm. In the period 1981-1984, four more radars of the same type were replaced.

In the first half of the period (1969-1978) anti-hail rockets, the Sako-6, produced in Yugoslavia, were used. These rockets had a range of 3,500 m and carried 400 g of silver iodide mixed with the burning mixture. Discharge of the reagent took place along about 400 m of the last part of the rocket path, giving $10^{11}$-$10^{12}$ ice niclei per gram of the mixture.

In 1979 new anti-hail rockets, Tg-10, were introduced in the hail control system of Serbia. The range of these rockets was 8,500 m, and the weight of the silver iodide mixture was the same. However, the reagent was greatly improved giving about $10^{13}$ ice nuclei per gram.

At the same time, the methodology of radar identification and seeding of the place of initiation of hail formation and growth was improved. That zone was precisely determined as a half a ring in front of the Cb cloud comprising the layer between -8°C and -12°C with the radius dependent on the speed of cloud. The goal was to have each $m^3$ in that zone seeded by $10^5$-$10^6$ artificial ice nuclei.

On the basis of the above mentioned changes,

it may be concluded that the hail control system in Serbia in the period 1978-1980 was greatly improved. Another important feature of that system was its continued extenssion until 1985 when about 95% of the agriculture surface of Serbia became covered by the hail control system. So, in recent years the hail control system has consisted of the 12 radar centers (hail control polygons) and about 1,300 hail rocket launching stations. These stations were connected by radio communications with the radar centers.

## 3. DATA USED IN EVALUATION

The hail control system in Serbia was not organized in a way to produce any particular data to set aside for evaluating the effectiveness of the system itself. Therefore, the evaluation of the effectiveness of hail control in this case has been based on two sources of data, which have been obtained independently of the hail control system. These are:

1) The size of the hail-swept agriculture area in hectares;

2) The percentage of the crops damaged; and

3) Frequency of hail occurrences observed at the regular network of meteorological stations.

The statistics of the size of the hail-swept area and percentage of the crops damaged have been obtained in a very specific way. Namely, the Parlament of SR Serbia many years ago established a law which required farmers income taxes be reduced in proportion to the percentage of hail damaged crops. Particular execution of has been taking place through qualified commissions, which have been set up by local authorities (the municipalities). Copies of the reports, made by these commissions, were sent to the Republic Hydrometeorological Institute of Serbia, which is conducting the hail control operations.

The quality of these data may be estimated in a following way. The typical size of a hail-swept area takes a few hundred to a few thousand hectares, and a typical size of an individual farmer's property is a few hectares only (in average less than 3 hectares). Since every individual farmer's property should be estimated, the possible error in determining the size of the hail-swept area is usually less than 1% of the total hail-swept area.

The estimation of the percentage of damaged crops is more delicate. It depends on the sort of crops as well as on its pheno-phases, which are usually not homogeneous. As a consequence the possible errors in this kind of data are estimated to be up to 10% of their total values.

Another problem connected with this data source was their collection. Every year certain municipalities did not send their reports to the Republic Hydrometeorological Institute of Serbia. Their data were missing in this analysis, particularly in the first part of the hail control operating period.

The network of meteorological stations in Serbia was reconstructed after World War II and started to work regularly 1949. From that year the total number of synoptical and climatological stations was changing from 47 as a minimum to 72 as a maximum. The average for the whole 37 year period (1949-1985) was 57 stations. The observations of the frequencies of hail occurrences have been published by the Federal Hydrometeorological Institute of Yugoslavia (Meteorological annual I - series 1949 to 1985).

In addition to these two aforementioned sources of data, the statistics of interruptions in the hail control operations in this analysis were used. These interruptions were caused partly by technical difficulties and partly by the Air Control Agency. Also, the statistics of the changes in methodology and technique of the hail control system were used to some extent.

## 4. EVALUATION BASED ON THE SIZE OF HAIL-SWEPT AREAS

The data used for the evaluation of the hail control system effectiveness, based on the size of hail-swept areas, are presented in Table 1. The hail-swept areas in protected territory in the cases when the system was not operating ($S_p^+$, column 4) are contained in the hail-swept areas, when the system was operating ($S_p$, column 3). The size of the observed territory $O_u$ is defined as the part of the unprotected territory $T_u$ for which the municipalities were sent commission reports about the hail damages. The calculations in this paper, concerning the hail damages in the unprotected territory, have been in relation to $O_u$ and to $T_u$ as the most unfavorable variant.

From the Table 1 it may be seen that the total agricultural area of Serbia (protected and unprotected) during the period 1971-1987 has been changed very little. It was decreased by 80,683 hectares or about 2%. A second important feature, that can be noted from Table 1 is the nearly steady increase of protected and decrease of unprotected territories. At the beginning of the period concerned, the protected territory amounted to about 28%, while at the end of the period it reached 95% of the total agricultural area. In spite of an increase of the protected territory by about 3.3 times, the size of the hail-swept area has been not changing very much and even shows some decrease.

Also, it may be noticed that the hail-swept area in the protected territory when the hail control system was not operating ($S_p^+$) was very large in the first half of the period. In that time the Air Control directed the aircraft by the radio beacon; as a result the prohibition of the anti-hail rocket launching were frequent and long lasting. At the same time, the hail control system was in a developing phase and frequently was not working.

Using the data shown in Table 1, the percentage R of hail-swept area in the protected and unprotected teritories has been calculated as

$$R_{p,i} = \frac{S_{p,i}}{T_{p,i}} 100\%, \quad R_{u,i} = \frac{S_{u,i}}{O_{u,i}} 100\%,$$

$$r_{u,i} = \frac{S_{u,i}}{T_{u,i}} 100\%$$

and corresponding mean values

$$\bar{R}_p = \frac{1}{N} \sum_{i=1}^{N} R_{p,i}, \quad \bar{R}_u = \frac{1}{N} \sum_{i=1}^{N} R_{u,i},$$

$$\bar{r}_u = \frac{1}{N} \sum_{i=1}^{N} r_{u,i}$$

Table 1. Sizes of protected ($T_p$) and unprotected ($T_u$) territories, hail-swept areas with ($S$) and without ($S^*$) operations and observed territory ($O_u$) in Serbia

| Years (1) | $T_{p(2)}$ | $S_{p(3)}$ | $S^*_{p(4)}$ | $T_{u(5)}$ | $O_{u(6)}$ | $S_{u(7)}$ |
|---|---|---|---|---|---|---|
| 1971 | 1130350. | 52003. | 30671. | 2909232. | 1750899. | 162424 |
| 1972 | 1093255. | 47526. | 25399. | 2948352. | 1889942. | 129823. |
| 1973 | 1137978. | 52762. | 37620. | 2879347. | 1198894. | 99519. |
| 1974 | 1184775. | 40818. | 23115. | 2839379. | 1260940. | 103398. |
| 1975 | 1648612. | 33727. | 13978. | 2375157. | 1733315. | 147994. |
| 1976 | 1888658. | 25936. | 2274. | 2126470. | 992721. | 54831. |
| 1977 | 2326575. | 120969. | 53023. | 1669271. | 1226792. | 112721. |
| 1978 | 2455712. | 67050. | 11783. | 1542450. | 622468. | 49972. |
| 1979 | 2912735. | 48387. | 940. | 1083221. | 711785. | 20370. |
| 1980 | 3079377. | 64043. | 2003. | 914658. | 462653. | 31920. |
| 1981 | 3133651. | 61767. | 25855. | 852049. | 299149. | 20488. |
| 1982 | 3330067. | 64823. | 0. | 657126. | 344121. | 38068. |
| 1983 | 3385784. | 31217. | 0. | 580994. | 266323. | 8800. |
| 1984 | 3753002. | 39313. | 0. | 220549. | 107181. | 1259. |
| 1985 | 3760870. | 23669. | 0. | 198029. | 0. | 0. |
| 1986 | 3760870. | 54837. | 3938. | 198029. | 28412. | 682. |
| 1987 | 3760870. | 33719. | 0. | 198029. | 28412. | 18. |

Table 2. Percentages of hail-swept areas at protected ($R_p$) and unprotected ($R_u$,$r_u$) territories as well as their ratio (Q,q)

| Years | $R_p$ | $R_u$ | $r_u$ | $Q$ | $q$ |
|---|---|---|---|---|---|
| 1971 | 4.60 | 9.28 | 5.58 | 0.496 | 0.824 |
| 1972 | 4.35 | 6.87 | 4.40 | 0.633 | 0.989 |
| 1973 | 4.64 | 8.30 | 3.46 | 0.559 | 1.341 |
| 1974 | 3.45 | 8.20 | 3.64 | 0.420 | 0.948 |
| 1975 | 2.05 | 8.54 | 6.23 | 0.240 | 0.329 |
| 1976 | 1.37 | 5.52 | 2.58 | 0.249 | 0.531 |
| 1977 | 5.20 | 9.19 | 6.75 | 0.566 | 0.770 |
| 1978 | 2.73 | 8.03 | 3.24 | 0.340 | 0.842 |
| 1979 | 1.66 | 2.86 | 1.88 | 0.580 | 0.883 |
| 1980 | 2.08 | 6.90 | 3.49 | 0.301 | 0.596 |
| 1981 | 1.97 | 6.85 | 2.40 | 0.288 | 0.821 |
| 1982 | 1.95 | 11.06 | 5.79 | 0.176 | 0.337 |
| 1983 | 0.92 | 3.30 | 1.51 | 0.279 | 0.609 |
| 1984 | 1.05 | 1.17 | 0.57 | 0.892 | 1.842 |
| 1985 | 0.63 | **** | **** | ***** | ***** |
| 1986 | 1.46 | 2.40 | 0.34 | 0.607 | 4.294 |
| 1987 | 0.90 | 0.06 | 0.01 | 14.152 | 90.000 |

The last formulas are not the best ones for estimating the mean R, as they weight all years equally even though, e.g., $T_p$ in 1987 is 3.3 times $T_p$ in 1971. We use, therefore, additional formulas

$$\bar{\bar{R}}_p = \Sigma S_{p,i}/\Sigma T_{p,i}, \quad \bar{\bar{R}}_u = \Sigma S_{u,i}/\Sigma O_{u,i}$$

Here i=1,2,...,N denotes year in the period and N the number of the years in the period. Further simple formulas for evaluating the effectiveness of hail control are

$$Q_i = \frac{R_{p,i}}{R_{u,i}}, \quad \bar{Q} = \frac{\bar{R}_p}{\bar{R}_u}, \quad \bar{\bar{Q}} = \frac{\bar{\bar{R}}_p}{\bar{\bar{R}}_u}$$

which give the ratio between the percentage of hail-swept areas in the protected and unprotected territories.

The results obtained by these calculations are presented in Table 2. In this Table it may be readily seen that from the beginning to the end of the period of operation the percentage of size of hail-swept area in the protected territory was gradually decreasing. During first few years it amounts to about 4% and in the last few years it amounts to about 1%. The percentage of hail-swept area in the unprotected territory from 1971 to 1982 was all the time rather high, from 5.5 to 11.0% except for the 2.9% in 1979. During the last 4-5 years the percentage of hail-swept area suddenly dropped. That could be a result of drastic decreasing of the size of unprotected territory. In that time it was already reduced to about 5% of the total agricultural area in Serbia and became surrounded by much larger protected territory.

The mean percentage of the hail-swept area in the protected territory amounts to $\bar{R}_p$ = 2.41% ($\bar{\bar{R}}_p$ = 1.97%) and in the unprotected territory $\bar{R}_u$ = 5.80% ($\bar{\bar{R}}_u$ = 7.60%). It gives mean ratio Q = =$^u$0.42 ($\bar{\bar{Q}}$ = 0.26) and an effectiveness expressed by formula E = 1-$\bar{Q}$ of 0.58 or 58% ($\bar{\bar{E}}$ = 0.74 or 74%).

In order to analyse the characteristics of the series of percentages of hail-swept areas in protected and unprotected territories, we shall apply the Abe's statistical test to investigate the trend of decreasing the size of hail-swept areas. This test uses the formula

$$q = \frac{\Sigma(X_{i+1} - X_i)^2}{\Sigma(X_i - \bar{X})^2}$$

where $X_i$ denotes a member and $\bar{X}$ mean value of the series considered. The existence of trend is characterized by small and non-existence by high value of q.

As a consequence of improvement of methodology and spreading the hail control system to greater territory, in the case that the hail control system has been efficient, a trend of percentage of hail-swept area decrease in the protected territory should exist. On the contrary, such a trend in the unprotected territory should not exist.

In application of Abe's test, the periods of 17 years for $R_p$ and 14 years for $R_u$ and $r_u$ are used. Namely, in the last three years of the period considered the unprotected territory became very small so that the percentages of hail-swept area were unrepresentative. After the abovementioned formula the results obtained as follow:

$R_p$: q=0.405 n=17(1971-1987) P(q≤0.405)≤0.005

$R_u$: q=0.790 n=14(1971-1984) P(q≤0.790)=0.210

$r_u$: q=0.980 n=14(1971-1984) P(q≤0.980)=0.470

These data show that a significant trend of percentage of hail-swept area decrease exist in the protected territory with a probability of 99% to be true. At the same time such a trend in the series of percentages of hail-swept areas in the unprotected territory has been not noted.

Further, the sign test is applied using null hypothesis Ho: no difference in number of negative (-) and positive (+) signs is true, than

$$P(-) = P(+) = 0.5$$

with an alternative that $P(+)>0.5$. If T represents the number of negative signs than small number of signs (-) is characteristic for Ho.

The difference $Z = R_u - R_p$ is positive in all years, i.e. T=0 and according to this test the probability that hail control system in Serbia is efficient amounts to 100%. However, if we take the most unfavorable case, i.e. that in the part of the unprotected territory for which the reports were not received, $Z = r_u - R_p$, we obtain

$$T = 2 \quad n = 14 \quad P(T \leq 2) = 0.0065$$

That means that between the percentages of hail-swept areas in the protected and unprotected territories a significant difference exist.

In order to be more confident in the aforementioned conclusion, the Student's test for investigation of the mean value of difference (coupled samples) to series $Z = r_u - R_p$ is applied. This test is made using the formula

$$t_o = \frac{\bar{Z} - m}{\bar{S}_z} \sqrt{n}$$

where $\bar{Z}=0.96$ represents the arithmetic mean value of the series considered and $\bar{S}_z = 1.45$ is standard deviation.

This test has $t_{n-1}$ distribution, i.e. Student's distribution with n-1 degrees of freedom. Simbol m in formula is assumed (theoretical) mean value. In our case we consider the series Z for which according to Ho is taken to be m=0. In that way we obtain

$$t_o = 2.48 \quad \text{and} \quad P(t_o \geq 2.48) \leq 0.01$$

showing that between $\bar{r}_u$ and $\bar{R}_p$ a significant difference exist. Also the Wilcoxon matched-pairs signed-ranks test, which utilizes both the direction and the relative magnitude of the differences within pairs, gives

$$n = 14 \quad T = 14 \quad P(T \leq 14) < 0.01.$$

That means that the difference between the percentage of hail-swept area in the unprotected territory taken as the most unfovarable case, and the percentage of hail-swept area in the protected territory is significant.

In the previous section it has been mentioned that great differences in technical means, efficiency of reagent and size of protected and unprotected territory exist between the periods 1971-1977 and 1978-1984. For that reason the Student's test has been applied to series $\bar{R}_p$, $\bar{R}_u$ and $\bar{r}_u$ separately to each of these two periods.

The Student's test for comparison two independent characteristics $X_1$ and $X_2$ and Ho: that $X_1$ and $X_2$ have the same mean value, is used by formula

$$t_o = \frac{\bar{X}_1 - \bar{X}_2}{\tilde{\delta}\sqrt{\frac{1}{n_1} + \frac{1}{n_2}}} = t_{n_1+n_2-2}$$

Here, $n_1$ and $n_2$ denote the sizes of samples and $\delta$ is standard deviation obtained by formula

$$\tilde{\delta} = \sqrt{\frac{(n_1-1)\tilde{S}_1^2 + (n_2-1)\tilde{S}_2^2}{n_1 + n_2 - 2}}$$

where

$$\tilde{S}_x^2 = \frac{1}{n-1} \Sigma(X_i - \bar{X})^2$$

The above formula for $t_o$ is used under assumption that the difference between $\tilde{\delta}_1 = S_{x_1}$ and $\tilde{\delta}_2 = S_{x_2}$ is not significant. In the case when the difference between $\tilde{S}_1^2$ and $\tilde{S}_2^2$ is significant, $t_o$ is calculated by formula

$$t_o = \frac{\bar{X}_1 - \bar{X}_2}{\sqrt{\frac{S^2}{n_1} + \frac{S^2}{n_2}}} = t_k$$

where k denotes the number of degrees of freedom, which may be obtained by formula

$$k \cong \frac{\left(\frac{S_1^2}{n_1} + \frac{S_2^2}{n_2}\right)^2}{\left(\frac{S_1^2}{n_1}\right)^2 \frac{1}{n_1+1} + \left(\frac{S_2^2}{n_2}\right)^2 \frac{1}{n_2+1}} - 2$$

On the basis of above shown formulas, the results are obtained as follow:

| Period 1971-1977 | | Period 1978-1984 | |
|---|---|---|---|
| $\bar{R}_p = 3.67$ | $\tilde{\delta} = 1.45$ | $\bar{R}_p = 1.77$ | $\tilde{\delta} = 0.62$ |
| $\bar{R}_u = 7.99$ | $\tilde{\delta} = 1.35$ | $\bar{R}_u = 5.74$ | $\tilde{\delta} = 3.45$ |
| $\bar{r}_u = 4.67$ | $\tilde{\delta} = 1.56$ | $\bar{r}_u = 2.70$ | $\tilde{\delta} = 1.69$ |

Using these data in comparison of the series $R_p$, $R_u$ and $r_u$ for the periods 1971-1977 and 1978-1984 we obtain the results

| | | | |
|---|---|---|---|
| $R_p$: | $t_o = 3.19$ | $k = 11$ | $P(t_o \geq 3.19) \leq 0.005$ |
| $R_u$: | $t_o = 1.61$ | $k = 8$ | $P(t_o \geq 1.61) \leq 0.070$ |
| $r_u$: | $t_o = 2.27$ | $k = 12$ | $P(t_o \geq 2.27) \leq 0.025$ |

These results show that there is a significant difference in the series $R_p$, i.e. in percentage of hail-swept area in the protected territory between the periods 1971-1977 and 1978-1984. These difference arises due to substantial decrease of hail-swept areas in the period 1978-1984 caused by an improment in the methodology and technique of hail control system in that period. Some tendencies of hail-swept area decrease which is seen in the same period in the unprotected territory it is supposed to be result of a great decrease of the size of unprotected territory and increase of protected territory. In that way the hail suppression influence has been transfered to unprotected territory.

## 5. EVALUATION BASED ON THE PERCENTAGE OF CROP DAMAGES

In the preceeding section it has been shown that the size of hail-swept area in protected territory in comparison to that in the unprotected territory is very much reduced. It is natural to assume that the decrease of the size of hail-swept areas has been followed by a decrease of the in-

tensity of the hail too. In order to prove this assumption, the sizes of hail-swept area were multiplied by the corresponding percentages of crop damages in the hail-swept area and thus reduced to 100% hail damaged area.

Here it should be pointed out that due to the varieties of crops and their phases of growth, this comparison will not be accurate enough for the small areas. However, such areas as protected and unprotected teritories of a size over a million hectares, for the sorts of crops, their phenophases and the time of hail-damaging, statistically may be considered as similar.

The sizes of hail-swept area reduced to areas damaged 100% in protected ($S'_p$) and unprotected ($S'_u$) territories, as well as corresponding percentages ($R'_p$) and ($R'_u$) and their ratio ($Q'$) are presented in Table 3. If we compare Tables 2 and 3 we can see that the decrease of the hail-swept areas damaged 100% in the protected territory is greater that the decrease in the unprotected one in 12 of the 16 years.

Table 3. Hail-swept areas reduced to area damaged 100% in protected ($S'_p$) and unprotected ($S'_u$) territories, as well as corresponding percentages ($R'_p$, $R'_u$) and their ratio ($Q'$)

| Years | $S'_p$ | $S'_u$ | $R'_p$ | $R'_u$ | $Q'$ |
|---|---|---|---|---|---|
| 1971 | 25102. | 99435. | 2.23 | 5.68 | 0.393 |
| 1972 | 22914. | 85949. | 2.10 | 4.55 | 0.461 |
| 1973 | 27231. | 56623. | 2.39 | 4.72 | 0.507 |
| 1974 | 18615. | 52443. | 1.57 | 4.16 | 0.378 |
| 1975 | 12374. | 81443. | 0.75 | 4.70 | 0.160 |
| 1976 | 13008. | 30194. | 0.69 | 3.04 | 0.226 |
| 1977 | 76912. | 65093. | 3.31 | 5.31 | 0.623 |
| 1978 | 36349. | 22743 | 1.48 | 3.65 | 0.405 |
| 1979 | 21710. | 9254. | 0.75 | 1.30 | 0.573 |
| 1980 | 25153. | 10525. | 0.82 | 2.27 | 0.359 |
| 1981 | 23724. | 5791. | 0.76 | 1.94 | 0.391 |
| 1982 | 24884. | 21205. | 0.75 | 6.16 | 0.121 |
| 1983 | 14010. | 5856. | 0.41 | 2.20 | 0.188 |
| 1984 | 13802. | 751. | 0.37 | 0.70 | 0.525 |
| 1985 | 6765. | 0. | 0.18 | 0.00 | ***** |
| 1986 | 22721. | 538. | 0.60 | 1.89 | 0.319 |
| 1987 | 14856. | 12. | 0.40 | 0.04 | 9.353 |

The mean percentage of the hail-swept area reduced to 100% of damage in the protected territory is $\bar{R}'_p = 1.15\%$ and for unprotected territory $\bar{R}'_u = 3.08\%$. Their ratio is $\bar{Q} = 0.37$ and value of effectiveness $E' = 0.63$ or 63%. These values show that the effectiveness of the hail control system in Serbia expressed through the decrease in hail intensity may be estimated as 5%.

In order to find out whether a decrease trend in series $R'_p$, $R'_u$ and $r'_u$ exist, the Abe' test has been applied. The results obtained are as follow:

$R'_p$: $q = 0.504$ $n = 17$ $P(q \leq 0.504) \cong 0.01$

$R'_u$: $q = 0.720$ $n = 14$ $P(q \leq 0.720) \cong 0.14$

$r'_u$: $q = 0.890$ $n = 14$ $P(q \leq 0.890) \cong 0.34$

These results show that in series $R'_p$ a significant trend of decreasing of hail-swept area in the protected territory. Such a trend in series $R'_u$ and $r'_u$, which relate the unprotected territory, has not been noted.

The Student's test applied to the signes of series $Z' = r'_u - \bar{R}'_p$ yields

$$T = 2 \qquad n = 14 \qquad P(t \leq 2) \leq 0.0065$$

This test shows a significant difference between the percentage of hail-swept areas in which the percentage of crop damages is taken into consideration compared to sizes of hail-swept area in the unprotected territory.

Application of Student's test to coupled samples of series $Z'$ gives

$$Z' = 0.68 \quad \tilde{\delta}_{z'} = 0.911 \quad n = 14 \quad t_o = 2.8$$

$$P(t_o \geq 2.8) \leq 0.01$$

This shows that the difference between mean values of the size of hail-swept areas in which the level of damages in protected and unprotected territories is significant.

A comparison of the mean values of series $\bar{R}'_p$, $\bar{R}'_u$ and $\bar{r}'_u$ for periods 1971-1977 and 1978-1984 yields the results as follow:

| Period 1971-1977 | | Period 1978-1984 | |
|---|---|---|---|
| $\bar{R}'_p = 1.84$ | $\tilde{\delta} = 0.94$ | $\bar{R}'_p = 0.76$ | $\tilde{\delta} = 0.36$ |
| $\bar{R}'_u = 4.95$ | $\tilde{\delta} = 0.85$ | $\bar{R}'_u = 2.60$ | $\tilde{\delta} = 1.82$ |
| $\bar{r}'_u = 2.70$ | $\tilde{\delta} = 0.95$ | $\bar{r}'_u = 1.25$ | $\tilde{\delta} = 0.94$ |

Using these data we obtain:

$R'_p$: $t_o = 2.89$ $k=7$ $P(t_o \geq 2.89) \cong 0.01$

$R'_u$: $t_o = 2.62$ $k=10$ $P(t_o \geq 2.62) \leq 0.025$

$r'_u$: $t_o = 2.62$ $k=12$ $P(t_o \geq 2.62) \cong 0.01$

From these values if follows that a significant difference in mean values of $R'_p$, $R'_u$ and $r'_u$ between above mentioned periods exist. That means that during the last years of hail control operation in the unprotected territory decrease of the hail intensity has been greater than decrease in the size of the hail-swept area.

## 6. TRENDS IN SIZES OF HAIL-SWEPT AREAS

Let we consider that the total agricultural surface in Serbia, which amounts about 4 million hectares, has been constant during the whole period of hail control operations. Then, if we assume that this system has been efficient, the following conditions should be fulfilled:

1) A decreasing trend of the percentage of hail-swept area in the total agricultural surface of Serbia, as a consequence of the hail control system spreading from year to year, should be shown.

2) A decreasing trend of the percentage of hail-swept area in the protected territory, as a consequence of the improvement of technology, particularly introducing the new reagent, during the

period of operations, should be observed.

3) A decreasing trend of the percentage of hail-swept area in the unprotected territory, due to radical decrease of that territory and becoming surrounded by protected territory, from which the effect was transferred, should be shown.

4) The percentage of hail-swept area in the protected territory should be less than that in the unprotected territory and the percentage in the total territory (protected and unprotected) should be between them.

In order to test these hypotheses, two techniques have been applied which will bring out the general trend of changes of the size of hail-swept area during the period of operations. Owing to the fact that there exist considerable fluctuations in the occurrences of these phenomena from year to year, both techniques are based on the time averaging of data.

The first techniques was a calculation of moving averages according to data of the annual sizes of hail-swept which were obtained by the formula:

$$\hat{R}_m = \left( \sum_{i=m}^{m+n} S_{p,i} \Big/ \sum_{i=m}^{m+n} T_{p,i} \right) \cdot 100\%$$

Here i = 1,2,...,17 denotes the years in the period and m = 1,2,...,M identifies the moving average. The number of moving averages is less than 17 number of years for a smoothing interval which has been taken here to be n=6. The results calculated by this formula are presented in Table 4.

Table 4. Trends of percentage of hail-swept areas in total ($\hat{R}_T$), protected ($\hat{R}_p$) and unprotected $\hat{R}_u$ territories

| Periods | $\hat{R}_T$ | $\hat{R}_p$ | $\hat{R}_u$ |
|---|---|---|---|
| 1971-1976 | 3.94 | 3.13 | 4.34 |
| 1972-1977 | 4.02 | 3.47 | 4.37 |
| 1973-1978 | 3.78 | 3.21 | 4.23 |
| 1974-1979 | 3.43 | 2.71 | 4.20 |
| 1975-1980 | 3.24 | 2.52 | 4.30 |
| 1976-1981 | 2.83 | 2.46 | 3.55 |
| 1977-1982 | 2.92 | 2.48 | 4.07 |
| 1978-1983 | 2.12 | 1.84 | 3.01 |
| 1979-1984 | 1.80 | 1.58 | 2.81 |
| 1980-1985 | 1.61 | 1.39 | 2.94 |
| 1981-1986 | 1.45 | 1.30 | 2.56 |
| 1982-1987 | 1.25 | 1.14 | 2.38 |

The second technique of averaging was the gradual average of the annual sizes of hail-swept areas obtained by the formula:

$$R_\mu = \frac{1}{\mu} \sum_{i=1}^{\mu} R_i$$

which gives the average values for each preceding period (μ) of time. The results obtained by this formula are presented in Fig.1

From Fig.1 and Table 4 it is obvious that the trends of the hail-swept area decrease are fully

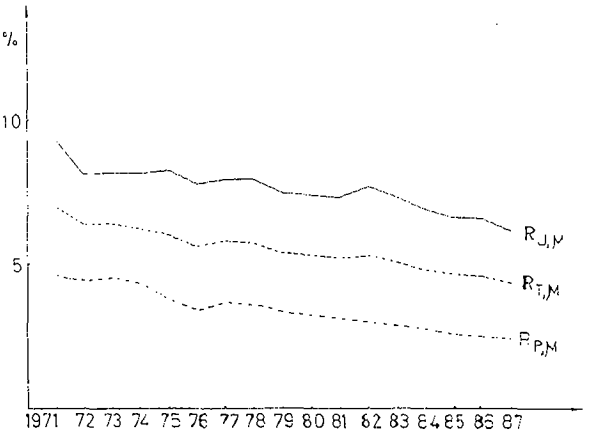


Fig.1 Graphical presentation of the gradual averages of the annual sizes of hail-swept areas at the total ($R_T$), protected ($R_p$) and unprotected ($R_u$) territories.

in accordance with above-mentioned hypotheses.

If we do not make smoothing but simply calculate the percentage of whole hail-swept areas ($S_p+S_u$) in relation to total protected and unprotected ($T_p+O_u$) territories we shall for the mean values obtain:

Period 1971-1977 Period 1978-1987

$\bar{R}_T = 5.79$ $\tilde{c} = 1.49$ $\bar{R}_T = 1.87$ $\tilde{c} = 1.03$

The Abe's criterion for trend gives

$q = 0.24$ $n = 17$ $P(q \leq 0.24) = 0.0007$

It shows that the trend of decrease of the percentage of whole hail-swept area in the protected and unprotected territories very pronounced. A comparison of mean values for the periods 1971-1977 and 1978-1987 yields

$t_o = 6.08$ $k=11$ $P(t_o \geq 6.08) = 0.0005$

It means that the difference in percentage of whole hail-swept areas for above-mentioned periods for total protected and unprotected territories is very high and statistically significant.

## 7. EFFECTIVENESS OF NON-INTERRUPTED OPERATIONS

In previous sections the hail-swept areas in the protected territory have been considered without taking into account the interruptions in the hail control system operations. Such cases were rather frequent and long lasting during the first half of the period (1971-1978). In such situations the protected territory or some part of it stayed practically unprotected. For that reason, the picture about the real effectiveness of the hail control system, obtained in above derived way, is not quite realistic one.

Determination of the part of territory where the system was not operating in a single situation was not practical. Two main reasons for that are: first, the part of the protected territory over

which the system was not operating did not coincide with the territories of the municipalities, from which the data about the hail-swept areas in summarized from have been obtained; second, it was not possible to control the effect of operations which took place in surrounding areas. Thus, it was decided not to consider individual cases but to omit all the territories and reports of the municipalities from consideration if the hail control system was not operating in a given year for as little as a single day. Thus, consideration was only given for those territories and reports of the municipalities in which the hail control system operated without interruption. The results calculated in this manner are presented in Table 5.

Table 5. Parts of protected territory ($T_p''$) and hail-swept areas ($S_p''$) in hectares where the hail control system have been operating without interruption

| Years | $T_p''$ | $S_p''$ | $R_p''$ | Q'' |
|---|---|---|---|---|
| 1971 | 667061. | 21133. | 3.17 | 0.342 |
| 1972 | 534992. | 19359. | 3.62 | 0.527 |
| 1973 | 804643. | 7364. | 0.92 | 0.110 |
| 1974 | 836379. | 15961. | 1.91 | 0.233 |
| 1975 | 1084288. | 14985. | 1.38 | 0.162 |
| 1976 | 1660759. | 21762. | 1.31 | 0.237 |
| 1977 | 1686442. | 54254. | 3.22 | 0.350 |
| 1978 | 2211108. | 53672. | 2.43 | 0.302 |
| 1979 | 2879785. | 47157. | 1.64 | 0.572 |
| 1980 | 3024419. | 60336. | 1.99 | 0.289 |
| 1981 | 3050817. | 35912. | 1.18 | 0.172 |
| 1982 | 3330067. | 64823. | 1.95 | 0.176 |
| 1983 | 3385784. | 31217. | 0.92 | 0.279 |
| 1984 | 3753002. | 39313. | 1.05 | 0.892 |
| 1985 | 3760870. | 23669. | 0.63 | ***** |
| 1986 | 3742912. | 50899. | 1.36 | 0.567 |
| 1987 | 3760870. | 33719. | 0.90 | 14.152 |

The mean value of percentage of the hail-swept area when the hail control system had been operating without interruption amounts to: $\bar{R}_p'' = 1.74$. Its ratio with mean percentage for unprotected territory gives $\bar{Q}'' = 0.3$.

The sizes of the hail-swept areas reduced to 100% of damages in their part of the protected territory, where the hail control system was operating without interruptions, are presented in Table 6. The mean percentage in this case is $\bar{R}_p'' = 0.82$ and its ratio to the percentage unprotected territory gives $\bar{Q}''=0.26$. That means that the hail-swept area reduced to 100% of damages in the part of protected territory where the hail control system has been operating without interruptions in comparison to unprotected territory has shown an effectiveness of $\bar{E}''= 0.74$ or 74%.

Looking at the differences between $R_p$ and $R_p''$ for individual years of the series considered, we can see that these differences were significant in the period 1971-1977 when the hail control system had been frequently out of operation. The mean difference $Z'' = R_p - R_p''$ for the period 1971-1977 amounts to $\bar{Z}''=1.45$ and $\tilde{\delta}'' = 1.19$. The Student's test applied to these values yields:

Table 6. The same as Table 5 but reduced to 100% of damages

| Years | $T_p''$ | $S_p''$ | $R_p''$ | $Q''$ |
|---|---|---|---|---|
| 1971 | 667061. | 9211. | 1.38 | 0.243 |
| 1972 | 534992. | 10362. | 1.94 | 0.426 |
| 1973 | 804643. | 3092. | 0.38 | 0.081 |
| 1974 | 836379. | 6445. | 0.77 | 0.185 |
| 1975 | 1084288. | 5212. | 0.48 | 0.102 |
| 1976 | 1660759. | 11263. | 0.68 | 0.223 |
| 1977 | 1686442. | 39032. | 2.31 | 0.436 |
| 1978 | 2211108. | 29339. | 1.33 | 0.363 |
| 1979 | 2879785. | 20844. | 0.72 | 0.557 |
| 1980 | 3024419. | 23564. | 0.78 | 0.342 |
| 1981 | 3050817. | 14638. | 0.48 | 0.248 |
| 1982 | 3330067 | 24884. | 0.75 | 0.121 |
| 1983 | 3385784. | 14010. | 0.41 | 0.188 |
| 1984 | 3753002. | 13802. | 0.37 | 0.525 |
| 1985 | 3760870. | 6765. | 0.18 | ***** |
| 1986 | 3742912. | 19325. | 0.52 | 0.273 |
| 1987 | 3760870. | 14856. | 0.40 | 9.051 |

$$t_o = 3.22 \qquad k=6 \qquad P(t_o \geq 3.22) \leq 0.01$$

It shows that the difference between the percentage of hail-swept area in the protected territory in the case when the hail control system had been operating with and without interruption was statistically significant.

During the period 1978-1987, as it has been said before, the interruptions in the hail control operations were rare and short. As a result, the differences between $R_p$ and $R_p''$ were rather small. These results are also supporting the theses that the hail control system in Serbia is efficient.

In order to be more sure about that conclusion we calculated the median for series $R_p''$ in Table 5, which amounts to 0.68, and made an analysis of the series of signs of deviations from the mean value. The test of number of series did not show a significant deviation from a series composed by chance. However, a more sensitive rank test has shown at a 5% of probability a significant deviation of a series composed by chance.

## 8. EVALUATION BASED ON OBSERVATIONS AT METEOROLOGICAL STATIONS

Cloud seeding with the aim of hail suppression, it is believed, do not affect much the cloud dynamics nor the general conditions of the atmosphere. Therefore, it may be expected that the number of storms on the average will stay unchanged. However, the frequency of occurrences, the length of duration and the intensity of hail phenomena should be decreased. That decrease, which should be seen in the hail observations at meteorological stations, is not so pronounced as the decrease of the size of hail-swept area and percentage of crop damaged. It is well known that in many cases the hailstones are too small and make insignificant damages; such cases were not taken into consideration in statistics of the municipality commissions. Nevertheless, such occurrences will be regularly registered by meteorological stations.

A radical decrease of the hail-swept areas in

Serbia, during the period of hail control operations, should be shown in the series of hail frequencies observed in the network of meteorological stations. In order to explore this hypothesis we used the series of number of days with hail observed in the network of synoptical and climatological stations in Serbia during the period 1949-1985. Data obtained are presented in Table 7.

Table 7. Number of days with hail observed at the meteorological stations in Serbia

| Years (1) | No of stations (2) | No of days (3) | Average No. of days (4) | Moving 5-years average of days (5) | Deviations (6) |
|---|---|---|---|---|---|
| 1949 | 48 | 39 | 0.81 | - | -0.25 |
| 1950 | 50 | 38 | 0.76 | - | -0.30 |
| 1951 | 48 | 71 | 1.48 | 1.08 | 0.42 |
| 1952 | 49 | 51 | 1.04 | 1.18 | -0.02 |
| 1953 | 52 | 67 | 1.29 | 1.27 | 0.23 |
| 1954 | 61 | 81 | 1.33 | 1.26 | 0.27 |
| 1955 | 68 | 83 | 1.22 | 1.40 | 0.18 |
| 1956 | 72 | 102 | 1.42 | 1.32 | 0.36 |
| 1957 | 69 | 121 | 1.75 | 1.21 | 0.69 |
| 1958 | 71 | 61 | 0.86 | 1.08 | -0.20 |
| 1959 | 69 | 54 | 0.78 | 1.03 | -0.28 |
| 1960 | 63 | 38 | 0.60 | 0.89 | -0.46 |
| 1961 | 63 | 72 | 1.14 | 0.89 | 0.08 |
| 1962 | 66 | 72 | 1.09 | 0.89 | 0.03 |
| 1963 | 64 | 54 | 0.84 | 1.01 | -0.22 |
| 1964 | 54 | 43 | 0.80 | 1.02 | -0.26 |
| 1965 | 57 | 68 | 1.19 | 1.15 | 0.13 |
| 1966 | 51 | 60 | 1.18 | 1.12 | 0.12 |
| 1967 | 51 | 89 | 1.74 | 1.14 | 0.68 |
| 1968 | 55 | 38 | 0.69 | 1.11 | -0.37 |
| 1969 | 53 | 48 | 0.90 | 1.16 | -0.16 |
| 1970 | 47 | 50 | 1.06 | 1.04 | 0.00 |
| 1971 | 55 | 77 | 1.40 | 1.07 | 0.34 |
| 1972 | 55 | 64 | 1.16 | 1.09 | 0.10 |
| 1973 | 49 | 41 | 0.84 | 1.25 | -0.22 |
| 1974 | 54 | 53 | 0.98 | 1.17 | -0.08 |
| 1975 | 49 | 92 | 1.88 | 1.18 | 0.82 |
| 1976 | 52 | 52 | 1.00 | 1.14 | -0.06 |
| 1977 | 53 | 65 | 1.23 | 1.16 | 0.17 |
| 1978 | 54 | 45 | 0.83 | 0.97 | -0.23 |
| 1979 | 54 | 47 | 0.87 | 0.97 | -0.19 |
| 1980 | 55 | 52 | 0.94 | 0.87 | -0.12 |
| 1981 | 64 | 62 | 0.97 | 0.87 | -0.09 |
| 1982 | 61 | 45 | 0.74 | 0.86 | -0.32 |
| 1983 | 63 | 53 | 0.84 | 0.84 | -0.22 |
| 1984 | 59 | 48 | 0.81 | - | -0.25 |
| 1985 | 59 | 51 | 0.86 | - | -0.20 |
| Average | 57 | - | 1.06 | - | - |

By dividing number of days with observed hail in the network of stations with the number of stations in each year we got the annual mean number of days with haul per station (or at a point) in Serbia (column 4). These annual mean number of days with hail, as a point value, has fluctuated between 0.60 as a minimum to 1.88 as a maximum. The average value for the whole period is 1.06 days. Here it should be pointed out that in the last 8 years (1978-1985) the mean number of days with hail was below normal. It suggests that the period in which the hail control system in Serbia was increased in size and technologically improved coincides with the period of hail frequency decrease.

The last column in Table 7 shows the deviations of the normal value of the annual number of days with hail at a point in Serbia. Let us suppose that the annual number of days with hail over the areas considered in two successive years is independent. Then, the probability that a number of successive years x in the series will have the same sign of deviation is given by

$$P(x) = \left(\frac{1}{2}\right)^x$$

It means that probability that 8 successive years will have the same sign of deviation, as it has been shown at the end of last column in Table 7, is below 0.4%.

Taking into consideration some characteristics of the series of hail days in Serbia in the period 1949-1985, which are relevant for statistical tests application, this series is divided into four separate periods. First period encircles the time 1949-1970 when the hail control system did not operate. Second period encompasses the time 1971--1977, i.e. the period when the hail control system had been developing and functioning with frequent interruptions. Third period encircles the time 1978-1985 when hail control system had been technically improved, functioning nearly without interruptions and covering the greatest part of Serbia. Fourth period makes sum of first two periods, i.e. the period when the hail control system did not exist and the period when it did not operate well and covered a small part of the territory of Serbia.

If we calculate the mean number of hail days ($\bar{A}$) and standard deviation ($\hat{\sigma}_A$) for above-mentioned periods, we obtain:

| | Period | $\bar{A}$ | $\hat{\sigma}_A$ |
|---|---|---|---|
| I | 1949-1970 | 1.09 | 0.32 |
| II | 1971-1977 | 1.21 | 0.35 |
| III | 1978-1985 | 0.86 | 0.07 |
| IV | 1949-1977 | 1.12 | 0.33 |

Application of Student's test to comparison of two series gives results as follow:

| | | | | |
|---|---|---|---|---|
| I | and II | $t_o = -0.84$ | k=27 | $P(t_o \leq -0.84) \approx 0.20$ |
| I | and III | $t_o = 3.17$ | k=26 | $P(t_o \geq 3.17) \leq 0.0025$ |
| II | and III | $t_o = 2.66$ | k= 7 | $P(t_o \geq 2.66) \leq 0.025$ |
| III | and IV | $t_o = 3.98$ | k=36 | $P(t_o \geq 3.98) \leq 0.0005$ |

Those results show that the difference between the number of hail days in the periods when the hail control system did not exist (I) and when it was not operating well (II) was not significant. The difference in the number of hail days between the periods I and III, i.e. when the hail control system did not exist and when it was working well, is statistically significant. The difference between the period when the hail control system was not operating well (II) and the period when it was functioning well (III) is also statistically signi-

ficant. Finally, the difference between the periods when the hail control system was operating well (III) and the joined periods when the system did not exist and not well operating (IV) is statistically highly significant.

Further, we mentioned above an interesting characteristic of the series of the annual number of hail days in Serbia, i.e. the last 8 successive years the number of hail days were below the average value for the whole period of observation. In order to test whether this event occured by chance or not we applied the median test and the test of the number of series.

Median for period 1949-1985 is 0.89 and the successive values below (-) and above (+) this value gives:

/--/+++++++/---/++/--/+++/--/+++/-0/+++/--------/

According to number of series test U=11, and expected number is 19. Standard deviation is 2.96 so we have

$$Z_o = \frac{U - 19}{2.98} = -2.7 \quad \text{and} \quad P(Z_o \leq -2.7) = 0.0035$$

This test show that the deviation of the last part of the series considered compared to that one obtained by chance is significant. In other words, this test suggests that the event of decreased values of number of annual hail days during the last 8 years in the series did not occured by chance.

Another calculation has been done using the ratio between the frequency of hail occurrences before and after hail control was introduced. For this calculation we used the network of meteorological stations for which the hail control operation existed for at least five years. Data used are presented in Table 8. From this table it may be seen that mean number of days before hail operations was 23, and after hail operations 13 years. The mean frequency of hail occurences in the period before hail control was 1.32 and after was 1.03 days with hail. This suggests a decrease of 22% in the frequency of days during hail control operation years.

Let us now consider the difference between the mean number of hail days in the period before and after the hail control system was introduced (presented in Table 8). From these differences we obtain the mean difference $\bar{Z} = 0.3$ and standard deviation $\delta = 0.77$. Application of Student's test gives

$$t_o = 1.87 \quad k=22 \quad P(t_o \geq 1.87) \leq 0.05$$

This show that the difference between the mean number of hail days in Serbia in the periods before and after the hail control system was introduced is statistically significant.

In the same way, the sign test show that at 5 out of 23 stations the number of hail days was less in the period before the hail control was introduced. So, the sign test for T = 5 gives

$$P(T \leq 5) \cong 0.013$$

The Wilcoxon test for the same data gives

Table 8. Number of days with hail observed at meteorological stations in Serbia before and after the hail control operation

| Stations | Before | | | After | | |
|---|---|---|---|---|---|---|
| | No. of years | No. of days | Mean No. of days | No of years | No of days | Mean No. of days |
| Loznica | 18 | 30 | 1.7 | 16 | 13 | 0.8 |
| U.Požega | 25 | 45 | 1.8 | 9 | 11 | 1.2 |
| Kuršumlija | 27 | 32 | 1.2 | 7 | 7 | 1.0 |
| Vrnjačka B. | 29 | 45 | 1.6 | 7 | 17 | 2.4 |
| Zaječar | 27 | 39 | 1.4 | 10 | 8 | 0.8 |
| Zlatibor | 27 | 69 | 2.6 | 9 | 23 | 2.6 |
| Bukovička B. | 18 | 21 | 1.2 | 19 | 12 | 0.6 |
| Ćuprija | 20 | 32 | 1.6 | 17 | 16 | 0.9 |
| Kragujevac | 20 | 24 | 1.2 | 17 | 13 | 0.8 |
| Kruševac | 20 | 25 | 1.2 | 16 | 6 | 0.4 |
| Negotin | 20 | 20 | 1.0 | 17 | 11 | 0.6 |
| Niš | 20 | 21 | 1.1 | 17 | 20 | 1.2 |
| Peć | 20 | 16 | 0.8 | 17 | 14 | 0.8 |
| Predejane | 21 | 52 | 2.5 | 16 | 23 | 1.4 |
| Priština | 30 | 36 | 1.2 | 7 | 4 | 0.6 |
| Prizren | 20 | 12 | 0.6 | 17 | 14 | 0.8 |
| Prokuplje | 27 | 10 | 0.4 | 10 | 7 | 0.7 |
| Kraljevo | 27 | 41 | 1.5 | 10 | 13 | 1.3 |
| Rekovac | 27 | 32 | 1.2 | 10 | 7 | 0.7 |
| S.Palanka | 17 | 17 | 1.0 | 19 | 15 | 0.8 |
| Šabac | 20 | 18 | 0.9 | 16 | 12 | 0.8 |
| Trošević | 30 | 39 | 1.3 | 7 | 3 | 0.4 |
| Valjevo | 21 | 29 | 1.4 | 16 | 30 | 1.9 |
| Mean values | 23.1 | 30.6 | 1.3 | 13.3 | 13.1 | 1.0 |

$$n=21 \quad T=19 \quad P(T=19) \leq 0.005$$

This also shows that the number of hail days in the period after the hail control was introduced is significantly less than the number of days before it was introduced.

## 9. CONCLUSIONS

The hail control system in Serbia during its 17 year operation shown an hail-swept area decrease in the protected compared to unprotected territories for about 58%. When the percentage of crop damages taken into consideration the effectiveness of hail suppression was increased for additional 5%, amounting 63%. Further, the part of protected territory over which the hail control system has been operating without interruptions, the effectiveness amounts to 74%.

An analysis of the number of hail days in Serbia observed in the network of meteorological stations, shown a decrease of number of days in last 8 years when the hail control system was functioning well. Also, an comparison of number of hail days observed before and after the hail control system was introduced, showed an decrease of hail days during the hail control operations for about 22%.

Several statistical tests have been applied to abovementioned data and they showed the significant differences between the protected and unprotected territories. They give a strong suport the concept that the hail control system, which has been operating in Serbia, is efficient. The rate of efficiency seems to be high enough to be

considered economically significant.

ACKNOWLEDGEMENTS

This work was supported by the Republic Hydrometeorological Institute of SR of Serbia in frame of the Hail Control Research Project, Contract No.92-1-52/85.

Appreciation is extended to Dr.Dragan Banjević for help in statistical tests application and to Mrs.Ljerka Opra for assistance in the preparation of data. Also, the author whishes to thank Mrs. Ljubica Radoja for typing the manuscript.

REFERENCES

Federer, B. et al., 1986: Main results of Grossversuch IV. J. Climate and Appl. Meteor., 25, 917-957.

Fedorov, E.K., 1965: Scientific problems of weather modification (in Russian). Leningrad, Gidrometizdat, p.57.

Gajvoronskij, I.I., and J.A. Seregin, 1965: The problem of introduction of reagent into cloud in modifying hail processes (in Russian). Tr. CAO, 5, 1.18.

Izrael, Yu.A., 1983: The role of atmospheric and geophysical sciences in the food supply programs (in Russian), Meteorology and Hydrology, 12, 9-15.

Karcivadze, A.I., 1964: Organization of experimental hail control in the Alzan Valley (in Russian). Tr. Geoph. Observ., Tbilisi, 15, 25-37.

Knight, C.A., G.B. Foote and P.W. Summers, 1979: Results of the randomized hail suppression experiment in northeast Colorado. Part IX. J.Climate and Appl. Meteor., 18, 1629-1639.

Radinović, D., 1972: Hail Control - Operative and scientific research project. Federal Hydrometeorological Institute, Belgrade (Translated and published for the U.S. Department of Commerce and National Science Foundation, Washington), p.124.

Sedunov, Yu.S., 1986: Influencing meteorological processes to the benefit of National economy. Meteorology and Hydrology 9, 5-17.

Sulakvelidze, G.K., 1967: Showers and hail (in Russian). Leningrad, Gidrometizdat, p.412.

# RECENT PROGRESS AND NEEDS IN OBTAINING PHYSICAL EVIDENCE FOR WEATHER MODIFICATION POTENTIALS AND EFFECTS

Roger F. Reinking
Weather Modification Program
NOAA Environmental Research Laboratories
Boulder, Colorado, USA

Rebecca J. Meitin
Cooperative Institute for Research in theEnvironmental Sciences (CIRES)
University of Colorado
Boulder, Colorado, USA

## ABSTRACT

Statistical and numerical modeling approaches to assess the effects of cloud seeding require the interactive input of, and understanding derived from, measurements that provide direct evidence of natural and altered development of precipitation. A brief review of recent progress in obtaining physical evidence to evaluate and verify potentials for and effects of precipitation enhancement and hail suppression is presented. Recent findings from the National Oceanic and Atmospheric Administration's Federal/State Cooperative Program in Weather Modification Research are emphasized, but other related results are included. In the context of many significant new advances toward proving hypotheses by direct measurement, a number of remaining needs for measurements and corresponding technologies are identified.

## 1. INTRODUCTION

Precipitation forms from many processes over many possible pathways in clouds. These processes and pathways may be altered by cloud seeding. The complexities and the natural variability of the processes and the consequent precipitation make it extremely difficult either to predict or to assess the effects of cloud seeding. Statistical and numerical modeling approaches to deal with the complexities and variability require the interactive input of, and the understanding derived from, direct measurements. To this end, some history, and some new advances, with a focus mainly on those from the National Oceanic and Atmospheric Administration's (NOAA) Federal/State Cooperative Program in Weather Modification Research (Reinking, 1985), are reviewed in this paper. In the context of these advances, some needs for other direct measurements and measurement technologies are identified.

## 2. BACKGROUND

Early cloud seeding experiments using rudimentary measurement technologies have demonstrated that precipitation can be stimulated to form and fall from relatively simple clouds. We define simple clouds as those that are either small, isolated or shallow, generally without natural ice, and with relatively uncomplicated internal structure and motions. Consider just a few examples to illustrate the foundation given to weather modification by the successes with simple clouds.

The supercooled stratocumulus cloud seeded by V.J. Schaefer in 1946 was not only dissipated but it was also quickly converted to precipitating snowflakes (see *Dennis*, 1980). Similarly, experimental and operational seeding of supercooled fogs has not only demonstrated a capability for dissipation; it has also shown that ice crystals that grow from the available liquid do indeed precipitate (e.g., Steele and Reinking, 1966).

Bethwaite et al. (1966) seeded isolated nonprecipitating cumuli from cloud base and measured subsequent rain at cloud base with a raindrop impactor. Cumuli with initial tops at $-10°$ to $-14°C$ that were seeded with 20 g of silver iodide-silver iodate produced rain volumes 13 times greater in the mean than those from nonseeded clouds. Substantially less seeding material (2 g) had no measurable effect. Kraus and Squires (1947) used dry ice to seed two cumuli in a seemingly uniformly sized population. Within 100 miles of the seeding aircraft, only these two clouds grew, explosively, above the general level of other tops, and produced radar echoes and rain.

New experiments using advanced measurement technologies quantify and confirm the early results. For example, an experiment with Alberta cumuli, using an aircraft with advanced "pointer" navigation and particle measuring probes to follow developing hydrometeors, is reported by Kochtubajda (1985) and Kochtubajda and English (1989). The size-concentration distributions of

growing and precipitating ice crystals from seeding were tracked and measured from the nucleation levels to the melting level near or below cloud base, and the rain from the melt was tracked to near the ground. In clouds with lifetimes enduring 20–40 minutes after seeding, aircraft-measurable precipitation was tracked and detected near the ground below 71% of clouds seeded with dry ice, 74% of clouds seeded with silver iodide-silver iodate flares, and only 15% of nonseeded clouds; 37% of the seeded clouds and none of the nonseeded clouds produced S-band radar echoes. As expected, the silver iodide-silver iodate was observed to take some 6–10 min longer to act than the dry ice, due to the difference in nucleation mechanisms.

The reader is referred to the many additional physical demonstrations that leave "no serious doubt about the existence of convective clouds which respond to artificial glaciation with increases in size and increases in precipitation" (Dennis, 1980). The thorough historical reviews by Dennis and in the volume edited by Braham (1986) show that the same is true for relatively simple clouds of other types.

These focused measurements add to the direct and quantitative physical evidence that the fundamental principles of cloud seeding are sound. One of the clouds seeded by Kraus and Squires produced 12 mm of rain over 130 km$^2$, thus providing good reason to explore seeding for dynamic effects. However, the more common result is that simple clouds do not yield substantial precipitation. For example, the precipitation from Schaefer's stratocumulus sublimed after falling 600 m into dry air, and the heaviest rainfall from the seeded Alberta cumuli was equivalent to only 1.6 cm over 1 km$^2$.

For more complex clouds with more natural ice, which might produce more added precipitation, Cooper's (1986) review shows that cloud conditions do occur where ice crystal concentrations are the result of temperature-dependent nucleation, rather than other processes. These concentrations, as compared with those from secondary ice production, are reasonably predictable and substantiate the hypothesis that some clouds may be ice deficient, depending on the flux of liquid water, cloud lifetime, and precipitation mechanisms. Knowledge of these factors is required for the next step: understanding the potentials. Hail suppression is more difficult to understand than precipitation enhancement. There are no measurements directly linking seeding materials and their effects to decreases in number or size of hailstones, although theories, models, and some sound statistical experiments with hail pad measurements suggest that seeding for hail suppression can work (Dennis, 1980; Steering Committee, 1988; Farley, 1987; Flueck et al., 1987; Smith et al., 1987). Therefore, central remaining challenges are (1) to demonstrate to the satisfaction of users and scientists that net precipitation can be beneficially increased from larger and more complex cloud systems, by either static or dynamic seeding, over the area of a watershed, and (2) to determine if either the microphysics or dynamics of complex convective storms can be sufficiently and predictably altered to suppress hail, in support of modeling and statistical experiments that suggest real possibilities for both precipitation increase and hail suppression.

Research toward these goals in the NOAA Federal/State Cooperative Program (Reinking, 1985) is focused on four key subsets of problems: (1) determination of the presence, persistence, and natural utilization of supercooled liquid water, (2) determination of potentials and methods for effective delivery of the seeding material to the supercooled liquid water, (3) evaluation and verification of the effects of seeding, and (4) quantification of benefits of any increased precipitation or suppressed hail. Satisfying proof of hypotheses in these areas will come only with measurements that provide direct physical evidence.

## 3. PHYSICAL EVIDENCE: ADVANCES AND NEEDS

### *3.1 Supercooled liquid water*

The invention of the dual-channel passive microwave radiometer (Hogg et al., 1983) to provide continuous measurements of liquid water and water vapor has heralded a wave of productive physical investigations centered on remote sensing. Many radiometer measurements show highly variable, commonly small, but often persistent levels of supercooled liquid water (SLW) in storms over mountains (e.g., Long, 1986; Long et al., 1986; Reynolds, 1988). The greatest advances are and will be made by applying sets and arrays of multiple remote sensors supported by airborne and surface measurements; for example, Long (1986), Long et al. (1986), Sassen et al. (1986), Snider et al. (1986), Meitin and Reinking (1989), Uttal et al. (1989) and others have applied combinations of Doppler and polarization radars, polarization lidar, and a radiometer to study orographic storms in Utah. These cases and composite studies spatially and temporally depict cloud and frontal structure; mesoscale kinematics; conditions for orographic enhancement, blocking with diversion or damming, gravity flows, etc; water release rates; precipitation generation processes; fluxes of water substance and forms of precipitating ice throughout storm passages. The coordinated use of satellite and radar remote sensing to follow the development and passage of warm cloud tops and rainbands, as was done in recent Bureau of Reclamation programs, is reviewed by Reynolds (1988).

The composite measurements are yielding an unprecedented but still partial understanding of the spatial and temporal evolution of SLW in relation to storm circulations and their interactions with the mountains. Such studies show in general that, for frontal/orographic storms, observable and potentially predictable "liquid water opportunities" occur within but not throughout storm periods, during periods with low and relatively warm could tops that minimize chances of natural ice formation, when either prefrontal or postfrontal moist air flow is perpendicular to the mountain barrier, or within embedded convective cells or bands. Concentrations of liquid water are greatly reduced when flow becomes oblique to the barrier, even though the regime may be under the influence of cyclonic convergence and lifting. The liquid water is most consistently observed close to terrain features that force lifting through the condensation level, rather than at higher altitudes in deep cloud systems or over the highest windward mountain slopes.

The vertically integrated precipitable liquid water has been observed to reach values of the order of 1 mm, but the probability of it exceeding 0.2 mm is only about 10% in the continental interior orographic storms in Utah and about 20% in storms over the Sierra Nevada or California. The liquid water can persist, albeit with high variability, for as long as 6 to 48 hours (Snider et al., 1986; Reynolds, 1988). Occurrences of lee-side losses of SLW to evaporation are often revealed by rimed trees on mountain crests. Such losses are not well documented, although measurements taken with scanning radiometers placed on or near crests could be used for this purpose. A significant opportunity to measure the budget of water vapor and liquid water fluxes over whole watersheds rests with the potential use of arrays of radiometers and wind profilers or Doppler radars.

Also needed are sensors to profile and horizontally locate the liquid water. The three-dimensional distribution of the liquid water in a cloud system might be measured using a technique of differential attenuation at two short radar wavelengths, as first suggested by Atlas (1954) and now being examined by NOAA's Wave Propagation Laboratory. Preliminary calculations show that ice particles would produce negligible attenuation in either the Ka-(0.86 cm) or the X-band (3.22 cm), but 0.2 g $m^{-3}$ of liquid water would produce 2-way attenuation of about 0.5 db/km in the Ka-band and an order of magnitude less attenuation in the X-band. The difference is measurable with state-of-the-art radars over pathlengths of several kilometers, so a synchronized dual-wavelength method is promising.

A dual-channel microwave radiometer for airborne use has been developed by NOAA's Wave Propagation Laboratory; this will allow investigators to take the SLW and vapor measuring device to desired locations and altitudes in clouds to be studied.

Knowledge of the temperature of the cloud liquid water is crucial to understanding, predicting and modifying conversion of the water to ice. A major advance, a combination of a Radio Acoustic Sounding System (RASS) with a wind profiler radar (Strauch et al., 1989), offers a solution to the temperature profiling problem in both orographic and convective regimes and can now provide a capability to profile the temperature of the water, within convective as well as orographic mixed phase clouds.

### *3.2 Delivery*

Given that ice particle deficiencies occur and that cloud volumes with significant liquid water can be identified, well-timed and well-dispersed delivery of seeding materials, to fill the cloud-liquid volumes, will require careful, innovative approaches. A recent assessment of experimental design considerations for transport and dispersion of seeding materials (Warburton et al., 1986) provides a good basis for discussing advances in gaining physical evidence for testing hypotheses of delivery. The questions of how to get the material to the target volume and how to mix it through the volume in stable or unstable air are very challenging.

Aerosol-hydrometeor interactions and the nucleation of ice depend on actual rather than average particle concentrations carried in a particular parcel or turbulent entity. Thus, the fraction of volume affected is pertinent, not the average concentration as derived from time-averaged Gaussian models; also, super-position of multiple Gaussian plumes overestimates the fraction of volume seeded. The ropes of aerosol or tracer need to become part of the theory, and the statistic most appropriate for determining the spread of the aerosol is not the mean concentration, but rather the concentration fluctuations enroute to and within the cloud volume (Warburton et al., 1986). Lagrangian particle diffusion and transport schemes are appropriate.

The plumes of aerosol released over complex terrain or into convection are best described as rope-like in structure; cloud- and meso-scale eddies do not mix two plumes, but cause them to weave or meander together. The history of an air parcel carrying a tracer depends on its path; the path varies for each passing section of a plume. Particularly in cloudy convection, successive steps in extension of the rope-like plume depend crucially on where the rope was in the previous "step" of the transport process. The meandering and the turbulence of eddies the size of the plume are the two physical mechanisms that produce concentration fluctuations.

The questions of delivery and verification are being effectively addressed by the use of airborne measurement technologies, $SF_6$ gas, indium oxide, oxygen isotopes, and silver (from AgI) to trace cloud motions and microphysical processes (Reinking, 1987; Smith et al., 1989).

Field research has proven the reality of the rope-like, spatially confined nature of plumes passing over complex terrain, by strategic sampling of fallen snow to find silver released as AgI from upwind ground-based, point source generators. While silver concentrations up to 35 times background have been observed in seeded Sierra Nevada snowfall, the "seeding silver" was present only 10–30% of the time in snow samples from periods of continuous seeding. The excess silver commonly appeared in narrow spatial and temporal zones as expected from narrow, meandering, precipitation-generating plumes. On some occasions, however, groups of silver sampling sites indicated relatively uniform dispersion in generating plumes and falling precipitation, throughout the area for extensive time periods during storms (Warburton, 1986; Reinking, 1987).

In recent experiments using aircraft with particle measuring probes and "pointer" navigation to follow advected and lifted air parcels, the enhancement of ice crystal concentrations above background by seeding has been documented quantitatively for both convective and orographic clouds. For example, Cooper and Lawson (1984) and Marwitz and Stewart (1981) have accomplished this in Bureau of Reclamation programs. Stith and Benner (1987) and Stith et al. (1989) have carried this another step in cumulus congestus clouds by identifying the ice due to seeding and separating it from natural ice by tagging the seeded air parcels with the $SF_6$ tracer gas. The rope-like structure of plumes during initial dispersion in convective clouds was confirmed, but turbulent mixing in the tops of convective currents tended to fill the volume and subsequent downdrafts. Also, Stith et al. (1989) compared, with some initial success, the concentrations of ice where $SF_6$ was detected to time- and temperature-dependent nucleation rates of the seeding material (AgI – AgCl) predicted from laboratory measurements.

For cloud-interactive seeding aerosols that do not immediately nucleate, there is the need to know whether the aerosol becomes involved in nucleation and both contributes to and is removed by precipitation, or whether it is merely removed by scavenging. Warburton et al. (1985) have approached this problem by releasing two tracers simultaneously at the same rates and locations: an active AgI ice-nucleating aerosol and a passive or inert (non ice-nucleating) indium sesquioxide ($In_2O_3$) aerosol. Both types of particles, as generated, were predominately submicron, and size distributions of the AgI complex and $In_2O_3$ were quite similar. If these particles were removed through precipitation by the same mechanisms, their masses in fallen snow would bear the same type of relationship to the water mass. Measured silver (iodide) contents showed a strong and positive correlation with the water mass of fallen snow; this is contrary to the normal negative correlations observed for atmospheric impurities scavenged by precipitation (the inert particle correlation is consistent with scavenging proportional to volume or surface area of the precipitation particulates). The data suggest independence or a slight positive correlation of the indium (oxide) mass concentrations with the mass of snow, which, within experimental tolerances, equates to the inert particle correlation, and is very distinctly different from the silver-snow mass relationship. The measurable difference indicates an ice nucleating component active in the removal of the silver iodide aerosol.

Overall, this work on the questions of effective delivery shows that ice from seeding can be identified and separated from natural ice by tagging seeded parcels of air with tracers, and that seeding material is producing some snow from complex clouds. However, this work also shows that current methods of delivery and the limits of dispersion processes make it very difficult to properly time and fill either an orographic or a convective cloud volume with seeding material. New strategies may be appropriate. A strategy for delivery with a design for seeding materials to reach only a portion of the available liquid water would appear to further compromise already limited seeding opportunities when the static mode of seeding is optimal, but may be appropriate for the dynamic mode. Cost effectiveness is a factor here. For example, the value of added water or reduced hail must be considered if delivery by multiple aircraft is otherwise desirable.

The problem of properly timing the seeding of an evolving volume of SLW could conceivably be sidestepped by seeding whenever there is cloud cover during storm passage or convective cloud development. If such an approach is cost effective, it would still require assessments of the effectiveness of targeting and potentials for decreasing precipitation.

Ground-based generators are in wide use for operationally seeding orographic clouds, and they continue to be used, albeit controversially, to seed convective clouds. Thus the release of seeding materials into clear air below cloud base is a standard practice. Drainage flows and thermally driven up-valley flows in mountain valleys have been mapped in detail with measurements from pulsed infrared Doppler lidar (Post and Neff, 1986). This device senses a frequency shift in infrared energy backscattered from aerosols that is proportional to the radial components of winds carrying the aerosol.

Many of the unresolved questions of ground-based delivery might be answered by applying lidar instrumentation and techniques to map tracer or natural aerosol gradients and airflows in clear air.

If cloud seeding technology is to advance very far beyond its present state, careful, innovative approaches that include real time monitoring of dispersion and SLW will likely be required for either research or operational application.

### *3.3 Evaluation and verification*

The questions and challenges of evaluation and verification of effects of seeding on the physical "chain of events" comprising the formation of precipitation are closely interwoven with the SLW and delivery problems, and much of the work already mentioned could equally well be examined in the evaluation and verification context. The liquid water must be available to form precipitation, and to determine and monitor its presence is to verify one link in the chain. Likewise, to determine that seeding material has reached the SLW and is producing ice crystals and snow is to verify that certain links in the chain have been modified.

The utilization of cloud water depends on the activity of various raindrop and ice processes. List et al. (1986) identify top priority laboratory experiments (which of late have been all too neglected in the scheme of obtaining meaningful measurements and insight); among these are production of secondary ice. Also included from the precipitation chain are ice crystal aggregation and large drop interactions with effects of electrostatic charging.

Pitter and Finnegan (1988), on the basis of laboratory observations, postulate a mechanism of secondary ice nucleation that proceeds only with aggregation and is correlated with high electrical freezing potentials of dissolved ionizable salts. Czys (1988) argues that shock-induced freezing (primary nucleation) may result from collisions of supercooled raindrops. The collisions may produce pressure fields which may induce local expansion and cooling of gas bubbles in the drops; the local cooling may cause nucleation on neighboring immersed nuclei. These new ideas are welcome because neither secondary nor primary ice is well predicted for complex clouds. This gap in physical evidence and understanding is limiting the utility of the advanced numerical cloud models, which have outpaced supporting observations.

Intense localized dynamics, large raindrops, and wet ice complicate our efforts to measure and understand isolated and embedded convective clouds. Determinations of the sum of factors affecting their precipitation efficiencies lag far behind those for more stratiform orographic clouds. Our inability to remotely detect and quantify first ice, particularly in the presence of large drops, is still a major obstacle. However, multiparameter radar measurement techniques offer hope of distinguishing various kinds of large ice particles and determining raindrop size distributions in mixed phase clouds (Bringi et al., 1989). This will help to identify active precipitation-forming processes and to quantitatively measure rates of precipitation in the varied forms.

Physical evidence from complex clouds that directly links released seeding material to precipitation on the ground has not been acquired, except in the physical-statistical experiments with simple cumuli reported by Kochtubajda (1985) and Kochtubajda and English (1989). Super and Heimbach (1989), for example, have effectively correlated AgI plumes and ice particle concentrations during a Bureau of Reclamation experiment; they conclude that "seeding the stable orographic clouds over the Bridger Range sometimes caused marked increases in ice particle concentration, presumably leading to more surface snowfall" (our underline). For a similar experiment with clouds over the Grand Mesa, Super and Boe (1989) concluded that precipitation rates estimated from ice particle images at flight level suggested increases within the seeded volumes" in eight tests. Correlated surface precipitation increases were observed in three of the tests and not evident in the others, and again, direct physical links between ice from seeding in the cloud and snow on the ground were not made.

This problem might be solvable by applying in combination, one or more of the gas and aerosol tracer technologies with the technique known as TRACIR (TRacking Air with Circular polarization Radar), which detects depolarized signal backscatter from chaff fibers released into a cloud. The chaff, which falls at velocities of small precipitation particles ($\sim 25$ cm $s^{-1}$), may be used as a tracer (Moninger and Kropfli, 1987; Martner and Kropfli, 1989) to simulate or tag first echo from seeding and the trajectories of resulting precipitation. This could be combined with polarization lidar which has already been effectively used to identify and monitor types of snow particles falling from cloud base to the ground (Sassen et al., 1986; Long et al., 1986).

The various tracer technologies, including TRACIR, also offer opportunities to determine the feeder cell vs. main cell sources and transport of hail embryos, beyond in-storm trajectories analyzed from multiple Doppler radar studies (Steering Committee, 1988).

Lee-side sublimation of unprecipitated ice may represent the greatest loss of water from mountain storms; likewise, the losses to glaciation of convective clouds may be very significant. This phenomenon is pertinent to the overall water budgets of targeted clouds which need to be determined to estimate the effects of seeding in causing net increases or decreases in precipitation. While instrumented aircraft may be helpful in addressing this problem, a

remote sensor to measure cloud ice mass and flux from large volumes of cloud is needed. Presently, K-band Doppler radars could be useful for crudely estimating the flux of large ice particles.

In related laboratory work, Finnegan and Pitter (1986) show how the dissolution of ionizable molecules of salts in ice crystals can cause aggregation, presumably by inducing electric multipoles. One can envision seeding nucleants with certain hygroscopic components to induce aggregation and enhance fallout. This kind of approach to enlargement of hydrometeors could be very important in reducing the lee-side losses to sublimation or in converting convective virga to precipitation.

### *3.4 Physical evidence of benefits*

Recent analyses of measured physical effects of added rain or snow, or reduced hail are generally lacking. Two exceptions are those reported by Knapp et al. (1988) and Changnon and Hollinger (1988).

Knapp et al. (1988) interactively used a model and measurements of plant processes and infiltration of rain into varied soils to estimate the effects of added July and August rainfall on the soil moisture, crop water use, and stream flow in the Midwest. The model simulations, based on the measurements, suggest that a large increase in rain (10–25%) directly on the crops would be required to sufficiently affect crops under stress to help growth, because any rain during crop stress periods is normally light and actual additions to the light rain would be small. However, actual additions for the same percentage increases would be greater during wet periods, and most of any increased summer rain would go to increase groundwater flows. This would improve water quality during dry periods. Also properly timed irrigation from (increased) groundwater could alleviate crop stress and add to growth.

Field experiments to evaluate the actual effects of enhanced rain on crop production have been needed. The unique experiment by Changnon and Hollinger (1988) uses a 9-m × 48-m mobile, plastic-covered shelter with a sprinkler system to exclude natural rain but otherwise expose crop plots to the prevailing weather. Watering is quantified and timed to the historical rain-day precipitation record, for wet, dry and average summers, with water added to simulate modification. Initial results indicate that rainfall increases of 10–40% in Illinois increase corn and bean yields by 4–20% if rainfall is below or near average.

In a more general analysis, Garcia et al. (1987) used a long period of records of standard measurements to study the effects of technological advance and weather conditions on crop production. They found that an increasing absolute variability in Midwest corn yield has accompanied a continued long-term trend of increasing average yield, such that increased precipitation and moderated crop heat stress might reduce risk by alleviating extreme year-to-year changes in yield.

Examination of crop-rainfall relationships by Schaffner et al. (1983) suggest that expected increases in crop yields and associated economic benefits from a 3 cm increase in growing season rainfall would boost the North Dakota state economy by $0.7 billion annually.

Southwest North Dakota has the highest ratio of hail damage claims paid to insured crop liability within the United States (9–11%). An exploratory statistical analysis of 61 years of hail loss ratios, which are crude but practical measurements, suggest 43.5% less hail damage to crops during 10 years of operational hail suppression. This is not explained by climate variations. Such a reduction, if attributable to seeding, supports a benefit-to-cost ratio of 8:1 for the operations (Smith et al., 1987). Only direct physical evidence from specific cloud, precipitation and other meteorological measurements will confirm such analyses.

## 4. CONCLUSIONS

The physical evidence accumulated so far proves that cloud seeding enhances precipitation when the right kind and amount of material is applied at the right time and place in a cloud. The task of determining what is "right" in microphysically and dynamically complex clouds is very difficult. The realized and potential advances in capabilities for cloud and precipitation measurement have taken the science of cloud seeding well beyond the plateau of the 1970's. These capabilities provide input and verification for statistical, theoretical and numerical modeling approaches which continue to be appropriate to use interactively with direct measurements to gain more complete understanding and predictability of the natural and modified precipitation processes. The new and emerging technologies may now enable us to meet the challenges of measuring if and when a complex cloud system is "right," if and how seeding material can be effectively delivered, and whether net precipitation over an area can or cannot be beneficially increased or hail can be reduced.

Central to all of this, detection of substantial liquid water within the lifetime of a cloud element is to be recognized as a necessary but not sufficient condition for finding seeding potential, which also depends on all of the factors that determine the natural precipitation efficiency and on the consequent effect of seeding on the net water budget of the entire volume of targeted clouds. Natural precipitation (in)efficiencies of complex cloud systems are unknown and need to be measured and under-

stood, as do the potentially modifiable links between hail embryos and hailstones.

## REFERENCES


Atlas, D., 1954: Estimates of cloud parameters by radar. J. Meteorol., 11, 309–317.

Bethwaite, F., E. Smith, J. Warburton, and K. Heffernan, 1966: Effects of seeding isolated cumulus clouds with silver iodide. J. Appl. Meteorol., 5, 513–520.

Braham, R., Jr., (ed.) 1986: Precipitation enhancement—a scientific challenge. Meteorological Monographs, Amer. Meteorol. Soc., Boston, 21, 171 pp.

Bringi, V., S. Sur, D. Musil, P. Smith, and R. Rasmussen, 1989: Microphysical evolution of convective clouds inferred from multiparameter radar measurements and aircraft penetrations. Preprints, 24th Conf. Radar Meteorol., Tallahassee, Amer. Meteorol. Soc., Boston (in press).

Changnon, S., and S. Hollinger, 1988: Use of unique field facilities to simulate effects of enhanced rainfall on crop production. J. Weather Modif., 20, 60–66.

Cooper, W., 1986: Ice initiation in natural clouds. Chap. 4 in R. Braham, Jr., ed., Precipitation enhancement—a scientific challenge. Meteorological Monographs, Amer. Meteorol. Soc., Boston, 21, 29–32.

Cooper, W., and R. Lawson, 1984: Physical interpretation of results from the HIPLEX-1 experiment. J. Climate Appl. Meteorol., 23, 523–540.

Czys, R., 1988: A new mechanism for ice initiation on warm-based Midwestern cumuli. Preprints, 10th International Cloud Phys. Conf., Bad Homburg. IAMAP/IUGG, 1, 25–27.

Dennis, A., 1980: Weather modification by cloud seeding. Academic Press, NY, 267 pp.

Farley, R., 1987: Numerical modeling of hailstorms and hailstone growth. Part II: The role of low density riming growth in hail production. J. Climate Appl. Meteorol., 26, 234–254.

Finnegan, W., and R. Pitter, 1986: Study of the initial aggregation of ice crystals. Preprints, 23rd Conf. Radar Meteorol. and Conf. Cloud Phys., Snowmass, Amer. Meteorol. Soc., Boston, C110–C112.

Flueck, J., M. Solak, R. Allen and T. Karacostos, 1987: An exploratory analysis of the National Hail Suppression Program in Greece. Preprints, 10th Conf. Wea. Modif., Amer. Meteorol. Soc., Boston, 124–128.

Garcia, P., S. Offutt, M. Pinar, and S. Changnon, 1987: Corn yield behavior: Effects of technological advance and weather conditions. J. Climate Appl. Meteorol., 26, 1092–1102.

Hogg, D., F. Guiraud, J. Snider, M. Decker and E. Westwater, 1983: A steerable dual-channel microwave radiometer for measurements of water vapor and liquid in the troposphere. J. Climate Appl. Meteorol., 22, 789–806.

Knapp, H., A. Durgunoglu and S. Changnon, 1988: Effects of added summer rainfall on the hydrologic cycle of Midwestern watersheds. J. Weather Modif., 20, 67–74.

Kochtubajda, B., 1985: The evolution of hydrometeor size distributions in seeded Alberta summertime cumulus clouds. Preprints, 4th WMO Sci. Conf. Weather Modif., Honolulu. WMO Tech. Doc., No. 53, Geneva, 1, 77–80.

Kochtubajda, B. and M. English, 1989: Summertime cumulus cloud seeding experiments in Alberta, Part II: Observations of seeded clouds. J. Appl. Meteorol. (submitted).

Kraus, E., and P. Squires, 1947: Experiments on the stimulation of clouds to produce rain. Nature, 159, 489–491.

List, R., J. Hallett, J. Warner and R. Reinking, 1986: The future of laboratory research and facilities for cloud physics and cloud chemistry. Bull. Amer. Meteorol. Soc., 67, 1389–1397.

Long, A., 1986: Investigations of winter mountain storms in Utah. Final Report to NOAA, Utah Division of Water Resources, Salt Lake City, 350 pp.

Long, A., K. Sassen, J. Snider and N. Fukuta, 1986: Remote sensing investigation of the mesoscale kinematics and the microphysics of a winter mountain storm. Preprints, 23rd Conf. Radar Meteorol. and Conf. Cloud Phys., Amer. Meteorol. Soc., Boston, J237–J240.

Martner, B., and R. Kropfli, 1989: Tracking chaff-filled air through clouds with circular polari-

zation diversity radar. 24th Conf. Radar Meteorol., Tallahassee. Amer. Meteorol. Soc., Boston (in press).

Marwitz, J., and R. Stewart, 1981: Some seeding experiments in Sierra storms. J. Appl. Meteorol., 20, 1129–1144.

Meitin, R., and R. Reinking, 1989: A Doppler radar analysis of a mountain winter storm. 5th WMO Conf. Weather Modif., Beijing. World Meteorological Organization, Geneva (in press).

Moninger, W. and R. Kropfli, 1987: A technique to measure entrainment in cloud by dual-polarization radar and chaff. J. Atmos. Oceanic Tech., 4, 75–83.

Pitter, R., and W. Finnegan, 1988: Field observations of ice crystal formation in clouds at warm temperatures. J. Wea. Modif., 20, 55–59.

Post, M., and W. Neff, 1986: Doppler lidar measurements of winds in a narrow mountain valley. Bull. Amer. Meteorol. Soc., 67, 274–281.

Reinking, R., 1987: Perspectives for research in wet chemistry and unintentional cloud modification from the discipline of purposeful cloud modification. Boundary-Layer Meteorology, 41, 381–405.

Reinking, R., 1985: An overview of the NOAA Federal-State Cooperative Program in Weather Modification Research. Fourth WMO Scientific Conference on Weather Modification, WMO/IAMAP Symposium, Honolulu, WMO/TD–No. 33, Geneva, II: 643–648.

Reynolds, D., 1988: A report on winter snowpack-augmentation, Bull. Amer. Meteorol. Soc., 69, 1290–1300.

Sassen, K., R. Rauber and J. Snider, 1986: Multiple remote sensor observations of supercooled liquid water in a winter storm at Beaver, Utah, J. Climate Appl. Meteor., 25, 825–834.

Schaffner, L., J. Johnson, H. Vruegdenhl and J. Eng, 1983: Economic effects of added growing season rainfall on North Dakota Agriculture. Agric. Econ. Report No. 172, Agricultural Experiment Station, North Dakota State University, Fargo, 19 pp.

Smith, P., J. Miller, Jr., and P. Mielke, Jr., 1987: An exploratory study of crop-hail insurance data for evidence of seeding effects in North Dakota. Final Report WMB-CARD– 86–1, North Dakota Weather Modif. Board, Bismarck, 21 pp.

Smith, P., H. Orville, J. Stith, B. Boe, D. Griffith, M. Politovich, and R. Reinking, 1989: Evaluation studies of the North Dakota cloud modification project. Preprints, 5th WMO Scientific Conference on Weather Modification and Applied Cloud Physics, Beijing. World Meteorological Organization, Geneva (in press).

Snider, J., T. Uttal and R. Kropfli, 1986: Remote sensor observations of winter orographic storms in southwestern Utah. NOAA Tech. Memo. ERL/WPL– 139, 99 pp.

Steele, R., and R. Reinking, 1966: Supercooled fog seeding and particle replication. In V.J. Schaefer (ed.), Sixth Yellowstone Field Research Expedition, Interim Report, State Univ. New York, Albany, Pub. No. 37, 114–125.

Steering Committee, 1988: Hailswath II, Preliminary Experimental Design. South Dakota School of Mines and Tech., Rapid City, 105 pp.

Stith, J., and R. Benner, 1987: Applications of fast response continuous $SF_6$ analyzers to in situ cloud studies, J. Atmos. Ocean. Tech., 4, 599–612.

Stith, J., A. Detwiler, R. Reinking and P. Smith, 1989: Investigating mixing and the production of ice in cumuli with gaseous tracer techniques. Atmospheric Research (accepted).

Strauch, R., K. Moran, P. May, A. Bedard, and W. Eckland, 1989: RASS temperature soundings with wind profiler radars. Preprints, 24th Conf. Radar Meterol., Tallahassee, Amer. Meteorol. Soc., Boston (in press).

Super, A., and J. Heimbach, Jr., 1989: Microphysical effects of winter time cloud seeding with silver iodide over the Rocky Mountains. Part II: Observations over the Bridge Range, Montana. J. Appl. Meteorol., 27, 1152–1165.

Super, A., and B. Boe, 1989: Microphysical effects of winter time cloud seeding with silver iodide over the Rocky Mountains. Part III: Observations over the Grand Mesa, Colorado. J. Appl. Meteorol., 27, 1166–1182.

Uttal, T., J. Snider, R. Kropfli and B. Orr, 1989: A remote sensing method of measuring atmospheric vapor fluxes: Application to winter mountain storms. J. Appl. Meteorol., (submitted).

Warburton, J., R. Elliott, W. Finnegan, B. Lamb, R. McNider, J. Telford, and L. Grant (ed.), 1986: A program of Federal/State/Local Cooperative Weather Modification Research: Design considerations. Part II: Transport and dispersion of seeding materials. Final report to NOAA; Colorado State University, Fort Collins, 80 pp.

Warburton, J., L. Young, M. Owens, and R. Stone, 1985: The capture of ice nucleating and non ice-nucleating aerosols by ice phase precipitation. J. Rech. Atmos., 19, 249–255.

# PAWS RESTRUCTURED

R C GROSH (PAWS Scientific Director, Rain Stimulation Project Leader)

C MüLLER (Rain Stimulation)

J GALPIN (Centre for Advanced Computing & Decision Support

I AURET (Centre for Advanced Computing & Decision Support)

M C HODSON (Rain Measurement, Project Leader)

D E PROCTOR (Lightning Probing, Project Leader)

G REUTER (Weather & Industry, currently with McGill Univ., Canada)

D vdS ROOS (Weather & Industry, Programme Manager)

CSIR

P O Box 395, PRETORIA 0001 South Africa

## INTRODUCTION

The Program for Atmospheric Water Supply (PAWS) is a randomized summer rain stimulation experiment utilizing dry ice released by Learjet as the seeding agent. Seeding is done during penetration into growing turrets of convective storms at the -10°C level. The main goal of the PAWS is to increase the water supply to all the people living in the dry climate of South Africa, but particularly to the Eastern Transvaal where rapid industrial and population growth will require additional water within the next generation. The experiment is now examining the physical effects of seeding on individual cloud systems. In the future, it is expected that statistical evaluations will be carried out over predetermined areas on the ground. The PAWS study has been on-going since 1981 and is partially described in Grosh (1988a), Dixon and Mather (1986), Morrison *et al.* (1986) and Mather *et al.* (1986), where initial radar and airborne microphysical analyses are briefly discussed. A series of lengthy annual reports supplies more complete and current information (Grosh, 1988b).

Funding and general management are provided by the Corporation for Atmospheric Water Supply (CRAWS). In January 1987 scientific direction for the project was placed in the hands of CSIR, a national science institute, to reduce

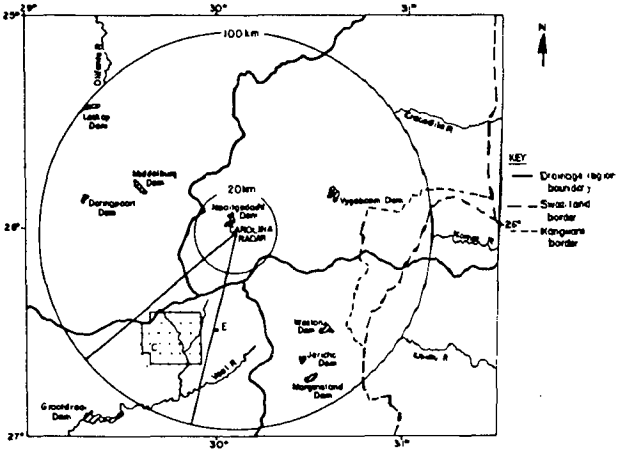


Figure 1: The new PAWS rain gauge network.

the dependence on and expense of foreign consulting firms, to develop local expertise, to expand the investigations, and to begin the process of independent confirmation of the very promising initial results. The importance of a

supporting institution with a broad scientific base to successful rain stimulation projects is discussed in Grosh (1989). Independent statistical analysis was contracted for within CSIR (Galpin, 1988) and preliminary cloud modelling undertaken at that time.

In 1988 a new scientific director was appointed within CSIR. At this point, three originally independent CSIR scientific projects also began to contribute to the rain stimulation studies through the office of the scientific director. These dealt with radar rainfall measurements, lightning locations, and investigations of ice particles in a coldroom laboratory. Thus, the project now has seven major components: scientific director, field operations (mainly CloudQuest), statistical analyses, rain measurement, electrical probing, laboratory studies, and cloud modelling. The purpose of this note is to describe the early stages of the CSIR development process, and the current state of the expanding project.

Field Equipment

The primary evaluation of PAWS is provided by the project radar which radiates at 5 cm wavelength and performs a fully digitised three-dimensional volume scan every 7 or 8 minutes. Recently the radar site has been moved to Carolina, about 110 km to the southwest of its original location at Nelspruit (Figure 1). The move was made to obtain improved viewing geometry and to be closer to the hydrologic centroid of the Eastern Transvaal. Plans are underway to expand the new rain gauge network to forty gauges, and improvement of the project radar facilities (to 10 cm) is thought likely to occur soon as well.

Two aircraft now serve the project, an Aerocommander for cloud base studies and a very maneuverable Learjet for seeding and penetration studies. The Learjet utilizes the 2D-C, FSSP, and King Hot Wire probes, amongst others. In addition, the jet engine is used as the evaporator in the first stage of a Lyman-alpha total water meter. The cloud base plane is equipped with a 2D-P probe. The nose radars of both planes are being developed for quantitative precipitation studies. All these facilities are maintained and operated by a commercial subcontractor, CloudQuest, which has been with the project since its inception.

The development of the jet engine evaporator/total water meter is one of the principal accomplishments of the PAWS project. Its main advantage over earlier total water meters is its very large sample volume, 15 $m^3$/sec (Morgan *et al.*, 1986; Kyle, 1975; Grosh, 1988a).

The two subprojects dealing with electrical effects on precipitation growth and radar rainfall measurements have additional special equipment including four radars (one a vertically pointing Doppler, one a long-wave lightning detector), several distrometers and rain gauges and an array of five VHF radio receivers for determining the location of lightning discharges. However, these are not located in the seeding area.

CloudQuest

In addition to field operations, CloudQuest has always played a strong role in planning and evaluating the PAWS experimental activities. One of the main contributions has been the identification of the very useful stratification variable, the coalescence time parameter. When the ratio of the cloud base temperature to the 500 mb temperature buoyancy is greater than two, coalescence drop growth is relatively favoured by the long time available for collisions as the cloud air rises slowly toward the -10°C flight level. The Learjet 2D-C observations confirm the effectiveness of this parameter in identifying conditions in which coalescence is dominant, as indicated by encounters with large droplets (>300 μm) at the -10°C level. The main use of this parameter is in analysis of the PAWS radar data. Early indications suggest that when large droplets are

present at the seeding level, seeding effects on storm size and rain are more likely to be significant. In other words, a "dynamic" seeding effect receives some support in the Eastern Transvaal.

Laboratory

A 23 $m^3$ coldroom (-10°C) is being obtained for cloud physic studies, such as of the" ice whiskers" associated with the dry ice seeding pellets. A small vertical wind tunnel is also available.

Lightning Probing

The programme of lightning research is carried out at a field station near Johannesburg. Paths of lightning flashes are traced by locating the sources of radio noise emitted by the flashes themselves. This is done by measuring the differences in the times of arrival of noise at the 5 widely spaced VHF receivers. The noise is retransmitted over microwavelengths to the main station where it is recorded on a laser optical recorder which can record 5 channels, each with a bandwidth of 6 MHz for an uninterrupted duration of 20 min.

These observations are supplemented by recordings of electrical field changes, by means of which the type of flash can be identified. In many cases the field-changes can be used to compute the current that flowed in the channel as well as the charge that was carried by a streamer, because its path is known. However, in order to do this it is necessary to assume the form of the charge distribution. The form of the charge distribution is not critical but the measured wave form cannot be regenerated from the data if a point distribution is assumed.

The Learjet will conduct limited studies in this network to determine if the meteorological conditions (draft structure, water contents) associated with the lightning locations can be ascertained.

Rainfall Measurement Usage

This investigation concentrates on finding the reasons for the differences in radar measured rainfall aloft and gauge measured rainfall at the ground using two different approaches, modelling and observation. A 9.3 GHz vertically pointing Doppler radar with eight nearby rain gauges and two anemometers are used to make observations.

Amongst several factors which change the rainfall structure with altitude, the combination giving the largest differences between rainfall aloft and at the ground appears to be the horizontal wind and differential drop fall velocities. Modelling these shows that differences in the rainfall rate of up to 100% can be obtained over a 600 m fall. An example of the output from a simple model for still air which uses measured rainfall rates as input is given in Figure 2. Here the maxima aloft and at the ground differ by 19%. In addition to amplitude reductions, phase shifts are also common. Both will become worse the higher the point of origin (radar observation level) is above ground. Testing these models by applying them to the Doppler radar measurements is currently being undertaken.

Few studies have dealt with the actual causes of the discrepancies in radar rain measurements. Thus, it is believed that this subproject will help determine the most efficient means of measuring surface rains when PAWS requires areal rain measurements.

Statistical Analyses

Full independent statistical and physical evaluations of the seeding effect on the PAWS storms will come only with time to resolve conflicts in sampling and statistical analysis procedures between CSIR and CloudQuest and to ponder the physical circumstances. For now, the seven radar variables (out of 250 available radar variables) which intuition tells us are the most closely related to the rain producing

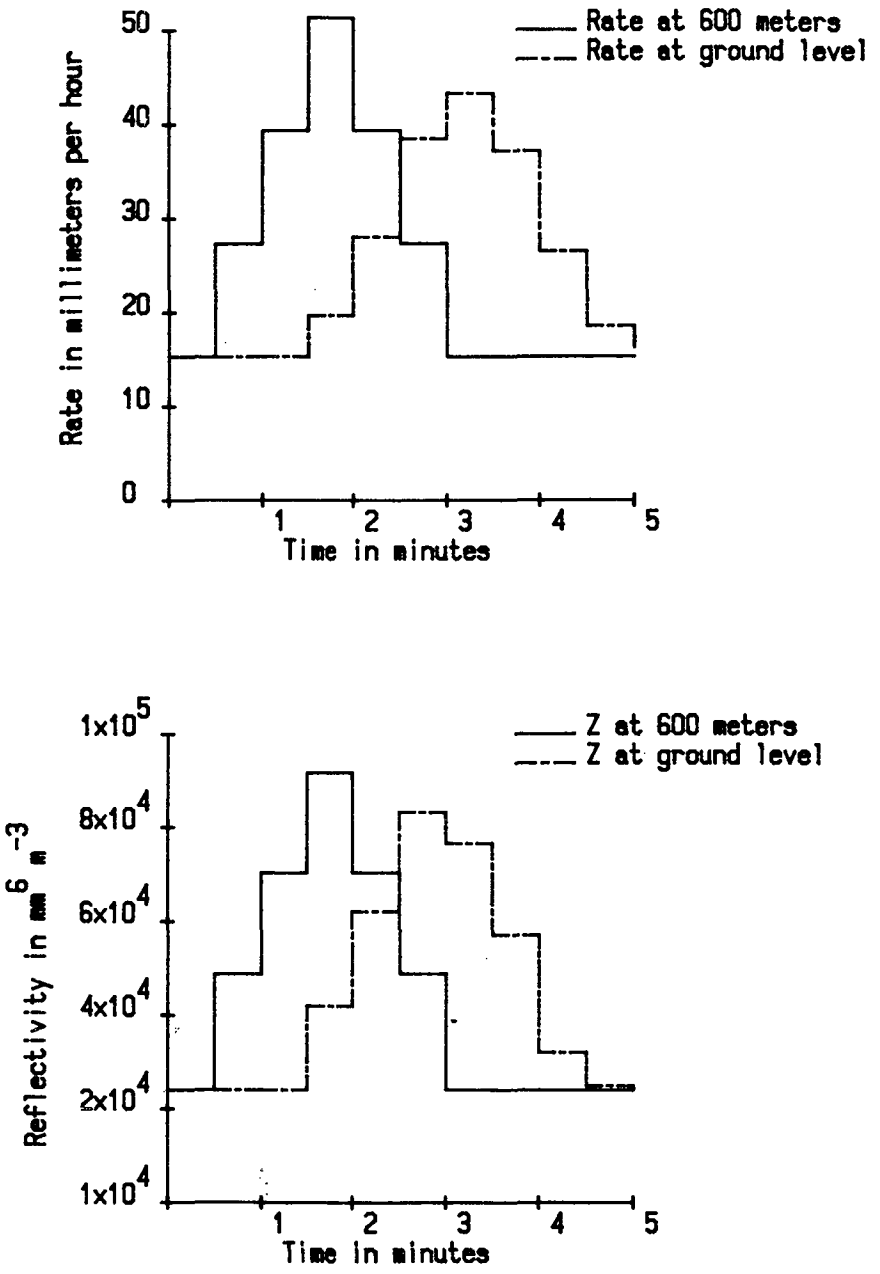


Figure 2. The effects of differential drop velocity on rain rates and reflectivity.

capabilities of storms are examined in a simple comparison of the two most relevant treatments. The significance of the difference between the seeded and unseeded (and unpenetrated) clouds for the mean echo top height (variable number 13), area (60), volume (28), mass (36), rainflux at 3° elevation angle (68), rainflux at 6 km (76) and precipitable water (84) are listed in Table 1 (Galpin, 1988; Appendix A, Table E). In this data stratification no cases are included without pretreatment echoes or with the coalescence time parameter less than 2.

This table looks promising for seeding effects with 23 significant cases at the 5% level. Obviously, however, further study is required to remove the effects of the pretreatment (-10 to 0) bias. This is being examined with a covariance analysis. Nevertheless, it appears that the requirement for the existence of pretreatment echo employed by the CSIR statisticians may be contributing to the difference with the earlier CloudQuest analysis. For example, this sample of 65 echoes only shows a factor of two rainflux (and echo area) enhancement for the seed group, compared with the factor of four increases for the total sample examined by CloudQuest in the 1986/87 Annual Report (N = 147 storms). The CloudQuest data included two categories not used in the CSIR analysis, (1) penetrated storms which were not seeded, and (2) storms with no pretreatment cell echo. The existence of pretreatment echo, makes it possible to examine one of the many possible bias indicators (the radar observations before seeding). Unfortunately, in the smaller 65 echo CSIR subsampler all but one of these seven echo variables is significantly different for the seeded case before treatment. This suggests a biased subsample. However, although the possibility of accidental bias in sampling is always going to be relatively high given the number of variables which must be controlled, the total sample does not appear to suffer bias. Furthermore, Gagin has also shown that early seeding (relative to echo life) may strongly impact on the effectiveness of the treatment. Thus, the early seeded PAWS cases must also receive more attention. These cases probably make a very substantial contribution to the overall PAWS seeding effect. Consequently, the pretreatment echo constraint will be relaxed for some future CSIR analyses.

The use of numerical cloud models is also suggested, both to eliminate the effects of bias and to better link cause to effect.

## Cloud Models

In the past, a broad spectrum of numerical cloud modelling studies have been undertaken at CSIR. These related to cloud growth processes and precipitation development, and included the use of large computers. One, two and three-dimensional cloud models (Steiner, 1973) studied the energy and water transformations during the lives of storms (Reuter, 1988).

Table 1: Significance probabilities for seeding effects (mean comparison via re-randomization). Data stratification, coalescence active, and echo required before treatment, N = 65 (see Galpin, 1988; Appendix A, Table E.)

| Period (min) | -10 to 0 | 0 to 10 | 10 to 20 | 20 to 30 | 30 to 40 |
|---|---|---|---|---|---|
| Variable | | | | | |
| Height (13) | - | - | .95 | .95 | - |
| Volume (28) | .99 | 1.00 | 1.00 | .99 | .95 |
| Mass (36) | .99 | 1.00 | 1.00 | .99 | .91 |
| Area (60) | .94 | 1.00 | .99 | .99 | .97 |
| Rainflux at 3° (68) | .99 | 1.00 | .99 | .99 | .98 |
| Rainflux at 6 km (76) | .97 | 1.00 | .99 | .98 | - |
| Precipitable water (84) | 1.00 | 1.00 | 1.00 | .99 | - |

However, more basic scientific studies have also been performed at CSIR. These related to the more realistic calculation of the collection kernel for cloud drop collisions in a turbulent environment via a stochastic model. The model assumes white noise random drop displacements proportional to the turbulent diffusion coefficient and introduced the use of stochastic differential equations into the field of precipitation studies. The Fokker- Plank type of differential equation needs to be solved numerically only once, yet covers the entire probabilistic nature of the problem. Thus, the new model avoids the high number of calculations required for the older Monte Carlo simulations. The results show that turbulence enhances the probability of collisions, particularly for droplet radii of less that 50 μm (Reuter *et al.*, 1988). However, the enhancement does not appear to be adequate to explain observations of the most rapid rain development rates.

Now, extensive application of simpler one-dimensional numerical cloud models will also be made to identify the atmospheric thermodynamic conditions suitable for successful cloud seeding.

In the future, it is planned to adopt the newer multi-dimensional cloud models which utilise Doppler radar observations as input to analyse the results of cloud seeding activities. These models are expected to be a powerful tool in identifying seeding signals amongst the otherwise great natural variability of convective rain processes since the rapidly updated radar input may supply very realistic pre-seeding in cloud conditions to the model predictions. Great reductions in experiment duration and in the uncertainty of establishing a seeding effect are possible. Most important, the actual physical mechanisms acting will be better identified.

REFERENCES


DIXON M J and MATHER G K, 1986: Radar evaluation of a randomized rain augmentation experiment - Some preliminary results. *Preprints: 10th Conference on Weather Modification*, AMS, Boston, 139-141.

GALPIN J S, 1988: Preliminary analysis of radar data concerning the Nelspruit cloud seeding experiment. CSIR/CACDS CKOMP 88/7. 27pp + Appendices A-E.

GROSH R C, 1988a: The science of rainmaking - An historical perspective. *Newsletter, SA Society for Atmos. Sci.*, **8**, 2-10.

GROSH R C, 1988b: Editor, 1987/88 PAWS report. CSIR/EMA C-88107, 200pp.

GROSH R C, 1989: Rainmaking - The promise for South Africa. *Proceedings First Biennial Conference*, Water Inst. South Africa, Parkhurst, 12pp.

KYLE T G, 1975: The measurement of water content by an evaporator. *J. Appl. Meteor.*, 14, 327-332.

MATHER G K, MORRISON B J and MORGAN G M, 1986: A preliminary assessment of the importance of coalescence in convective clouds of the Eastern Transvaal. *J. Clim. Appl. Meteor.*, 25, 1780-1784.

MORGAN G M, 1986: Accepted: *Theoretical and Applied Climatology*, Springer Verlag, Vienna.

MORRISON B J, MATHER, G K and MORGAN G M, 1986: Aircraft observations of target turrets on multicellular storms showing radar response to dry-ice seeding. *Preprints: 10th Conference on Weather Modification*, AMS, Boston, 204-209.

REUTER G W, DE VILLIERS R and YAVIN Y, 1988: *J. Atmos. Sci.*, **45**(5), 765-773.

REUTER G W, 1988: *Beitr. Phys. Atmosph.*, 61, 30-38.

STEINER J T, 1973: *J. Atmos. Sci.*, 30, 414-435.